Università Politecnica delle Marche
Corso di Dottorato di Ricerca in Ingegneria Civile, Ambientale, Edile e Architettura
Curriculum in Ingegneria Civile, Ambientale, Edile e Architettura
XVI edition - new series

Self-healing potential and RAP inclusion as sustainable strategies for never-ending bituminous materials

Ph.D. Dissertation of

Giorgia Mazzoni

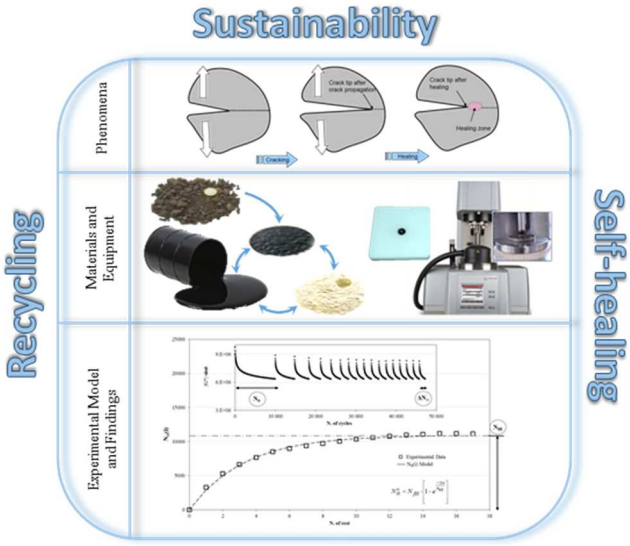

Advisor: **Prof. Francesco Canestrari**

Curriculum Supervisor: **Prof. Stefano Lenci**

Università Politecnica delle Marche
Corso di Dottorato di Ricerca in Ingegneria Civile, Ambientale, Edile e Architettura
Curriculum in Ingegneria Civile, Ambientale, Edile e Architettura
XVI edition - new series

Self-healing potential and RAP inclusion as sustainable strategies for never-ending bituminous materials

Ph.D. Dissertation of:

Giorgia Mazzoni

Advisor:

Prof. Francesco Canestrari

Curriculum Supervisor:

Prof. Stefano Lenci

XVI edition - new series

Università Politecnica delle Marche
Dipartimento di Ingegneria Civile, Edile e Architettura
Via Brecce Bianche — 60131 - Ancona, Italy

To my Family

"…What we have to learn to do,

we learn by doing …"

Aristotle

Acknowledgements

Completion of this doctoral dissertation would have never been possible without the support of several people to whom I would like to express my deep gratitude.

First, I am extremely thankful to my advisor Prof. Francesco Canestrari for giving me the possibility to reach this prestigious goal. He has been a charismatic and admirable guide with his immense knowledge and enthusiasm, and his exemplary dedication to work and outstanding researches.

Besides my advisor, a particular mention is due to Prof. Maurizio Bocci and Prof. Amedeo Virgili for the opportunity to collaborate in important scientific tasks (e.g. co-relator of master theses, co-author of scientific publications).

My sincere appreciation goes to the staff of the department ICEA (infrastructure area): Pierluigi Priori, Stefania Mercuri, Nicola Agostinacchio and, especially, Gabriele Galli who was like a "second father" to me. They have been very kind and always willing to lend their service whenever I approached them.

A special thank is dedicated to the entire research group of the department ICEA (infrastructure area) and other affiliated departments, in particular Gilda Ferrotti, Fabrizio Cardone, Andrea Graziani, Andrea Grilli, Edoardo Bocci and Musaab Abuadouss, for the daily scientific support and especially sincere friendship.

A loving mention to some fundamental colleagues:

- Emiliano, Carlotta, Arianna and Francesca, before being valued office- and work-mates, you are close friends with whom shared efforts, concerns as well as a lot of fun;
- Davide, irreplaceable work-mate and friend, thank you so much for being my first supporter and making me laugh even in the toughest times;
- Chiara, precious office-mate and friend, I am very grateful for your essential help received in the last months of my Ph.D.

I owe a lot to my family, who supported and encouraged me at every stage of my personal and academic life. To them I dedicate this doctoral dissertation as a sign of never-ending gratitude.

Above all, I bless God for granting me the wisdom, health and strength to undertake this research task and enabling me to its completion.

Abstract

Economic and environmental advantages encourage the use of Reclaimed Asphalt Pavement (RAP), coming from the milling of old pavements, to be introduced in new bituminous mixture. In particular, hot recycling of RAP allows a reduction of production costs and disposal issues as well as natural resources conservation thanks to the exploitation of both bituminous and lytic component. However, regulations of road agencies and public administrations usually impose restrictions on RAP percentages (from 10 to 30%) due to uncertainties concerning the interaction between bitumen released from RAP and virgin bitumen. Inaccurate assumptions on the related effects could lead to mixtures subjected to premature distresses, such as fatigue failure, considering the higher oxidation, and consequently viscosity (stiffness), of aged bitumens if compared to that of virgin bitumens.
In this context, the Ph.D research aimed at evaluating the effects caused by hot recycling of high RAP contents. Since it is expected that field performance of bituminous mixtures is mainly led by mastic phase and its components (i.e. filler and bitumen), the experimental study focused on analysing interactions among different types and dosages of RAP bitumens, rejuvenators and fillers. Besides the "classical" rheological characterisation, more innovative tests and analyses were performed in order to get an overall picture of the mechanical behaviour of the materials investigated in terms of fatigue, self-healing and thixotropy.
Based on the overall findings, the inclusion of higher RAP contents appears possible, without negatively affecting the final mixture performance, when an appropriate design is considered. Production process, paving technology, source, properties and dosage of RAP and, eventually, rejuvenator need to be properly selected so as to improve low and intermediate temperature properties of the mixture without penalising its high temperature performance.

Sommario

Benefici economico-ambientali incoraggiano l'uso di fresato (RAP), proveniente dalla demolizione di vecchie pavimentazioni stradali, da introdurre nella produzione di nuove miscele. In particolare, riciclare a caldo il RAP permette una riduzione dei costi di produzione e dei problemi di smaltimento, oltre a un risparmio delle risorse naturali, grazie allo sfruttamento della fase sia bituminosa sia litica. Tuttavia, i regolamenti delle agenzie stradali e pubbliche amministrazioni impongono restrizioni sulle percentuali di RAP implementabili (10÷30%) per la scarsa conoscenza dei meccanismi di interazione tra bitume riattivato da RAP e bitume vergine. Assunzioni inaccurate possono causare ammaloramenti prematuri della miscela, come fessurazioni da fatica, data la più severa ossidazione, e conseguente rigidezza, del bitume da RAP rispetto a quello vergine.

In questo contesto, l'attività di dottorato si è posta l'obiettivo di valutare gli effetti causati dal riciclaggio a caldo di alti quantitativi di RAP. Poiché la prestazione in sito di miscele bituminose è strettamente legata alla fase legante e ai suoi costituenti (filler e bitume), la sperimentazione è stata indirizzata all'analisi delle interazioni tra diverse tipologie e dosaggi di bitumi da RAP, rigeneranti e filler. Accanto alla "classica" caratterizzazione reologica, protocolli di prova innovativi sono stati applicati per ottenere un quadro globale del comportamento dei materiali e comprensivo di risposta a fatica, self-healing e tixotropia.

Sulla base delle evidenze sperimentali, l'impiego di un maggior contenuto di RAP è possibile, senza l'insorgenza di effetti dannosi sulla miscela finale, con una corretta progettazione. La tecnica di produzione, stesa e compattazione, la provenienza e le proprietà del RAP e dell'eventuale rigenerante devono essere selezionate opportunamente per migliorare le proprietà della miscela alle basse e intermedie temperature senza comprometterne le prestazioni alle alte temperature.

Contents

List of Figures

List of Tables

Introduction

Chapter 1

Background and problem statement

The word “sustainability” is currently dominating research trends and practical interests in many different fields.

Within the past 25 years, it has become important for political strategies, for goals of nations, cities and communities, and for companies’ business strategies. A long-term sustainable development can be achieved only if the idea of sustainability is implemented at different levels, from national guidelines to the practical application on site. The different levels should exchange information and knowledge to guarantee an efficient advancement.

The origins of contents discussed in connection with the term “sustainability” go back to the beginning of the 20th century and are rooted in the historic development of environmentalism (Pepper, 2005). During the 1970s and 1980s, problems caused by environmental pollution and consumption of resources became increasingly important. The most significant report of that time that deals with this topic was by Meadows et al. (1972), which analyses the growth of the world’s population and the resulting consumption of resources over the following 100 years. The results predict a failure of the world economy in case the economic system and the treatment of the environment were not changed. The Brundtland report “Our Common Future” can be identified as a milestone (Brundtland, 1987). It covers the relationship between development and environmental policies and defines the model of sustainable development for the first time: “*Sustainable development is development that meets the needs of the present without compromising the ability of future generations to meet their own needs*” (Brundtland, 1987). This report provided the impetus for the convention of the first United Nations Conference on Environment and Development, also known as the “Earth Summit,” in Rio de Janeiro, Brazil, in 1992. The most important result was the adoption of Agenda 21, an action program containing specifications, inter alia, to fight poverty and create effective energy policy, as well as fostering financial and technological cooperation of industrialised and developing countries (UNCED 1993). In addition, the results were extended and strengthened during the Johannesburg summit in 2002 (UN 2002). For the first time, the transcription into specific policy goals was realised at the United Nations Framework Convention on Climate Change in Kyoto in 1997 (UN 1998) by determining mandatory targets for the limitation of environmental impacts, such as the reduction of CO_2 emissions. Based on the above-mentioned conventions and reports, a broad discussion dealing with sustainability and sustainable development took place. As a result, an understanding of three different dimensions or pillars was developed, which specified the conceptual model of sustainability:

- Economic sustainability, intended as the ability of an economy to generate a lasting growth able to maintain a healthy balance with ecosystem. This pillar supports initiatives like fair distribution and efficient allocation of resources;
- Environmental sustainability, intended as the maintenance of the factors and practices that contribute to the quality of environment on a long-term basis. This pillar supports initiatives like renewable energy, reducing fossil fuel consumption and emissions, sustainable agriculture and fishing, organic farming, tree planting and reducing deforestation, recycling and better waste management;
- Social sustainability, intended as the ability of a community to develop processes and structures which not only meet the needs of its current members, but also support the ability of future generations to maintain a healthy community. This pillar supports initiatives like peace, social justice, reducing poverty and other grassroots movements that promote social equity.

These three dimensions of sustainability are internationally accepted as a well-established framework these days (Otto, 2007).
Several other categories for organising sustainability indicators and criteria can be used. Depending on the different countries and fields of application, various arrangements for the criteria can be applied. In particular, sustainability assessment in the construction sector has become increasingly important since the year 1990. It also goes along with the global development of sustainability, which supported life-cycle thinking, with the model of the three sustainability dimensions above-mentioned and with the importance of holistic analysis. Most activities can be found in the building sector, whereas fewer approaches are available for infrastructure sector, although this latter produces the highest level of greenhouse gas, directly through fossil energy used in mining, transportation, paving works and indirectly through the emissions coming from vehicles. For this reason, there is a deep need to face the challenge of sustainability by limiting the impact of infrastructures on the environment to a minimum through different sustainable practices. Nowadays, pavement-engineering strategies aim at performance improvement, resources conservation (e.g. recycling techniques) and environment protection (e.g. reduction of harmful emissions). The goal is to maximise the lifetime of a road pavement while restricting its emissions.
In this context, the optimum solution to reach sustainability is recycling, which entails environmental benefits with a reduction in the consumption of natural resources, energy and landfill spaces and concurrently economic advantages thanks to costs saving for new materials, disposal and transport. In particular, sustainability applied in road pavement design and construction deals with the insertion of recycled materials, as substitution of virgin one, whose origins can be different. In fact, according to the further field of application, it is possible to reuse materials coming from old pavement demolition (i.e. road by-product, usually referred as Reclaimed Asphalt Pavement, RAP), rubber tire recovery (i.e. industrial by-product, coded as PFU) or generic old structure demolition (i.e. demolition by-product, referred to Construction and Demolition, C&D).

Over the years, the use of RAP has been widely promoted due to its environmental and economic benefits, as the construction of new roads has gradually satisfied the constant growth in traffic volume. Various recycling technologies for asphalt pavement, such as hot recycling in asphalt plant, hot in-place recycling and cold in-place recycling, have been developed and proved to possess their own advantages and characteristics (Wang et al., 2017). For years, using RAP in unbound granular layers pavement was a common practice (Kazmee et al., 2016). However, in addition to aggregates, RAP also contains binder; therefore, when referred to hot recycling, the presence of RAP implies the introduction of both bituminous and lytic components, hence offering a higher advantage compared with the other recycled materials above-mentioned. In particular, the higher the RAP content within a mixture, the higher the corresponding economic and environmental advantages that include reduction of production costs, conservation of natural resources and avoidance of disposal problems (Rubio et al., 2012). In spite of the benefits above-mentioned, it is important to specify that more effort is needed to design a mixture containing a certain amount of RAP. Production process (plant type, production temperature, mixing time and discharge temperature), paving technology and RAP source and properties are fundamental factors on the final recycled mixture properties. In general, the presence of high RAP contents would increase the risk of premature distresses, such as thermal and fatigue cracking, as result of higher oxidation and viscosity (stiffness) of RAP bitumen component compared to virgin bitumen. In this context, the use of a rejuvenating agent represents a common practice to restore the aged bitumen properties to a condition that resembles that one of a virgin bitumen. Obviously, type and amount of rejuvenator need to be properly selected so as to improve low and intermediate temperature properties of the mixture without negatively affecting its high temperature performance. Also the implementation of RAP obtained from high-trafficked roads (highways) offers a positive contribution in terms of asphalt pavement performance. In fact, in this type of roads the likely presence of Styrene Butadiene Styrene (SBS) copolymer modified bitumen limits oxidation with beneficial effects on the RAP mix in terms of permanent deformation, thermal and fatigue cracking resistance (Dondi et al., 2016).

Actually, many agencies and public administration limit the use of RAP ranging from 10 to 30% due to concerns for pavement performances and production technologies. Uncertainties concern the interaction between bitumen reactivated from RAP and virgin bitumen. Inaccurate assumptions on the effects of interaction might create problems in both mix design and pavement performance (Mogawer et al., 2012). However, several studies have indicated that recycled pavements including over 40% RAP were feasible without detrimental effects on their mechanical properties (Valdes et al., 2011; Pereira et al., 2004; Celauro et al., 2010), especially on fatigue response (Stimilli et al., 2015a, 2015b, 2016, 2017; Mazzoni et al., 2016, 2017b and 2017c).

Anyway, it should be emphasised that fatigue cracking represents the major cause of failure for asphalt pavements, hence it is fundamental the correct understanding of cracking performance of bituminous materials, which is strictly linked to the properties of mastic phase and its components (i.e. filler and bitumen) (Jakarni, 2012; Kim, 2008). In particular, fatigue

resistance is the result of several mechanisms, such as self-healing which can be classified among environmentally sustainable strategies designed to decrease maintenance costs, extend service life and reduce greenhouse gas emission as well (Chung et al., 2015). In fact, when exposed to damage, some materials (e.g. metals, polymers, concrete or bituminous mixtures) have the intrinsic ability to repair small cracks and partial restore their original properties through thermo-mechanical or induced mechanisms. However, other recoverable phenomena of viscoelastic materials, such as thixotropy and heating, can permanently recover material properties. In order to avoid misleading-analyses, it is important to distinguish between recovery due to real healing and recovery due to intrinsic responses, especially with respect to thixotropy since the latter does not contribute to the fatigue life.

Therefore, research studies on this field are necessary to achieve a proper know-how about the best recycling process and the best laboratory practices for the recycled material property investigation, the best source and properties of milled material including its maximum content that can be incorporated in a new mixture. In particular, the best technical standards to characterise these new materials and reliable parameters should be identified, considering, among all the time and temperature dependent mechanisms involved in fatigue response, also the recoverable phenomena of viscoelastic materials, such as self-healing and thixotropy, in order to estimate the pavement service life under different climatic and traffic loading conditions. It is important to achieve comparable field performance for recycled and virgin materials, taking into account aspects related to both safety and maintenance costs.

Based on the above-mentioned discussions, it can be concluded that road pavement sustainability deals with high- quality and long-lasting pavements whose design, construction and management consider economic and social development, as well as environmental preservation. Specifically, the aim of the work presented in this Ph.D thesis is to quantify the fatigue life of bituminous mastics, considering self-healing potential and thixotropy and concurrently identifying useful insights in varying mastic components (types, contents and interactions). In fact, it is expected that the prediction of field performance of bituminous mixtures is closely linked to mastic self-healing properties. Moreover, the increasing reuse of Reclaimed Asphalt (RA) for the production of new, more performing and environmental friendly bituminous mixtures leads to a further need of understanding the influence of aged bitumen reactivated from RA (reclaimed bitumen) on the final mastic behaviour. A wide experimental study focused on analysing interactions among different types and amounts of reclaimed bitumen, eventually rejuvenator, virgin bitumen and filler, investigating the related effects on the bituminous mastic performance.

Chapter 2.

Research description and objectives

The Ph.D research work aims at developing all the topics above-mentioned. In particular, the valorisation of the milled material coming from old asphalt pavements results a fundamental objective to pursue, especially when dealing with highway network system, where the new bituminous mixtures produced and the milled material substituted are quantitatively equivalent. As a consequence, the possibility to include higher percentages of milled material than the current limit allowed by the national technical specifications represents the main goal to be achieved in the production of new bituminous mixtures, whatever the recycling techniques adopted (both cold and hot recycling). At the same time, this demand must be supported by an adequate performance-based laboratory investigation focused on the identification of advantages and disadvantages compared to the mixtures currently used in the highway system. Ultimately, such an investigation aims at providing useful information for technical and economic assessments of the recycling process. One of the main concerns for the use of RAP in the production of new bituminous mixtures is related to the properties of the aged bitumen included in the RAP and how it can affect the quality of the final bituminous phase of the recycled mixture. Given the complexity of such a topic, a rational planning of the experimental activities on a multiannual basis is required. In particular, the investigations described in the following chapters first focused on the evaluation of the rheological properties of different bitumens considered during their overall service life that includes their reuse in hot recycling by adopting eventually different rejuvenators. Subsequently, since the whole experimental program aims at verifying the actual possibility to produce recycled mixture with high RAP content without compromising field performance with regard to the main distress suffered by flexible pavements (i.e. fatigue cracking), fatigue performance, which is strictly linked to the properties of mastic phase and its components (i.e. filler and bitumen), was investigated for different bituminous materials. In particular, an evaluation of the overall response of different bitumens and mastics including different RAP contents is provided in terms of fatigue, self-healing and thixotropy and concurrently useful insights for fillers and bituminous blends and their interactions are identified.

The main objectives are briefly summarised in the following section. In particular, the overall research activities discussed in this dissertation are carried out in the Department of Civil and Building Engineering and Architecture of the Polytechnic University of Marche and address the main issues related to hot recycling production techniques, such as effect of RAP and eventually rejuvenator inclusions on different bituminous materials.

The analysis focused first on the characterisation of different bitumens (primary bitumen and vis-breaking bitumen) during the three main phases of their service life: the first service life (service life after the bituminous mixture production using virgin bitumen), hot recycling

process (bituminous phase of recycled mixtures made with virgin bitumen and aged bitumen reactivated from RAP) and second service life (service life after the recycling process using rejuvenated bitumen). In particular, the presence of aged RAP bitumen was simulated by subjecting the reference bitumen to a laboratory long-term ageing, as described in a following paragraph in detail (§ 5.2).
Subsequently, since the milled material used for the production of new mixtures for the highway system comes exclusively from old highway pavements that can be implemented only with modified bitumens, in accordance with the standard technical specifications, the analysis focused on materials modified with Styrene Butadiene Styrene (SBS) copolymers. Moreover, the choice of these materials depends on their highly established efficacy in improving fatigue cracking and reducing ageing, thanks to the presence of elastomeric polymers (SBS) that modify bitumen rheology by enhancing its elastic response. Different bituminous and binder (bituminous mastic) phase of recycled mixtures, made with SBS polymer modified bitumens, composed partially of the virgin polymer modified bitumen and partially of the old aged bitumen released from RAP, polymer modified itself, and different types and amounts of filler were characterised, especially in terms of fatigue, self-healing and thixotropy.

2.1 Outline of the dissertation

In order to achieve the objectives above-mentioned, the research activities have been planned and structured in two main phases, as shown by the scheme of Figure 2.1 that summarises the research activity subjects of each step.

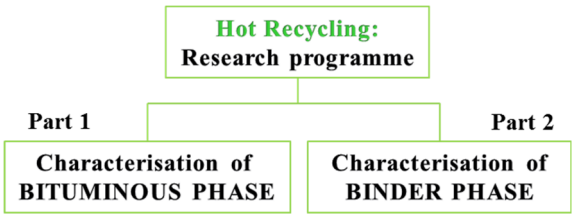

Figure 2.1. Research program: main steps.

Prior to performing the experimental activities, an extensive literature review was conducted for each phase investigated. It allowed the assessment of the current state of knowledge on hot recycling for bituminous mixtures and the related performance in terms of fatigue, thixotropy and self-healing. Afterwards, laboratory activities were structured in two main steps: the first one aimed at evaluating rheological properties of bitumens considered during their overall service life that includes their reuse in hot recycling by adopting eventually

different rejuvenators; the second one focused on the response of the binder component within hot recycled pavement, especially in terms of fatigue, self-healing and thixotropy.
This Ph.D dissertation is composed of several chapters, whose contents deal with the topics above-mentioned.

Part 1

Characterisation of the bituminous phase

Chapter 3

Literature review

The implementation of high RAP contents in new bituminous mixtures represents an important challenge to be taken and a fundamental goal to be achieved. Over the last decades, the re-use of old pavements is become a common practice to face up to the increment of the oil price and low availability of good quality aggregates.
However, RAP component is rich in aged bitumen that could cause a significant increment in the mixture stiffness, with consequences both in terms of production process and lay down phase. Hence, when dealing with high RAP inclusion, the addition of a rejuvenator is suggested so as to soften the aged bitumen reactivated from RAP and minimise the negative impact of ageing. Many experimental studies linked to the re-use of milled materials are available in literature and, in particular, the main experiences on hot recycling with the related issues concerning the use of RAP and rejuvenators in a new bituminous mixture are discussed in this chapter, especially with respect to the effects of RAP and rejuvenators on the bituminous phase.

3.1 Main experiences on hot recycling of asphalt pavements

Hot Mix Asphalt (HMA) is the most commonly used material for road pavement construction worldwide. During road pavement service-life, the HMA suffers structural damage, such as rutting, fatigue and thermal cracking, mainly due to repeated traffic loading, severe climatic conditions and problems related to the bituminous mixture production, compaction and paving. It is estimated that the amount of RAP that is milled off roads is approximately 100 million tons pro year (Boomquist et al., 1993) and is totally recyclable (Hansen et al., 2011). In accordance with Directive 2008/98/EC, Member States of EU shall take measures to promote the re-use of products and preparing for re-use activities (2008/98/EC Directive). The new circular economy package issued by the European Commission in December 2015 aims at increasing the use of recycled material and RAP in road construction by promoting cradle-to-cradle strategy to save raw materials, reduce carbon footprint of construction process and save money. For instance, in Germany, France and the Netherlands the available quantity of RAP is 11.5, 6.9 and 4.5 million tonnes, respectively, and the percentage of RAP incorporated in hot/warm recycling is 90%, 64% and 76%, respectively. However, re-use and hot/warm asphalt recycling practices struggle in Italy, where10 million tonnes of RAP are available, but only 20% of RAP is used in hot/warm recycling processes. This means that RAP is accumulating in stockpiles, used in non-bituminous applications or being dumped. Many agencies and public administrations insert restrictions on RAP percentages ranging from 10 to 30% in their regulations due to concerns for pavement performances and

production technologies. Also most state Departments of Transportation (DOTs) allow the use of RAP in preparing bituminous mixtures at low percentages ranging between 15 and 45%. The main reason of such low RAP contents used in new bituminous mixtures is the uncertainty concerning the interaction between bitumen released from RAP and virgin bitumen. Despite considerable efforts in characterising the interaction between virgin and RAP bitumens (Navaro et al., 2012; Nguyen, 2009; Booshehrian et al., 2013) and consequently the degree of blending the two constituent of the bituminous phase (Shirodkar et al., 2010; Yousefi, 2013; Bressi et al., 2015) only few fundamental information on physicochemical phenomena and mechanisms during a mixing phase of a new mixture with RAP are available in literature. Moreover, the main obstacle to incorporate high RAP contents into asphalt pavements is the aged RAP bitumen which causes premature distresses, such as fatigue failure or low temperature cracking in pavement structure. To overcome this problem, the use of specific additives is usually recommended to achieve adequate workability and final mechanical performance (Chen et al, 2007; Shen et al., 2007; Yu et al., 2014). The same rheological properties of the target virgin bitumen can be obtained by mixing the aged RAP bitumen with a rejuvenator, but the chemical composition (e.g. the ratio of asphaltenes to maltenes) of the rejuvenated bitumen is significantly different from that of the virgin bitumen which may affect the long-term performance of the RAP mix (Asli et al., 2012; Shen et al., 2007; Zargar et al., 2012). The performance of the rejuvenated bitumen is obviously also high dependent on the type and dosage of the rejuvenator. Additives should be non-hazardous and stable over a wide range of temperatures, from production to application and must not experience any exudation or evaporation, in order to ensure a good performance over asphalt pavement lifetime designed. Numerous studies have been undertaken on the effect of recycling additives within aged bitumen, but the ageing process of rejuvenated bitumen is still a challenge. For this reason, an overview of the knowledge acquired about the proper rejuvenator to be used (type and dosage) as well as its effect on the properties of aged bitumen and mixture will be widely discussed in the following sections.

3.1.1 Major issues related to the use of RAP

Reclaimed Asphalt Pavement (RAP), coming from the demolition and milling of old asphalt pavements, can be incorporated in the production process of new bituminous mixtures (Copeland, 2011), thus obtaining a recycled bituminous mixture that guarantees appropriate characteristics if a proper design is planned. In particular, several studies highlighted the necessity to address the following issues (Copeland, 2011; Ipavec et al., 2012):

- quality control of materials and production process adopted;
- characterisation of RAP in agreement with the European standard EN 13108-8;
- dosage and type of external materials eventually included in RAP;
- type and age of bituminous component;
- average bitumen content;
- type and grading distribution of original aggregates;

- nominal maximum aggregate size;
- homogeneity;
- type and percentage of the virgin bitumen added.

The recycling technique chosen and the properties of RAP components are of fundamental importance to obtain good recycled mixtures and consequently suitable field performance. In particular, recycling techniques can be divided in two main categories: hot and cold recycling. In this literature review, only the main experiences on hot recycling technique are described in order to provide a comprehensive picture of the current state of the art.

Usually, with respect to hot recycling process, RAP constitutes a percentage of the total amount of materials around 10 to 50% to be mixed with aggregates and bitumen preventively heated at high temperature. Two different production methods can be adopted:

- in plant recycling: the milled material is moved from the old pavement location to the plant site where it is processed through crushing and screening to discard foreign matters and clumps too large. Then, it is usually sieved and divided in more fractions prior to being re-used. Thanks to the higher possibility to monitor and control the milled material prior to be re-introduced in the production process, this method avoids high variability of RAP and guarantees a better quality and a more uniform homogeneity of the final mixture. Moreover, it provides the advantage of having higher flexibility in the production sequences that can be adapted according to several requirements and different types of mixture. At the same time, this method has few drawbacks mainly related to the higher costs due to the transport and the stocking of the milled material in the plant where it is necessary to ensure a big amount of appropriate spaces;
- in place recycling: in this case, all the production activities (milling, mixing, compaction) are implemented directly in field using specific equipments. Lower control of the milled materials and the quality of the production process have to be considered. However, these drawbacks are balanced by higher economic benefits and shorter production time. The so produced mixtures are usually employed to build binder or base layers, depending on type and volume of traffic (Tebaldi et al., 2012).

The choice to adopt the in plant production process is mainly determined by the following factors:

- type of application: the in plant recycling is usually taken into account when the recycled material is used to build a new layer of the pavement;
- in site material: since high quality and good properties are required for surface layers, when they are produced with milled material, the variability usually related to RAP can justify a pre-treatment that can be fulfilled only in plant.

Another aspect to be mentioned, strongly associated to the production method adopted, is the water content of RAP, namely its humidity that represents one of the most important characteristic to check when RAP is re-used, since it can negatively affect the overall quality of the mixture.

In fact, a pavement is subjected to maintenance and rehabilitation activities when its distresses are already significant and compromise the integrity of the surface, hence allowing

the access of the water inside the pavement structure. In particular, in the case of in place recycling, RAP is used right after the milling in the exact conditions that it has in situ. Therefore, it is necessary to control a priori that the water content in the old pavement is able to guarantee the goodness of the re-building activity.
On the contrary, in the in plant production the initial water content of RAP is less important since this parameter can be easily monitored over time and varied if needed. In fact, once RAP is moved to the plant site, it can be managed and preserved as a traditional aggregate fraction. However, it is necessary to remind that the milled material has the tendency to keep the humidity without allowing the water to progressively drain as usually happens for the virgin aggregates. Therefore, also in plant the water content of RAP must be regularly monitored (Tebaldi et al., 2012b) and the contact between RAP and water should be avoided, for example stoking the material in a covered space.
As initially highlighted, besides the production techniques, also the homogeneity of RAP, especially in terms of type and dimension of the original aggregates and type of the original bitumen, should be considered among the factors affecting the quality of a recycled bituminous mixture.
The ideal production process should allow the use of RAP coming from only a single source (intended as pavement layer). Such a precaution can be achieved by stocking the material coming from different layers separately. This is particularly important since different layers of a pavement are made with different materials in order to obtain specific characteristics. For example, the surface layers are usually composed of bitumen with improved quality and aggregates of smaller size (Al-Qadi et al., 2007; Copeland, 2011; de la Roche et al., 2012).
Since this practice requires several efforts in terms of logistic organisation and costs (time and a lot of spaces for the stockpiles), it is difficulty fulfilled and often milled materials coming from different locations and pavement layers are mixed together.
In any case, in the attempt to increase the homogeneity of the milled material, a previous fractioning and sieving of RAP is fundamental. Obtaining several RAP sizes (e.g. 0/4 mm and 4/11 mm or 0/8 mm and 8/16 mm) should be recommended also for the in plant production, since it allows to meet more easily and effectively the aggregate grading curve requirements (de la Roche et al., 2012). Moreover, such a precaution can encourage the use of higher RAP content in new mixtures, since the fractioning in more sizes is believed to enhance the integrity and the homogeneity of RAP with positive consequences on interaction with the virgin aggregates (Copeland, 2011).
Among the aspects previously mentioned, also the aggregate gradation of the recycled mixture and the type and quantity of the virgin bitumen added have a fundamental importance in the production of optimum hot recycled mixtures. Consequently, before producing recycled mixtures, specific investigations are needed about these two fundamental aspects. In particular, with respect to the virgin bitumen, one of the major concern, not fully investigated yet, is the degree of blending between the virgin bitumen and the aged bitumen reactivated from RAP and the effects of the blending on the properties of the final bituminous component of the recycled mixture. The performance of the bituminous mixture is

significantly affected by the degree of blending which determines type and quantity of the virgin bitumen to be used as well as the maximum amount of RAP to be included in a recycled mixture. As suggested by the fundamental importance of this aspect, a specific paragraph of the literature review hereby presented (§ 3.2.5) is completely dedicated on it.

3.1.2 Major issues related to the use of rejuvenators

Among recycling additives, a distinction can be made between rejuvenators and softening agents (Wu et al, 2002; Pradyumna et al., 2013). The softening agents play the role of agents reducing aged bitumen viscosity, whereas rejuvenators act as agents restoring the chemical and rheological properties of aged bitumen (Grilli et al., 2017; Karlsson et al., 2006; Garcia et al., 2010).
According to Carpenter et al. (1980), the diffusion process of a rejuvenator includes four steps. In the first step, the rejuvenator forms a very low viscosity layer surrounding the aggregate particles coated with aged bitumen. In the second step, it starts penetrating into the aged bitumen and consequently softens the bitumen. In the third step, the rejuvenator penetrates into the aged bitumen and viscosities of both inner and outer layers are gradually decreased. Finally, by passing time, equilibrium is reached over the majority of the recycled bituminous film. Different factors influence diffusion rate, as listed below (Cussler, 1997; Karlsson et al., 2003):

- Size and shape of molecules or agglomerations;
- Intermolecular forces;
- Temperature;
- Structural rigidity of the diffusing molecules (restrictions on bending and twisting);
- Microscopic structure of a relatively stationary phase, if any.

In 2003, Karlsson and Isacsson investigated the influence of different parameters on diffusion rate using Fourier Transform Infrared Spectroscopy by Attenuated Total Reflectance (FTIR-ATR). These parameters included temperature, bituminous film thickness, type of bitumen, and chemical properties of the bitumens. According to their results, temperature had the highest influence on the diffusion rate (Karlsson et al., 2003). In long-term criteria, chemical properties should be altered in addition to bitumen rheology to minimise fatigue and low temperature cracking without negatively affecting rutting properties, as a consequence of a softer bitumen. Additionally, the rejuvenated bitumen should provide sufficient adhesion and cohesion between the aggregate particles to prevent moisture damage and ravelling (Zaumanis et al., 2014). Another long-term issue is related to the ageing of the rejuvenated bitumen. It was reported that ageing process is faster in a rejuvenated bitumen than in a virgin bitumen. Therefore, performance of rejuvenated bituminous mixture should be accurately evaluated (Ongel et al., 2015). Typical changes in chemical compositions for a typical aged and rejuvenated bitumen are depicted in Figure 3.1.

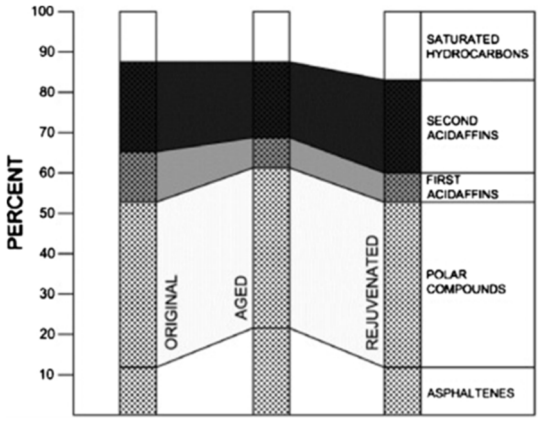

Figure 3.1. Alterations in chemical compositions of aged and rejuvenated bitumen.

Three rejuvenating methods are suggested by literature. The most common way to use rejuvenators is mixing them with aged bituminous mixture at high temperature (140–150 °C) or spraying them onto the surface of asphalt pavement (Lin et al., 2014; Garcia et al., 2011). The second procedure is called Rejuvenator Seal Materials (RSM), which is typically used after three to four years of pavement construction (Lin et al., 2014). Two factors are important in the RSM procedure: (1) effective penetration depth of rejuvenator; (2) diffusion effect with bitumen. RSM method can improve mixture properties against catastrophic effects caused by the presence of moisture, gasoline, diesel and weathering, and can even enhance surface cracking properties of road mixtures (Fwa, 2006; King et al., 2007). It can also prevent bitumen oxidation by penetrating into the voids in bituminous mixture (Lin et al., 2012). Although the advantages above-mentioned, RSM method presents some weak points. Firstly, rejuvenator must penetrate into pavement surface to a required depth or it might reduce surface skid resistance which can cause delay to open traffic after RSM application (Prapaitrakul et al., 2005; Garcia et al., 2010; Su, 2012; Qureshi et al., 2013). Another negative aspect about RSM is that it might harm the environment (Garcia et al., 2010). The third concept of using rejuvenators is encapsulation process. In this method, a rejuvenator is contained in capsules. Figure 3.2 shows the working mechanism of a capsule: under the application of repeated traffic loads the capsule within the mixture starts degrading until it breaks and rejuvenator comes out and diffuses through the bitumen (Garcia et al., 2011). Recently, the microencapsulation process has been developed (Su et al., 2013). In the theory of microcapsule, after the microcapsule cracks, the released rejuvenator will leak into the micro-cracks which help with healing process. Shells in microcapsules are commonly fabricated by polymeric materials that provide not only appropriate strength and toughness, but also exhibit good thermal stability at high temperatures (Su et al., 2013; Pan et al., 2012).

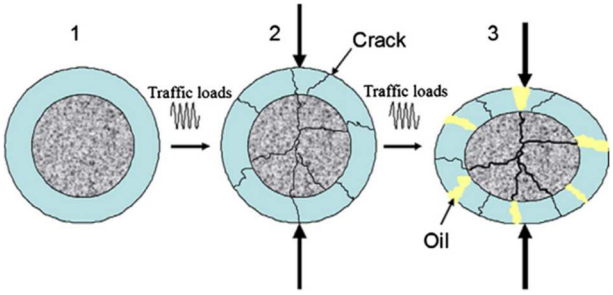

Figure 3.2. Capsules mechanism scheme (Garcia et al., 2011).

A crucial step is the selection of the appropriate type and dosage of rejuvenator. In particular, rejuvenators come from different sources and include plant oils, waste-derived oils, engineered products, as well as traditional and non-traditional refinery base oils (Zaumanis et al., 2013). Good rejuvenators should properly react with aged bitumen and produce high quality recycled bitumen. However, according to Ping-Sien Lin et al. (2011), there is the lack of a complete knowledge about rejuvenating mechanism responsible of the improvement of aged bitumen properties and consequently recycled mixture quality. In addition, concerns are associated with rejuvenator ability to diffuse within RAP bitumen and to provide the long-term performance required for another pavement service period (Zaumanis et al, 2015). Moreover, overdosage of rejuvenator can create problems such as adhesion and stripping of the bituminous film from the aggregate (Zaumanis et al., 2013).
However, introducing rejuvenators provides major benefits as compared to merely bumping the virgin bitumen grade, as follows:
– Unrestricted RAP content using a single rejuvenator;
– Cheap storage, since in most cases rejuvenators do not require heating;
– Simple addition to the mixture using volumetric pump or existing liquid additive dosage system;
– Ability to add the precise required dose based on the RAP bitumen properties.
These advantages would allow an increase in the average RAP content to be incorporated in HMA asphalt pavements, if the rejuvenating mechanism were better understood.

3.1.3 Incorporation of high RAP contents and rejuvenators in asphalt pavements

Both hot and cold in place recycling processes potentially allow the incorporation of RAP percentages up to 80-100%. However, the common practices limit the use of RAP ranging to 10-30% by aggregate weight due to the extreme variability of RAP gradation. This aspect is especially important when RAP is not appropriately processed and stocked, with previous sieving and fractioning actions that avoid excessive variability and segregation. Additionally, the milling process produces a recycled material with high fine aggregates content, RAP

component rich in (aged) bitumen that, hence, could cause a significant increment in mixture stiffness, with consequences in terms of both production process and lay down phase.
In order to soften the aged RAP bitumen and minimise the negative impact of ageing, a rejuvenator should be used. From a chemical point of view, an ideal rejuvenator should replenish the volatiles and light chemical fractions that have been lost during pavement ageing (Nahar et al., 2014) by providing a homogeneous system where asphaltenes are well dissolved and prevented from precipitation or flocculation, as suggested by some researchers (Karlsson et al., 2006). Another study has demonstrated that high amounts of resin or aromatic fractions provide a better rejuvenating effect (Roberts et al., 2009).
In any case, rejuvenators have the potential to significantly increase RAP content incorporated in HMA mix design, and, perhaps even provide a chance for total (100%) hot-mix recycling (Zaumanis et al., 2014). This would require ensuring homogeneous RAP material with low fines content, adequate mix design and modified production plants. Despite the economic and environmental benefits promised by higher RAP contents, some state agencies are reluctant to allow the use of rejuvenators, mostly due to potential rutting damage (Shen et al., 2007), which may result from ineffective blending of the rejuvenator with the RAP bitumen and resultant low stiffness micro-layer on RAP surface (Zaumanis et al., 2015). Hence, careful selection of the rejuvenator is required to guarantee the pavement the necessary short-and long-term properties, as follows:

- Short-term properties: rejuvenators should allow the production of high RAP content mixture by rapidly diffusing into RAP bitumen and mobilising aged bitumen in order to produce uniformly coated mixtures. Rejuvenator should soften bitumen in order to produce a workable mixture that can be easily paved and compacted to the required density without the hazard of producing harmful emissions. Major part of diffusion process should be completed before traffic is allowed to avoid reduction of friction and increased susceptibility to rutting;
- Long-term properties: rejuvenators should reconstitute chemical and physical properties of the aged bitumen and maintain stability for another service period. Bitumen rheology should be altered to reduce fatigue and low temperature cracking potential without over softening the bitumen to cause rutting failure. In order to prevent moisture damage and ravelling, a mix exhibiting sufficient adhesion and cohesion have to be designed.

However, there is still the need to bridge the lack of a systematic approach aimed at exploring how the rejuvenator modifies the chemical, microscopic and mechanical properties of the aged bitumen.

3.2 Effect of RAP on the bituminous phase of bituminous mixtures

One of the main concerns for the use of RAP in the production of new bituminous mixtures is related to the properties of the aged bitumen included in RAP and how it can affect the quality of the final bitumen phase of the recycled mixture. In fact, the most critical issue is related to the ageing process which affects physical and chemical characteristics of RAP bitumen entailing a general hardening of the final bituminous blend. Moreover, the phenomena of RAP bitumen mobilisation and its blending and interaction with the new virgin bitumen during mix production represent uncertainties that are still under investigation worldwide. Inaccurate assumptions on the effects of interaction could create problems both in mix design and pavement performance, leading to a final mixture more susceptible to cracking, ravelling, moisture damage and rutting (Zaumanis et al, 2015; Dondi et al., 2016; Noferini et al., 2017).
In this regard, ageing effects on the chemical and rheological properties of the bitumen and the current state of the art about the knowledge acquired on the interactions between virgin and RAP bitumen are discussed in the following paragraphs.

3.2.1 Basic bitumen chemistry and structure

In order to have a better understanding about RAP bitumen and ageing phenomenon, an exhaustive overview about bitumen chemistry and structure is first provided.
Bitumen is defined in the current European specifications (EN 12597) as a "*virtually involatile, adhesive and waterproofing material derived from crude petroleum, or present in natural asphalt, which is completely or nearly completely soluble in toluene, and very viscous or nearly solid at ambient temperatures*". The elemental composition of bitumen depends on its crude source, which is composed of hydrocarbons. The chemical nature of the crude oil is described as paraffinic, naphtenic or aromatic if a majority of saturate, cyclic or aromatic structures, respectively, are present. Hydrocarbons are organic compound consisting entirely of hydrogen and carbon, where carbon atom is the molecule skeleton. The complexity of bitumen chemistry lies in the fact that many different chemicals are present. In fact, even if bitumen mainly consists in carbon (typically 80÷88 wt.%) and hydrogen atoms (8÷12 wt.%), which give a hydrocarbon content generally superior to 90 wt.%, heteroatoms, such as sulphur (0÷9 wt.%), nitrogen (0÷2 wt.%) and oxygen (0÷2 wt.%), and traces of metals, such as vanadium, up to 2000 parts per million (ppm), and nickel (up to 200 ppm) are generally present (Table 3.1) (Speight, 1999; Read, 2003; Jiménez-Mateos, 1996; Branthaver, 1994).

Table 3.1. Elemental analysis for the core SHRP bitumens (Mortazavi et al., 1993).

Origin		AAA-1	AAB-1	AAC-1	AAD-1	AAF-1	AAG-1	AAK-1	AAM-1
		Canada	USA	Canada	USA	USA	USA	Venezuela	USA
C	wt.%	83.9	82.3	86.5	81.6	84.5	85.6	83.7	86.8
H	wt.%	10.0	10.6	11.3	10.8	10.4	10.5	10.2	11.2
H+C	wt.%	93.9	92.9	97.8	92.4	94.9	96.1	93.9	98.0
H/C	Molar	1.43	1.55	1.57	1.59	1.48	1.47	1.46	1.55
O	wt.%	0.6	0.8	0.9	0.9	1.1	1.1	0.8	0.5
N	wt.%	0.5	0.5	0.7	0.8	0.6	1.1	0.7	0.6
S	wt.%	5.5	4.7	1.9	6.9	3.4	1.3	6.4	1.2
V	ppm	174	220	146	310	87	37	1480	58
Ni	ppm	86	56	63	145	35	95	142	36
Mn	g/mol	790	840	870	700	840	710	860	1300

In particular, heteroatoms influence in saturated molecules: they combine with the carbon atoms of some unsaturated molecules making them more active (polar). However, molecules saturated by heteroatoms are joined by relatively weak chemical bonds that can be easily broken by heating or applying tangential actions; this fact explains the viscoelastic and thermoplastic nature of bitumen. It should be emphasised that, if the bonds are broken by heating, they will be replaced after the bitumen cooling by a different structure, if compared with the original one characterising the bond before undergoing heating (oxidation).
The presence of some compounds constituted by heteroatom provides useful indication on bitumen behaviour. For example, the presence of ketones and sulphides is a marker of a bitumen with a strong tendency to oxidation that is, conversely, inhibited by phenols, sulfides do not react directly with oxygen, whereas the presence of amphoteres improves bitumen viscosity.
Approaching bitumen chemistry on a global basis is not sufficient to fully understand its properties, thus it is fundamental the knowledge of bitumen structures, or better its homogeneous fractions, each one with peculiar characteristics, to which certain properties of the bitumen are common. In fact, through different fractionation methods, it is possible to separate bitumen molecules into different chemical families, depending on their size and solubility in polar, aromatic or non-polar solvents. In particular, chromatographic method is the main tool worldwide used for the evaluation of the bitumen structural constitution. It identifies four separate fractions allowing the so-called SARA analysis to be performed: Saturates, Aromatics, Resins and Asphaltenes (SARA). Bitumen must be thought as a chemical continuum with a gradual increase of molar mass, aromatic content and polarity from saturates to asphaltenes (Table 3.2.)

Table 3.2. Chemical properties of bitumen and the SARA fractions.

Chemical properties of bitumen and the SARA fractions:
typical H/C, elemental analysis, number average molar mass and solvent used in ASTM D-4124

	H/C	C	H	O	N	S	M_n	Solvent in ASTM D4124
	–	%	%	%	%	%	g/mol	
Bitumen	1.5	80–88	8–12	0–2	0–2	0–9	600–1500	–
Saturates	1.9	78–84	12–14	<0.1	<0.1	<0.1	470–880	n-heptane
Aromatics	1.5	80–86	9–13	0.2	0.4	0–4	570–980	toluene and toluene/methanol 50/50
Resins	1.4	67–88	9–12	0.3–2	0.2–1	0.4–5	780–1400	trichloroethylene
Asphaltenes	1.1	78–88	7–9	0.3–5	0.6–4	0.3–11	800–3500	n-heptane insoluble

In details, saturates usually amount for 5÷15 wt.% of a paving grade bitumen and form a colourless or lightly coloured liquid at room temperature (Corbett, 1969). They are composed of mainly aliphatic with different branching structures and some long aliphatic chains (paraffins) and very few polar atoms or aromatic rings are present. They function as jelling agent for bitumen components, as they favour asphaltene flocculation and therefore bitumen solid-elastic phase.
Aromatics form a yellow to red liquid at room temperature and are the most abundant constituents of a bitumen together with the resins, since they amount for 30÷45 wt.% of the total bitumen (Corbett, 1969). Their carbon skeleton is slightly aliphatic with lightly condensed aromatic rings (Piéri, 1995). They are somewhat more viscous than saturates at the same temperature and function as solvents for the peptised asphaltenes.
If saturates and aromatics are oily liquids at room temperature, resins form a black solid at room temperature (Corbett, 1969) and can be numerous (30÷45 wt.%) (Corbett, 1969). Their composition is close to that of asphaltenes except a less complex aromatic structure content (Koots et al., 1975). Piéri (1995) showed that they can sometimes be more polar than asphaltenes, but again with less condensed aromatic rings. They typically contain fused aromatic rings, with a most probable structure corresponding to 2–4 fused rings. They play a crucial role in the stability of bitumen, since they act as flocculent agents for the asphaltenes.
Asphaltenes form a black powder at room temperature (Corbett, 1969) and are largely responsible for the black colour of bitumen. They exhibit many condensed aromatic rings and polar groups, some fused aromatic rings and pending aliphatic chain. They represent generally between 5 and 20 wt.% of a paving grade bitumen (Corbett, 1969; Speight, 2004) and are by far the more studied bitumen fractions because of their viscosity building role (Branthaver, 1994). The higher the asphaltenes content, the higher the stiffness as well as the viscosity of the associated bitumen. However, bitumen behaviour is determined by the compatibility and the interactions among these homogeneous fractions rather than the relative amount of the components.
Different models were proposed to link bitumen composition and rheological properties. Early colloidal systems were proposed by Rosinger (1914)-Errera-Nellensteyn (1924) and described bitumen as a dispersion of asphaltene micelles (solid) in an oily phase (fluid) thanks to the presence of peptising agents, i.e. resins, adsorbed on their surface. Resins and oils are called maltenes (Read and Whiteoak, 2003; Redelius 2004).
Resins, the polar components of the maltenes, are thought to stabilise the asphaltene micelles that are very close in structure to free carbon. In particular, if resins keep asphaltenes highly peptised (or dispersed) in the oily phase so that micelles are no interacting, the associated bitumen is characterised by sol-model as defined by Pfeiffer and Saal (1940) and Labout (1940). This model results in a newtonian liquid behaviour at high temperature and very viscous (not elastic) behavior at low temperature. Whereas, if resins are not very effective in peptising asphaltenes, which result fully interconnecting, gel-model is obtained for the associated bitumen. This model results in a non newtonian fluid (viscoelastic) behaviour at high temperature and elastic solid behaviour at low temperature. Also an excessive presence

of paraffins (saturates) in relation to nitrogen bases tends to reduce solubility, leading to increased gel characteristics, but, if the asphaltenes are very branched, it is higher their interaction with the resins and lower destabilising effect of saturates. In practice, most of the bitumens has intermediate characteristics between these two structures above-mentioned that represent the limit cases. Coexistence of sol-type micelles and a gel structure as a function of temperature and aggregation state of micelles (ratio among asphaltenes, resins, aromatics and saturates) is defined as a gel-sol model. Modern colloidal models developed, but the only difference between former sol and gel would be the amount of solid phase that is asphaltenes plus stabilising resins. Moreover, the effective volume fraction must account for the solvent entrapped inside the open asphaltene micelles and the possibility that asphaltene aggregation and conformation change with temperature and concentration.
However, in each bitumen the molecules are subjected to an irreversible oxidative phenomenon (i.e. ageing) that significantly alters chemical properties of the material over time.

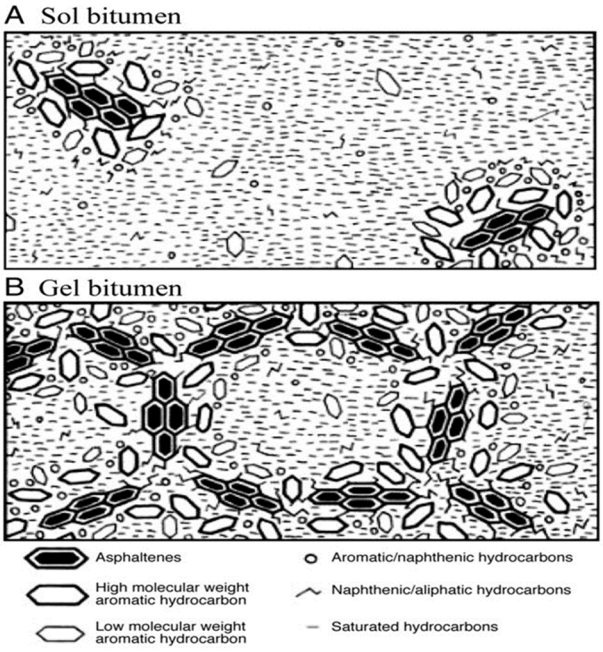

Figure 3.3. Internal structure of bitumen (Read and Whiteoak, 2003).

3.2.2 Ageing of bitumen

Chemical ageing is a sum of oxidation reactions and polymerisation and, to a lesser extent, lighter components evaporation (Read and Whiteoak, 2003; Traxler, 1961; Bell, 1989). As a

result, chemical ageing causes a global hardening of the material (Read and Whiteoak, 2003; Wright, 1965) and consequently an increase in cracking probability (Isaccson et al., 2003). In details, bitumen undergoes two different ageing phases: short- and long-term ageing. The former occurs during production, transport and paving, when bitumen is exposed to high temperatures, and is mainly linked to oxidation and evaporation leading to a doubling of the viscosity due to the increase in asphaltenes (from 1 to 4% in weight) (Groupe National Bitume, 1997). It is well simulated by means of Rolling Thin Film Oven Test (RTFOT) (ASTM D2872 - EN 12607) which "cooks" the bitumen in 1.25-mm thick moving films at 163 °C for 85 minutes. The latter occurs for a much longer period of time, since service life of the pavement can last several decades. It is most closely related to oxidation, physical hardening, polymerisation and photo-oxidation for surface layers and depends on several factors. Bitumen thickness and position inside the pavement, mix formulation and mix porosity together with local climate represent important parameters involved and making quite complicated to properly describe in-situ ageing. However, the Pressure Ageing Vessel (PAV) Test (ASTM D6521 - EN 14769) preceded by Rolling Thin Film Oven Test (RTFOT) (ASTM D2872 - EN 12607) represents a laboratory testing procedure widely used to reproduce satisfyingly the in-situ ageing of bitumen in surface courses for approximately 4 to 8 years in locations such as Wyoming and Florida (Anderson, 1994).

3.2.3 Ageing effects on bitumen chemistry

Ageing process causes a progressive change within bitumen chemical composition. In particular, it does not alter the molecules of saturates due to their poor reactivity neither those of the asphaltenes, since they are the most stable components of bitumen. On the contrary, the polar components are mostly subjected to oxidation (Rostler et al., 1970). In fact, oxidation converts the aromatics into resins that, in turn, generate asphaltenes (Read and Whiteoak, 2003; Wright, 1965; Moschopedis et al., 1978; Farcas, 1998), thus determining a reduction of the ratio maltenes/asphaltenes and a consequent increase in bitumen viscosity and stiffness. Another direct effect linked to chemical modifications caused by ageing phenomenon is a slight increase in the glass transition temperature.
In the Sixties, Corbett and Swarbrick (1960) observed an increase in asphaltene molecular weight after ageing, thus suggesting the existence of polymerisation reactions demonstrating that the asphaltenes produced during ageing process are different than the initial ones. This result was partially confirmed by Kats et al. (1976) who observed in one of the two bitumens investigated the conversion of asphaltenes into carbenes and carboids, due to a photo-oxidation. This latter is believed to generate polymerisation reactions, not only for asphaltenes (Kats et al., 1976), but also for lower fractions down to the saturates (Huang, 1997).
Ageing leads to the formation of sulfoxides, ketones and then carboxylic acids (Farcas, 1998; Petersen, 1993). Sulfoxides are rapidly formed, but are thermally unstable. Therefore, they reach a steady-state level that depends on both initial sulphur content and oxygen diffusion

within bitumen (Petersen, 1993). Ketones and carboxylic acids are more stable and do not reach an asymptotic value in laboratory ageing experiments (Petersen, 1993). The in-situ ageing seems to yield a steady-state level not only of sulfoxides, but also of carboxylic acids, after 2 years of service life in Southern France (Lamontagne et al., 2002). As a result, after ageing functional group content may rise up to more than 1 mol/l (Branthaver, 1994). Based on oxygen up-take, the ageing kinetics is initially linear and tends to slow down as the reaction proceeds (Wright, 1965; Petersen, 1993).

3.2.4 Ageing effects on bitumen rheology

Ageing has a great impact also on bitumen mechanical properties (e.g. hardening) and consequently its importance is quantified using rheological indicators, such as viscosity (Bell, 1989; Groupe National Bitume, 1997). The latter undergoes alterations more or less evident depending on ageing extent and bitumen structure. In fact, Traxler (1961) observed a linear increase in room temperature viscosity as a function of ageing time up to 15 h in thin film (3.2 mm) at 163 °C. The increments recorded varied between 5 and 20 times, depending on the bitumen origin. The more structured the bitumen ("gel type"), the higher the viscosity increase rate. On the contrary, for ageing time longer than 15 hours lower viscosity increments were detected, allowing the viscosity to be modelled over time by a hyperbolic interpolation line (Bell, 1989). In addition, Petersen (1993) demonstrated that at lower temperatures (around 60 °C) bitumens with high asphaltene content can easily aggregate, thus preventing oxygen from easily penetrating bitumen and, subsequently, ageing process to take place. On the contrary, at high temperatures (around 130 °C) the higher dispersion of the solid particles facilitates oxygen penetration within bitumen, thus determining a consequent higher degree of ageing (Figure 3.4 B). Whereas, bitumens with low amounts of asphaltenes show an ageing temperature-independent behaviour, since they always guarantee particle dispersion (Figure 3.4 A).
Other fundamental parameters used to assess ageing effects on bitumen are the norm of the complex modulus, $|G^*|$, and the phase angle, δ. In particular, Bahia and Anderson (1995) observed significant modification in the trends of $|G^*|$ and δ values of some bitumens subjected to oxidation in laboratory by applying different ageing durations and temperatures in comparison with unaged bitumens (Figure 3.5). In general, experimental test carried out within the typical frequency and temperature range of road applications pointed out an increment in the norm of the complex modulus and a reduction in the phase angle, as a general consequence of ageing.
The higher the $|G^*|$ values, the higher the stiffness and, hence, the lower the tendency to accumulate permanent deformations under traffic loading. However, besides the advantages in terms of rutting, a negative impact in terms of fatigue and thermal cracking could be induced. On the contrary, phase angle reduction allows different analysis to be drawn. In fact, the tangent of the phase angle represents the ratio between the dissipated modulus and the storage modulus at each loading cycle, corresponding to the viscous component and the

elastic component of the complex modulus, respectively. Hence, a decrease in such a parameter indicates a dissipated energy lower than the storage one and consequently a bitumen more resistant to fatigue and rutting, but more sensible to the effects induced by the thermal strains. In fact, the decrease in the dissipated strains leads to an increase in the tensile tension accumulated after each loading cycle (Bahia and Anderson, 1995).

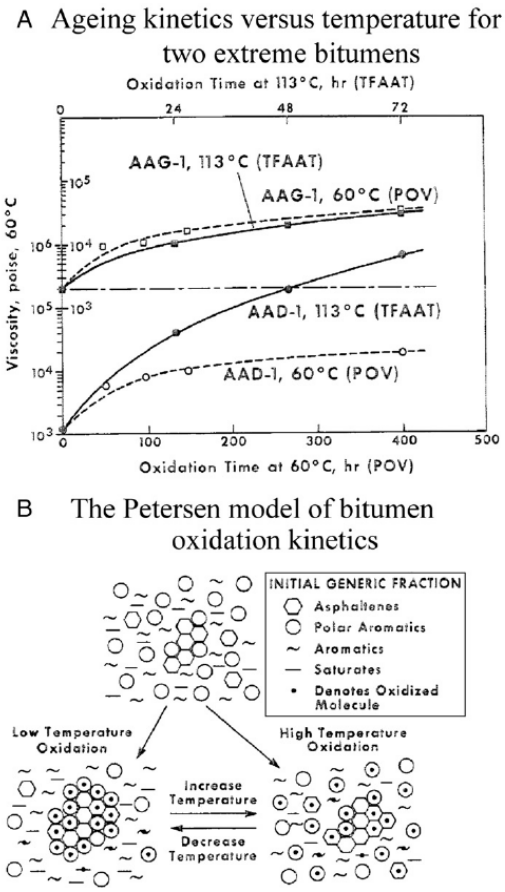

Figure 3.4. Ageing model of bitumen (Petersen, 1993).

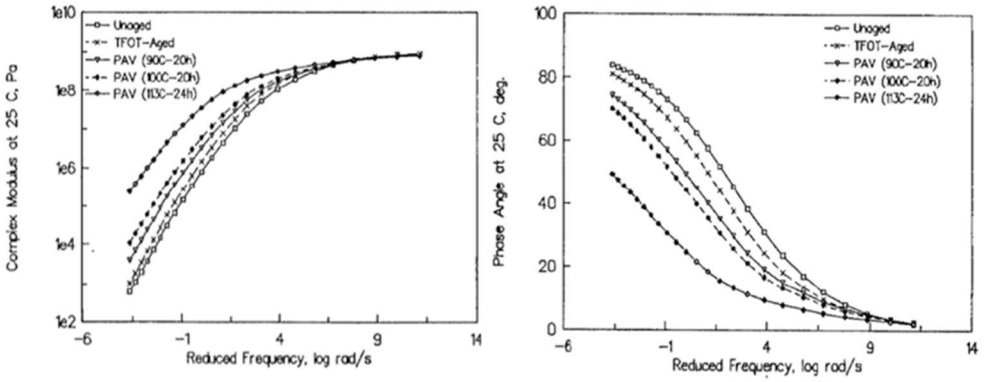

Figure 3.5. Ageing effect on the complex modulus and phase angle master curve (Bahia and Anderson, 1995).

3.2.5 Blending efficiency of RAP bitumen

Both industry and academia have a great interest in determining blending efficiency of bitumen reactivated from Reclaimed Asphalt Pavement (RAP) in new pavement mixtures as more and more RAP has been recycled in pavement construction to conserve natural resources.

It is well known that RAP bitumen is stiffer than a new, virgin bitumen, as a consequence of oxidation caused by thermal effects during mixing process and environmental effects during pavements life cycle. Moreover, it is generally expected that, when a certain RAP content is recycled into a new pavement mixture, RAP bitumen is completely blending with the new virgin bitumen. This is a critical assumption considering the long-term performance of the new pavement mixture. In fact, if RAP bitumen does not blend with the virgin bitumen, the pavement performance could be compromised. At higher percentages of RAP (>15%) the virgin bitumen grade is often decreased in order to account for the increased stiffness of the mixture due to RAP bitumen (Kandhal et al., 1997). This creates an even more complicated problem if the bitumens are not efficiently blending because there will potentially be pockets of stiff, RAP bitumen and virgin bitumen which is too soft for the climatic region. Thus, it is very important to establish blending efficiency and consequently to engineer the pavement to serve its entire expected life span. Many studies have been conducted to investigate the blending efficiency of RAP in bituminous mixtures. Soleymani et al. (2000) investigated this aspect by creating three very different mixes for comparison: case A, B and C, at 10% and 40% RAP content. Case A is the ‘‘black rock’’ scenario, meaning that RAP simply acts as an aggregate and consequently RAP bitumen is not reactivated at all. Case B is a ‘‘true’’ mixing scenario where the RAP is simply added to the mixture as it would be in typical mixing cases. Case C is the considered the ‘‘total blend’’ scenario because the recovered

RAP bitumen from Case A was blended mechanically with the virgin bitumen before adding it to the mixture. All the three mixtures were then tested using the Simple Shear Tester (SST). After testing over 64 cases, it was found that for 40% RAP content, 45% of the samples performed similar to the Case C, 100% blend. Only 5% of the mixtures performed close to the ‘‘black rock’’ scenario, and the remaining samples were somewhere in between in terms of performance. At 10% RAP content, little to no difference was detectable between Case A, B and C. Another study was conducted by McDaniel et al. (2012) that evaluated field mixtures with different RAP contents and similar gradations, and then defined their blending based on the ‘‘Bonaquist Approach’’. This approach takes into account the fully recovered bitumen from a mixture. In the case of a full recovery of a mixture, the bitumen is considered to be completely blended. The recovered bitumen was tested using the Dynamic Shear Rheometer (DSR) and the Bending Beam Rheometer (BBR). The Hirsch Model was applied to estimate the mix master curve. The mixtures were then tested and compared to the predicted master curve. If the master curves overlapped, the mixture was considered to be a total blend. Twenty mixtures were considered with RAP contents ranging between 0% and 40% and two different performance grade virgin bitumens. Three of the mixtures that included RAP were thought to exhibit poor blending, one had partial blending, and the remaining 16 mixtures were considered to be well blended. Mogawer et al. (2012) used a similar method to investigate the blending efficiency of plant produced mixtures. The Christensen-Anderson (CA) model was used to develop the mixture master curve. An important finding of this research is that the discharge temperature may have an impact on the relative degree of blending. Additional studies for blending efficiency assessment were conducted by Huang et al. (2005) and Bowers et al. (2014). In both studies a mixture was created with two different sized materials. A virgin bitumen was mixed with large virgin aggregate and a smaller RAP.

After mixing, the large and small aggregates were separated. The small (RAP) aggregate was then subjected to a ‘‘staged extraction’’ method where the aggregate was washed four times with solvent, removing ‘‘layers’’ of bitumen. In the study conducted by Huang et al. the bitumen was recovered and characterised using the DSR and Finite Element Analysis. Huang et al. found that a composite layer was formed between the virgin and RAP bitumens, but effectively a three layer system was formed with the innermost layer being stiffer. Bowers et al. (2014) also recovered the bitumen, but then tested it using the analytical chemistry techniques Gel Permeation Chromatography (GPC) and Fourier Transform Infrared Spectroscopy (FTIR). In the work of Bowers et al. it was determined that a partial blend occurred in all four layers, with the outermost layer being the softest and gradually stiffening when moving to the innermost layer.

Zhao et al. (2014) investigated the blending efficiency of Recycled Asphalt Shingles (RAS) using DSR and GPC. Three different sized aggregates were used in this study and separated after mixing. The fine particles were blended with the RAS before mixing with a medium and large aggregate. Mixing scenario’s varied in this research from different mixing time and temperature.

The researchers concluded that aggregate size and mixing temperature did not play a role in the blending efficiency of the RAS, but they did identify an effect of mixing time. It is also worth noting that the RAS never completely blended with the virgin bitumen. Navaro et al. (2012) studied the blending of RAP microscopically by using a virgin bitumen that is clear under white light, but has polymers that fluoresce under UV light. The researchers created mixtures at 110 °C, 130 °C, and 160 °C. The mixtures were then examined microscopically and the researchers determined that at higher mixing temperatures the RAP particles were less likely to cluster, implying that better blending occurs at higher temperatures. Shirodkar et al. (2011) conducted a study with large virgin aggregates and small RAP aggregates. Virgin aggregates were superheated and then RAP aggregates were added for 30 minutes before mixing. RAP was then mixed with virgin aggregates and put in oven for 2.5 h. The mass loss from RAP was then calculated and was considered to be the amount of bitumen that could mobilise. At the conclusion of the research, it was found that 70% blending occurs in a 25% RAP content with a PG 70-28. The researchers also found that up to 96% blending occurs when 35% RAP is blended with a PG 58-28 bitumen. Both these findings were based on the authors given gradation.

In the last decades, the use of Warm Mix Asphalt (WMA) is increasing, since it allows the production of bituminous mixtures at temperatures between 10 and 38 °C lower than traditional HMA temperatures and consequently economic and environmental benefits. The use of WMA additionally limits the susceptibility of bitumen to oxidation during the mixing process. Zhao et al. (2013) investigated the use of foamed bitumen and a surfactant based WMA product with high RAP contents ranging from 0% to 40% and compared the rutting resistance, fatigue resistance, and moisture susceptibility. Shu et al. (2012) investigated the impact of RAP in both HMA and WMA mixtures and found that RAP is beneficial for resistance to moisture damage. Further work studying the combination of WMA and RAP by Zhao et al. (2012) found that foamed WMA actually had better resistance to rutting, moisture damage and fatigue performance when compared to HMA equivalents. There are obviously economic and environmental benefits to the use of RAP and WMA together; however, the question still remains on how the use of WMA may affect the blending efficiency of RAP considering the lower mixing temperatures.

3.3 Effect of rejuvenators on the bituminous phase of bituminous mixtures

According to literature, the use of vegetable-based rejuvenators represents a good option, if the asphaltene content is sufficient (Simonen et al., 2012) and for in-place or in-plant cold mix recycling, since they can properly reactivate the aged bitumen wihin RAP (Hugener et al., 2014). Zaumanis et al. (2014) compared the influence of six rejuvenators on the properties of aged bitumen. The results obtained in their study showed the potential of waste vegetable (WV) oil to rejuvenate aged bitumen by reducing the performance grade and fatigue parameters to a higher degree as compared to other rejuvenators. However, it was noted that

using adhesion promoting additive might be necessary to contend with the high moisture susceptibility caused by using WV oil. The effects on the performance and microstructure of aged bitumen when using light weight oil, with high aromatic content (common rejuvenator), and composite oil, which is the blend of lightweight oil and chemical compounds containing polar groups, were investigated. The conclusive results of this study demonstrated that composite rejuvenator could be used for rejuvenating severely aged bitumen by more effectively restoring the colloidal structure of aged bitumen through the composition regulation and chemical reaction between asphaltenes and composite rejuvenator. The common rejuvenator could restore bitumen rheological properties; however, its effect was much lower than that of the composite rejuvenator (Kuang et al., 2014). Effects of using rejuvenators and softer bitumen in bituminous mixtures containing different percentages of RAP were investigated in another study. The moisture susceptibility test was performed using indirect tensile strength ratio. An asphalt pavement analyser was also used to evaluate rutting properties of mixtures. The results of this study indicated that mixtures fabricated with rejuvenators had higher strength values and the lowest rut depth compared to mixtures produced using softer bitumen. Tensile strength ratio results for these mixtures were slightly different than those of fabricated with softer bitumen (Shen et al., 2007a). Shen et al. (2007b) conducted a study to evaluate the effects of using a soft bitumen with low asphaltene content (2 wt%) as a rejuvenator and with different percentages on aged bitumen and mixture properties. The results achieved in this study demonstrated that rutting resistance parameter ($|G^*|/\sin\delta$) of aged bitumen decreased linearly as the rejuvenator percentage increased. The linear trend was observed for the fatigue parameter, $|G^*|\sin\delta$, that diminished with the incremental increase in rejuvenator content, thus providing a better fatigue resistance. Moreover, results in terms of Dynamic Stability (DS) of mixtures showed a considerable decrease in DS values in the case of rejuvenated mixture compared to the control mixture (mixture without rejuvenator). In particular, the lower the DS value, the lower the mixture performance at high temperature which could be of concern for the rejuvenated mixture. However, according to Thermal Stress Restrained Specimen Test (TSRST) result, the rejuvenated mixture performed better at low temperature when the fracture temperature decreased from 22.0 to 29.5 °C and fracture strength increased by 0.5 MPa by adding a higher rejuvenator content from 0% to 7.4% (Shen et al., 2007a). The effects of using three rejuvenators have been evaluated on the properties of bitumen and mixtures containing high RAP content. These rejuvenators are BituTech RAP, SonneWarmix RJT and SonneWarmix RJ. As authors mentioned, bitumen non-recoverable creep compliance was enhanced by the addition of rejuvenators. Fatigue properties of the rejuvenated bitumen improved, as suggested by Linear Amplitude Sweep (LAS) test results in comparison with virgin bitumen. A decrease in mixture air voids was detected thanks to the presence of rejuvenators and their diffusing effect in hard bitumen. Additionally, using rejuvenator could mitigate mixture cracking properties, whereas rutting and moisture susceptibility were adversely affected (Mogaver et al., 2013). In 2014, a comprehensive study was carried out by Zaumanis et al. to evaluate the use of different recycling agents on the properties of rejuvenated bitumens

and mixtures. Effects of six recycling agents were investigated with similar dosages (12%). Waste vegetable oil (WV oil), waste vegetable grease (WV grease), organic oil, distilled tall oil, aromatic extract and waste engine oil (WEO) were designated in this study. The properties of the agents are listed in Table 3.3.

Table 3.3. Recycling agent properties and description (Zaumanis et al., 2015).

RECYCLING AGENT	SPECIFIC GRAVITY	MOLECULAR STRUCTURE	POLARITY
WV OIL	0.924	Ring and strand	Non[(a)]
WV GREASE	0.924	Ring and strand	Mild
ORGANIC OIL	0.947	Ring and strand	Very[(b)]
DISTILLED TALL OIL	0.950	Ring and strand	Mild
WASTE ENGINE OIL	0.872	Aliphatic	Slight
AROMATIC EXTRACT	0.995	Aromatic ring	Very
VIRGIN BINDER	1.020	Ring and strand	Mixed[(c)]

[(a)] Products with very few if any polar compounds.
[(b)] Products with high percentage of polar compounds.
[(c)] reference to the mixture of oil fractions with different degrees of polarity comprising bitumen.

Results of this study revealed that at an intermediate temperature (25 °C) all agents could reduce bitumen viscosity to the level of virgin bitumen; however, bitumen viscosity was higher than that of virgin bitumen at higher temperature. Lower dosages of organic oils were required in comparison to the petroleum additives in order to provide similar softening effects. The application of 12% recycling agents improved workability of RAP bitumen, without reaching workability of the virgin bitumen. In details, the addition of organic agents led to an improvement in fatigue performance of aged bitumen, as suggested by LAS test results. The best effect was detected when vegetable oil products were added that guaranteed a comparable fatigue performance with virgin bitumen, whereas the petroleum products did not affect aged bitumen performance in terms of fatigue. Among all the agents selected, using 12% of organic oil determined the best overall performance, followed by WV grease and distilled tall oil. Conversely, WEO was considered as the worst agent. However, Zaumanis et al. (2015) suggested the quantification of the optimum dosage, according to each rejuvenator selected, as a fundamental task for future works. Using similar recycling agents, a complementary study was carried out on recycled mixtures. Results obtained and compared to virgin mixture showed positive rutting and fatigue resistance for recycled mixtures with the exception of the WEO-rejuvenated mixture. The workability of the mixtures was improved through the application of recycling agents, though in some cases using antistripping additive was deemed to be necessary (Zaumanis et al., 2014) . It is worth noting that polar aromatic ring structure is carcinogenic and therefore using polar aromatic oils, such as aromatic extract, in bitumen rejuvenation is being limited (Zaumanis et al., 2013). Another comparative study was performed using three rejuvenated bitumens. A rejuvenator, waste cooking oil and cotton seed oil were used with different percentages (0%, 5% and 10% by

rejuvenated bitumen weight). Results of this study showed a reduction in rutting resistance factors for rejuvenated bitumens, $|G^*|/\sin\delta$, due to the presence of rejuvenator. In general, the bitumens blended with rejuvenator performed better than the bitumens containing waste cooking oil or cotton seed oil, in terms of elastic recovery and resistance to flow deformation. Chen et al. (2014) assessed 5% of waste cooking oil and cotton seed oil as the optimum dosage to produce a bitumen exhibiting a superior PG equal to 64. Effects of nine rejuvenators were examined on bitumen and mixture properties, when RAP contents were involved. The rejuvenators were distilled tall oil, WEO, WEO bottoms, WEO + FT wax, naphthenic flux oil, aromatic extract, paraffinic base oil, refined tallow and organic blend. Among these, the refined tallow resulted to be the most effective agent at lowering the viscosity of aged bitumen, whereas the presence of WEO bottoms determined a considerably higher viscosity value as a likely consequence of higher mixing and compaction temperatures. Indirect tensile creep compliance and strength tests were performed to evaluate mixture performance at lower temperatures. In most cases, results obtained showed an improvement in low temperature properties of a mixture by adding rejuvenator (Zaumanis et al., 2013). Im et al. (2014) investigated impact of three commercial rejuvenators (R1, R2 and R3) on performance and engineering properties of HMA mixtures containing 19% RAP. In this study, rejuvenators R1 and R2 were directly added to virgin bitumen, whereas R3 was blended with recycled materials. Results achieved showed an improvement in terms of cracking, deformation and moisture susceptibility of mixtures containing a rejuvenator. Waste cooking oil was used in different percentages (1÷5% by bitumen weight) as a potential rejuvenator for aged bitumen. Physical properties of aged and rejuvenated bitumens were then evaluated by performing penetration, softening point and viscosity tests. As a result, it was concluded that for rejuvenated aged-bitumen group of 40/50, aged bitumen containing 3–4% of WCO could approximate the physical properties of virgin 80/100 bitumen (Asli et al., 2012). Additionally, the chemical analysis showed a decrease in Asphaltenes/Maltenes ratio for WCO-rejuvenated bitumen compared to the aged bitumen (Zargar et al., 2012). Aromatic oil (AO), vegetable oil (VO) and soft bitumen (SB) (160/220 penetration grade) were used as rejuvenating agents for RAP and added in percentage equal to 40% by total bitumen weight. All the bitumens were subjected to a laboratory ageing by means of Rolling Thin Film Oven Test (RTFOT) and Pressure Ageing Vessel (PAV) procedures. Results in terms of fatigue showed a better response for rejuvenated bitumen than for pure bitumen (Dony et al., 2013). Another study evaluated the effects of emulsion, maltene and vegetable-oil based rejuvenators on physical and rheological properties of three bitumens coded as AAA-1, AAD-1 and AAM-1. The result of this study showed that the flow property of highly aged bitumen was improved similarly for both vegetable-oil based and maltene based rejuvenators. A faster enhancement in fatigue resistance of bitumen type AAD-1 was detected using vegetable-oil based rejuvenator rather than the other rejuvenator types; however, comparing bitumen type AAM-1 to the other two types, the presence of emulsion based rejuvenator guaranteed a faster improvement in fatigue resistance of highly oxidised bitumen. In addition, aged bitumens containing vegetable-oil based rejuvenator exhibited the

best thermal behaviour (Huang et al., 2015). In another study, composite castor oil (30% coke oven gas condensate and 70% castor oil) and pongamia oil were selected thanks to their ability to increase maltene fraction and dissolve asphaltenes in rejuvenated bitumen, thus allowing the recovery of laboratory aged bitumen properties. Overall, three dosages (5%, 10% and 15%) of rejuvenators were used and thermal and rheological properties of the bitumens were investigated. The results revealed a similar rutting resistance for bitumens containing 10% of rejuvenator and virgin bitumen. Moreover, the bitumen rejuvenated by pongamia oil showed the best fatigue response, even if fatigue life of all the rejuvenated bitumens was quantified to be longer than that of the virgin bitumen, whatever the rejuvenator dosage considered. Overall, 5% of both oil types was found to be the optimum value to reach the desired fatigue and rutting performance (Nayak et al., 2015). Recently, effects of using paraffinic oil, aromatic oil and organic blend rejuvenators with 9% dosage by bitumen weight were investigated on mixtures including 50% RAP. The flexural beam fatigue test results revealed that all types of rejuvenators improved fatigue resistance of bituminous mixtures even more than the control mixtures fabricated to PG 58-28 and PG 64-28 specifications. Mixtures rejuvenated by paraffinic oil displayed the highest fatigue life among the mixtures. However, it should be highlighted that fatigue improvement in rejuvenated mixtures is generally a consequence of lower strength and stiffness, and higher creep rate (Mogawer et al., 2015).

Chapter 4.

Rheological investigation of bitumens: background

4.1 Viscoelastic properties

Bitumen is a viscoelastic and time-temperature dependent material. Therefore, its properties modify according to temperature and loading frequency applied. For a proper characterisation, fundamental parameters mainly related to the material rheological behaviour should be introduced. In particular, the main parameters depend on the stiffness properties of the material that are in turn associated with the viscous and elastic behaviour of bitumens. Thus, the norm of the complex shear modulus |G*| and the phase angle δ are often used to identify the material behaviour. |G*| is a measure of the total resistance of a material to deforming when repeatedly sheared. It consists of two components: an elastic recoverable component and a viscous unrecoverable component. The phase angle δ is an indicator of the relative amounts of recoverable and unrecoverable deformation (Figure 4.1).

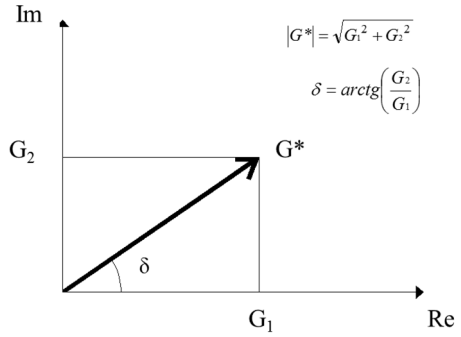

Figure 4.1. Complex modulus and phase angle representation.

The Strategic Highway Research Program (SHRP) developed detailed specifications, providing bitumen classification based on its performance measured through different rheological tests (Performance Grade). In particular, the Dynamic Shear Rheometer (DSR) is a reliable device used to determine rheological properties and thus identify the viscous and elastic behaviour of bituminous materials over a wide range of conditions. In particular, it

allows the application of oscillatory or continuous shear sinusoidal loading stress or strain, characterised by a given amplitude and frequency.
In details, the sinusoidal loads should simulate the effect induced by the intermittent passage of traffic in road pavement. The different vehicles speed can be reproduced by adopting different loading frequencies. Usually, the frequency is set equal to 1.59 Hz (i.e. 10 rad/s), since this value corresponds to a loading time of 0.1 s that represents a reference value in laboratory for all the tests aimed at simulating the effects caused by traffic on pavements (Christensen and Anderson, 1992). Therefore, in order to define a parameter that can allow the comparison between different types of bitumen, it must be always taken into account that external loads applied to a pavement are not static forces, but dynamic forces, schematically assumed as sinusoidal and periodic for laboratory purposes.
The main geometric configuration used by the DSR is the plate-plate configuration. The bitumen sample is sandwiched between two metal parallel plates. The bottom is fixed, whereas the upper can rotate and is able to apply sinusoidal loading waves described as follows:

$$\tau = \tau_0 \cdot sen(\omega t) \tag{4.1}$$

where τ is the shear stress, τ_0 is the amplitude of the stress, ω is the angular frequency and t is the time.

As a consequence of this loading action, the material reacts with a response that is sinusoidal itself and characterised by the same frequency of loading wave, but with a time lag equal to δ:

$$\gamma = \gamma_0 \cdot \mathrm{sen}(\omega t - \delta) \tag{4.2}$$

In this way, it is possible to characterise the material behaviour through its stiffness properties. In particular, the complex shear modulus G* can be determined in accordance with the following relationship:

$$G^*(\omega) = \frac{\tau^*(t)}{\gamma^*(t)} \tag{4.3}$$

where $\tau^*(t) = \tau_0 \cdot [\cos(\omega t) + i \cdot \sin(\omega t)]$

$\gamma^*(t) = \gamma_0 \cdot [\cos(\omega t - \delta) + i \cdot \sin(\omega t - \delta)]$

By substituting these expressions (periodic sinusoidal loads) into the previous equation, the following form can be obtained:

$$G^*(\omega) = \frac{\tau_0}{\gamma_0} e^{i\delta} \tag{4.4}$$

This equation represents a complex number with an absolute value equal to the ratio between the maximum amplitude of the stress applied and the maximum amplitude of the

corresponding strain. The vector direction is rotated respect to the horizontal axis of a quantity equal to the phase angle δ (Figure 4.1). Based on what introduced so far, it is worth noting that the complex modulus G* is independent on the loading time, but is function of temperature, frequency and stress/strain level (if the linear viscoelastic limit of the material is exceeded).

As previously mentioned, the complex modulus can be divided in two components:

- $G_1 = |G^*| \cdot \cos(\delta) =$ *storage modulus*, used as indicator of the elastic behaviour of the material;
- $G_2 = |G^*| \cdot \text{sen}(\delta) =$ *loss modulus*, used as indicator of the dissipated energy when a load is applied to the material and, hence, represents the viscous component of the material behaviour.

Therefore, the phase angle δ concurs to identify material behaviour: when the phase angle tends to 0 °, bitumen mainly behaves as an elastic material, whereas phase angle values close to 90 ° denotes a mainly viscous behaviour. These two components, storage and loss modulus, are used especially to characterise material behaviour at high and intermediate temperatures to directly address two main pavement distress modes: rutting caused by permanent deformation of the paving mix and fatigue cracking related to energy absorbed during repeated loading applications to the pavement. The first one occurs at high temperature, whereas fatigue is more likely at low-intermediate temperature. In particular, rutting resistance is mainly associated with creep behaviour of a viscoelastic material such as bitumen. While a constant load is applied, the material creeps. The initial response is elastic, but it tends to becomes viscous after a certain time of loading application. The stress is proportional to the load applied and the strain is the deformation response. The creep compliance in shear (J(t), reciprocal of the shear modulus G*) can be calculated as the ratio between strain and stress. After removing the load, the material relaxes, but only part of the strain accumulated is recovered. The reciprocal of the creep compliance (express in terms of shear modulus as |G*|/sinδ, rutting resistance parameter in the Superpave specification) can be assumed as a measure of the permanent strain resulting after the application of a unit stress, which simulates the effect of a single wheel load to the development of rutting on a flexible pavement. With respect to the fatigue resistance, bitumen stiffness represents an important parameter in determining the level of stress at the bottom of the bound layers where the crack initiates. When one deals with thick pavements, a stiff mixture is preferable, since it limits the stress at the bottom by distributing it over a wider area. On the contrary, thin pavements should require low stiff mixtures in order to limit the stress caused by large deflection of the subgrade. In particular, the fatigue phenomenon is mainly linked to energy dissipation. Therefore, the fatigue parameter introduced by Superpave specification to control the fatigue damage is |G*|·sinδ, which directly measures the energy dissipation during cyclic loading.
Finally, it can be stated that the complex modulus G* (and hence |G*| and the phase angle δ) provides fundamental information in the performance analysis of a bitumen. However, as

often mentioned, their value depends on the temperature, the loading frequency and the stress/strain applied. Anyway, it is possible to eliminate the stress/strain dependency by verifying that the loads applied (stress or strain) is lower than a limit value, referred as Linear Viscoelastic limit (LVE). Below this value, the material behaviour is independent on the loading magnitude. Such a value can be experimentally determined by applying several stress/strain values at a given temperature and frequency. Then, the stress/strain value corresponding to a reduction of the initial complex modulus |G*| equal to 5% is calculated and constitutes the LVE threshold. This type of test is usually named as strain sweep test.

Chapter 5.

Rheological experimental investigation

5.1 Materials

5.1.1 Bitumens

The binders selected were both 50/70 pen bitumens, but manufactured through different technologies. In details, the first bitumen selected was obtained as the residue from a visbreaking process and coded as VB. Visbreaking (i.e. viscosity breaking) is a relatively mild thermal cracking process operated at 455÷510 °C and 0.3÷2 MPa (i.e. 3÷20 bars) for a short residence time (1÷3 min), which allows to reduce the viscosity of residua without attempting coke formation and significant conversion to distillates (Mazzoni et al., 2017a). The main limitation of the visbreaking process is that the products can be unstable. In fact, thermal cracking at low pressure gives olefins that, in turn, produce a very unstable material tending to undergo secondary reactions (oxidation) to form intractable residua (Speight, 1999). The second bitumen selected was obtained as the vacuum residue from a typical distillation process and coded as PB.
The basic properties of the bitumens used in this study are summarised in Table 5.1.

Table 5.1. Basic properties of the bitumens selected.

	Code	Penetration at T = 25 °C [dmm]	Softening point [°C]
Visbreaking Bitumen	**VB**	62	46-54
Primary Bitumen	**PB**	63	44-52

5.1.2 Rejuvenators

In the present research, three commercial rejuvenators, commonly used for hot recycling, have been chosen. The first (Rejuvenator type A) is a miscible crude tall oil derived from the processing of pine wood in paper industry and contains fatty acids, resin acids and unsaponifiables. The second (Rejuvenator type B) is a mix of different chemicals and consists of modified polyamines and vegetal oils. The third (Rejuvenator type C) is an organic refined additive consisting of alkylates and fatty acids (Mazzoni et al., 2017a). The physical characteristics of the three rejuvenators are shown in Table 5.2.

Table 5.2. Basic properties of the rejuvenators (Mazzoni et al., 2017a).

Rejuvenator	Density at T = 20 °C [g/cm^3]	Kinematic viscosity at T = 20 °C [mm^2/s]
A	0.93	98
B	0.80	45
C	0.88	47

5.2 Bituminous blends preparation

Starting from each one of the two bitumens and the three rejuvenators above-mentioned, fifteen bituminous blends were artificially manufactured in laboratory to simulate the overall service life of each bitumen selected (i.e. ageing of a bitumen within a new Hot Mix Asphalt (HMA), rejuvenation of bituminous blends within a new HMA containing a high RAP content by means of three different additives and ageing of rejuvenated bitumens).
The first service life of each bitumen selected was simulated by subjecting it to a short- and long-term ageing, by means of Rolling Thin Film Oven Test (RTFOT) and Pressure Ageing Vessel (PAV) testing procedures, in accordance with European Standards EN 12607-1 and EN 14769, as summarised in a following paragraph (§5.3.1). It should be highlighted that the same aged bitumen obtained with the procedure above-mentioned was also used to reproduce the RAP bitumen. Hot recycling was simulated by blending 50% of the virgin bitumen, 50% of RAP bitumen and, in case, one of the three additives selected. The dosage of each additive complied with manufacturer instructions and previous experimental results as well (6% by RAP bitumen weight for both additives A and B and 3% by total bitumen weight for additive C).
A total of thirty bituminous blends was investigated in this study as summarised in Table 5.3.

Table 5.3. Bituminous blends investigated.

a) First step of testing

Bituminous blend		Bituminous sample preparation
Code	**Name**	
VB	Visbreaking virgin bitumen	The first reference bitumen selected
$STAG_{VB}$	Short-term aged bitumen	Visbreaking virgin bitumen subjected to a short-term ageing by means of RTFOT
$LTAG_{VB}$	Long-term aged bitumen/RAP bitumen	Visbreaking virgin bitumen subjected to a long-term ageing by means of RTFOT + PAV and simulating bitumen reactivated from RAP
$LTAG_{VB}$+VB	Unrejuvenated bitumen	RAP bitumen blended with virgin bitumen in proportion 50/50
$LTAG_{VB}$+VB+A	Rejuvenated bitumen type A	RAP bitumen blended with 6% of rejuvenator A and virgin bitumen in proportion 50/50
$LTAG_{VB}$+VB+B	Rejuvenated bitumen type B	RAP bitumen blended with 6% of rejuvenator B and virgin bitumen in proportion 50/50
$LTAG_{VB}$+VB+C	Rejuvenated bitumen type C	RAP bitumen blended with virgin bitumen in proportion 50/50 and 3% of rejuvenator C
$LTAG_{VB}$+VB_STAG	Short-term aged unrejuvenated bitumen	Unrejuvenated bitumen subjected to a short-term ageing by means of RTFOT
$LTAG_{VB}$+VB+A_STAG	Short-term aged rejuvenated bitumen type A	Rejuvenated bitumen type A subjected to a short-term ageing by means of RTFOT
$LTAG_{VB}$+VB+B_STAG	Short-term aged rejuvenated bitumen type B	Rejuvenated bitumen type B subjected to a short-term ageing by means of RTFOT
$LTAG_{VB}$+VB+C_STAG	Short-term aged rejuvenated bitumen type C	Rejuvenated bitumen type C subjected to a short-term ageing by means of RTFOT
$LTAG_{VB}$+VB_LTAG	Long-term aged unrejuvenated bitumen	Unrejuvenated bitumen subjected to a long-term ageing by means of RTFOT + PAV
$LTAG_{VB}$+VB+A_LTAG	Long-term aged rejuvenated bitumen type A	Rejuvenated bitumen type A subjected to a long-term ageing by means of RTFOT + PAV
$LTAG_{VB}$+VB+B_LTAG	Long-term aged rejuvenated bitumen type B	Rejuvenated bitumen type B subjected to a long-term ageing by means of RTFOT + PAV
$LTAG_{VB}$+VB+C_LTAG	Long-term aged rejuvenated bitumen type C	Rejuvenated bitumen type C subjected to a long-term ageing by means of RTFOT + PAV

b) Second step of testing

Bituminous blend		Bituminous sample preparation
Code	**Name**	
PB	Primary virgin bitumen	The second reference bitumen selected
$STAG_{PB}$	Short-term aged bitumen	Primary virgin bitumen subjected to a short-term ageing by means of RTFOT
$LTAG_{PB}$	Long-term aged bitumen/RAP bitumen	Primary virgin bitumen subjected to a long-term ageing by means of RTFOT + PAV and simulating bitumen reactivated from RAP
$LTAG_{PB}$+PB	Unrejuvenated bitumen	RAP bitumen blended with virgin bitumen in proportion 50/50
$LTAG_{PB}$+PB+A	Rejuvenated bitumen type A	RAP bitumen blended with 6% of rejuvenator A and virgin bitumen in proportion 50/50
$LTAG_{PB}$+PB+B	Rejuvenated bitumen type B	RAP bitumen blended with 6% of rejuvenator B and virgin bitumen in proportion 50/50
$LTAG_{PB}$+PB+C	Rejuvenated bitumen type C	RAP bitumen blended with virgin bitumen in proportion 50/50 and 3% of rejuvenator C
$LTAG_{PB}$+PB_STAG	Short-term aged unrejuvenated bitumen	Unrejuvenated bitumen subjected to a short-term ageing by means of RTFOT
$LTAG_{PB}$+PB+A_STAG	Short-term aged rejuvenated bitumen type A	Rejuvenated bitumen type A subjected to a short-term ageing by means of RTFOT
$LTAG_{PB}$+PB+B_STAG	Short-term aged rejuvenated bitumen type B	Rejuvenated bitumen type B subjected to a short-term ageing by means of RTFOT
$LTAG_{PB}$+PB+C_STAG	Short-term aged rejuvenated bitumen type C	Rejuvenated bitumen type C subjected to a short-term ageing by means of RTFOT
$LTAG_{PB}$+PB_LTAG	Long-term aged unrejuvenated bitumen	Unrejuvenated bitumen subjected to a long-term ageing by means of RTFOT + PAV
$LTAG_{PB}$+PB+A_LTAG	Long-term aged rejuvenated bitumen type A	Rejuvenated bitumen type A subjected to a long-term ageing by means of RTFOT + PAV
$LTAG_{PB}$+PB+B_LTAG	Long-term aged rejuvenated bitumen type B	Rejuvenated bitumen type B subjected to a long-term ageing by means of RTFOT + PAV
$LTAG_{PB}$+PB+C_LTAG	Long-term aged rejuvenated bitumen type C	Rejuvenated bitumen type C subjected to a long-term ageing by means of RTFOT + PAV

5.3 Test program

5.3.1 Rheological investigation

As bitumen is a viscoelastic material, it exhibits both elastic and viscous components of response and its stress-strain relationship is both temperature- and time- dependent. Bitumen rheology is consequently defined by its strain-stress-time-temperature response. However, within the linear viscoelastic (LVE) region, the interrelation between strain and stress is influenced by temperature and time alone and not by the strain magnitude (Van der Poel, 1954). Based on the above-mentioned bitumen properties, a rheological characterisation of each bitumen selected was carried out running tests, under different conditions, that allowed two main parameters to be determined: the LVE strain limit (γ_{lim}) and the complex modulus (G*). To this aim, both strain and frequency sweep tests were performed by means of a Dynamic Shear Rheometer (DSR). The tests were set up in plate-plate configuration (diameter of 8 mm and gap of 2 mm for low and intermediate temperatures; diameter of 25 mm and gap of 1 mm for high temperatures) and the sinusoidal load was applied in control-strain mode.
More details of each test are provided in the following section together with the corresponding experimental procedures. Table 5.4 shows a summary of the overall experimental plan in terms of number of replicates for each test implemented.

Table 5.4. Experimental program.

Bituminous blend	Number of replicates for each test condition		
	Strain sweep	Frequency sweep	
	PP08	PP08	PP25
VB	-	2	2
STAG$_{VB}$	-	2	2
LTAG$_{VB}$	-	2	2
LTAG$_{VB}$+VB	-	2	2
LTAG$_{VB}$+VB+A	-	2	2
LTAG$_{VB}$+VB+B	-	2	2
LTAG$_{VB}$+VB+C	-	2	2
LTAG$_{VB}$+VB_STAG	-	2	2
LTAG$_{VB}$+VB+A_STAG	-	2	2
LTAG$_{VB}$+VB+B_STAG	-	2	2
LTAG$_{VB}$+VB+C_STAG	-	2	2
LTAG$_{VB}$+VB_LTAG	2	2	2
LTAG$_{VB}$+VB+A_LTAG	-	2	2
LTAG$_{VB}$+VB+B_LTAG	-	2	2
LTAG$_{VB}$+VB+C_LTAG	-	2	2
PB	-	2	2
STAG$_{PB}$	-	2	2
LTAG$_{PB}$	-	2	2
LTAG$_{PB}$+PB	-	2	2
LTAG$_{PB}$+PB+A	-	2	2
LTAG$_{PB}$+PB+B	-	2	2
LTAG$_{PB}$+PB+C	-	2	2
LTAG$_{PB}$+PB_STAG	-	2	2
LTAG$_{PB}$+PB+A_STAG	-	2	2
LTAG$_{PB}$+PB+B_STAG	-	2	2
LTAG$_{PB}$+PB+C_STAG	-	2	2
LTAG$_{PB}$+PB_LTAG	2	2	2
LTAG$_{PB}$+PB+A_LTAG	-	2	2
LTAG$_{PB}$+PB+B_LTAG	-	2	2
LTAG$_{PB}$+PB+C_LTAG	-	2	2
TOTAL	**4**	**60**	**60**

5.4 Laboratory equipments, test methods and data analysis

In the following paragraphs, the equipments used in laboratory and their main operation principles are first described. Subsequently, the test protocols and the basic theory behind the

analysis methods applied to elaborate the test data are discussed for a better understanding of the results obtained through the laboratory investigation.

5.4.1 Ageing procedures

Short-term ageing

As mentioned in a previous paragraph (§ 3.2.2), short-term ageing occurs during production, transport and paving, when bitumen is exposed to high temperatures, and is mainly linked to oxidation and evaporation. In this study, it was simulated by means of the Rolling Thin Film Oven Test (RTFOT) (Figure 5.1), in accordance with the European standard EN 12607-1.
The RTFOT procedure requires an electrical heated convection oven at 163 °C that contains a vertical circular carriage to accommodate eight sample bottles covered by a film of bitumen for 85 minutes. The oven is also equipped with an air jet that blows air in each bottle while the carriage circulates.
Thanks to this test procedure, a short-term aged bitumen can be easily and quickly obtained and thus used for further testing.

Figure 5.1. RTFOT equipments.

Long-term ageing

As previously mentioned (§ 3.2.2), long-term ageing occurs during the whole service life of an asphalt pavement and is most closely related to oxidation, physical hardening, polymerisation and photo-oxidation for surface layers. In this study, it was simulated by means of the Pressure Ageing Vessel (PAV) used in combination with RTFOT and in agreement with the European standard EN 14769. The equipment consists of a vessel including a cylindrical chamber with a top lid secured through a shear ring assembly composed of an aluminum lock ring and bronze shear ring segments. The chamber can accommodate ten sample pans placed in a sample rack (Figure 5.2). The combined action of temperature and pressure should be able to reproduce in only 20 hours the same effects

caused by the climate agents on the pavements over a service period from 5 to 10 years. In particular, in this study, the test is conducted at 100 °C and 2.1 MPa.

Figure 5.2. PAV equipments.

5.4.2 Viscoelastic properties

Dynamic Shear Rheometer (DSR)

The Dynamic Shear Rheometer is an instrument that allows the concurrent evaluation of time and temperature effects on bitumen samples (see § 4.1 for the theoretical background). In this research study, all the bituminous blends investigated were rheologically characterised by means of an Anton Paar Modular Compactor Rheometer (MCR 302) (Figure 5.3). In particular, the DSR measures the rheological properties (e.g. norm of the complex shear modulus and phase angle) in a wide range of temperatures and loading conditions. Oscillatory or rotational tests can be performed in control strain or control stress mode and in plate-plate or cone-plate configuration depending on the type of measurements required.

For the purposes of this study, only oscillatory tests in plate-plate configuration and control strain mode were carried out. Bituminous blend samples were prepared following the procedure summarised in the next section and, when testing, sandwiched between a fixed

plate and a moving plate that oscillates back and forth. The distance between the two plates is maintained constant and is referred as gap. The dimension of the plates to be used varies depending on the bitumen stiffness measured and the temperature selected. In this study plates with a diameter of 8 (PP08) and 25 mm (PP25) and a corresponding gap of 2 and 1 mm, respectively, were used.

Figure 5.3. Anton Paar Modular Compactor Rheometer MCR 302.

Specimens preparation

Bitumen specimens are little disks of bitumen with a diameter equal to the oscillating plates and a height equal to the gap. They are prepared by heating bitumen until fluid enough to pour into a rubber mould of appropriate dimensions (slightly larger and higher than the space and the gap, respectively, between the parallel plates). Heating temperature may vary depending on bitumen consistency (stiffness). Afterwards, each disk must be stored at room temperature for a minimum of 2 hours (or 12 hours for modified bitumens) and a maximum of 3 days, according to UNI EN 14770. Then, after removal from the mould, the specimen to be tested is placed between DSR plates (Figure 5.4÷5.6). Before running the test, trimming of the edge specimen through a spatulas is needed in order to remove the bitumen in excess and obtain a specimen with the dimensions required.

Test configuration, loading steps and equipment setting can be controlled through the software associated to the instrument. In particular, all the tests carried out with the DSR provide two fundamental steps:

- a conditioning phase at the test temperature to allow the specimen to reach the desired temperature homogeneously (i.e. thermal equilibrium). In this step, no loads are applied;
- a loading phase where the different loading conditions are applied, depending on the specific test performed.

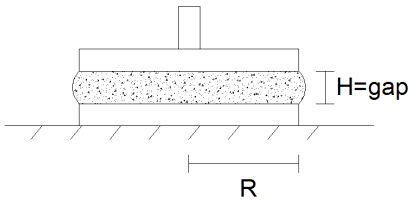

Figure 5.4. Schematic representation of the plate-plate configuration.

Figure 5.5. DSR plate-plate configuration: 8 mm (left) and 25 mm (right).

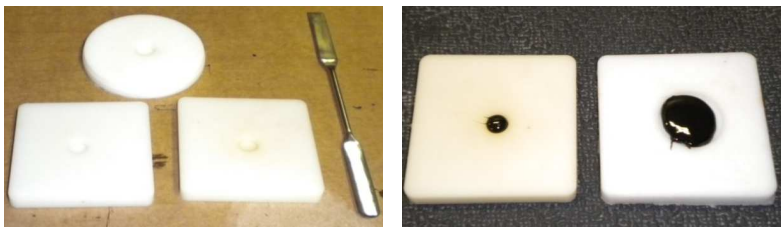

Figure 5.6. Rubber moulds with trimming spatulas (left) and bitumen samples (right).

5.4.3 Data analysis

Strain sweep test

Strain sweep tests were performed in order to determine the LVE region of the bitumens, i.e. where the norm of the complex modulus |G*| is not influenced by the strain magnitude. In particular, bitumen response was studied at a constant frequency (f = 1.59 Hz) by applying a range of strains (γ = 0.003-3%) for each temperature selected (T = 4, 16 and 28 °C) in order to monitor |G*| and thus determine the threshold of LVE region, γ_{lim} (defined as the strain corresponding to a |G*| deviation equal to 5% referred to its initial value $|G^*_{in}|$) (Figure 5.7).

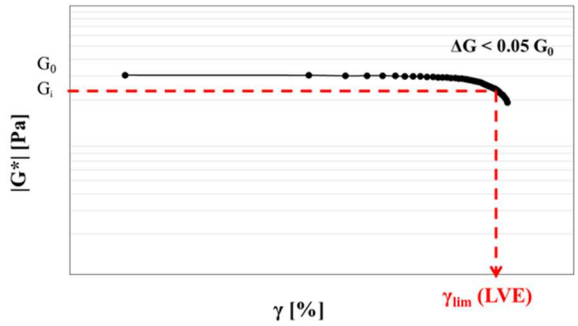

Figure 5.7. Strain sweep test result and γ_{lim} identification.

Frequency sweep test

Frequency sweep tests conducted under different temperatures and loading conditions represent a useful tool for a complete characterisation of bitumen viscoelastic properties. In addition, these tests implemented for thermo-rheologically simple bitumens at a strain within LVE region (i.e. $\gamma < \gamma_{lim}$) enable experimental data to be shifted between different frequencies and temperatures by applying the time-temperature superposition principle (TTSP) and thus master curve construction. In particular, frequency sweep tests were carried out at a constant strain ($\gamma = 0.5\% < \gamma_{lim}$) over a range of frequencies (from 0.159 to 15.9 Hz) and temperatures (from 4 to 82 °C, with 6 °C intervals) (using a PP08 for testing low and intermediate temperatures and PP25 for high temperatures) (Figure 5.8). Besides the construction of the master curves, Black and Cole-Cole diagrams were plotted as useful representations of raw data obtained from frequency sweep tests for all the bitumens investigated.

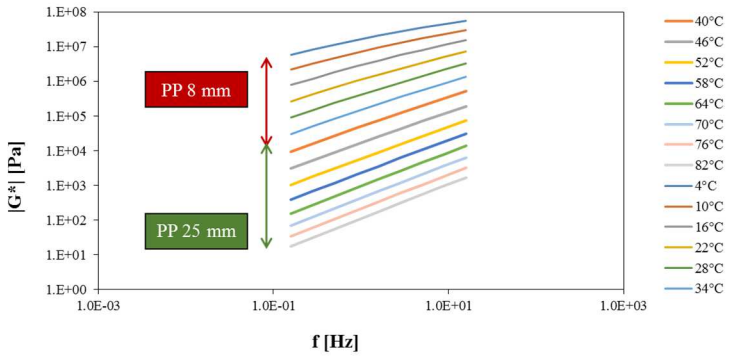

Figure 5.8. Frequency sweep test result.

Black Diagram

The Black diagram is the graph of the norm of the complex modulus, |G*|, versus the phase angle, δ. A smooth curve in Black diagram is a useful indicator of time-temperature equivalency and thermo-rheologically simplicity for the bitumens tested (Lesueur et al, 1996) as well as no discrepancies in experimental results (Airey, 2002); moreover, through this plot the magnitude of the glassy asymptote can be reasonably estimated and used in the master curve construction.

Cole-Cole Diagram

The Cole-Cole diagram is the graph of the loss modulus, G_2 as a function of the storage modulus G_1; it allows immediately appreciating the ratio between the two complex modulus components and thus estimating the preponderance of the viscous or elastic behaviour at the different temperatures investigated.

Master curve construction

Master curves provide a fundamental rheological understanding of viscoelastic materials and allow an estimation of mechanical properties at wide ranges of temperature and frequency that could be achieved in field, but that are not practical to directly simulate in laboratory.
Since the bitumens studied can be considered as linear viscoelastic under the conditions considered and characterised as thermo-rheologically simple thanks to smooth curves in Black diagrams, TTSP was applied to generate complex modulus master curves and shift factor relationship. A reference temperature equal to 34 °C was selected and the rheological data at all the other temperatures were shifted with respect to time until the curves merge into a single smooth function. The modified Christensen-Anderson-Marasteanu (CAM) Model was adopted to relate the complex modulus norm to the reduced frequency, following a shift factor variation based on the William-Landel-Ferry (WLF) law. In details, according to the modified CAM model, the equation for complex modulus norm is given by:

$$G^* = G_e^* + \frac{G_g^* - G_e^*}{\left[1+\left(\frac{f_c}{f'}\right)^k\right]^{\frac{m_e}{k}}} \quad (5.1)$$

Where:
$G^*_e = G^*(f \to 0)$, equilibrium complex modulus, $G^*_e = 0$ for bitumens and $G^*_e > 0$ for mixtures in shear;
$G^*_g = G^*(f \to \infty)$, glass complex modulus;
f_c, location parameter with dimension of frequency (i.e. crossover frequency);
f', reduced frequency, function of both temperature and strain;
k, m_e, shape parameters, dimensionless.

Figure 5.9(a) illustrates the complex modulus master curve in Equation 5.1. It can be seen that G^*_g is the horizontal asymptote at $f \to \infty$, and G^*_e is the horizontal asymptote at $f \to 0$. The G^*_e asymptote is zero for bitumens. The third asymptote is the one with a slope of m_e and represents the viscous asymptote.

The G^*_g and m_e asymptotes intercept at f_c, whereas the G^*_e and m_e asymptotes intercept at:

$$\mathbf{f'_c = f_c \left(\frac{G^*_e}{G^*_g}\right)^{\frac{1}{m_e}}} \quad (5.2)$$

For bitumens, $f'_c=0$

The distance between $G^*(f_c)$ and G^*_g for bitumens is given by:

$$\mathbf{R = Log \frac{2^{\frac{m_e}{k}}}{1+\left(2^{\frac{m_e}{k}}-1\right)\frac{G^*_e}{G^*_g}}} \quad (5.3)$$

For bitumens, $G^*_g=0$ and $R = \frac{m_e}{k} Log2$.

The distance between $G^*(f'_c)$ and G^*_e for bitumens is given by:

$$\mathbf{R' = Log\left\{1+\left(\frac{G^*_g}{G^*_e}-1\right)\left[1+\left(\frac{G^*_g}{G^*_e}\right)^{\frac{k}{m_e}}\right]^{\frac{-m_e}{k}}\right\}} \quad (5.4)$$

For bitumens, $G^*_g=0$ and $R' = Log2$.

The William-Landel-Ferry formulation is then used in the modified CAM model to express the temperature-shift factor in this study:

$$\mathbf{Log \frac{a_T(T)}{a_T(T_0)} = -\frac{C_1(T-T_0)}{C_2+(T-T_0)}} \quad (5.9)$$

Where:
a_T, temperature-shift factor;
T_0, reference temperature;
C_1, constant;
C_2, temperature constant.

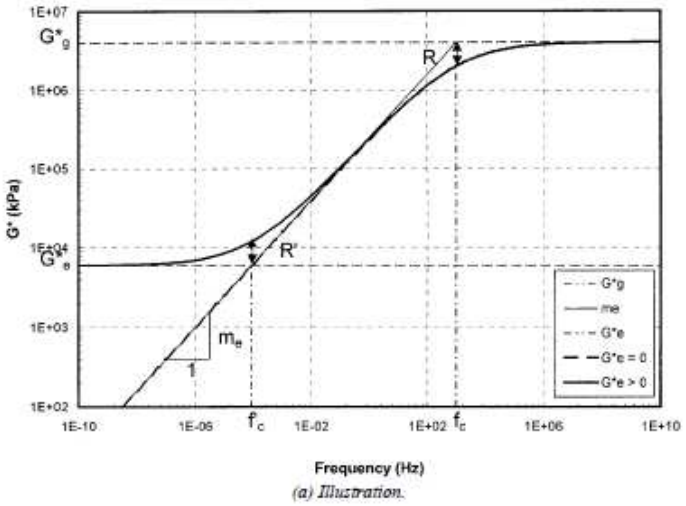

(a) Illustration.

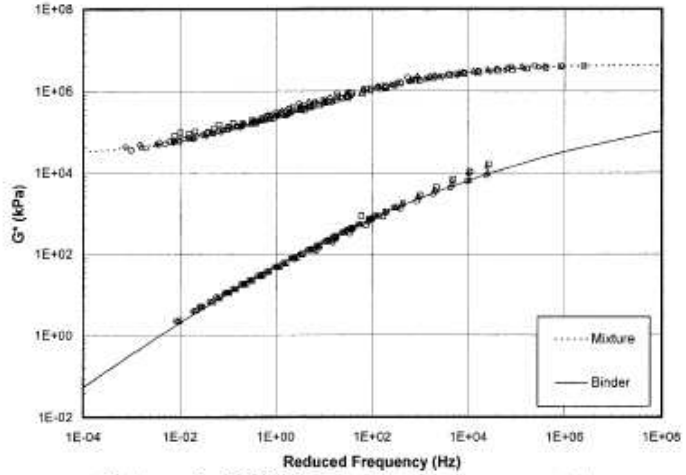

(b) An example (PG 82 SBSr binder, limestone coarse aggregates).

Figure 5.9. Model for complex modulus master curve (Bahia et al., 2001).

Chapter 6.

Rheological experimental investigation

6.1 Strain sweep test

6.1.1 Identification of LVE region

Before running the frequency sweep tests, strain sweep tests were carried out on the long-term aged unrejuvenated bitumens ($LTAG_{VB}$+VB_LTAG and $LTAG_{PB}$+PB_LTAG in the first and second step of testing, respectively), which exhibit the worst condition in terms of brittleness, as a consequence of oxidative hardening linked to ageing. In fact, the more severe the oxidation subjected by the bitumen considered, the higher the |G*| values measured and the lower the γ_{lim} value calculated (Grilli et al., 2017).
Results summarised in Table 6.1 and depicted in Figures 6.1 and 6.2 allow the threshold of LVE region, γ_{lim}, to be identified and consequently a proper strain value within LVE region to be selected for frequency sweep test implementation.

Table 6.1. Strain sweep test data for the long-term aged unrejuvenated bitumens investigated in the first and second phase of testing.

1st step of testing							
Bitumen	**Repetition**	**Temperature**					
		28 °C		**16 °C**		**4 °C**	
	N.	|G*| [Pa]	γ_{lim} [%]	|G*| [Pa]	γ_{lim} [%]	|G*| [Pa]	γ_{lim} [%]
$LTAG_{VB}$+VB_LTAG	1	1.21E+07	1.53	3.33E+07	1.44	7.85E+07	1.40
	2	1.21E+07	1.68	3.35E+07	1.51	7.84E+07	1.47
2nd step of testing							
Bitumen	**Repetition**	**Temperature**					
		28 °C		**16 °C**		**4 °C**	
	N.	|G*| [Pa]	γ_{lim} [%]	|G*| [Pa]	γ_{lim} [%]	|G*| [Pa]	γ_{lim} [%]
$LTAG_{PB}$+PB_LTAG	1	5.44E+06	2.15	1.87E+07	1.83	5.72E+07	1.94
	2	5.38E+06	2.15	1.85E+07	1.75	5.48E+07	1.87

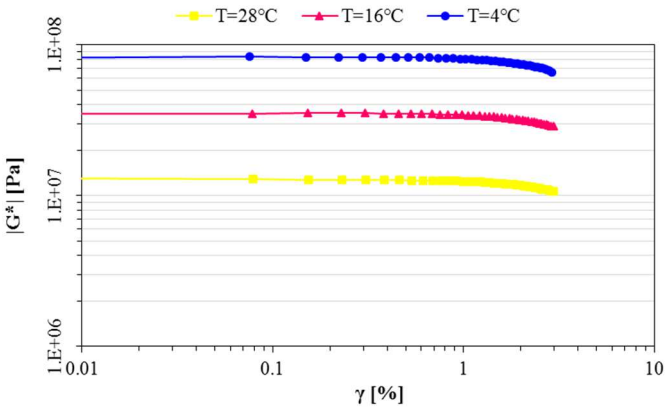

Figure 6.1. Strain sweep test isotherms for the long-term aged unrejuvenated bitumen, $LTAG_{VB}$+VB_LTAG, investigated in the first step of testing (Mazzoni et al., 2017a).

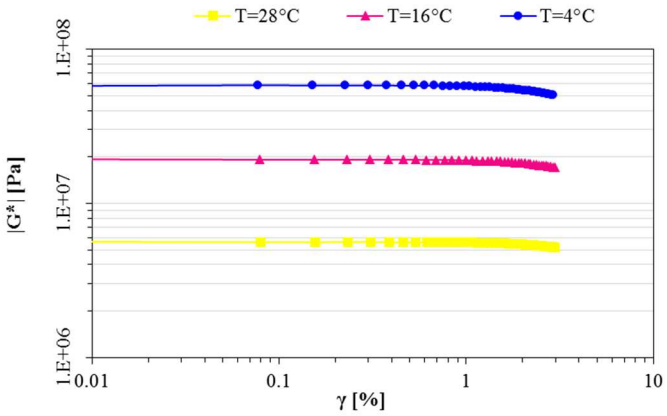

Figure 6.2. Strain sweep test isotherms for the long-term aged unrejuvenated bitumen, $LTAG_{PB}$+PB_LTAG, investigated in the second step of testing.

6.2 Frequency sweep test

6.2.1 Effects of ageing on virgin bitumen

First step of testing

All the curves plotted in Figure 6.3 and data summarised in Table 6.2 clearly show an increase in |G*| values, indicating a marked bitumen hardening, and a reduction in phase angles, δ. Hence, the results denote a prevalence of the elastic component G_1 on the viscous component

G_2, as a consequence of the ageing subjected by the reference virgin bitumen investigated in the first step of testing (Mazzoni et al., 2017a). Moreover, considering the CAM model parameters summarised in Table 6.3, oxidation phenomena determine the following effects on the reference bitumen (Mazzoni et al., 2017a):
- lower shape index S, as an evidence of a higher sensitivity to frequency changes, generally higher |G*| values and lower phase angles within the intermediate range of frequency;
- lower crossover frequency f_c, suggesting lower phase angles and thus a greater overall elastic component in the behaviour;
- higher C_1 and C_2 values, according to the reduction in fractional free volume (i.e. reduction of molecular mobility) (Mazzoni et al., 2016).

Table 6.2. Rheological data obtained for the reference bitumen investigated at different stages of ageing (virgin, short- and long-term aged bitumen) for f = 1.59 Hz in the first step of testing (Mazzoni et al., 2017a).

Bitumen	T = 4 °C				T = 58 °C			
	|G*| [Pa]	G_1 [Pa]	G_2 [Pa]	δ [°]	|G*| [Pa]	G_1 [Pa]	G_2 [Pa]	δ [°]
VB	2.09E+07	1.49E+07	1.46E+07	44.3	3.60E+03	2.58E+02	3.59E+03	85.9
$STAG_{VB}$	3.74E+07	3.12E+07	2.06E+07	33.5	1.63E+04	3.03E+03	1.61E+04	79.3
$LTAG_{VB}$	6.79E+07	6.18E+07	2.81E+07	24.4	1.19E+05	4.97E+04	1.08E+05	65.1

Table 6.3. Calibrated parameters of the modified CAM model and WLF law for the reference bitumen investigated at different stages of ageing (virgin, short- and long-term aged bitumen) in the first step of testing (Mazzoni et al., 2017a).

CAM modified model	$G^* = G_e^* + \frac{G_g^* - G_e^*}{[1+(\frac{f_c}{f})^k]^{\frac{m_e}{k}}}$						
	G^*_e [Pa]	G^*_g [Pa]	f_c [Hz]	k	m_e	$S = \mathrm{Log}\frac{2^{\frac{m_e}{k}}}{1+(2^{\frac{m_e}{k}}-1)\cdot\frac{G_e^*}{G_g^*}}$	R^2
VB	0	1E+09	360	0.16	1.12	2.107	0.996
$STAG_{VB}$	0	1E+09	290	0.16	0.96	1.797	0.995
$LTAG_{VB}$	0	1E+09	280	0.14	0.70	1.479	0.987

WLF law	$\mathrm{Log}(a_t) = -\frac{C_1(T-T_0)}{C_2+(T-T_0)}$		
	C_1	C_2	T_0 [°C]
VB	15	168	34
$STAG_{VB}$	21	210	34
$LTAG_{VB}$	26	210	34

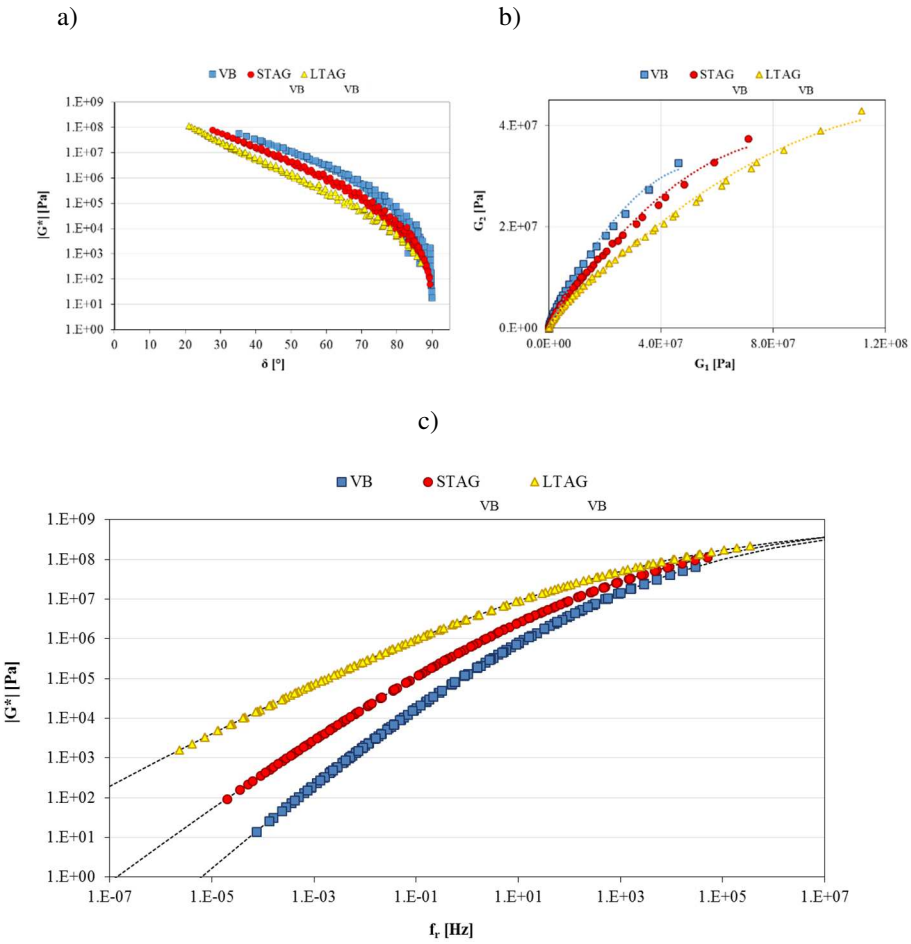

Figure 6.3. Rheological characterisation of the reference bitumen investigated at different stages of ageing (virgin, short- and long-term aged bitumen) in the first step of testing: a) Black Diagram; b) Cole-Cole Diagram; c) Master curves of |G*| at 34 °C (Mazzoni et al., 2017a).

Second step of testing

Oxidation causes the same above-mentioned effects as for the virgin reference bitumen investigated in the first step of testing:

- A curve contraction in Black Diagram, as a consequence of an increase in |G*| values and a decrease in δ values (Figure 6.4a);
- Elastic domain predominance pointed out in Cole-Cole Diagram. Setting a G_2 value, an increase in G_1 value with ageing evolution is observed (Figure 6.4b);

- A general increase in |G*| values, indicating a material stiffening (Table 6.4). The master curve of the virgin bitumen seems upward shifted, even if at the highest frequencies it tends to the same asymptotic value G_g equal to 1 GPa (Figure 6.4c). Analysing the master curve parameters, a decrease in the crossover frequency f_c, suggesting a stiff behaviour, is detected, besides a decrease in the shape index S, indicating a high energy level storage during deformation (Table 6.5).

Table 6.4. Rheological data obtained for the reference bitumen investigated at different stages of ageing (virgin, short- and long-term aged bitumen) for f = 1.59 Hz in the second step of testing.

Bitumen	T = 4 °C				T = 58 °C			
	|G*| [Pa]	**G_1 [Pa]**	**G_2 [Pa]**	**δ [°]**	**|G*| [Pa]**	**G_1 [Pa]**	**G_2 [Pa]**	**δ [°]**
PB	1.92E+07	1.29E+07	1.43E+07	48.1	3.10E+03	2.31E+02	3.09E+03	85.8
$STAG_{PB}$	2.98E+07	2.30E+07	1.91E+07	39.8	9.66E+03	1.63E+03	9.53E+03	80.3
$LTAG_{PB}$	4.92E+07	4.17E+07	2.62E+07	32.1	3.88E+04	1.26E+04	3.67E+04	71.2

Table 6.5. Calibrated parameters of the modified CAM model and WLF law for the reference bitumen investigated at different stages of ageing (virgin, short- and long-term aged bitumen) in the second step of testing.

CAM modified model	$G^* = G_e^* + \frac{G_g^* - G_e^*}{\left[1 + \left(\frac{f_c}{f}\right)^k\right]^{\frac{m_e}{k}}}$						
	G^*_e [Pa]	G^*_g [Pa]	f_c [Hz]	k	m_e	$S = \mathrm{Log}\frac{2^{\frac{m_e}{k}}}{1 + (2^{\frac{m_e}{k}} - 1)\cdot\frac{G_e^*}{G_g^*}}$	R^2
PB	0	1E+09	418	0.165	1.162	2.120	0.998
$STAG_{PB}$	0	1E+09	340	0.161	1.028	1.927	1.000
$LTAG_{PB}$	0	1E+09	290	0.160	0.910	1.710	0.997

WLF law	$\mathrm{Log}(a_t) = -\frac{C_1(T-T_0)}{C_2+(T-T_0)}$		
	C_1	C_2	T_0 [°C]
PB	13.00	153.00	34
$STAG_{PB}$	16.78	183.25	34
$LTAG_{PB}$	21.80	220.00	34

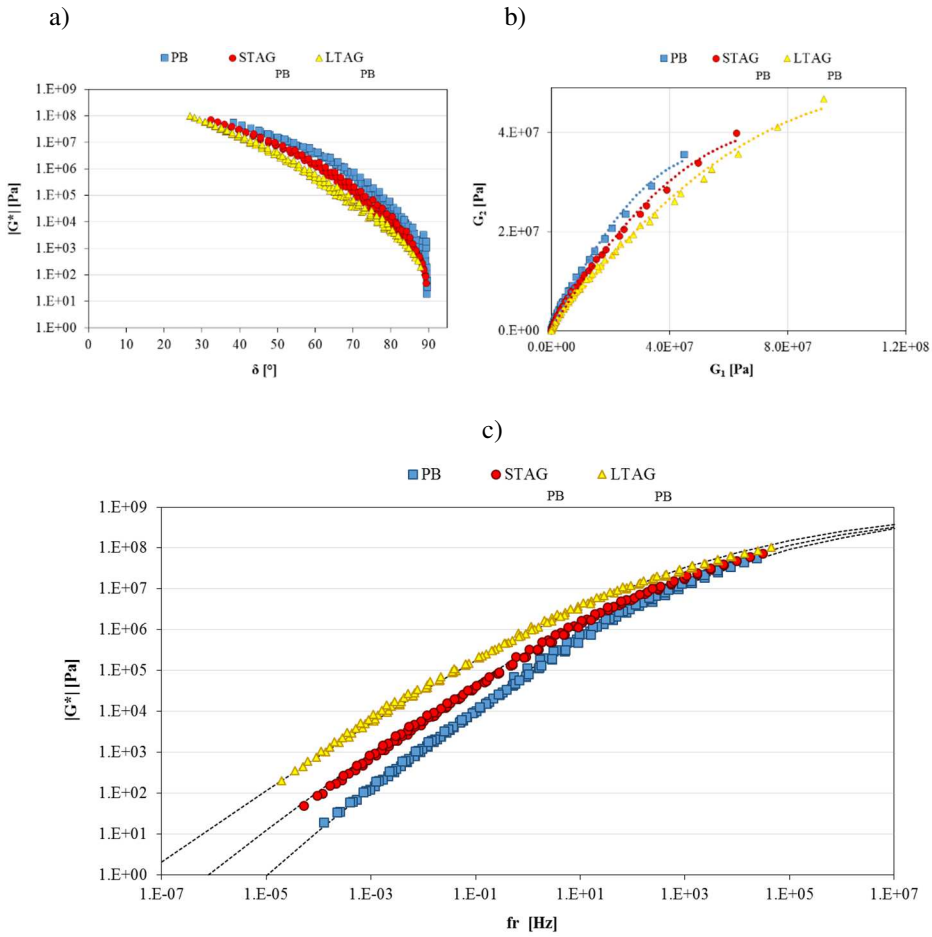

Figure 6.4. Rheological characterisation of the reference bitumen investigated at different stages of ageing (virgin, short- and long-term aged bitumen) in the second step of testing: a) Black Diagram; b) Cole-Cole Diagram; c) Master curves of |G*| at 34 °C.

6.2.2 Effects of bitumen rejuvenation

First step of testing

Rejuvenators modify bitumen chemistry and, consequently, rheology by enhancing the viscous response of the bitumen (Nahar et al, 2014, Xu et al., 2014). This behaviour results in a decrease in |G*| values, denoting a bitumen softening, and a rise of phase angles, δ, corresponding to a lower G_1/G_2 ratio, as shown in Figure 6.5 and Table 6.6, comparing the rejuvenated bitumens to the associated composite bitumen without additive

($LTAG_{VB}$+VB+A/B/C versus $LTAG_{VB}$+VB) (Mazzoni et al., 2017a). In addition, with respect to the CAM model parameters summarised in Table 6.7, the presence of each rejuvenator leads to the following effects on the corresponding composite bituminous blend ($LTAG_{VB}$+VB+A/B/C versus $LTAG_{VB}$+VB) (Mazzoni et al., 2017a):
- higher shape index S, as an indication of a more gradual transition from the elastic to the viscous behaviour;
- higher crossover frequency f_c and thus a remarkable retrieval of viscous component in the behaviour;
- lower C_1 and C_2 values, as a consequence of higher molecule mobility.
On the overall, the additives used are even approaching to restore the rheological properties of the virgin bitumen contained in each composite bituminous blend where they are implemented ($LTAG_{VB}$+VB+A/B/C versus VB). This result is confirmed by the comparable values of the calibrated parameters summarised in Table 6.7 and the nearing of the rheological data and curves shown in Table 6.6 and Figure 6.5 ($LTAG_{VB}$+VB+A/B/C versus VB) (Mazzoni et al., 2017a).

Table 6.6. Rheological data obtained for the bitumens rejuvenated or not compared to the associated virgin and long-term aged bitumens investigated in the first step of testing at f = 1.59 Hz (Mazzoni et al., 2017a).

Bitumen	T = 4 °C				T = 58 °C			
	|G*| [Pa]	G_1 [Pa]	G_2 [Pa]	δ [°]	|G*| [Pa]	G_1 [Pa]	G_2 [Pa]	δ [°]
VB	2.09E+07	1.49E+07	1.46E+07	44.3	3.60E+03	2.58E+02	3.59E+03	85.9
$LTAG_{VB}$+VB+A	1.98E+07	1.59E+07	1.19E+07	36.8	7.45E+03	1.04E+03	7.39E+03	82.0
$LTAG_{VB}$+VB+B	2.66E+07	2.11E+07	1.62E+07	37.6	7.62E+03	9.48E+02	7.56E+03	82.9
$LTAG_{VB}$+VB+C	2.20E+07	1.77E+07	1.30E+07	36.4	1.08E+04	1.71E+03	1.07E+04	80.9
$LTAG_{VB}$+VB	4.47E+07	3.84E+07	2.30E+07	31.0	1.64E+04	3.09E+03	1.61E+04	79.1
$LTAG_{VB}$	6.79E+07	6.18E+07	2.81E+07	24.4	1.19E+05	4.97E+04	1.08E+05	65.1

Table 6.7. Calibrated parameters of the modified CAM model and WLF law for the bitumens rejuvenated or not compared to the associated virgin and long-term aged bitumens investigated in the first step of testing (Mazzoni et al., 2017a).

CAM modified model	$G^* = G_e^* + \frac{G_g^* - G_e^*}{\left[1 + \left(\frac{f_c}{f}\right)^k\right]^{\frac{m_e}{k}}}$						
	G^*_e [Pa]	G^*_g [Pa]	f_c [Hz]	k	m_e	$S = \mathrm{Log}\frac{2^{\frac{m_e}{k}}}{1 + (2^{\frac{m_e}{k}} - 1) \cdot \frac{G_e^*}{G_g^*}}$	R^2
VB	0	1E+09	360	0.16	1.12	2.107	0.996
$LTAG_{VB}$+VB+A	0	1E+09	360	0.16	1.06	1.994	0.993
$LTAG_{VB}$+VB+B	0	1E+09	400	0.16	1.03	1.938	0.994
$LTAG_{VB}$+VB+C	0	1E+09	400	0.16	1.01	1.900	0.991
$LTAG_{VB}$+VB	0	1E+09	380	0.16	0.92	1.731	0.969
$LTAG_{VB}$	0	1E+09	280	0.14	0.70	1.479	0.987

WLF law	$\mathrm{Log}(a_t) = -\frac{C_1(T-T_0)}{C_2+(T-T_0)}$		
	C_1	C_2	T_0 [°C]
VB	15.0	168	34
$LTAG_{VB}$+VB+A	18.5	190	34
$LTAG_{VB}$+VB+B	17.0	180	34
$LTAG_{VB}$+VB+C	15.5	165	34
$LTAG_{VB}$+VB	22.5	200	34
$LTAG_{VB}$	26.0	210	34

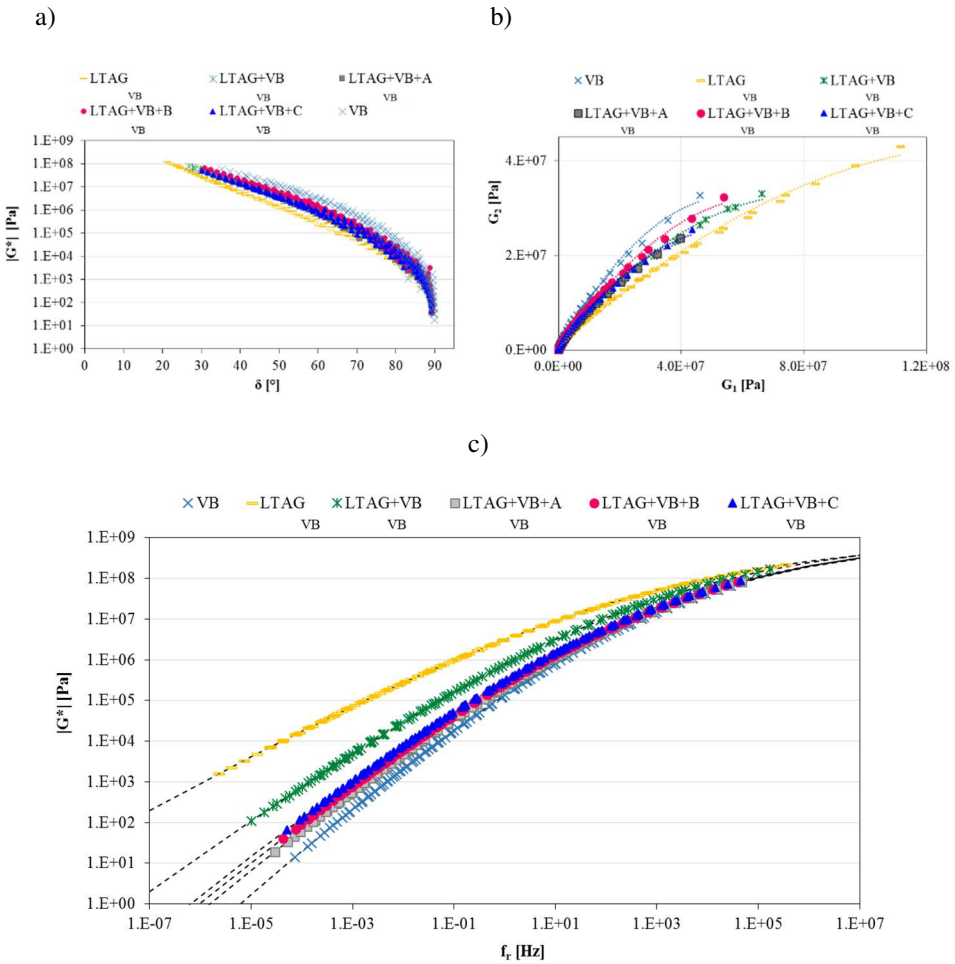

Figure 6.5. Comparison among the bitumens rejuvenated or not and the associated virgin and long-term aged bitumens investigated in the first step of testing: a) Black Diagram; b) Cole-Cole Diagram; c) Master curves of |G*| at 34 °C.

Second step of testing

Rejuvenation determines the same effects above-mentioned for the bitumens investigated in the first step of testing:

- A more flat curve in Black Diagram, as a consequence of a decrease in |G*| values and an increase in δ values ($LTAG_{PB}$+PB+A/B/C versus $LTAG_{PB}$ or $LTAG_{PB}$+PB) (Figure 6.6a);

- Viscous response enhancement pointed out in Cole-Cole Diagram. Setting a G_1 value, an increase in G_2 value is detected in the rejuvenated bitumens compared to the associated unrejuvenated aged bitumens ($LTAG_{PB}$+PB+A/B/C versus $LTAG_{PB}$/$LTAG_{PB}$+PB) (Figure 6.6b);
- A general decrease in |G*| values, denoting a material softening (Table 6.8). With respect to the associated aged bitumen or hot recycled bituminous blend without additives, the master curve of the rejuvenated bitumens are downward shifted, even if at the highest frequencies it tends to the same asymptotic value G_g equal to 1 GPa ($LTAG_{PB}$+PB+A/B/C versus $LTAG_{PB}$ or $LTAG_{PB}$+PB) (Figure 6.6c). Analysing the master curve parameters, it can be observed an increase in the crossover frequency f_c, suggesting a soft behaviour, besides an increase in the shape index S, indicating a high energy dissipation in form of deformation (Table 6.9).

On the overall, the additives used are even approaching to restore the rheological properties of the virgin bitumen contained in each composite bituminous blend where they are implemented ($LTAG_{PB}$+PB+A/B/C versus PB). This result is confirmed by the comparable values of the calibrated parameters summarised in Table 6.9 and the nearing of the rheological data and curves shown in Table 6.8 and Figure 6.6 ($LTAG_{PB}$+PB+A/B/C versus PB). In particular, the rejuvenator C provides a greater softening effect to the corresponding hot recycled bituminous blend, as confirmed by the comparable or even lower |G*| values of the rejuvenated bitumen type C compared to the associated virgin bitumen alone at high temperatures (low frequencies) or low temperatures (high frequencies), respectively ($LTAG_{PB}$+PB+C versus PB) (Table 6.8 and Figure 6.6). In particular, the related master curves are almost superimposed, denoting a great restoring potentiality of the rejuvenator C.

Table 6.8. Rheological data obtained for the bitumens rejuvenated or not compared to the associated virgin and long-term aged bitumens investigated at f = 1.59 Hz in the second step of testing.

Bitumen	T = 4 °C				T = 58 °C			
	|G*| [Pa]	**G_1 [Pa]**	**G_2 [Pa]**	**δ [°]**	**|G*| [Pa]**	**G_1 [Pa]**	**G_2 [Pa]**	**δ [°]**
PB	1.92E+07	1.29E+07	1.43E+07	48.1	3.10E+03	2.31E+02	3.09E+03	85.8
$LTAG_{PB}$+PB+A	1.75E+07	1.27E+07	1.21E+07	43.6	6.27E+03	9.88E+02	6.20E+03	81.0
$LTAG_{PB}$+PB+B	2.07E+07	1.50E+07	1.42E+07	43.4	5.55E+03	6.99E+02	5.50E+03	82.8
$LTAG_{PB}$+PB+C	1.05E+07	6.89E+06	7.90E+06	48.9	3.65E+03	4.32E+02	3.62E+03	83.2
$LTAG_{PB}$+PB	3.60E+07	2.83E+07	2.22E+07	38.1	1.30E+04	2.55E+03	1.27E+04	78.7
$LTAG_{PB}$	4.92E+07	4.17E+07	2.62E+07	32.1	3.88E+04	1.26E+04	3.67E+04	71.2

Table 6.9. Calibrated parameters of the modified CAM model and WLF law for the bitumen rejuvenated or not compared to the associated virgin and long-term aged bitumens investigated in the second step of testing.

CAM modified model	$G^* = G_e^* + \frac{G_g^* - G_e^*}{[1+(\frac{f_c}{f})^k]^{\frac{m_e}{k}}}$						
	G^*_e [Pa]	G^*_g [Pa]	f_c [Hz]	k	m_e	S $= \text{Log}\frac{2^{\frac{m_e}{k}}}{1+(2^{\frac{m_e}{k}}-1)\cdot\frac{G_e^*}{G_g^*}}$	R^2
PB	0	1E+09	418	0.165	1.162	2.12	0.998
$LTAG_{PB}$+PB+A	0	1E+09	400	0.150	1.060	2.12	0.997
$LTAG_{PB}$+PB+B	0	1E+09	400	0.150	1.070	2.14	0.997
$LTAG_{PB}$+PB+C	0	1E+09	400	0.158	1.160	2.21	0.999
$LTAG_{PB}$+PB	0	1E+09	370	0.146	0.955	1.97	0.995
$LTAG_{PB}$	0	1E+09	290	0.160	0.910	1.71	0.997

WLF law	$Log(a_t) = -\frac{C_1(T-T_0)}{C_2+(T-T_0)}$		
	C_1	C_2	T_0 [°C]
PB	13.00	150.0	34
$LTAG_{PB}$+PB+A	16.50	182.5	34
$LTAG_{PB}$+PB+B	17.00	184.0	34
$LTAG_{PB}$+PB+C	14.70	185.0	34
$LTAG_{PB}$+PB	18.75	187.0	34
$LTAG_{PB}$	21.80	220.0	34

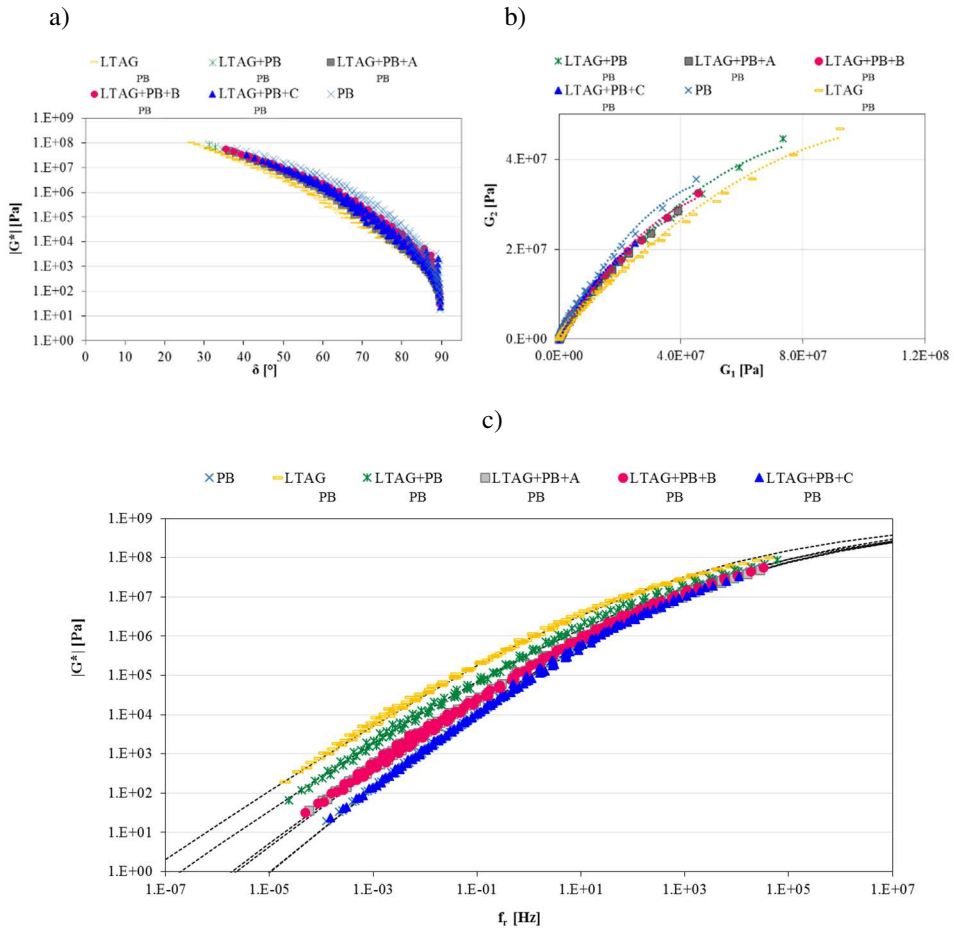

Figure 6.6. Comparison among the bitumens rejuvenated or not and the associated virgin and long-term aged bitumens investigated in the second step of testing: a) Black Diagram; b) Cole-Cole Diagram; c) Master curves of |G*| at 34 °C.

6.2.3 Effects of ageing on hot recycled bituminous blends

First step of testing

The results from the bituminous blends, including 50% of RAP bitumen and 50% of virgin bitumen, with or without rejuvenator ($LTAG_{VB}$+VB and $LTAG_{VB}$+VB+A/B/C versus $LTAG_{VB}$+VB_LTAG and $LTAG_{VB}$+VB+A/B/C_LTAG) and referring to different oxidative levels, are shown in Tables 6.10 and 6.11 and the corresponding master curves are plotted in Figure 6.7 (Mazzoni et al., 2017a). For these bitumens, ageing causes the same above-

mentioned effects as for the reference virgin bitumen (Figure 6.3 and Tables 6.2 and 6.3). However, since the hot recycled bituminous blends (rejuvenated or not) are composed of 50% RAP bitumen, oxidation is less detrimental on them than on the virgin bitumen, as confirmed by a lower variation of the parameter values with ageing (Mazzoni et al., 2017a). Moreover, it should be highlighted that the addition of a rejuvenator in hot recycling leads to a composite bituminous blend which can be even less stiff (lower |G*| values) than the associated virgin bitumen alone at the end of service life, suggesting significant benefits when dealing with high RAP contents (Figure 6.8) ($LTAG_{VB}$+VB+A/B/C_LTAG versus $LTAG_{VB}$) (Mazzoni et al., 2017a). In details, with respect to the associated reference bitumen alone, the rejuvenated bitumens type B or A guarantee lower ageing effects at $T < 58$ °C and a comparable or slightly higher hardening at $T \geq 58$ °C, respectively (Figure 6.9) ($LTAG_{VB}$+VB+B/A_LTAG versus $LTAG_{VB}$). Whereas the long-term aged rejuvenated bitumen type C exhibits similar stiffness values at temperatures lower than 58 °C and a doubling in stiffness values at higher temperatures ($T \geq 58$ °C), if compared to the associated reference bitumen alone (Figure 6.9) ($LTAG_{VB}$+VB+C_LTAG versus $LTAG_{VB}$) (Mazzoni et al., 2017a).

In particular, regarding the associated reference bitumen alone, the additive A provides a lower consistency to the corresponding rejuvenated bitumen also when it is unaged or short-term aged, especially at $T < 58$ °C, as shown by the rheological data in Tables 6.11 and 6.2 ($LTAG_{VB}$+VB+A and $LTAG_{VB}$+VB+A_STAG versus VB and $STAG_{VB}$). Whereas the presence of additives B in the bituminous blends allows obtaining optimum performance during all the service life, as confirmed by the positive rheological values in Table 6.11 compared to those from the associated reference bitumen in Table 6.2 ($LTAG_{VB}$+VB+B pre- and post-ageing versus VB/LTAG). This positive behaviour results in a slightly higher stiffness for this rejuvenated bitumen, when it is unaged or short-term aged ($LTAG_{VB}$+VB+B, $LTAG_{VB}$+VB+B_STAG), and lower stiffness after long-term ageing process ($LTAG_{VB}$+VB+B_LTAG), suggesting a likely higher resistance to rutting, fatigue and thermal cracking, respectively. As concerns the rejuvenated bitumen type C, its mechanical response is quite comparable to that of the associated reference bitumen alone at the different stages of ageing, except for $T \geq 58$ °C when doubled stiffness values occur, as suggested by the comparison of the rheological data in Tables 6.11 with Table 6.2 ($LTAG_{VB}$+VB+C pre and post ageing versus VB/$LTAG_{VB}$) (Mazzoni et al., 2017a).

Table 6.10. Calibrated parameters of the modified CAM model and WLF law for the hot recycled bitumens (rejuvenated or not) investigated at different ageing stages in the first step of testing (Mazzoni et al., 2017a).

CAM modified model	$G^* = G_e^* + \frac{G_g^* - G_e^*}{\left[1+\left(\frac{f_c}{f}\right)^k\right]^{\frac{m_e}{k}}}$						
	G^*_e [Pa]	G^*_g [Pa]	f_c [Hz]	k	m_e	$S = \text{Log}\frac{2^{\frac{m_e}{k}}}{1+(2^{\frac{m_e}{k}}-1)\cdot\frac{G_e^*}{G_g^*}}$	R^2
$LTAG_{VB}$+VB	0	1E+09	380	0.16	0.90	1.693	0.970
$LTAG_{VB}$+VB_STAG	0	1E+09	260	0.15	0.78	1.565	0.982
$LTAG_{VB}$+VB_LTAG	0	1E+09	225	0.15	0.65	1.339	0.983
$LTAG_{VB}$+VB+A	0	1E+09	360	0.16	1.06	1.994	0.993
$LTAG_{VB}$+VB+A_STAG	0	1E+09	350	0.16	0.89	1.728	0.990
$LTAG_{VB}$+VB+A_LTAG	0	1E+09	240	0.16	0.75	1.457	0.988
$LTAG_{VB}$+VB+B	0	1E+09	400	0.16	1.03	1.938	0.994
$LTAG_{VB}$+VB+B_STAG	0	1E+09	340	0.15	0.86	1.726	0.990
$LTAG_{VB}$+VB+B_LTAG	0	1E+09	260	0.15	0.75	1.495	0.988
$LTAG_{VB}$+VB+C	0	1E+09	400	0.16	1.01	1.900	0.991
$LTAG_{VB}$+VB+C_STAG	0	1E+09	340	0.15	0.86	1.726	0.992
$LTAG_{VB}$+VB+C_LTAG	0	1E+09	250	0.17	0.73	1.332	0.990

WLF law	$\text{Log}(a_t) = \frac{C_1(T-T_0)}{C_2+(T-T_0)}$		
	C_1	C_2	T_0 [°C]
$LTAG_{VB}$+VB	19.5	175	34
$LTAG_{VB}$+VB_STAG	22.0	185	34
$LTAG_{VB}$+VB_LTAG	27.0	215	34
$LTAG_{VB}$+VB+A	18.5	190	34
$LTAG_{VB}$+VB+A_STAG	22.0	220	34
$LTAG_{VB}$+VB+A_LTAG	27.5	240	34
$LTAG_{VB}$+VB+B	17.0	180	34
$LTAG_{VB}$+VB+B_STAG	22.0	200	34
$LTAG_{VB}$+VB+B_LTAG	27.5	230	34
$LTAG_{VB}$+VB+C	15.5	165	34
$LTAG_{VB}$+VB+C_STAG	21.5	200	34
$LTAG_{VB}$+VB+C_LTAG	24.0	220	34

Table 6.11. Rheological data obtained for the hot recycled bitumens (rejuvenated or not) at f = 1.59 Hz investigated at different ageing stages in the first step of testing (Mazzoni et al., 2017a).

Bitumen	T = 4 °C				T = 58 °C			
	|G*| [Pa]	G_1 [Pa]	G_2 [Pa]	δ [°]	|G*| [Pa]	G_1 [Pa]	G_2 [Pa]	δ [°]
$LTAG_{VB}$+VB	4.47E+07	3.84E+07	2.30E+07	31.0	1.64E+04	3.09E+03	1.61E+04	79.1
$LTAG_{VB}$+VB_STAG	5.88E+07	5.28E+07	2.59E+07	26.2	8.75E+04	3.45E+04	8.04E+04	66.8
$LTAG_{VB}$+VB_LTAG	8.36E+07	7.78E+07	3.05E+07	21.4	3.47E+05	2.01E+05	2.83E+05	54.6
$LTAG_{VB}$+VB+A	1.98E+07	1.59E+07	1.19E+07	36.8	7.45E+03	1.04E+03	7.39E+03	82.0
$LTAG_{VB}$+VB+A_STAG	3.25E+07	2.77E+07	1.70E+07	31.5	3.38E+04	1.05E+04	3.21E+04	71.9
$LTAG_{VB}$+VB+A_LTAG	5.39E+07	4.91E+07	2.23E+07	24.5	1.42E+05	7.10E+04	1.23E+05	60.0
$LTAG_{VB}$+VB+B	2.66E+07	2.11E+07	1.62E+07	37.6	7.62E+03	9.48E+02	7.56E+03	82.9
$LTAG_{VB}$+VB+B_STAG	4.01E+07	3.46E+07	2.02E+07	30.2	3.13E+04	8.84E+03	3.00E+04	73.6
$LTAG_{VB}$+VB+B_LTAG	5.90E+07	5.36E+07	2.45E+07	24.6	1.14E+05	5.04E+04	1.02E+05	63.7
$LTAG_{VB}$+VB+C	2.20E+07	1.77E+07	1.30E+07	36.4	1.08E+04	1.71E+03	1.07E+04	80.9
$LTAG_{VB}$+VB+C_STAG	3.87E+07	3.32E+07	1.99E+07	30.9	3.13E+04	8.78E+03	3.00E+04	73.7
$LTAG_{VB}$+VB+C_LTAG	6.57E+07	6.02E +07	2.64E +07	23.7	1.99E+05	1.02E+05	1.71E+05	59.2

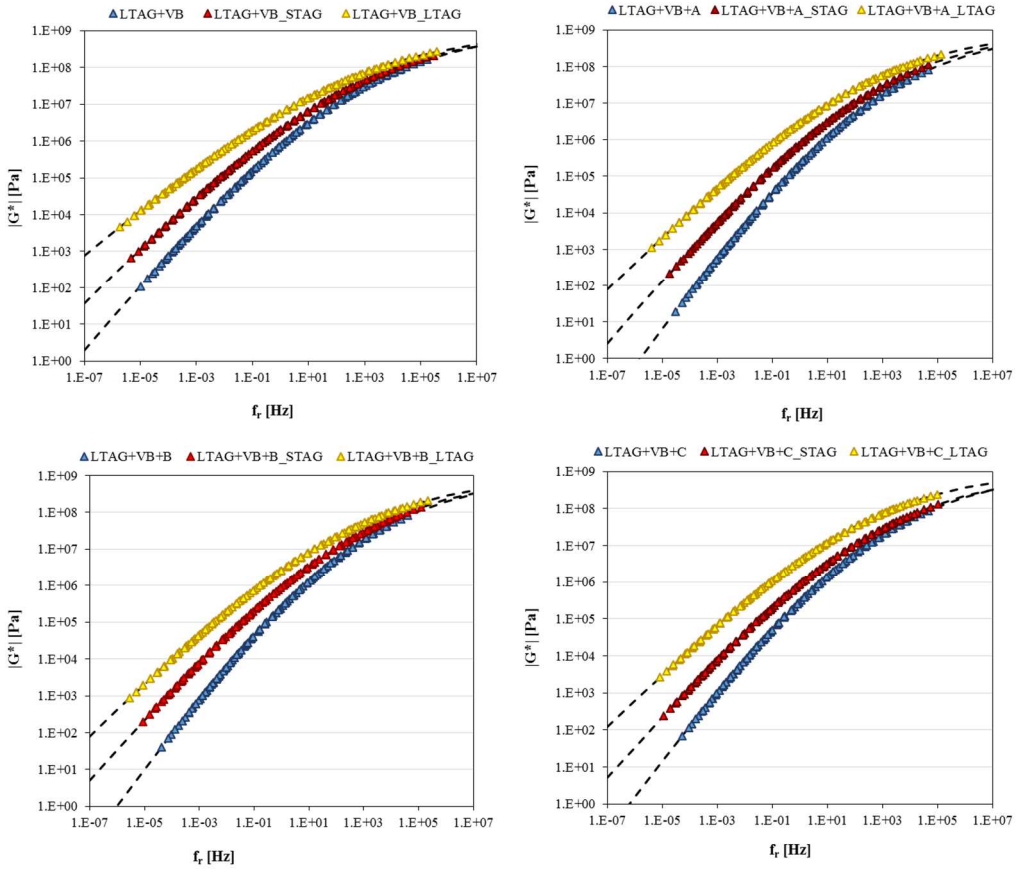

Figure 6.7. Master curves of |G*| at 34 °C for the hot recycled bitumens (rejuvenated or not) investigated at different ageing stages in the first step of testing.

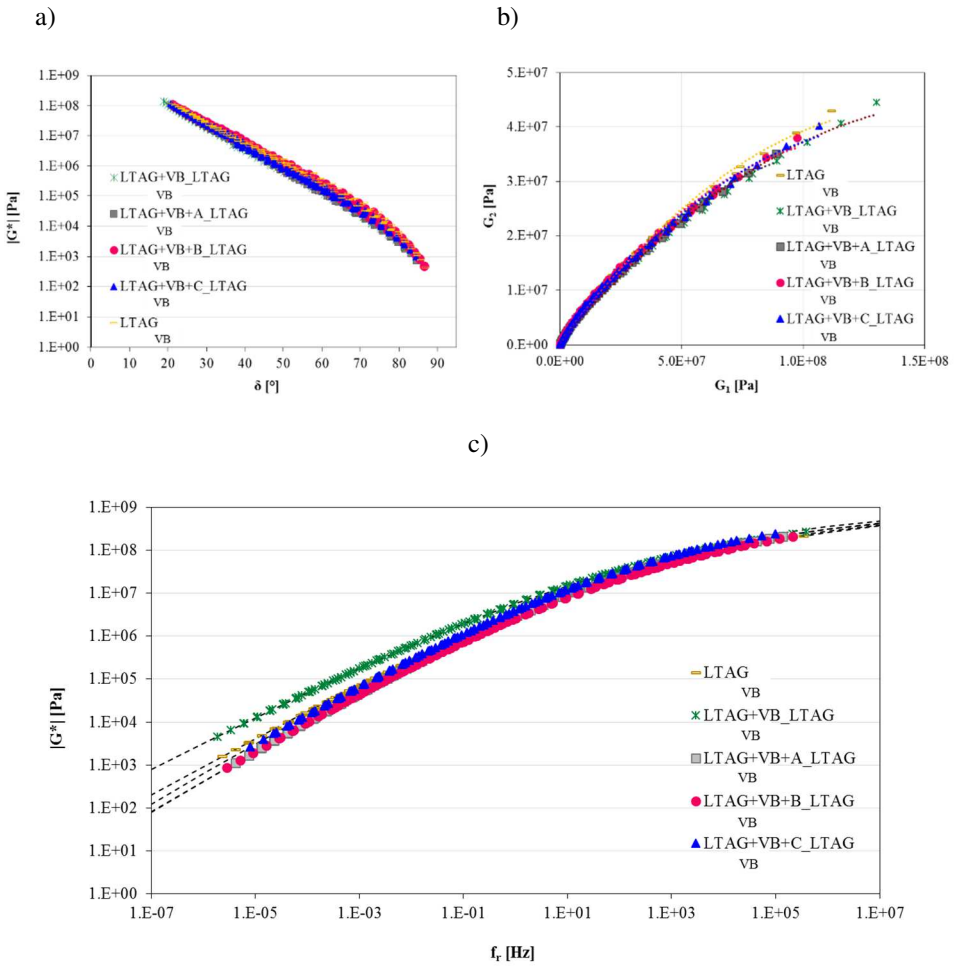

Figure 6.8. Comparison among all the long-term aged bitumens investigated in the first step of testing: a) Black Diagram; b) Cole-Cole Diagram; c) Master curves of |G*| at 34 °C.

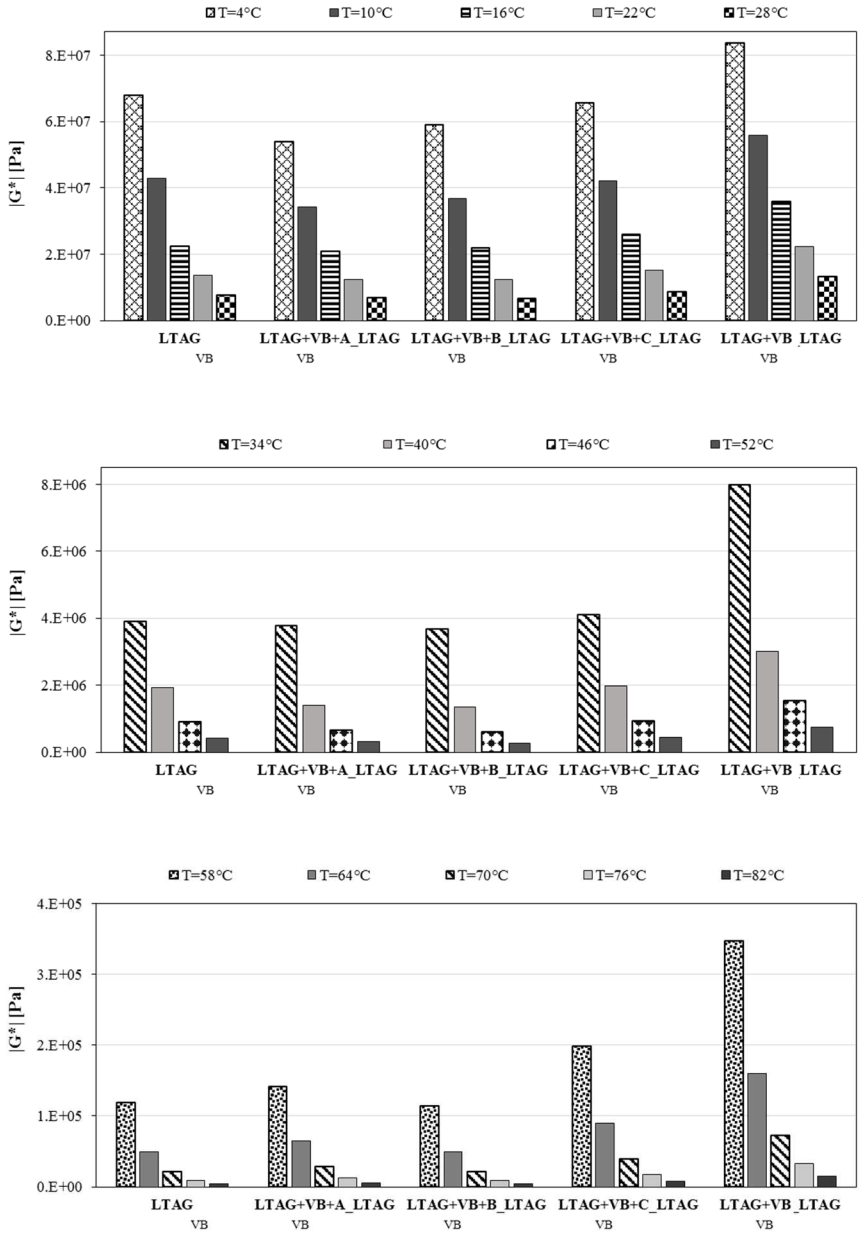

Figure 6.9. Comparison in terms of |G*| at f = 1.59 Hz among all the long-term aged bitumens investigated in the first step of testing (Mazzoni et al., 2017a).

Second step of testing

A comparison among all the long-term aged bitumens investigated in the second step of testing is shown in Tables 6.12 and 6.13 and in Figures 6.10 and 6.11 in terms of rheological data and parameters. It should be noted that the addition of a rejuvenator in hot recycling leads to a composite bituminous blend which can be even less stiff (lower |G*| values) than the associated virgin bitumen alone at the end of service life, suggesting significant benefits when dealing with high RAP contents (Figures 6.10 and 6.11) ($LTAG_{PB}$+PB+A/B/C_LTAG versus $LTAG_{PB}$). In details, with respect to the associated reference bitumen alone, the rejuvenated bitumens type A or C guarantee lower ageing effects at T < 34 °C and a similar or slightly higher hardening at T ≥ 34 °C (Figure 6.11 and Tables 6.12) ($LTAG_{PB}$+PB+A/C_LTAG versus $LTAG_{PB}$). Whereas response of the long-term aged rejuvenated bitumen type B is comparable to that of the long-term aged associated bitumen alone, except for high temperatures (low frequencies) when a slight increase in stiffness occurs (Figures 6.10 and 6.11 and Tables 6.12) ($LTAG_{PB}$+PB+B_LTAG versus $LTAG_{PB}$). However, it is worth noting that the long-term aged rejuvenated bitumen type B is less susceptible to temperature changes than the other long-term aged rejuvenated bitumen ($LTAG_{PB}$+PB+B_LTAG versus $LTAG_{PB}$+PB+A/C_LTAG), showing a behaviour more similar to the associated bitumen alone and the unrejuvenated bitumen when long-term aged (Figure 6.11).

Table 6.12. Rheological data obtained for all the long-term aged bitumens at f = 1.59 Hz investigated in the second step of testing.

Bitumen	T = 4 °C				T = 58 °C			
	|G*| [Pa]	G_1 [Pa]	G_2 [Pa]	δ [°]	|G*| [Pa]	G_1 [Pa]	G_2 [Pa]	δ [°]
$LTAG_{PB}$	4.92E+07	4.17E+07	2.62E+07	32.10	3.88E+04	1.26E+04	3.67E+04	71.15
$LTAG_{PB}$+PB+A_LTAG	3.73E+07	3.17E+07	1.97E+07	31.80	5.25E+04	2.18E+04	4.78E+04	65.55
$LTAG_{PB}$+PB+B_LTAG	5.06E+07	4.34E+07	2.61E+07	31.00	4.89E+04	1.86E+04	4.52E+04	67.65
$LTAG_{PB}$+PB+C_LTAG	3.45E+07	2.88E+07	1.89E+07	33.25	5.19E+04	2.11E+04	4.74E+04	66.00
$LTAG_{PB}$+PB_LTAG	6.15E+07	5.42E+07	2.91E+07	28.20	1.08E+05	5.08E+04	9.49E+04	61.85

Table 6.13. Calibrated parameters of the modified CAM model and WLF law for all the long-term aged bitumens investigated in the second step of testing.

CAM modified model	$G^* = G_e^* + \frac{G_g^* - G_e^*}{[1+(\frac{f_c}{f})^k]^{\frac{m_e}{k}}}$						
	G^*_e [Pa]	G^*_g [Pa]	f_c [Hz]	k	m_e	$S = \text{Log}\frac{2^{\frac{m_e}{k}}}{1+(2^{\frac{m_e}{k}}-1)\cdot\frac{G_e^*}{G_g^*}}$	R^2
$LTAG_{PB}$	0	1E+09	290	0.160	0.910	1.71	0.997
$LTAG_{PB}$+PB_LTAG	0	1E+09	280	0.180	0.869	1.45	0.994
$LTAG_{PB}$+PB+A_LTAG	0	1E+09	360	0.154	0.877	1.71	0.996
$LTAG_{PB}$+PB+B_LTAG	0	1E+09	350	0.140	0.820	1.76	0.996
$LTAG_{PB}$+PB+C_LTAG	0	1E+09	365	0.158	0.90	1.71	0.996

WLF law	$Log(a_t) = \frac{C_1(T-T_0)}{C_2+(T-T_0)}$		
	C_1	C_2	T_0 [°C]
$LTAG_{PB}$	21.8	220.0	34
$LTAG_{PB}$+PB_LTAG	21.0	239.0	34
$LTAG_{PB}$+PB+A_LTAG	21.0	225.0	34
$LTAG_{PB}$+PB+B_LTAG	24.5	227.5	34
$LTAG_{PB}$+PB+C_LTAG	20.0	223.0	34

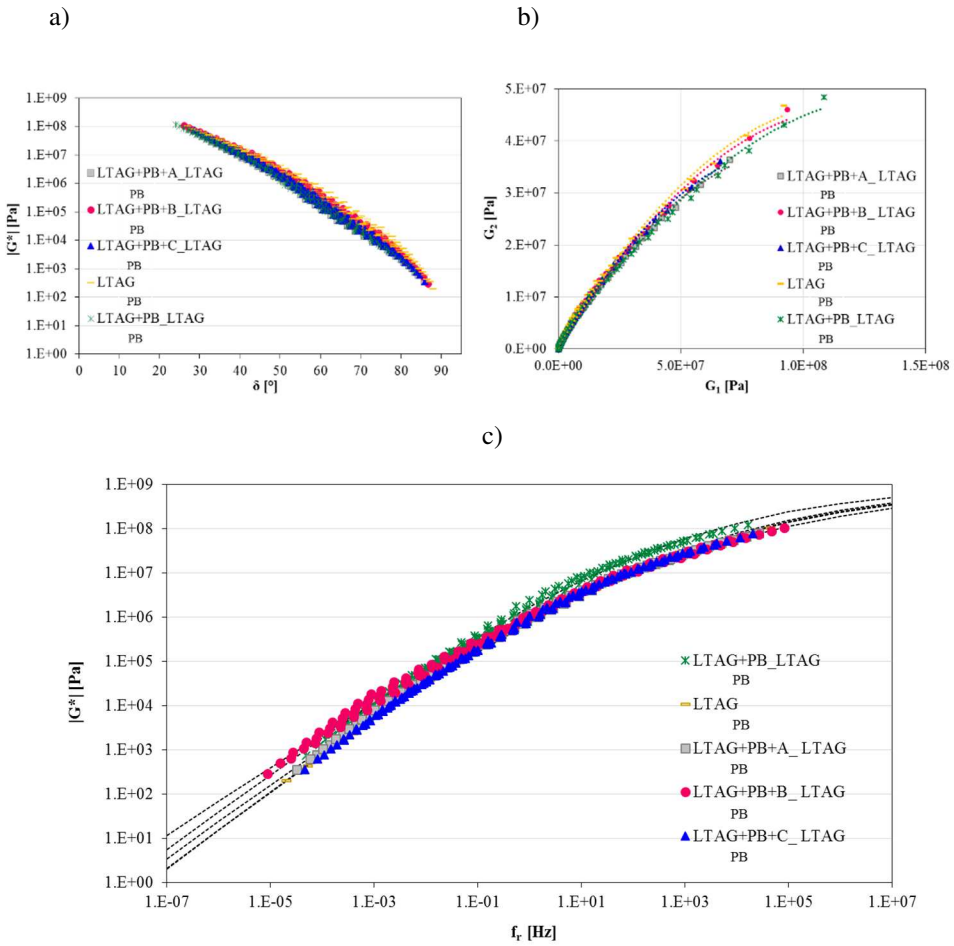

Figure 6.10. Comparison among all the long-term aged bitumens investigated in the second step of testing: a) Black Diagram; b) Cole-Cole Diagram; c) Master curves of |G*| at 34 °C.

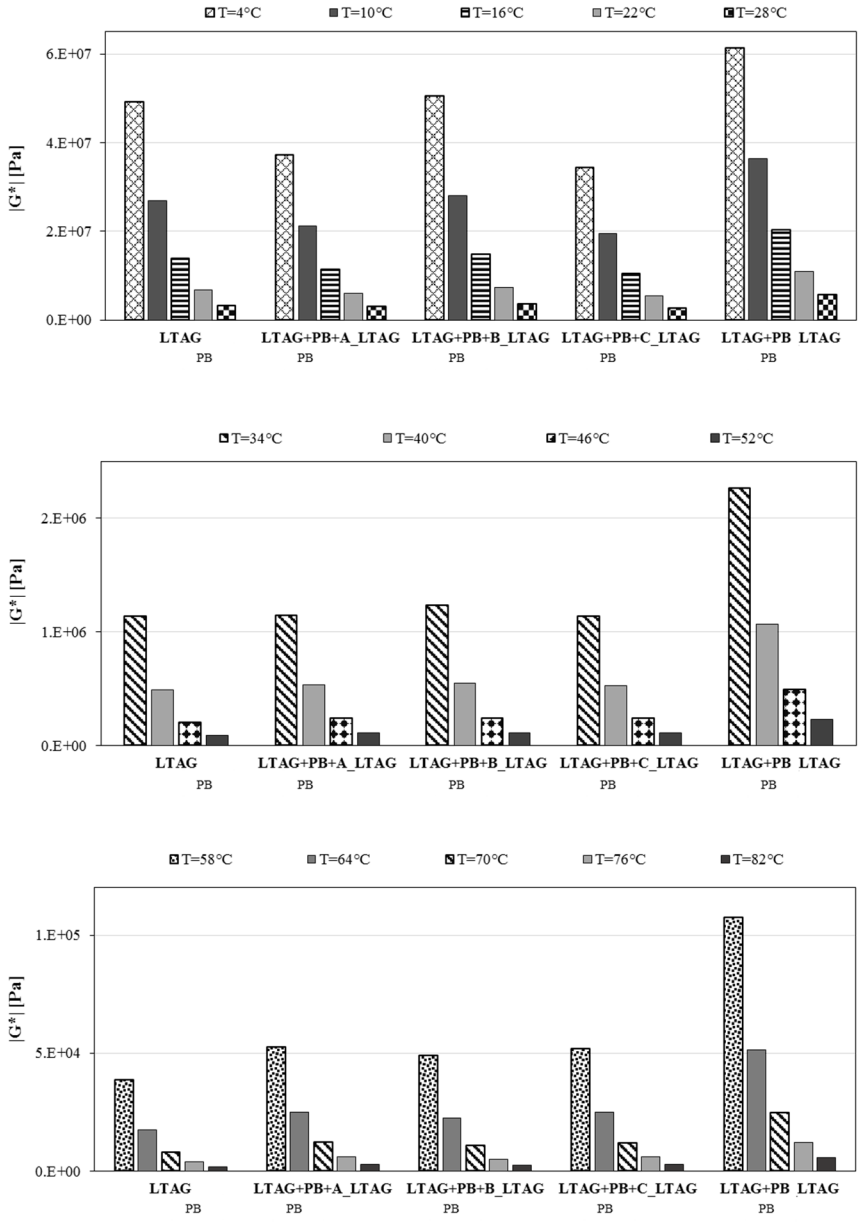

Figure 6.11. Comparison in terms of |G*| at f = 1.59 Hz among all the long-term aged bitumens investigated in the second step of testing.

6.2.4 Influence of the base bitumen on hot recycling

Bitumen ageing

A comparison between the two reference bitumens, before and after ageing, is presented in Tables 6.14 and 6.15 and in Figure 6.12 in terms of rheological data and parameters. In particular, when unaged, their related master curves are almost superimposed, suggesting a comparable rheological response (PB versus VB) (Figure 6.12a). This result is confirmed by an almost perfect agreement between their rheological data and also parameters, as summarised in Tables 6.14 and 6.15. However, a marked difference in stiffness is detected between the two reference bitumens, after ageing. In details, the different manufacturing process makes the first bitumen selected (VB) more unstable and consequently subjected to a more severe oxidation. As a consequence of oxidation, a higher hardening (higher |G*| values and consequently lower δ values) occurs ($LTAG_{VB}$ versus $LTAG_{PB}$) (Tables 6.14 and 6.15 and Figure 6.12b).

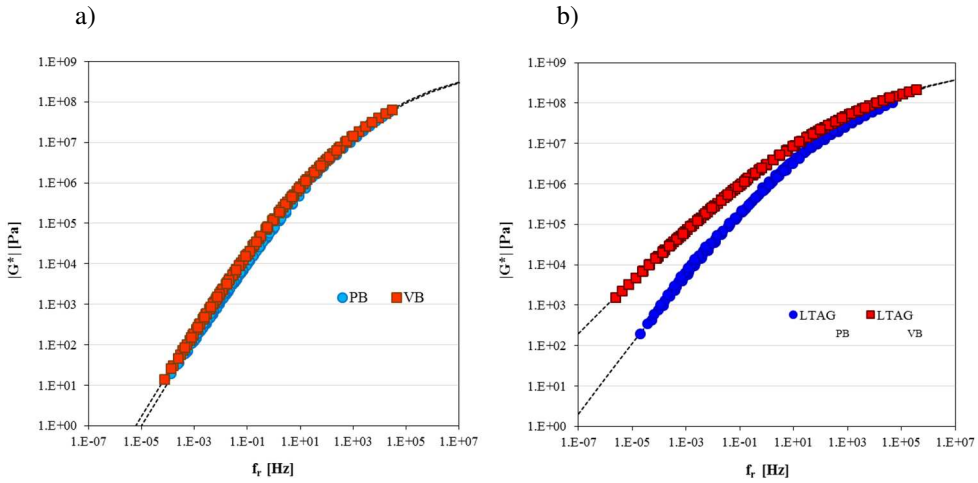

Figure 6.12. Comparison between the two reference bitumens, before and after ageing, in terms of |G*| master curves at 34 °C.

Table 6.14. Rheological data obtained for the two reference bitumens investigated before and after ageing at f = 1.59 Hz.

Bitumen	T = 4 °C				T = 58 °C			
	|G*| [Pa]	G_1 [Pa]	G_2 [Pa]	δ [°]	|G*| [Pa]	G_1 [Pa]	G_2 [Pa]	δ [°]
PB	1.92E+07	1.29E+07	1.43E+07	48.1	3.10E+03	2.31E+02	3.09E+03	85.8
VB	2.09E+07	1.49E+07	1.46E+07	44.3	3.60E+03	2.58E+02	3.59E+03	85.9
$LTAG_{PB}$	4.92E+07	4.17E+07	2.62E+07	32.1	3.88E+04	1.26E+04	3.67E+04	71.2
$LTAG_{VB}$	6.79E+07	6.18E+07	2.81E+07	24.4	1.19E+05	4.97E+04	1.08E+05	65.1

Table 6.15. Calibrated parameters of the modified CAM model and WLF law for the two reference bitumens investigated before and after ageing.

CAM modified model	$G^*=G_e^*+\frac{G_g^*-G_e^*}{[1+(\frac{f_c}{f})^k]^{\frac{m_e}{k}}}$						
	G^*_e [Pa]	G^*_g [Pa]	f_c [Hz]	k	m_e	$S = \mathrm{Log}\frac{2^{\frac{m_e}{k}}}{1+(2^{\frac{m_e}{k}}-1)\cdot\frac{G_e^*}{G_g^*}}$	R^2
PB	0	1E+09	418	0.17	1.16	2.120	0.998
VB	0	1E+09	360	0.16	1.12	2.107	0.996
$LTAG_{PB}$	0	1E+09	290	0.16	0.91	1.710	0.997
$LTAG_{VB}$	0	1E+09	280	0.14	0.70	1.479	0.987

WLF law	$Log(a_t)=-\frac{C_1(T-T_0)}{C_2+(T-T_0)}$		
	C_1	C_2	T_0 [°C]
PB	13.0	153	34
VB	15.0	168	34
$LTAG_{PB}$	21.8	220	34
$LTAG_{VB}$	26.0	210	34

Hot recycling with or without rejuvenators

A comparison among all the hot recycled bitumens (rejuvenated or not) obtained from the two different reference bitumens is presented in Tables 6.16 and 6.17 and in Figure 6.13 in terms of rheological data and parameters. Since the unrejuvenated bitumens are composed of 50% RAP bitumen ($LTAG_{VB}$ or $LTAG_{PB}$) and 50% virgin bitumen (VB or PB), their rheological response is obviously included between that of their components, as confirmed comparing rheological data and curves shown in Figure 6.12 versus Figure 6.13 and Table 6.16 versus Table 6.14 ($LTAG_{VB}$+VB versus $LTAG_{VB}$/VB and $LTAG_{PB}$+PB versus $LTAG_{PB}$/PB). In addition, a nearing of the rheological data, parameters and curves is detected

comparing the two unrejuvenated bitumens obtained from the two different reference bitumens (Tables 6.16 and 6.17 and Figure 6.13) ($LTAG_{VB}$+VB versus $LTAG_{PB}$+PB). With respect to the rejuvenated bitumens, the presence of the additive type A or B determines comparable behaviour, whatever the reference base bitumen, as suggested by the similar values of the calibrated parameters in Table 6.17 and the further nearing of the rheological data and curves in Table 6.16 and Figure 6.13 ($LTAG_{VB}$+VB+A/B versus $LTAG_{PB}$+PB+A/B and $LTAG_{VB/PB}$+VB/PB+A/B versus $LTAG_{VB/PB}$+VB/PB). Whereas using the rejuvenator type C with a different base bitumen strongly changes the performance likely due to compatibility. In fact, the rejuvenator type C allows a more than doubling restoring potentiality if blended with the primary bitumen rather than with the visbreaking bitumen ($LTAG_{PB}$+PB+C versus $LTAG_{VB}$+VB+C) (Table 6.16). Consequently, the distance between the related master curves get larger than that between the associated unrejuvenated bitumens ($LTAG_{VB}$+VB+C versus $LTAG_{PB}$+PB+C compared to $LTAG_{VB}$+VB versus $LTAG_{PB}$+PB).

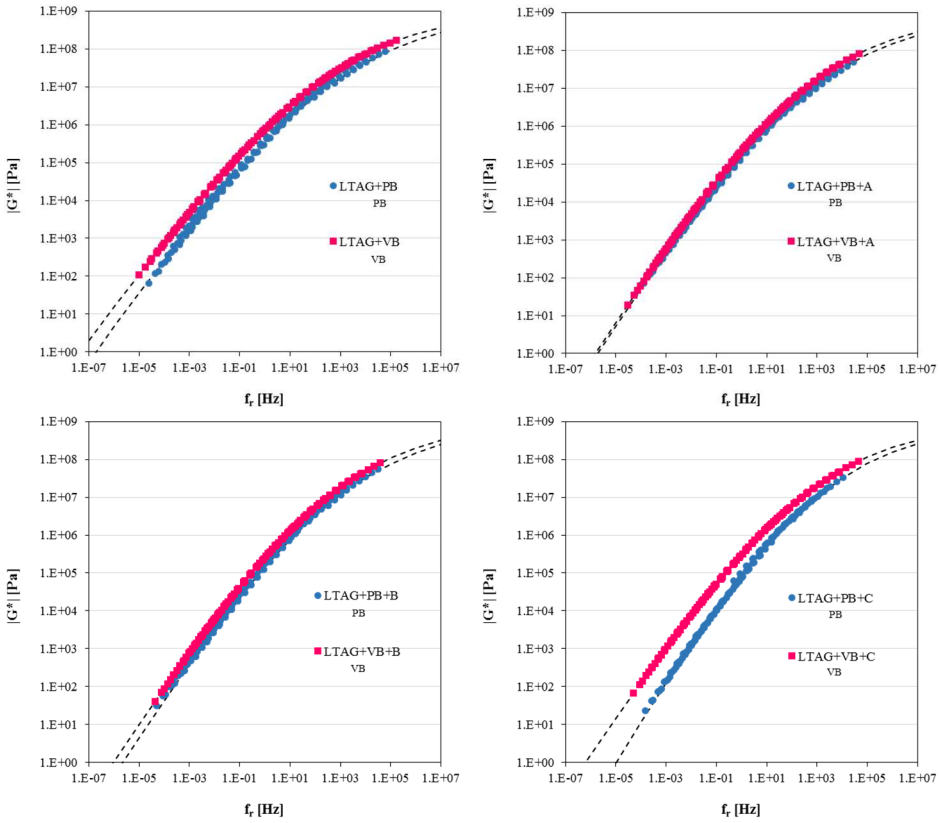

Figure 6.13. Comparison among the hot recycled bitumens (rejuvenated or not) obtained from the two different reference bitumens, in terms of |G*| master curves at 34 °C.

Table 6.16. Comparison among the hot recycled bitumens (rejuvenated or not) obtained from the two different reference bitumens and investigated in terms of |G*| at f = 1.59 Hz.

Bitumen	T = 4 °C		T = 58 °C	
	|G*| [Pa]	**ΔG_{VB-PB} [%]**	**|G*| [Pa]**	**ΔG_{VB-PB} [%]**
$LTAG_{PB}$+PB	3.60E+07	19.5	1.30E+04	20.7
$LTAG_{VB}$+VB	4.47E+07		1.64E+04	
$LTAG_{PB}$+PB+A	1.75E+07	11.6	6.27E+03	15.8
$LTAG_{VB}$+VB+A	1.98E+07		7.45E+03	
$LTAG_{PB}$+PB+B	2.07E+07	22.6	5.55E+03	27.2
$LTAG_{VB}$+VB+B	2.66E+07		7.62E+03	
$LTAG_{PB}$+PB+C	1.05E+07	52.3	3.65E+03	66.2
$LTAG_{VB}$+VB+C	2.20E+07		1.08E+04	

Table 6.17. Comparison among the modified CAM model and WLF law parameters for the hot recycled bitumens (rejuvenated or not) obtained from the two different reference bitumens.

CAM modified model	$G^* = G_e^* + \frac{G_g^* - G_e^*}{[1+(\frac{f_c}{f})^k]^{\frac{m_e}{k}}}$						
	G^*_e [Pa]	G^*_g [Pa]	f_c [Hz]	k	m_e	$S = \mathrm{Log}\frac{2^{\frac{m_e}{k}}}{1+(2^{\frac{m_e}{k}}-1)\cdot\frac{G_e^*}{G_g^*}}$	R^2
$LTAG_{PB}$+PB	0	1E+09	370	0.15	0.96	1.97	0.995
$LTAG_{VB}$+VB	0	1E+09	380	0.16	0.92	1.73	0.969
$LTAG_{PB}$+PB+A	0	1E+09	400	0.15	1.06	2.12	0.997
$LTAG_{VB}$+VB+A	0	1E+09	360	0.16	1.06	1.99	0.993
$LTAG_{PB}$+PB+B	0	1E+09	400	0.15	1.07	2.14	0.997
$LTAG_{VB}$+VB+B	0	1E+09	400	0.16	1.03	1.94	0.994
$LTAG_{PB}$+PB+C	0	1E+09	400	0.16	1.16	2.21	0.999
$LTAG_{VB}$+VB+C	0	1E+09	400	0.16	1.01	1.90	0.991

WLF law	$Log(a_t)=-\frac{C_1(T-T_0)}{C_2+(T-T_0)}$		
	C_1	C_2	T_0 [°C]
$LTAG_{PB}$+PB	18.75	187.0	34
$LTAG_{VB}$+VB	22.50	200.0	34
$LTAG_{PB}$+PB+A	16.5	182.5	34
$LTAG_{VB}$+VB+A	18.5	190.0	34
$LTAG_{PB}$+PB+B	17.0	184.0	34
$LTAG_{VB}$+VB+B	17.0	180.0	34
$LTAG_{PB}$+PB+C	14.7	185.0	34
$LTAG_{VB}$+VB+C	15.5	165.0	34

Hot recycled bituminous blend ageing

All the hot recycled bitumens (rejuvenated or not), obtained from the two different reference bitumens and investigated after a long-term ageing, are compared in terms of rheological data and parameters in Tables 6.18÷6.20 and in Figure 6.14. The comparison between each hot recycled bitumen (rejuvenated or not) contained the primary bitumen with the corresponding blend including the visbreaking bitumen shows a further increase in gap between the related rheological data and curves moving from the unaged condition to the aged one, particularly at high temperatures ($LTAG_{PB}$+PB+(A/B/C) versus $LTAG_{VB}$+VB+(A/B/C) compared to $LTAG_{PB}$+PB+(A/B/C)_LTAG versus $LTAG_{VB}$+VB+(A/B/C)_LTAG) (Table 6.16 versus Table 6.20 and Figure 6.13 versus Figure 6.14). This behaviour is attributed to a more severe oxidation subjected by each hot recycled bitumen (rejuvenated or not) containing the visbreaking bitumen rather than the corresponding blend including the primary bitumen, as a consequence of the manufacturing process ($LTAG_{PB}$+PB+(A/B/C) versus $LTAG_{PB}$+PB+(A/B/C)_LTAG compared to $LTAG_{VB}$+VB+(A/B/C) versus $LTAG_{VB}$+VB+(A/B/C)_LTAG) (Table 6.20). Moreover, regardless of the presence or not of rejuvenators within the blends considered, the primary bitumen guarantees the corresponding bituminous blends a lower hardening effect than the visbreaking bitumen, whatever the ageing level ($LTAG_{PB}$+PB+(A/B/C) versus $LTAG_{PB}$+PB+(A/B/C)_LTAG compared to $LTAG_{VB}$+VB+(A/B/C) versus $LTAG_{VB}$+VB+(A/B/C)_LTAG) (Table 6.19).

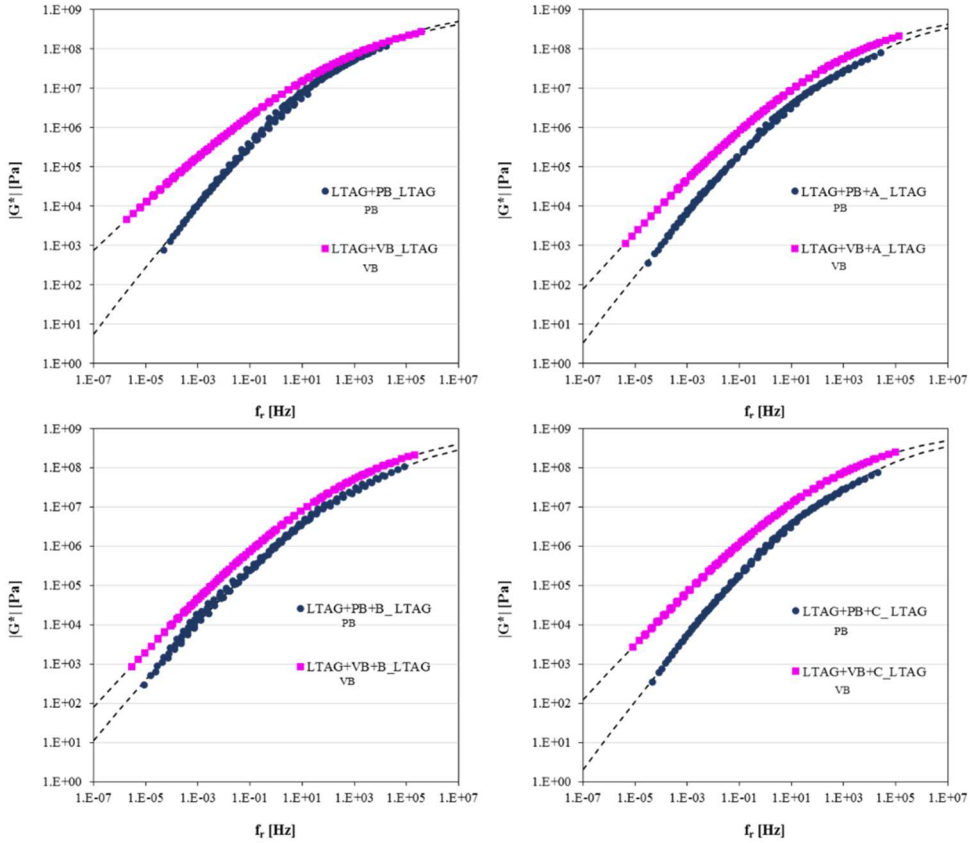

Figure 6.14. Comparison among the long-term aged hot recycled bitumens (rejuvenated or not), obtained from the two different reference bitumens in terms of |G*| master curves at 34 °C.

Table 6.18. Comparison among the modified CAM model and WLF law parameters for the long-term aged hot recycled bitumens (rejuvenated or not), obtained from the two different reference bitumens.

CAM modified model	$G^* = G_e^* + \frac{G_g^* - G_e^*}{[1+(\frac{f_c}{f})^k]^{\frac{m_e}{k}}}$						
	G^*_e [Pa]	G^*_g [Pa]	f_c [Hz]	k	m_e	$S = \text{Log}\frac{2^{\frac{m_e}{k}}}{1+(2^{\frac{m_e}{k}}-1)\cdot\frac{G_e^*}{G_g^*}}$	R^2
$LTAG_{PB}$+PB_LTAG	0	1E+09	280	0.180	0.87	1.450	0.994
$LTAG_{VB}$+VB_LTAG	0	1E+09	225	0.15	0.65	1.339	0.983
$LTAG_{PB}$+PB+A_LTAG	0	1E+09	360	0.154	0.88	1.710	0.996
$LTAG_{VB}$+VB+A_LTAG	0	1E+09	240	0.16	0.75	1.457	0.988
$LTAG_{PB}$+PB+B_LTAG	0	1E+09	350	0.140	0.82	1.760	0.996
$LTAG_{VB}$+VB+B_LTAG	0	1E+09	260	0.150	0.75	1.495	0.988
$LTAG_{PB}$+PB+C_LTAG	0	1E+09	365	0.158	0.90	1.710	0.996
$LTAG_{VB}$+VB+C_LTAG	0	1E+09	250	0.17	0.73	1.332	0.990

WLF law	$\text{Log}(a_t) = -\frac{C_1(T-T_0)}{C_2+(T-T_0)}$		
	C_1	C_2	T_0 [°C]
$LTAG_{PB}$+PB_LTAG	21.0	239.0	34
$LTAG_{VB}$+VB_LTAG	27.0	215.0	34
$LTAG_{PB}$+PB+A_LTAG	21.0	225.0	34
$LTAG_{VB}$+VB+A_LTAG	27.5	240.0	34
$LTAG_{PB}$+PB+B_LTAG	24.5	227.5	34
$LTAG_{VB}$+VB+B_LTAG	27.5	230.0	34
$LTAG_{PB}$+PB+C_LTAG	20.0	223.0	34
$LTAG_{VB}$+VB+C_LTAG	24.0	220.0	34

Table 6.19. Comparison among the hot recycled bitumens (rejuvenated or not), obtained from the two different reference bitumens and investigated in terms of |G*| values at f = 1.59 Hz before and after ageing.

Bitumen	T = 4 °C		T = 58 °C	
	|G*| [Pa]	ΔG [%]	|G*| [Pa]	ΔG [%]
$LTAG_{PB}$+PB	3.60E+07	41.5	1.30E+04	88.0
$LTAG_{PB}$+PB_LTAG	6.15E+07		1.08E+05	
$LTAG_{PB}$+PB+A	1.75E+07	53.1	6.27E+03	88.1
$LTAG_{PB}$+PB+A_LTAG	3.73E+07		5.25E+04	
$LTAG_{PB}$+PB+B	2.07E+07	59.1	5.55E+03	88.7
$LTAG_{PB}$+PB+B_LTAG	5.06E+07		4.89E+04	
$LTAG_{PB}$+PB+C	1.05E+07	69.6	3.65E+03	93.0
$LTAG_{PB}$+PB+C_LTAG	3.45E+07		5.19E+04	
Bitumen	**T = 4 °C**		**T = 58 °C**	
	|G*| [Pa]	**ΔG [%]**	**|G*| [Pa]**	**ΔG [%]**
$LTAG_{VB}$+VB	4.47E+07	46.5	1.64E+04	95.3
$LTAG_{VB}$+VB_LTAG	8.36E+07		3.47E+05	
$LTAG_{VB}$+VB+A	1.98E+07	63.3	7.45E+03	94.8
$LTAG_{VB}$+VB+A_LTAG	5.39E+07		1.42E+05	
$LTAG_{VB}$+VB+B	2.66E+07	54.9	7.62E+03	93.3
$LTAG_{VB}$+VB+B_LTAG	5.90E+07		1.14E+05	
$LTAG_{VB}$+VB+C	2.20E+07	66.5	1.08E+04	94.6
$LTAG_{VB}$+VB+C_LTAG	6.57E+07		1.99E+05	

Table 6.20. Comparison among the long-term aged hot recycled bitumens (rejuvenated or not) obtained from the two different reference bitumens and investigated in terms of |G*| at f = 1.59 Hz.

Bitumen	T = 4 °C		T = 58 °C	
	|G*| [Pa]	ΔG_{VB-PB} [%]	|G*| [Pa]	ΔG_{VB-PB} [%]
$LTAG_{PB}$+PB_LTAG	6.15E+07	26.4	1.08E+05	68.9
$LTAG_{VB}$+VB_LTAG	8.36E+07		3.47E+05	
$LTAG_{PB}$+PB+A_LTAG	3.73E+07	30.8	5.25E+04	63.0
$LTAG_{VB}$+VB+A_LTAG	5.39E+07		1.42E+05	
$LTAG_{PB}$+PB+B_LTAG	5.06E+07	13.7	4.89E+04	57.1
$LTAG_{VB}$+VB+B_LTAG	5.90E+07		1.14E+05	
$LTAG_{PB}$+PB+C_LTAG	3.45E+07	47.5	5.19E+04	73.9
$LTAG_{VB}$+VB+C_LTAG	6.57E+07		1.99E+05	

6.3 Summary

The experimental investigation described in the first phase of Ph.D investigation focused on the assessment of the rheological properties of two reference bitumens considered during their overall service life that includes their reuse in hot recycling by adopting different rejuvenators.

Based on the results obtained, the following conclusions can be drawn:

1. Although a comparable rheological behaviour of the two reference bitumens when unaged, these latter exhibit a different oxidative level because of the different manufacturing process that makes the visbreaking bitumen more unstable and consequently subjected to a more severe ageing;
2. Regardless of the reference bitumen considered, ageing entails an increase in |G*| values, indicating a bitumen hardening, and a reduction in phase angles δ, corresponding to a prevalence of the elastic component G_1 over the viscous component G_2. In addition, the analysis of the master curve parameters shows a decrease in shape index S, as an evidence of a higher sensitivity to frequency changes, and in crossover frequency f_c, suggesting a greater overall elastic behaviour. Moreover, higher C_1 and C_2 values are a further consequence of oxidation according to the reduction in fractional free volume (i.e. reduction of molecular mobility);
3. Whatever the reference bitumen considered, rejuvenators modify bitumen chemistry and consequently rheology by enhancing the viscous response of the bitumen, as confirmed by a decrease in |G*| values and a rise of phase angles δ, corresponding to a lower G_1/G_2 ratio. In terms of master curve parameters, compared to the corresponding unrejuvenated bitumen, bitumens including any rejuvenator exhibit higher shape index S, as an indication of a more gradual transition from the elastic to

the viscous behaviour, and crossover frequency f_c and thus a remarkable retrieval of viscous component in the behaviour. Moreover, all the additives used are even approaching to restore the rheological properties of the virgin bitumen, because of the comparable values obtained for both model and rheological parameters;

4. Ageing has a similar effect on virgin bitumen and bituminous blends including RAP bitumen, independently of the reference bitumen considered. However, as confirmed by a lower variation of parameter values pre and post ageing, oxidation is less detrimental on the hot recycled bitumens (rejuvenated or not) than on the virgin bitumen, since the former include 50% of aged RAP bitumen;
5. The addition of a rejuvenator in hot recycling leads to a corresponding composite bituminous blend which can be even less stiff than the associated virgin bitumen alone at the end of service life, suggesting significant benefits when dealing with high RAP contents.

In conclusion, this experimental study provides an important contribution to understand the effect of ageing on the rheological properties of the bituminous blends containing virgin and RAP bitumens.

Based on the above-described findings, it is reasonable to expect that recycled bituminous mixtures prepared with virgin bitumens, rejuvenators and high amounts of RAP (which releases a percentage of the same aged bitumen) suffer less ageing phenomena and could also be less stiff than virgin mixtures. However, great importance should be given to the choice of the most suitable components of the mixture due to compatibility. In particular, type and dosage of rejuvenator and bitumen should be properly selected, since their interaction strongly affects the final mixture performance.

Part 2

Characterisation of the binder phase (bituminous mastic)

Chapter 7.

Literature review

A fundamental aspect in asphalt pavements is the correct understanding of cracking performance of bituminous materials, which is strictly linked to the properties of mastic phase and its components (i.e. filler and bitumen) (Jakarni, 2012; Kim, 2008).
These materials are subjected to a wide range of thermo-mechanical stresses that cause premature failure if not properly addressed during their entire service life. Fatigue is one of the main failure modes for flexible pavements. It consists in the formation of micro-cracks due to repeated loading cycles which leads to the appearance of macro-cracks by coalescence. Nevertheless, once a crack is opened in the pavement, it starts healing and, if there is enough time for the process to be completed, it may even close (Garcia, 2012). In particular, researchers believe that an asphalt pavement with extended service life is an achievable aim, since healing process is able to counter the development of micro-cracks (Karki et al., 2014; Roque et al., 2012). Nowadays, investigations regarding healing phenomenon in asphalt pavements have been classified within environmentally sustainable strategies in the construction engineering domain. In fact, when asphalt pavements have the ability to repair small cracks, it will considerably decrease maintenance costs, extend service life and eventually reduce greenhouse gas emission (Chung et al., 2015). Recently, preventive maintenance approaches via the promotion of the healing capability of bituminous materials, such as induction heating technology, are considered as a new way of increasing durability and service life of road pavements (Liu et al., 2012a; Menozzi et al., 2015) and it also potentially guarantees economic and environmental benefits. In addition, healing property becomes even more important when materials are engineered for long-term service like road pavements and where repair and maintenance are not easy (Joseph et al., 2009; Wool, 2008).
As a key issue which has not been highlighted in the majority of studies, healing phenomenon in bituminous materials refers to diminishing micro-cracks and eventually partial recovery of properties. Subsequently, all types of recovery of the properties in bituminous materials should not be considered as a healing process. In general, healing is related to the recovery of structural damages (microcracks), whereas recoverable phenomena, such as thixotropy, can be observed when there are no microcracks and can permanently restore material properties (Ashouri, 2014; Moreno-Navarro et al., 2015). Therefore, in order to avoid misleading-analyses, it is important to distinguish between real recovery due to self-healing and recovery due to intrinsic viscoelastic responses (Ayar, 2015), especially with respect to thixotropy, since the latter does not contribute to fatigue life.

7.1 Fatigue phenomenon

Each time a vehicle passes, bituminous materials in road pavement are subjected to short-term loading that can result in a loss of rigidity of the material, if sufficiently high, or even lead to failure, by accumulation in the long-term. Consequently, in pavement construction the correct understanding of fatigue deterioration process is fundamental for a proper structural design.

Two main phases of the degradation process are usually considered during fatigue cracking. The first phase corresponds to degradation, resulting from damage that is uniformly spread in the material. Hence, this phase is manifested by the initiation and propagation of a "micro-crack" network (in a diffuse way), which results in a decrease in the macroscopic rigidity (modulus). In the second phase, as a consequence of the micro-cracks coalescence, a "macro-crack" appears and propagates within the material. The coalescence appears at a certain value of micro-cracking (or level of damage, or level of fatigue). The two phases may be governed by quite different physical evolution laws and consequently are usually modelled within different theoretical frameworks. In details, damage mechanics (DM) and linear elastic fracture mechanics (LEFM), respectively, are examples of frameworks used for the deterioration phases. At present, it is theoretically challenging to model both phases jointly in a unified approach. During experimental fatigue testing of bituminous materials, the two phases can be considered as appearing successively or, for some test geometries, parallel in time. Besides deterioration related to damage initiation and propagation, other phenomena can contribute to stiffness reduction during fatigue testing, but they are not interpreted as fatigue. One of these artefact phenomena is self-heating caused by dissipated energy generation, resulting from the tested material's inherent viscous property (de La Roche et al., 1996a; de La Roche et al., 1996b; Di Benedetto et al., 1996; Di Benedetto et al., 1997a). Another phenomenon which may determine a pronounced stiffness decrease during mechanical excitation seems to be bitumen thixotropy (Di Benedetto et al., 1997b; de La Roche, 1996; Soltani, 1998). Fatigue response is very sensitive to boundary and loading conditions (Di Benedetto et al., 2014) and this behaviour induces a scatter of the results, which makes more complex the general interpretation of the tests. As previously mentioned, fatigue damage affects material stiffness and consequently implies a reduction of the modulus recorded. However, fatigue should not be mistaken for permanent deformation. When only compressive excitation (or tensile) is applied, the irreversible accumulated strain can become substantial, which may hide the effect associated with fatigue.

7.2 Damage accumulation

Damage analysis is often based on the concept of effective stress (Lemaitre and Desmarat, 2005). Damage is assumed to cause a decrease in the surface area over which stresses are applied. This reduction of effective area occurs because the surface area which is stressed decreases due to the formation and growth of defects and voids. This is the basic concept

used in continuum damage modelling. In fatigue testing of bituminous mixtures, it is reasonable to assume that repeated loading leads to the formation of micro-voids and defects. Whereas the cause for changes in material response during DSR fatigue testing of bitumens are less clear.

7.3 Thixotropic contribution

Mewis and Wagner (2009) defined thixotropy as "*the continuous decrease of viscosity with time when flow is applied to a sample that has been previously at rest and the subsequent recovery of viscosity in time when flow is discontinued*". Thixotropy is a form of structural nonlinearity and, thus, not a form of damage. Structural nonlinearity is associated with reversible micro-structural changes (Malkin, 1995). Structural changes can include changes in "regular" structure or configuration and "rupture" of inner micro-structure. Structural nonlinearity is possible even if the material is being loaded outside the linear viscoelastic regime or when continuous, reversible changes evolve over time (i.e. thixotropy).
The changes in microstructure leading to thixotropic behaviour are not well understood. Generally, thixotropy is thought to be associated with relatively weak attractive forces. There are two competing mechanisms during flow: break-down due to stresses and build-up due to random collisions between particles and Brownian motion (Barnes, 1997). Brownian motion is the random thermal motion of molecules. When molecules collide due to this random motion, they can attach to each other, given the necessary attractive forces, forming flocs. During loading, stresses can cause flocs to break apart over time, leading to thixotropic behaviour. When loading is ceased, Brownian motion dominates and molecules will collide and flocs will be formed. Recovery/formation of flocs can take significantly longer than break-down (Barnes, 1997). Both increased shear rate and loading time increase breakage (Mewis and Wagner, 2009). With respect to bituminous materials, Shan et al. (2011) demonstrated that thixotropy affects the entire performance of the bitumen, especially in terms of fatigue and healing response at high temperatures. In fact, thixotropy is associated with the colloidal nature of bitumen, which forms by the source of bitumen, the degree of processing and the temperatures (Qiu, 2012). Previous experiment shows that during repetitive loadings thixotropy causes a progressive change from a gel to a sol structure, whereas during rest periods the gel structure starts to reform (Gaskin, 2013).

7.4 Self-healing capability

"*Self-healing materials are inspired in nature. They are artificial counterparts of a tree, which can recover damage to its trunk by itself, or a cut in a finger, which seemingly spontaneously stops bleeding*" (NL Agency, 2010). Materials that possess healing capability are able to (partially) recover themselves when suffering mechanically or thermally induced damage and thus restore their original set of properties (Liu, 2012; Wool, 2008). Self-healing materials generally include polymers, metals, ceramics (Wool, 2008), glass, concrete,

bitumen (Qiu, 2012; Shen and Carpenter, 2007) and their composites. Few materials, however, have the ability to heal as an intrinsic property (Wool, 2008) and the majority of studies have focused on the use of novel self-healing systems, particularly the case of polymers for the repair of cracks (Liu, 2012). Some of these systems have a shell structure with an embedded liquid (such as microcapsules, hollow fibers, microvascular networks, etc.) and, when a crack passes through it, the shell will tear and the embedded liquid flows to fill and repair the crack (Joseph et al., 2009; Qiu, 2012). Since the mechanisms thought to underlie healing remain unclear (Qiu, 2012), there is no exact definition of healing capability in asphalt pavements. Nevertheless, healing capability is generally regarded as the intrinsic response of bitumen to diminish the generated cracks within the bituminous body and consequently initiate the partial recovery of its original properties (Canestrari et al., 2015; Shen and Carpenter, 2007).

Usually material properties degrade over time due to the initiation of damage (like micro-cracking) on a microscopic scale that tends to grow and will ultimately lead to failure of the material. In this respect, the self-healing capability of asphalt pavements is limited to the repair of microcracks, since macrocracks do not close unless external forces are applied to press the cracked surfaces together (Jones and Dutta, 2010) and self-healing cannot recover the damage due to permanent deformations (Menozzi et al., 2015).

Two main types of healing exist in bituminous mixtures: adhesive healing at the bitumen-aggregate interface and cohesive healing within the bituminous phase. More in details, the healing process of bituminous materials consists of a three-step-mechanism: (1) surface approach due to the consolidation of stresses and flow of bitumen; (2) wetting (adhesion of two crack surfaces driven together by surface energy); (3) the complete recovery of mechanical properties due to diffusion and randomisation of asphaltene structures (Phillips, 1998). According to Phillips (1998), during pavement service life there is competition between fatigue and healing. Figure 7.1 shows a schematic diagram of this mechanism. Of these steps, the first is the fastest one, whereas the other two steps are much slower. Further, the first step almost leads to recovery of modulus (stiffness) and the other two steps determine an improvement of both modulus and strength. Wetting ability is related to the type of bitumen, such that bitumen with a higher surface energy has a higher wetting ability (Ashouri, 2014). Additionally, the capability of diffusion is directly linked to mobility potential of the molecules in the bitumen and a bitumen containing more molecules with longer chains and fewer branches has a higher molecular mobility (Kim et al., 1990).

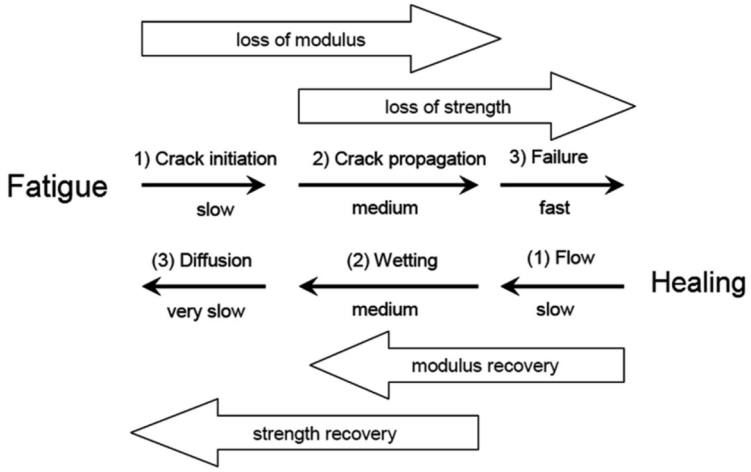

Figure 7.1. A schematic diagram of the three step healing mechanism in bitumen (Qiu, 2012).

7.4.1 Characterisation of bituminous material self-healing

Since the 1960s, healing phenomenon or recovery capability in bituminous materials have been a focus of research in both laboratory and field (Bazin and Saunier, 1967; Raithby and Sterling, 1970). In particular, studies focused on different levels, dependent on the subject. They include bitumen, bituminous mastic, bituminous mixture and the asphalt pavement itself characterised using fatigue, fracture or non-destructive tests. Fatigue tests with the insertion of rest periods represent the main method for self-healing capability evaluation in laboratory. This test method was performed on bituminous mixtures by means of Four Point Bending Test (4PBT) or Indirect Tensile Test (ITT) (Qiu, 2012; Shen and Caerpenter, 2007) and diffusely on bitumens, especially by means of Dynamic Shear Rheometer (DSR) (Lu et al., 2003; Bodin et al., 2004; Stimilli et al., 2012; Stimilli et al., 2014; Canestrari et al., 2015; Santagata et al., 2015) and seldom by means of Binder Bond Strength (BBS) (Huang et al, 2016; Lv et al., 2017). Besides, fatigue tests with rest periods were carried out on mastics on limited scale by means of Three Point Bending Test (3PBT) or DSR (Garcia, 2012; Underwood, 2016; Mazzoni et al., 2016, 2017b and 2017c). With respect to non-destructive tests, Atomic Force Microscopy (AFM) (Das Kumar et al., 2012; Nazzal, 2012) and Scanning Electron Microscopy (SEM) (Lu, 2013, Qiu, 2012) were used to evaluate bitumen self-healing capability. Moreover, non-destructive methods were also employed to measure field healing potential by means of Falling Weight Deflectometer (FWD) or Stress Waves (Groenedijk, 1998; Williams et al., 2001).

7.4.2 Influence factors on bituminous material self-healing

Internal factors

Bitumen properties strongly affect asphalt pavement self-healing capability (Liu, 2012, Qiu, 2012), since the latter is mainly related to the interdiffusion of bitumen components (Wool, 1981). However, it is clear that self-healing potential of bitumen allows the corresponding bituminous mixture to recover. In the following paragraphs, bitumen and bituminous mixture characteristics as well as modifiers are presented as internal factor influencing self-healing capability.

Physical properties

Many researchers demonstrated that a soft bitumen with a high penetration grade and a low softening point exhibits a higher self-healing capability than a hard bitumen (Van Dijk et al., 1972; Bonnaure et al., 1982). Moreover, low viscosity is considered as a positive factor for healing process occurrence in bitumen (Garcia et al., 2014; Kim et al., 2003).

Chemical composition

Previous researches concluded that bitumens with low amphoteric and high aromatic contents (low molecular weight fractions) possess a higher healing capability (Little et al., 1999; Schmets et al., 2010). Indeed, there is a direct relationship between aromatic content in terms of the acid-base component of surface energy and long-term healing rate (Little et al., 1999). The surface free energy can be divided into two parts, including the Lifshitz-Van der Waals and the Lewis acid-base components. The Lewis acid-base component positively affect long-term healing, whereas the Lifshitz-Van der Waals component can have a detrimental effect on short-term healing (Lytton, 2000; Williams et al., 2001). Additionally, a high amount of heteroatoms favours healing process, since sulfur, oxygen, and nitrogen promote bitumen polarity. A high presence of waxes is also helpful for healing due to the Van der Waals force of the interactions between long chains of hydrocarbons and aliphatic molecules within the wax (Schmets et al., 2010; Williams et al., 2001). Since it is recognised that a higher diffusion capability in a bitumen is linked to a higher molecular mobility, Kim et al. (1990) introduced two parameters to quantify this aspect: MMHC ratio and CH_2/CH_3 ratio. The former stands for methylene and methylene hydrogen atoms to methyl and methylene carbon atoms and is related to the amount of the branching in chains, whereas the latter means methylene to methyl and is associated with the length of chains. Thanks to their research, Kim et al. (1990) demonstrated that the diffusivity and rate of healing increases with the decrease in MMHC ratio (the amount of branching).

Ageing

In literature, there are discordant opinions about ageing effect on self-healing capability in bituminous materials. According to Little et al (1999), ageing negatively affects the self-healing capability of a laboratory aged sand mixture specimen, even if he also indicated the addition of hydrated lime as an enhancement for self-healing potential of an aged specimen.

On the opposite, Canestrari et al. (2015) found a positive effect in term of healing capability in Styrene Butadiene Styrene (SBS) modified bitumens including a certain amount of the same long-term aged bitumen (up to 45%), suggesting a beneficial interaction between the shorter polymer chains caused by ageing process and the unaged chains of virgin bitumen.

Volumetric properties

For a bituminous mixture, a high self-healing potential is found to be related to a high bitumen content (Molenaar, 2007, Van Gooswiligen et al., 1994). In addition, an improvement in self-healing is also favoured by high voids filled with bitumen (VFA), low voids in mineral aggregate skeleton (VMA) as well as a low air void content (VA) (Qiu, 2012; Van den Bergh, 2011). Further researchers concluded that the healing properties of bituminous mixtures are more affected by composition characteristics (which in turn affect the aggregate interlock, the film thickness, etc.) than by polymer modifications (Kim and Roque, 2006; Grant 2001). In particular, self-healing process within coarse-graded bituminous mixture is much faster than fine-graded mixture. A coarse gradation with a lower surface area can provide a thicker bitumen film and fewer transition zones between aggregate and bitumen. This condition is therefore favourable for improving crack healing (Abo-Qudais and Suleiman, 2005; Grant, 2001). Moreover, Lee found that Stone Matrix Asphalt (SMA) shows the highest healing capacity compared to other types of bituminous mixtures (Lee et al., 1995 and 2000).

Modifiers

As reported in literature, the influence of modifiers on self-healing capability of bituminous materials is not clear. In particular, many researchers indicated that the presence of elastomers (e.g. SBS) improved self-healing capability of the corresponding bitumen and also bituminous mixtures (Lee et al, 2000; Shen and Carpenter, 2007; Canestrari et al, 2015). In contrast, Little et al. (1999) concluded that the addition of SBS polymer modifier acts as a filler interrupting the ability of pure bitumen to recover and thus causing detrimental effect in terms of self-healing occurrence. Moreover, Kim and Roque found that SBS modification has a relatively small effect on healing rate of bituminous mixtures. Qiu (2012) stated to assess effects of SBS modification according to the related damage level present in the corresponding bituminous material. In particular, SBS polymer modification negatively affects on the healing capability of bituminous mastic when considering the healing of an open crack, whereas it positively acts at a lower damage level where micro-cracks develop thanks to the confinement effect of the undamaged SBS polymer network.

With respect to other modifiers, using rejuvenators is a well-known technique not only for the recovery of aged bitumen properties, but also for enhancing self-healing capability of asphalt pavements (Menozzi et al., 2015; Su et al., 2013a).

External factors

Besides the internal factors above-mentioned, some important boundary conditions favour self-healing detection in bituminous material. In the following paragraphs, the major external factors influencing self-healing capability are discussed.

Rest periods

Many researchers accepted the beneficial effect of rest periods on self-healing capability in bituminous materials under different loading conditions (Stimilli et al, 2012; Van Dijk et al., 1972; Bazin et al., 1967; Kim et al., 2002; Bahia et al., 1999). In particular, the longer the rest period, the higher the damage recovery (Kim et al., 2002; Van Dijk et al., 1972). However, rest period duration required for healing occurrence in laboratory depends on both loading condition (Qiu, 2012) and type of bituminous mixture (Castro and Sanchez, 2006).

Temperature

Temperatures play a fundamental role as self-healing influencer. It is well-established that at high enough temperatures healing rapidly occurs (Daniel and Kim, 2001; Kim and Roque, 2006; Grant, 2001), whereas low temperature values inhibit molecular mobility, preventing the restoration of the original chemical structure and initial physicomechanical properties.

Loading condition and damage level

Loading amplitude is considered as one of the most important factors influencing asphalt pavement self-healing capability. Various studies have shown that a high tensile stress/strain level has detrimental effects on self-healing capability (Van Dijk et al., 1972; Castro and Sanchez, 2006). The lower the damage level, the higher the healing capability (Song et al., 2005; Zhang et al., 2001). In fact, when macro-cracks occur, it becomes difficult to recover material properties through healing phenomena (Molenaar, 2007; Zhang, 2000).

Moisture

Previous studies demonstrated that moisture negatively affects self-healing of adhesive bonds, since it has a higher affinity for the aggregates than bitumen and therefore could prevent self-healing occurrence (Hefer and Little, 2005).

7.4.3 Modelling of bituminous material self-healing

As previously mentioned, most of the relevant studies concerning healing evaluation were carried out in laboratory. Consequently, there is the need to bridge the lack of a proper understanding of healing process, at a field scale, and the quantification of its contribution in pavement durability improvement and service life extension. The best method for analysing healing mechanisms in bituminous materials is the simultaneous investigation of the mechanical and chemical characteristics through healing experiments. With respect to self-healing detection in bituminous material, two main models can be found in literature: physical-chemical based healing model and mechanical based healing model. The former is

a somewhat conceptual model to explain healing phenomenon using physical-chemical theories, whereas the latter is basically a regression model to pattern healing phenomenon in a macroscopic continuum damage state. Details of these two models can be found hereafter.

Physical-chemical based healing model

Multi-step healing model

In the 1980s, an extensive research dealt with crack healing of thermoplastic polymers. It was noticed that, when two pieces of the same polymer are brought into contact at a temperature above its glass transition temperature (T_g), the interface gradually disappears and the mechanical strength at the polymer–polymer interface increases as the crack heals across the interface. As shown in Figure 7.2, Wool and his colleagues suggested a five stages model to explain the crack healing process in terms of surface rearrangement, surface approach, wetting, diffusion and randomisation (Kim et al., 1983; Wool et al., 1981; Wool et al., 1982). They concluded that the stages of wetting and diffusion are responsible for the majority of mechanical property recovery or healing, and control the intrinsic healing function $R_h(t)$. The observed macroscopic recovery R is a convolution product as shown in Equation (7.1):

$$R = \int_{-\infty}^{t} R_h(t-\tau)\frac{d\Phi(\tau)}{d\tau}d\tau \quad (7.1)$$

where,

$R_h(t)$ is an intrinsic healing function of time t;

$\Phi(t)$ is a wetting distribution function of time t;

τ is a time variable.

Intrinsic healing functions for strength, elongation at break, impact energy and fracture parameters were obtained as a function of time, molecular weight, temperature, pressure and processing conditions, in perfect agreement with the theory.
Because of the similarity between healing process of bituminous materials and healing process of thermoplastic polymers above-mentioned, Phillips (1998) adopted this five stages model to describe fatigue and healing capability of bituminous materials.
Figure 7.1 depicted in paragraph § 7.4 shows that not only fatigue can be described using a three-step model (namely crack initiation, crack propagation and failure), but also self-healing process of bituminous material is believed to be a three-step process. This three-step healing process consists of: (1) closure of macro-cracks due to consolidating stresses and flow; (2) closure of micro-cracks linked to wetting (adhesion of two crack surfaces driven together by surface energy); (3) complete recovery of mechanical properties related to diffusion. Step (1) is believed to be the fastest one and implies only a stiffness recovery, whereas steps (2) and (3) are thought to occur much slower, but to improve both stiffness and strength of the material that consequently exhibits mechanical properties comparable with the virgin condition.

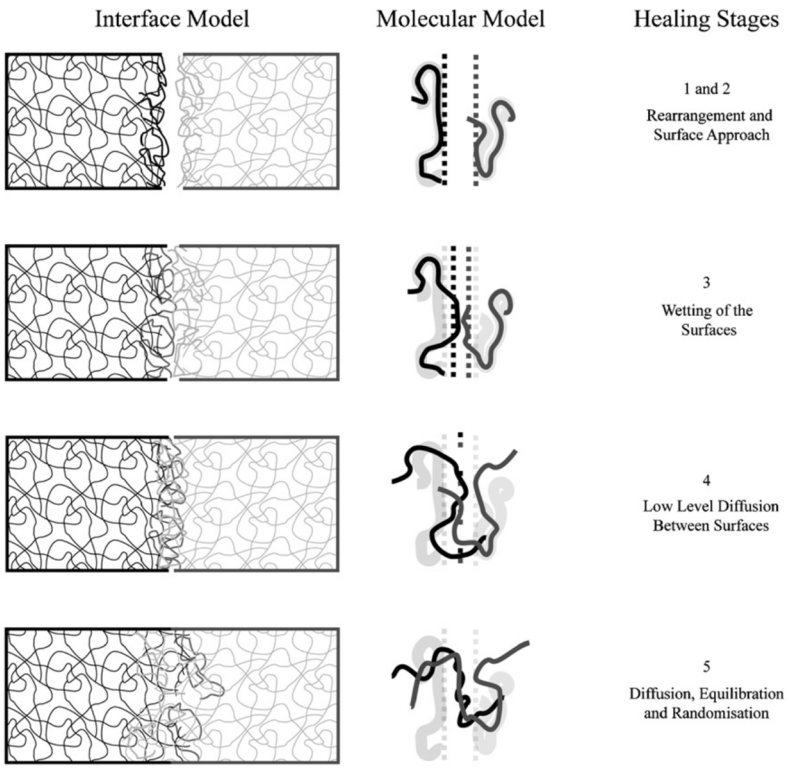

Figure 7.2. Schematic diagram showing the five steps of crack healing (Wool et al., 1982; Wu et al., 2008).

Thixotropy model

As previously described in paragraph § 3.2.1, bitumen is traditionally considered as a colloidal system where high molecular weight asphaltene micelles are dispersed or dissolved in a lower molecular weight oily medium (maltenes) (Figure 7.3) (Read and Whiteoak, 2003). The micelles are considered to be asphaltene clusters covered by an absorbed layer of high molecular weight aromatic resins which act as a stabilising solvating medium. Away from the centre of the micelle there is a gradual transition to less polar aromatic resin layers which extend outwards to the less aromatic oily dispersion medium. According to the colloidal nature of bitumen, the latter can be divided into three categories: sol bitumen, gel bitumen and sol-gel bitumen. The sol bitumen has a sufficient amount of resins and aromatics, with enough solvating power to fully peptise the asphaltenes. Therefore, the resulting micelles have a good mobility within bitumen. The gel bitumen has not enough aromatic/resin fractions to peptise the micelles. The asphaltenes can associate further in a gel type bitumen.

This can lead to an irregular open packed structure of linked micelles. The rest of the space is filled with an intermicellar fluid of mixed constitution. In practice, most bitumens show an intermediate colloidal character, called sol-gel bitumen.

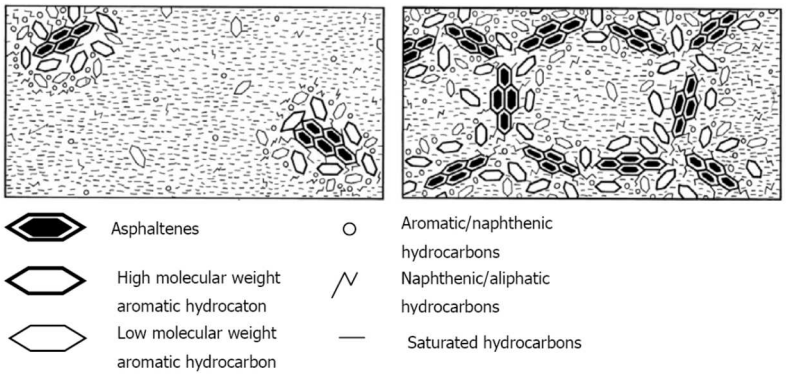

Figure 7.3. Schematic representation of sol (left) and gel (right) type bitumen (Read and Whiteoak, 2003).

Since 1930s bitumen was found to exhibit a so-called thixotropic behaviour (Saal et al., 1940; Traxler et al., 1935; Mouillet et al., 2012) which is also widely observed in many colloidal systems. Thixotropy is defined as the tendency of a material's viscosity to decrease with time when subjected to flow/stress, and to recover with time when the flow/stress is stopped (Tan et al., 2011). Thixotropy is demonstrated to be an inherent material property of bitumen and to have a significant effect on bitumen rheological properties (Traxler et al., 1935). In addition, thixotropy is strictly linked to the colloidal nature of bitumen, which depends on the source of bitumen, the degree of processing and the temperatures. Thixotropy is also thought to be related to the changes in a material's microstructure (Tan et al., 2011). The microstructure of the material breaks down and its viscosity decreases by applying stress/flow. After a period of rest, the material regains the broken-down structure and its viscosity increases to the initial value thanks to molecular movement. Verstraeten (1991) related the thixotropic effect to the stiffness decrease during fatigue tests and its recovery during rest periods (Castro and Sanchez, 2006). Based on fatigue test results performed on bituminous mixtures at the Belgium Road Research Centre, he proposed that at temperatures higher than 15 °C fatigue of bituminous mixtures is mainly caused by thixotropic effect in the bitumen. During load repetitions, bitumen changes progressively from a gel to a sol type structure. Whereas during rest periods bitumen returns from a sol to a gel structure. If rest time is sufficiently long, recovery would be almost total. However, at low temperatures (less than 5 °C), fatigue is determined by structural damage because of load repetitions and recovery of the structural damage at low temperatures would be only partial. This proposition has been proven by many researchers. Soltani and Anderson (2005) concluded that the loss

in modulus during a fatigue test and the gain in modulus during rest periods are the result of thixotropy. Di Benedetto et al. (2011) considered thixotropy as one of the artefacts which influences the real fatigue performance of bituminous mixtures and it can be modelled using an equivalent temperature increase. Shan and her colleagues (2012) introduced the Cox-Merz relationship of the thixotropy model to characterise fatigue and healing behaviour using the break-down and build-up coefficients of the microstructure. It is observed that thixotropy plays a role in fatigue and healing characteristics of bituminous binders. When comparing the thixotropic model with the multi-step healing model, both models explain the recovery process during rest periods. However, the multistep healing model illustrates the healing process in case of damage (micro-cracks, macro-cracks), whereas the thixotropy model interprets the recovery process in case of molecular motion and the rebuilt of the microstructure, which is not necessarily related to a crack.

Mechanical based healing model

VECD model

The theory that fatigue in bitumen and mastic is the result of the combined effects of linear viscoelasticity (LVE), non-linear viscoelasticity (NLVE) and damage represents the basis for the modelling approach developed by Underwood (2016). For each of the three mechanisms, separate material models are proposed and then integrated into the final formulation. A key component for fatigue response is damage, which is supposed to exist in the form of micro-cracks that upon continued loading coalesce to form a localised macro-crack that then dominates the behaviour. This hypothesis stems from studies that have examined the morphology of failure surfaces in time-sweep fatigue tests on bituminous binders and shown the presence of radial cracks (Wen et al., 2009; Asphalt Research Correspondent, 2013). This model is able to describe material response between the intact and localisation stages. Linear viscoelastic materials exhibit time-temperature dependent behaviours, which can be modelled through a convolution integral representation:

$$\sigma_{ij}(t_r) = \int_0^{t_r} C_{ijkl}(t_r - \xi)\frac{d\varepsilon_{kl}}{d\xi}d\xi \tag{7.2}$$

$$\varepsilon_{kl}(t_r) = \int_0^{t_r} S_{klij}(t_r - \xi)\frac{d\sigma_{ij}}{d\xi}d\xi \tag{7.3}$$

$$t_r = \int_0^{t}\frac{dt}{a_T} \tag{7.4}$$

where $C_{ijkl}(t_r)$ and $S_{klij}(t_r)$ are the relaxation moduli and creep compliances, respectively; t is the time; t_r is the reduced time; a_T is the time–temperature shift factor; ξ is an integration variable; σ_{ij} is stress; and ε_{kl} is strain.

If temperature is constant for a prescribed period, Equation (7.4) simplifies to a more common form $t_r = t/a_T$. The experimental configuration in this study involved oscillatory

loading and thus the constitutive equations are further specialised according to Equations (7.5) and (7.6).

$$\tau(t_r) = \int_0^{t_r} G(t_r - \xi) \frac{d\gamma}{d\xi} d\xi \tag{7.5}$$

$$\gamma(t_r) = \int_0^{t_r} J(t_r - \xi) \frac{d\tau}{d\xi} d\xi \tag{7.6}$$

where G is the relaxation modulus in shear, J is the creep compliance in shear, σ is shear stress, and γ is shear strain. As common practice, Prony series represent the relaxation and compliance functions:

$$G(t_r) = \sum_{i=1}^{m} G_i e^{\frac{-t_r}{\rho_i}} \tag{7.7}$$

$$J(t_r) = J_g + \frac{\eta}{t_r} + \sum_{j=1}^{n} J_j \left(1 - e^{\frac{-t_r}{\lambda_i}}\right) \tag{7.8}$$

where G_i are relaxation modulus Prony terms, ρ_i are relaxation times, J_i are compliance Prony terms, η is the steady-state viscosity, λ_i is the retardation times, and J_g represents the glassy compliance. These formulations are used because of their computational efficiency and because they allow relatively easy manipulation between time and frequency domains. This aspect is particularly important in fatigue modelling applications with viscoelastic materials as it can simplify the characterisation process without sacrificing the predictive capabilities in the time domain. Fourier transformation is used to derive these relationships, see Equations (7.9) and (7.10), where *R'* is the real component of the response function in the frequency domain (the in-phase component) and *R''* is the imaginary or out of phase component of this function. By first substituting Equations (7.7) or (7.8) and then simplifying the relaxation and creep functions are given in the frequency domain by Equations (7.11) and (7.12).

$$R' = Re\left\{j\omega \int_0^{\infty} R(t) e^{-j\omega t}\, dt\right\} \tag{7.9}$$

$$R'' = Im\left\{j\omega \int_0^{\infty} R(t) e^{-j\omega t}\, dt\right\} \tag{7.10}$$

$$G' = \sum_{i=1}^{m} \frac{G_i \rho_i^2 \omega^2}{1 + \rho_i^2 \omega^2} \tag{7.11}$$

$$G'' = \sum_{i=1}^{m} \frac{G_i \rho_i \omega}{1 + \rho_i^2 \omega^2} \tag{7.11}$$

$$J' = J_g + \sum_{j=1}^{n} \frac{J_j}{1 + \tau_j^2 \omega^2} \tag{7.12}$$

$$J'' = \frac{1}{\eta\omega} + \sum_{j=1}^{n} \frac{J_j \tau_j \omega}{1 + \tau_j^2 \omega^2} \tag{7.12}$$

Bitumen and mastic can be considered as purely LVE materials only within a limited range of strain levels and thus consideration for nonlinear behaviours is necessary for a proper fatigue process modelling (Tan et al., 2012; Motamed et al., 2012; Motamed et al., 2013; Masad et al., 2009; Rajagopal et al., 1998; Narayan et al., 2013). These behaviours are thought to be distinct from damage, but they can occur simultaneously. A technique has been devised (RSS test) and a model developed to separate and account for these behaviours (Underwood et al., 2015). The resulting formulation, shown in Equation (7.13), is based on the single-integral nonlinear function proposed by Schapery.

$$\tau(t_r') = h_1 \int_0^{t_r'} G(t_r' - \xi) \frac{d(h_2 \gamma)}{d\xi} d\xi \tag{7.13}$$

$$t_r' = \frac{t}{a_T a_\gamma} \tag{7.14}$$

where t'_r is the strain dependent reduced time, a_γ is the strain shift factor, and h_1 and h_2 are the nonlinearity coefficients. These coefficients are found to express higher order strain dependency in the Helmholtz free energy, whereas a_γ is noted to relate to the influence of strain on free energy and entropy production (Schapery, 1966; Schapery, 1969). In the strictest sense, Equation (7.13) may not represent a fully NLVE model, since it lacks certain aspects linked to frame invariance of stresses and strains and it is inherently 1-D (it does not predict normal stresses due to shear). However, the model provides a rational and thermodynamically admissible solution to the issue of strain dependent deformation response independent of permanent changes in the materials structure, such as damage. In addition, although it is not shown here, these coefficients can be generalised to 3-D so as to provide an accurate representation of nonlinearity (Levesque et al., 2008). In the case of steady-state sinusoidal loading (approximately true for the time sweep experiments performed by Underwood) Equation (13) can be further simplified, as follows:

$$\tau(\omega_r) = h_1 \; x \; G^*(\omega_r')[\gamma_e(\omega_r)] \tag{7.15}$$

where γ_e is the effective strain during the cycle (h_1 multiplied strains) and ω'_r is dependent upon the actual frequency, ω (rad/s), and is referred to as the strain dependent reduced frequency, Equation (7.16).

$$\omega_r' = \omega_r \; x \; a_\gamma = (\omega \; x \; a_T) \; x \; a_\gamma \tag{7.16}$$

A continuum damage model motivated by Schapery's work-potential theory is adopted to explain the damage process (Schapery, 1990). The extended elastic–viscoelastic correspondence principle is first used to cast an elastically derived damage potential function to an equivalent viscoelastic form by replacing the physical strains with pseudo strains, γ^R, (Schapery, 1984). Pseudo strains shown in Equation (7.17) are represented as the linear viscoelastic stresses occurring from an applied strain multiplied by a reference modulus that ensures dimensional compatibility. This reference modulus could take on any value, but is

usually chosen to be either one or a value equal to the initial apparent elastic modulus of a test. Since this decision is arbitrary and ultimately does not impact the modelling effort, it is assumed to have a value of one in Underwood's study. The importance of the pseudo strain concept is that it removes all of the time dependency associated with the deformation process as long as these processes are wholly described via the single relaxation function and the nonlinear related parameters.

$$\gamma^R = \frac{h_1}{G_R}\int_0^{t_r'} G(t_r' - \xi)\frac{d(h_2\gamma)}{d\xi}d\xi \tag{7.17}$$

The calculation of pseudo strain in the time domain is facilitated by the use of a state variable based solution to Equation (7.17). Starting with this function and recognising that the relaxation modulus can be expressed as shown in Equation (7.7), the pseudo strain value at a time-step, n can be determined from the following expression:

$$(\gamma^R)^n = \frac{h_1}{G_R}\sum_{i=1}^{m} G_i \int_0^{(t_r')^n} e^{-\left[(t_r')^n - \xi\right]\lambda_i}\dot{f}(\xi)d\xi \tag{7.18}$$

From which the following internal state variable associated with the relaxation function is defined, as follows:

$$\eta_i^n = G_i \int_0^{(t_r')^n} e^{-\left[(t_r')^n - \xi\right]\lambda_i}\dot{f}(\xi)d\xi \quad i > 0 \tag{7.19}$$

Thus, the total pseudo strain can be determined using the following equation:

$$(\gamma^R)^n = \frac{h_1}{G_R}\sum_{i=1}^{m} G_i\eta_i^n \tag{7.20}$$

To determine the updating procedure for each of the η_i^n, their value at time step, t_{n+1}, can be written as;

$$\eta_i^{n+1} = \int_0^{(t')^{n+1}} e^{-\left[(t')^{n+1} - \xi\right]\lambda_i}\dot{f}(\xi)d\xi$$

$$= \int_0^{(t_r')^n} e^{-\left[(t_r')^{n+1} - \xi\right]\lambda_i}\dot{f}(\xi)d\xi + \int_{(t')^n}^{(t_r')^{n+1}} e^{-\left[(t_r')^{n+1} - \xi\right]\lambda_i}\dot{f}(\xi)d \tag{7.21}$$

On the right hand side, the first integral can be separated trough a proper manipulation of the exponential and the second integral can be simplified by assuming that the input, f, varies linearly between successive data points with a slope of $C_1 = \frac{(\varepsilon^{n+1} - \varepsilon^n)}{\Delta t}$. With these two adjustments, the updating rule becomes:

$$\eta_i^{n+1} = e^{\frac{-\Delta t_r'}{\lambda_i}} \int_0^{(t_r')^n} e^{-\left[(t_r')^n - \xi\right]\lambda_i} \dot{f}(\xi) d\xi + C_1^{n+1} \, x \int_{(t_r')^n}^{(t_r')^{n+1}} e^{-\left[(t_r')^{n+1} - \xi\right]\lambda_i} d\xi \quad (7.22)$$

It should be noticed that the first integral simply represents the state variable from the previous time step and the second integral can be analytically solved leading to the following result:

$$\eta_i^{n+1} = e^{\frac{-\Delta t_r'}{\lambda_i}} \eta_i^n + C_1^{n+1} \lambda_i \left[1 - e^{\frac{-\Delta t_r'}{\lambda_i}}\right] \quad (7.23)$$

With respect to fatigue, such time step dependent quantities may not be necessary. In this case, a primary interest is the magnitude of the pseudo strain response to a sinusoidal variation in strain input. By letting the pseudo strain response reach a steady state condition, Equation (7.17) can also be simplified, as follows:

$$\left(\gamma_{pp}^R\right)_i = \frac{h_1}{G_R}\left[\left(\gamma_{0,pp}\right)_i\right] |G^*|(\omega_r') \quad (7.24)$$

where the subscript *pp* refers to the peak-to-peak value of strain and the subscript *i* indicates the cycle number. As with other continuum damage models the approach here considers a damaged body to have a spatial distribution of stiffness, but treats this body as an undamaged one with a homogeneous, but reduced stiffness. Hence, macro-scale observations are used to characterise a material rather than micro-scale behaviours. On the macro-scale, the most convenient method to evaluate the effective stiffness is the instantaneous secant modulus defined for the continuum damage model in the stress–pseudo strain space and normalised for specimen-to-specimen variability using the DMR:

$$C = \frac{\tau}{\gamma^R \, x \, DMR} \quad (7.25)$$

Where the variable *C* denotes the pseudo secant modulus. Damage is quantified by analogy to Schapery's work potential theory originally derived for axial loading conditions and then further generalised for complete three dimensional representations (Schapery, 1990). The basic equations necessary for the damage theory are summarised below:

- Pseudo strain energy density function:

$$W^R = \frac{1}{2} C(S)(\gamma^R)^2 \quad (7.26)$$

- Stress-pseudo strain relationship:

$$\tau = \frac{\partial W^R}{\partial \gamma^R} \quad (7.27)$$

- Damage evolution law:

$$\frac{dS}{dt_r'} = \left(-\frac{\partial W^R}{\partial S}\right)^{\alpha} \tag{7.28}$$

In Equations (7.26) and (7.28), *S* is the internal state variable and quantifies microstructural changes that result in the stiffness reduction, and α is the damage evolution rate. For bitumen and mastic under oscillatory shear, *S* is related primarily to radial micro-cracking from anti-plane shearing. The relationship between *S* and the pseudo secant modulus, *C*, is known as the damage characteristic relationship and is the primary function in this model. The parameter α is introduced to consider that, although the time dependency of deformation is accounted for through pseudo strain, an additional time dependence associated with damage growth is not. It has been shown that its value is related to the inherent viscoelastic time-dependence, as expressed in the log–log slope of the relaxation modulus, *m* (Park, 1994). In the case of a single macro-crack if the material's fracture energy and failure stress are constant, then $\alpha = 1 + \frac{1}{m}$, but, if the fracture process zone size and fracture energy are constant, then $\alpha = \frac{1}{m}$. In the case of distributed micro-cracks, there are no such theoretical relationships, but it is considered advantageous to relate α to the inherent LVE. Damage can be characterised via the method outlined in (Underwood et al., 2010) wherein the damage evolution law is rearranged to yield a discrete form by first substituting the pseudo strain energy density function, Equation (7.26), into Equation (7.28). Since only pseudo stiffness is a function of damage, this substitution yields;

$$\frac{dS}{dt_r'} = \left(-\frac{1}{2}\,(\gamma^R)^2\,\frac{dC}{dS}\right)^{\alpha} \tag{7.29}$$

Then the chain rule is applied to the right hand side derivative to yield;

$$\frac{dS}{dt_r'}\left(-\frac{1}{2}\,(\gamma^R)^2\,\frac{dC}{dt_r'}\,\frac{dt_r'}{dS}\right)^{\alpha} \tag{7.30}$$

which can be subsequently rearranged and cast into a discrete form for finding damage at each time step, *j*;

$$S_{j+1} = S_j + \left[-\frac{1}{2}\left(\gamma_{j+1}^R\right)^2\left(C_{j+1} - C_j\right)\right]^{\frac{\alpha}{1+\alpha}}\left(t_r'^{(j+1)} - t_r'^{(j)}\right)^{\frac{1}{1+\alpha}} \tag{7.31}$$

Equation (7.31) is applicable to any loading history, but to use it with cyclic fatigue data can be cumbersome due to the large number of time steps. For example, a fatigue test that captures 100 points per data cycle and lasts for 100000 cycles includes 10000000 time steps. The calculation can be simplified by casting the function in a cycle-wise manner and observing that an approximate state of steady-state is detected after only few cycles (Underwood et al., 2010). Applying this technique requires a return to the damage rate function, Equation (7.29), and a calculation for the amount of damage occurring during a load cycle, Equation (7.32).

$$\Delta S = \int_{t'_{r,initial}}^{t'_{r,final}} \left(-\frac{1}{2}\,(\gamma^R)^2\,\frac{dC}{dS}\right)^{\alpha} dt'_r \tag{7.32}$$

The reduce interval, $t'_{r,final} - t'_{r,inital}$, is the interval during which damage occurs and for fatigue loading γ^R is given by Equation (7.33) where γ^R_{pp} is the peak-to-peak pseudo strain magnitude.

$$\gamma^R(t'_r) = \gamma^R_{pp}\frac{sin(\omega_r t'_r)}{2} = \gamma^R_{pp} f(t'_r) \tag{7.33}$$

Since damage occurs during both the forward and reverse loading, $t'_{r,final} - t'_{r,inital}$ is equal to the reduced period of loading, t'_{rp}, or the inverse of reduced frequency. Next, a cycle-wise damage function is proposed, Equation (7.34), where pseudo stiffness is defined according to the slope of the stress–pseudo strain relationship in the entire loading cycle and differentiated from the time dependent pseudo strain by denoting it as *C**:

$$\Delta S = \left(-\frac{1}{2}\left(\gamma^R_{pp}\right)^2\,\frac{dC}{dS}\right)^{\alpha}\left(t'_{r,final} - t'_{r,inital}\right) x\, B_1 \tag{7.34}$$

$$C^* = \frac{\tau_{pp}}{\gamma^R_{pp}\, x\, DMR} \tag{7.35}$$

Fatigue progresses by steady accumulation of damage under repeated loading, thus the incremental damage developing during a single cycle is relatively small and the *C** parameter closely approximates the time varying *C* value throughout the entire cycle. It cannot be assumed that the damage growth during the cycle is absolutely zero or else the model would be incapable of predicting damage growth during the experiment. Instead, a more realistic cycle-wise approximation is that the rate of pseudo stiffness change with respect to damage during a single cycle is constant. With this approximation, Equation (7.32) simplifies to:

$$\Delta S = \left(\frac{dC}{dS}\right)^{\alpha}\left[\int_{t'_{r,initial}}^{t'_{r,final}} \left(-\frac{1}{2}\,(\gamma^R)^2\right)^{\alpha} dt'_r\right] \tag{7.36}$$

Setting Equation (7.36) equal to Equation (7.34), substituting Equation (7.33) for the pseudo strain history and setting *C** equal to *C* produce the following equality:

$$\Delta S = \left(-\frac{1}{2}\left(\gamma^R_{pp}\right)^2\right)^{\alpha} \int_{t'_{r,initial}}^{t'_{r,final}} \left(f(t'_r)\right)^{2\alpha} dt_r$$

$$= \left(-\frac{1}{2}\left(\gamma^R_{pp}\right)^2\right)^{\alpha}\left(t'_{r,final} - t'_{r,inital}\right) x\, B_1 \tag{7.37}$$

which can be rearranged and solved for B_1.

$$B_1 = \frac{1}{\left(t'_{r,final} - t'_{r,inital}\right)} \int_{t'_{r,initial}}^{t'_{r,final}} \left(f(t'_r)\right)^{2\alpha} dt'_r = f_r \int_{t'_{r,initial}}^{t'_{r,final}} \left(f(t'_r)\right)^{2\alpha} dt'_r \qquad (7.38)$$

In the preceding derivations, two separate assumptions were made: (1) constant damage rate during a loading cycle; (2) steady-state deformation existence. Analytical study of fatigue data loading conditions suggests that these two assumptions are valid for bitumens and mastics except during the first few loading cycles. Changes to the material state can develop quite rapidly in the first loading cycle and thus the more rigorous time-step based damage formulation must be used during this portion of the test. Therefore, the damage model should be represented in the piecewise form shown in Equations (7.39) and (7.41) depending on the portion of the test examined. In Equation (7.41) the variable *N* refers to cycle number and is included to represent the fact that, as long as $\frac{dC}{dS}$ is constant, calculations can be performed over groups of cycles, which can further reduce the necessary computational time.

$$C = \begin{cases} C = \frac{\tau}{\gamma^R \, x \, DMR} & t'_r \le t'_{rp} \\ C^* = \frac{\tau_{pp}}{\gamma^R_{pp} \, x \, DMR} & t'_r > t'_{rp} \end{cases} \qquad (7.39)$$

$$\gamma^R = \begin{cases} \gamma^R = \frac{h_1}{G_R} \int_0^{t'_r} G(t'_r - \xi) \frac{d(h_2 \gamma)}{d\xi} d\xi & t'_r \le t'_{rp} \\ \left(\gamma^R_{pp}\right)_i = \frac{h_1}{G_R} \left[\left(\gamma_{pp}\right)_i\right] |G^*|(\omega'_r) & t'_r > t'_{rp} \end{cases} \qquad (7.40)$$

$$\Delta S = \begin{cases} \left[-\frac{1}{2}\left(\gamma^R_{j+1}\right)^2 \left(C_{j+1} - C_j\right)\right]^{\frac{\alpha}{1+\alpha}} \left(t_r^{\prime(j+1)} - t_r^{\prime(j)}\right)^{\frac{1}{1+\alpha}} & t'_r \le t'_{rp} \\ \left[-\frac{1}{2}\left(\gamma^R_{pp}\right)^2 (C_{i+N} - C_i)\right]^{\frac{\alpha}{1+\alpha}} \left(t'_{rp} \, x \, N\right)^{\frac{1}{1+\alpha}} \, x \, B_1 & t'_r > t'_{rp} \end{cases} \qquad (7.41)$$

Once the incremental values of damage are known, they can be cumulated to find the total *S* at any cycle and then subsequently used to characterise the relationship between *S* and *C*. This relationship can be fitted to a convenient analytical function, which can be then substituted into either Equation (7.29) or (7.34) to predict the damage growth for any known loading history. Note that the piecewise formulations are only important during the characterisation phase. For predicting the modulus evolution during repetitive loading, the steady-state assumptions can be used from the beginning of the simulation and the initial cycle damage can be ignored, as long as the strain levels being evaluated result in a fatigue life that is substantially greater than one cycle.

PH model

Pronk et al. (2009; 2000) proposed the so-called partial healing (PH) model to describe the evolution of the complex stiffness modulus (loss and storage modulus) due to irreversible and reversible damage in a fatigue (bending) test, assuming that damage is related to the

dissipated energy per cycle and that bituminous mixture self-healing happens not only during rest periods, but also during loading periods. The PH model is mainly based on two equations:

- Loss modulus:

$$S_{mix}\sin(\varphi) = F\{t\} = F_0 - \int_0^t \left[F\{t\}\left(\alpha_1 e^{-\beta(t-\tau)} + \gamma_1\right)\right] d\tau \quad (7.42)$$

- Storage modulus:

$$S_{mix}\cos(\varphi) = G\{t\} = G_0 - \int_0^t \left[F\{t\}\left(\alpha_2 e^{-\beta(t-\tau)} + \gamma_2\right)\right] d\tau \quad (7.43)$$

The parameters α_1, α_2, γ_1, γ_2 and β are the products of material constants times the occurring strain squared (ε^2). The values α and γ also depend on the frequency applied. Since no energy will be dissipated during a rest period, the function $F\{t\}$ in the integral equals zero during the rest period. When no loading is applied after a time t_1 (rest period), the loss modulus can be described by the following equation.

$$F\{t\} = F_0 - e^{-\beta t}\int_0^{t_1} \alpha_1 F\{\tau\} e^{+\beta\tau}\, d\tau - \int_0^{t_1} \gamma_1 F\{\tau\} d\tau \quad (7.44)$$

The second term on the right hand represents the reversible damage and the third term the non recoverable (irreversible) damage P_{L1}, which is equal to the accumulation of the permanent damage in the loading period. The reversible damage is subjected to the exponential time function at the end of the load period, which will vanish in time. The evolution of the loss modulus during the rest period is given by Equation (7.45). Similarly, we can obtain the development of the storage modulus during healing time given in Equation (7.46).

$$F\{t\} = F_0 - R_{L1} e^{-\beta(t-t_1)} - P_{L1} \quad for\ t \geq t_1 \quad (7.45)$$

$$G\{t\} = G_0 - R_{S1} e^{-\beta(t-t_1)} - P_{S1} \quad for\ t \geq t_1 \quad (7.46)$$

After the first rest period a second loading period starts at $t = t_2$ and will end at $t = t_2 + t_1 = t_2 + \Delta t_L$. The equations (7.47) and (7.48) are valid for the evolutions of the loss modulus and the storage modulus.

$$F\{t\} = F\{t_2\} - \int_{t_2}^{t} [F\{\tau\}(\alpha_1 e^{-\beta(t-\tau)} + \gamma_1)] d\tau \quad for\ t_2 < t < t_2 + \Delta t_L \quad (7.47)$$

$$G\{t\} = G\{t_2\} - \int_{t_2}^{t} [F\{\tau\}(\alpha_2 e^{-\beta(t-\tau)} + \gamma_2)] d\tau \quad for\ t_2 < t < t_2 + \Delta t_L \quad (7.48)$$

By moving the origin of the time scale to $t = t_2$, the same equations are obtained as for the first load period ($t^* = t - t_2$) as indicated by equations (7.49) and (7.50).

$$F\{t^*\} = F_0^* - \int_0^{t^*} [F\{\tau\}(\alpha_1 e^{-\beta(t^*-\tau)} + \gamma_1)] d\tau \quad for\ 0 < t^* < \Delta t_L (= t_1) \quad (7.49)$$

$$G\{t^*\} = G_0^* - \int_0^{t^*} [F\{\tau\}(\alpha_2 e^{-\beta(t^*-\tau)} + \gamma_2)]d\tau \quad for\ 0 < t^* < \Delta t_L \qquad (7.50)$$

The only differences between the first loading and the loading after healing are the start values for the loss modulus *F{t}* and the storage modulus *G{t}* at the beginning of the (second) load period. Therefore, the same solutions with shifted time scales can be used for all the load and rest periods.

Examples of the simulation of a continuous fatigue test and a fatigue related healing with storage periods (FHS) test are depicted in Figures 7.4 and 7.5, respectively. It should be noted that for the FHS simulation the material parameters were chosen by fitting the first two cycles of loading rather than only one cycle of loading. Pronk stated that this could be related to the real healing, which cannot be fully explained by the current PH model based on stiffness modulus development. He believes that there is a distinction between the stiffness recovery and the fatigue strength recovery (fatigue life recovery) (Pronk et al., 2009).

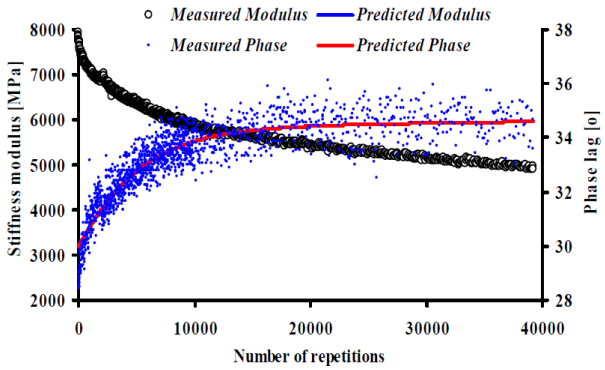

Figure 7.4. Simulation of stiffness and phase lag development for a continuous fatigue test using the PH model (Pronk, 2009).

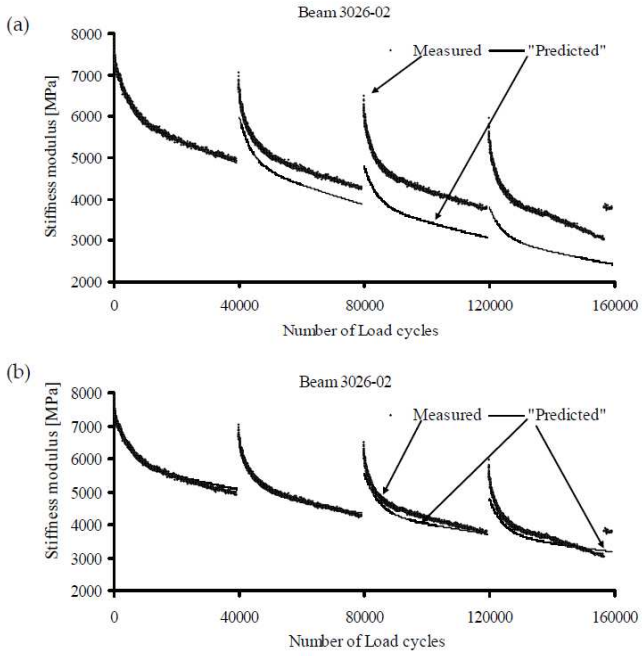

Figure 7.5. Simulation of stiffness development for a FHS test using the parameters determined from: (a) the first load period only; (b) the first two load periods (Pronk et al., 2009).

DER approach

As previously mentioned, cohesive healing is considered as the result of several mechanisms which develop at crack interfaces, such as wetting (which depends on surface energy of the material), interfacial cohesion and interdiffusion and randomisation of molecules between wetted surfaces (Little et al., 2007; Bhasin et al., 2009; Bommavaram et al., 2009). Such processes within a bitumen contribute to crack repair and original internal structure restoration. Moving from the assumption that any change in material internal structure due to damage reflects in a change in their energy dissipation processes, Santagata et al. (2017) introduce a methodology based on the comparison of dissipated energy measured under continuous oscillatory shear loading without rest periods (fatigue tests) and after single long rest periods introduced at fixed values of complex modulus loss (healing tests). In such a context, the Dissipated Energy Ratio (DER) concept originally proposed by Pronk and Hopman (1991) is used to analyse fatigue and healing test data. The DER parameter after N loading cycles is calculated through the following expression:

$$DER = \frac{\sum_{i=1}^{N} W_i}{W_N} \quad (7.51)$$

where W_i and W_N are the energy dissipated per unit volume in the generic i-th and N-th cycle, respectively, and are calculated pre the following general expression:

$$W_i = \pi \tau_{0,i} \gamma_{0,i} \sin(\delta_i) \quad (7.52)$$

where $\tau_{0,i}$ and $\gamma_{0,i}$ are respectively the stress and strain amplitudes, whereas δ_i is the phase angle value. In Figure 7.6. a typical plot of DER as a function of the number of loading cycles N in the case of stress-controlled tests is depicted. It can be observed that after an initial phase of testing with no damage accumulation, the experimental data points gradually deviate from the equality line (with 45 ° horizontal slope). A peak value is reached, after which DER values decrease until complete failure of the specimen. Several fatigue life indicators can be derived from the DER function obtained from continuous oscillatory loading test data (Bahia et al., 2001; Santagata et al., 2008):

- N_p, which identifies the onset of crack propagation and corresponds to the intersection between the equality line and the horizontal line passing through the maximum DER value;
- N_{p20}, which is associated with 20% deviation of DER from the equality line;
- N_{max}, which corresponds to DER peak.

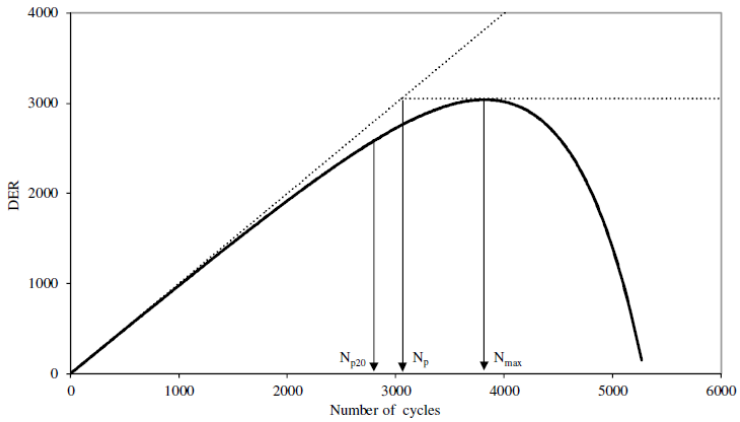

Figure 7.6. Example of a typical DER function obtained from a stress-controlled fatigue test (Santagata et al., 2017).

Figure 7.7 show a comparison between the DER functions derived from fatigue tests and those obtained from the reloading phases in healing tests carried out on the three bitumens investigated at two stress levels and three values of complex modulus loss.

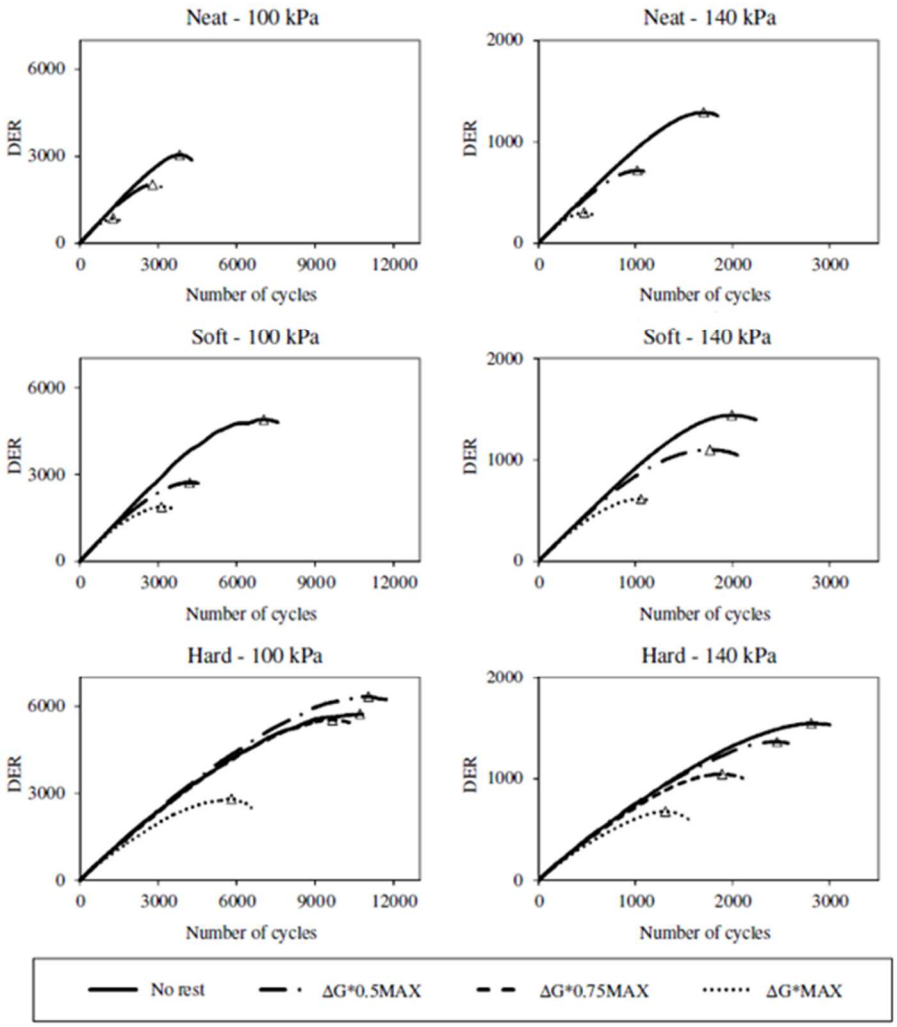

Figure 7.7. Comparison of DER functions obtained from fatigue and healing tests (Santagata et al., 2017).

In particular, the DER function obtained from fatigue tests is considered as a reference point for healing evaluation, since it represents material response in its original state. Its comparison with the DER function obtained after a certain amount of damage induced in bitumen may provide information on material healing capability.
In order to quantify the magnitude of healing occurring during rest time, a Healing Ratio (HR) was defined as follows:

$$HR = \frac{N_{max-RP}}{N_{max}} \quad (7.53)$$

where $N_{max\text{-}RP}$ is the number of loading cycles at peak DER determined from the reloading phase of healing tests and N_{max} is the number of loading cycles at peak DER determined from the corresponding fatigue tests.
By definition, HR can vary in the interval comprised between 0 and 1. The lower limit is obtained when $N_{max\text{-}RP} << N_{max}$ and refers to an ideal material which exhibits a negligible fatigue resistance after being subjected to a first loading phase. The upper limit is achieved when $N_{max\text{-}RP} = N_{max}$ and is related to a material which attains a full recovery of its original fatigue resistance after rest time.

Healing index

In order to assess bitumen healing capability and study healing factors, Tan et al. (2012) introduce two healing indices symbolised as HI^1 and HI^2 and described by Equations (7.54) and (7.55), respectively.

$$HI^1 = \frac{|G^*|_{after}}{|G^*|_{initial}} x100 \quad (7.54)$$

where HI^1 is the healing index calculated by the ratio of the initial modulus value after rest to the initial modulus value before rest; $|G^*|_{initial}$ is the initial modulus value before rest; $|G^*|_{after}$ is the initial modulus value after rest.

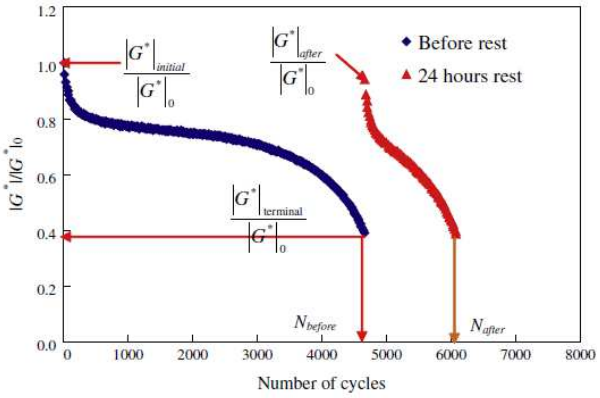

Figure 7.8. Schematic of the fatigue indices (Tan et al., 2012).

Taking Figure 7.8 as an example, all the modulus values are normalised by $|G^*|_0$ to eliminate the differences between the replicates. The solid diamond series represent the normalised modulus change curve before rest and the triangle series denotes the normalised modulus

change curve after 24 h of rest. The rest periods are not shown in Figure 7.8. The normalised $|G^*|_{initial}$ is the value at the beginning of the Before rest curve and normalised $|G^*|_{after}$ is the value at the beginning of the 24 h rest curve. HI^1 can show only the degree of healing of the initial modulus and not the degree of healing that is needed to resist loading. To fix this deficiency, another healing index, symbolised as HI^2, is introduced here, as shown in the following equation:

$$HI^2 = \left(\frac{|G^*|_{terminal}}{|G^*|_{initial}}\right)\frac{(N_{after}-N_{before})}{N_{before}}x100 \quad (7.55)$$

where HI^2 is the healing index calculated by the ratio of cycle numbers, and $|G^*|_{terminal}$ is the dynamic modulus value when the loading stops.

In the example shown in Figure 7.8, $\frac{|G^*|_{terminal}}{|G^*|_0}$ is the modulus value at the end of the Before rest curve and N_{before} is the number of cycles when the loading stops before a rest period. N_{after} represents the number of cycles when the loading stops after a rest period. $\frac{|G^*|_{terminal}}{|G^*|_{initial}}$ is the decrease in the percentage of the dynamic modulus when the loading stops. If $\frac{(N_{after}-N_{before})}{N_{before}}$ equals 1, bitumen ability to resist loading allows a totally healing.

Chapter 8.

Advanced investigation of binders: background

The rheological properties of the bituminous components of bituminous mixtures contribute significantly to the major distresses of flexible pavements. In particular, bitumen and fillers create a blend known as bituminous mastic that, depending on its nature and composition, strongly affects the durability of pavement asphalt layers. The main effect of filler is to stiffen bitumen, therefore, when a mix includes also Reclaimed Asphalt Pavement (RAP) that release aged bitumen, the final mastic constituted by virgin and aged RAP bitumen together with filler exhibits a high stiffening capacity that influences the ability to resist permanent deformation at high temperatures, fatigue life at intermediate temperatures and cracking resistance at low temperatures.
In this study, three fillers (limestone, basalt and Portland cement) and a high polymer modified bitumen (3.8% of Styrene Butadiene Styrene, SBS) were selected. The latter was first blended with various percentages of an aged bitumen (itself polymer modified), long-term aged in laboratory, and then analysed. Subsequently, mastics composed of the same bituminous phase above-mentioned and different types and amounts of filler were investigated. Classical and advanced rheological tests besides a basic morphological analysis were performed. The materials used, the test methods with the associated data analysis applied and the corresponding results are presented in the following paragraphs. First, an overview to describe the background of the topic is provided. Then the morphological characterisation is described and afterwards the rheological investigation is addressed. In particular, the analysis of the rheological data was carried out by means of a Dynamic Shear Rheometer (DSR) and was based on a classical approach along with innovative test methods previously implemented for bitumens and then found suitable also for mastics. Moreover, the influence of morphological properties of filler on filler-bitumen interactions was assessed by means of a Scanning Electron Microscope (SEM).

8.1 Binder response in terms of fatigue, self-healing and thixotropy

Asphalt pavement performance is strictly linked to the properties of mastic phase and its components (i.e. filler and bitumen) (Jakarni, 2012; Kim, 2008). Filler is a key element in mastic behaviour, from mixture production to pavement layer construction. Several researches have demonstrated that, besides aggregate blend gradation adjustment, filler

particles are able to accomplish important tasks within bituminous mixtures, reducing thermal susceptibility and fixing the thickness and mechanical properties of the mastic film covering stone particles (Harris et al., 1995; Puzinauskas, 1983). The filler fraction passing No. 200 (63 μm) sieve, be it natural (i.e. dust of mineral aggregates) or manufactured (e.g. Portland cement), causes, primarily, an increase in binder stiffness.

Although the mastic-to-bitumen relative stiffness is mainly related to the filler/bitumen ratio (f/b), many researches carried out over the last years have highlighted the dependence of mastic stiffness on the properties of both materials (i.e. filler and bitumen) and their specific interactions (Cardone et al., 2015; Antunes et al., 2016). Great importance should be given to filler physicochemical nature, particle density, size and shape, surface area and, in particular, fractional voids (i.e. Rigden voids, RV) (Antunes et al., 2015; Faheem and Bahia, 2010; Grabowsky and Wilanowicz, 2008; Rigden, 1947). The volume of voids in the dry compacted filler sample (i.e. Rigden voids, RV) corresponds to the volume fraction of bitumen that is fixed and only the fraction in excess of this volume is able to lubricate the filler matrix (Kandhal et al., 1998). The higher the Rigden voids (RV) of a certain filler, the higher the amount of bitumen needed to make the mixture fluid as well as the stiffness of the corresponding mastic.

Buttlar et al. (1999) identified mastic behaviour as the result of a three-step-reinforcement mechanism: (1) volume-filling reinforcement (i.e. the presence of a rigid inclusion in a less rigid matrix causes stiffening effects); (2) physicochemical reinforcement (i.e. stiffening is caused by interfacial effects between bitumen components and filler particles); (3) particle interaction reinforcement (i.e. particles interlocking inside the lytic skeleton). The latter mechanism is usually considered negligible because of its limited role in filler stiffening effect (Shashidhar et al., 1998).

Mastic stiffness affects the ability to resist permanent deformation at high temperatures, fatigue life at intermediate temperatures and cracking resistance at low temperatures (Airey et al., 2006; Wang et al., 2011). Fatigue cracking represents the major cause of failure for asphalt pavements. Hence, it is fundamental to identify reliable fatigue parameters in order to estimate pavement service life under traffic loading conditions.

Nowadays, pavement-engineering strategies aim at performance improvement, resources conservation (e.g. recycling techniques) and environment protection (e.g. reduction of harmful emissions). In this sense, it should be emphasised that fatigue resistance is the result of several mechanisms, such as self-healing which can be classified among environmentally sustainable strategies designed to decrease maintenance costs, extend service life and reduce greenhouse gas emission as well (Chung et al., 2015). In fact, when exposed to damage, some materials (e.g. metals, polymers, concrete or bituminous mixtures) have the intrinsic ability to repair small cracks and partial restore their original properties through thermo-mechanical or induced mechanisms. However, other recoverable phenomena of viscoelastic materials, such as thixotropy and heating, can permanently recover material properties. In order to avoid misleading-analyses, it is important to distinguish between recovery due to real healing and

recovery due to intrinsic responses, especially with respect to thixotropy, since the latter does not contribute to fatigue life.

Over the last years, many studies focused on the determination of bituminous mixture self-healing capability, since this property can constitute an important future for the development of long-lasting asphalt pavements (Liu et al., 2012; Wool et al., 2012). Healing process of bituminous materials consists of a three-step-mechanism: (1) surface approach due to the consolidation of stresses and flow of bitumen; (2) wetting (adhesion of two crack surfaces driven together by surface energy); (3) complete recovery of mechanical properties due to diffusion and randomisation of asphaltene structures (Phillips, 1998).

Although previous researches demonstrated that self-healing is mainly related to the interdiffusion of bitumen components (Wool, 1981) and, consequently, the majority of experimental studies mainly focused on bitumen analyses, mastic is the real binder phase in bituminous mixtures, which should be considered as mastic-coated aggregates rather than pure bitumen-coated aggregates (Wang et al., 2011).

Mastic self-healing response differs from the associated pure bitumen behaviour because of the presence of filler which determines a discontinuity within the material, as result of volume filling and physicochemical interactions with bitumen (Delaporte et al., 2007; Frigio et al., 2016). In fact, fatigue process of mastics involves chemical and mechanical phenomena due to the interaction between the bituminous phase and the lytic component (i.e. filler). In particular, the presence of filler particles within the continuous bituminous phase further complicates crack propagation by altering the overall cohesive potential of the real binder component of a mixture (i.e. mastic) (Mazzoni et al., 2016).

Because of the combination of two main mechanisms (adhesive healing at the bitumen-aggregate interface and cohesive healing within the bitumen) (Little et al., 2001), self-healing of bituminous materials has an impact on asphalt pavements service life.

Various internal and external factors influence self-healing capability of asphalt pavements. Chemical and mechanical characteristics of bituminous materials are identified as the most important internal factors, whereas high air temperatures and long rest periods are the major external factors.

In literature, self-healing capability was studied using different methods, but a specified protocol has not been yet standardised to examine this issue (Ayar et al., 2016; Little et al., 2015). This phenomenon was investigated at the bitumen, bituminous mastic and bituminous mixture level using fatigue, fracture or non-destructive tests. Fatigue tests with the insertion of rest periods represent the main method for self-healing capability evaluation in laboratory. This test method was performed on bituminous mixtures by means of Four Point Bending Test (4PBT) or Indirect Tensile Test (ITT) (Qiu, 2012; Shen and Carpenter, 2007) and diffusely on bitumens, especially by means of Dynamic Shear Rheometer (DSR) (Lu et al., 2003; Bodin et al., 2004; Stimilli et al., 2012; Stimilli et al., 2014; Canestrari et al., 2015; Santagata et al., 2015) and seldom by means of Binder Bond Strength (BBS) (Huang et al, 2016; Lv et al., 2017). Besides, fatigue tests with rest periods were carried out on mastics on a limited scale by means of Three Point Bending Test (3PBT) or DSR (Garcia, 2012;

Underwood, 2016; Mazzoni et al., 2016, 2017b and 2017c). Moreover, most investigations were characterised by the lack of discrimination between real healing and other recoverable phenomena in bituminous materials, such as thixotropy. In addition, few of them dealt with the simultaneous interaction among fatigue, self-healing and thixotropy (Soltani et al., 2005; Shan et al., 2010; Canestrari et al., 2015; Mazzoni et al., 2016, 2017b and 2017c). It should be noted that there is a basic difference between self-healing capability and thixotropy in bituminous materials properties recovery during rest periods. In fact, as previously mentioned, self-healing is regarded as an effort to recover initial properties by wetting and interdiffusion, whereas thixotropy occurs due to molecular rearrangement in the bituminous phase (Butt et al., 2012; Mouillet et al., 2012).

Given this background, there is a need to bridge the lack of an analytical consolidated approach to determine self-healing potential and thixotropy of bituminous mastics, concurrently identifying useful insights for filler types and contents. In fact, it is expected that the prediction of field performance of bituminous mixtures is closely linked to mastic self-healing properties. Moreover, the increasing reuse of RAP, containing polymer modified bitumen, for the production of new, more performing and environmental friendly bituminous mixtures, leads to a further need of understanding the influence of aged polymer modified bitumen from RAP on the final mastic behaviour. Thus, it is fundamental to analyse interactions among aged polymer modified bitumen from RAP, new virgin polymer modified bitumen and filler, investigating the related effects on fatigue, thixotropy and self-healing capability.

Chapter 9.

Advanced experimental investigation

9.1 Materials

Different materials were analysed and compared (Table 9.1). In details, the first phase of the experimental investigation focused on the evaluation of the overall response of aged and unaged mastics and the associated bitumens, since it is well-established that bituminous material response is affected by the bituminous phase, but it is strictly related to the real binder phase represented by bituminous mastic.

In particular, since Styrene Butadiene Styrene (SBS) polymers represent the most commonly elastomers employed in bituminous mixture modification, they were added to a base bitumen (coded as BB) in quantity equal to 3.8% by bitumen weight so as to produce a high modified bitumen (coded as H). In fact, the 3.8% value represents the most common level of polymer modification for bituminous mixtures in Italian motorways. The other bitumens were obtained by blending bitumen H to different percentages (0%, 45%, 100%) of a same SBS modified aged bitumen (coded as R) in order to account for the effects due to the addition of RAP. In fact, the aim of adding bitumen R is to simulate the presence of the reactivated bitumen released by RAP during the in-plant production of Hot Mix Asphalt (HMA). In particular, bitumen R was obtained by subjecting virgin bitumen H to a long-term ageing by means of Rolling Thin Film Oven Test and Pressure Ageing Vessel testing procedure, in accordance with European Standards EN 12607-1 and EN 14769. It is worth noting that the choice to use a laboratory aged bitumen rather than a bitumen directly extracted from milled material does not limit the general validity of this study as each extracted bitumen would have its own characteristics and could be considered in any case not exhaustive of all the possible conditions, analogously to the laboratory aged one. Moreover, the laboratory aged bitumen is always reproducible for further investigation or comparative purpose.

Three types of mastic were then produced by adding to each of the bitumens above-mentioned a filler whose nature and dosage selected are expressed below. A limestone filler (coded as L) was set because it consists mostly of angular particles with smooth to slightly rough surface, with a low propensity to agglomerate (Antunes et al., 2015), and it is the most commonly used for bituminous mixtures thanks to its high affinity with bitumen with which develops strong chemical bonds and high adhesion also in presence of water. A constant filler/bitumen ratio equal to 1.00 by bitumen weight (corresponding to a filler/mastic ratio equal to 28% by mastic volume) was selected in agreement with Superpave specifications (Kennedy et al, 1994), which recommend a ratio by bitumen weight within 0.60 and 1.20 and a maximum filler concentration by volume of total mastic equal to 28%.

It should be highlighted that the three mastics studied in this first experimental step represented the reference materials for the following steps which aim at evaluating the effect of different dosages and types of filler. In details, further amounts of limestone filler were studied and compared to the 28% value by mastic volume previously investigated. In particular, filler/mastic ratios equal to 14% and 42% by mastic volume (corresponding to 0.40 and 1.90 filler/bitumen ratio by bitumen weight, respectively) were considered. If the 28% value represents the reference value, as previously mentioned, the other two percentages were adopted for a better understanding of filler contribution on final mastic behaviour. Subsequently, the influence of filler nature was assessed by selecting further filler types to be compared to the reference limestone whose dosage was set equal to 28% by mastic volume. In details, another mineral filler (basalt "B") and a manufactured one (Portland cement "PC") were chosen. In order to obtain a constant filler/mastic ratio equal to 28% by mastic volume for each filler investigated, a corresponding 1.16 and 1.04 filler/bitumen ratio by bitumen weight resulted for Portland cement and basalt, respectively, according to their different particle densities (Table 9.2) and complying with the Superpave specifications (Kennedy et al., 1994). As previously mentioned, limestone represents the reference filler thanks to its suitable physicochemical properties (fineness, basicity, lack of clay) that promote and strengthen bitumen-aggregate adhesion and concurrently ensure an optimum mastic response. Whereas the other two fillers, basalt and Portland cement, were chosen because their geometrical and physical characteristics are such as to guarantee a good dispersion within the bitumen and consistently assure final bituminous mastic homogeneity (Antunes et al., 2015). Besides, the different chemical composition of basalt and Portland cement influences filler-bitumen interaction and consequently determines evident changes in final mastic behaviour, making their comparison with limestone more interesting and exhaustive.

All the materials investigated were prepared following an optimised protocol so as to obtain homogeneous mixes (Cardone et al., 2015). At first, bitumens H and R and the filler selected (L, PC or B), if present, were heated in oven at 165 °C until the consistency of the bitumens became sufficiently fluid. Then bitumen H was blended with the set percentage of bitumen R using a low shear mixer operating at 60 rpm and 165 °C for 5 minutes; finally, in the case of mastics, filler was gradually added to the bituminous phase and blended using the same mixer. The rotation speed was progressively increased in proportion to the amount of the material and the addition of filler was completed in about 10 minutes. The parameters of the blending procedure were selected so as to prevent bitumens from severe processing conditions and to minimise additional ageing effects. Moreover, during the preparation of the mastics, further aspects were carefully taken into account in order to avoid inhomogeneities in the materials studied:

- segregation (due to different specific weights of mastic components);
- hardening (steric hardening was controlled by standardising all sample preparation times before testing);

– heterogeneity (all the components in the samples comply with the percentages selected).

All the materials investigated in this study are summarised in Table 9.1.

Table 9.1. Bituminous materials investigated.

	Code	SBS content, by weight [%]	Bitumen R, by weight [%]	Filler/Bitumen ratio, by weight [/]	Filler/Mastic ratio, by volume [%]
1st step: comparison between mastics and the associated bitumens					
BITUMEN	**BB**	/	0	/	/
SBS MODIFIED BITUMEN	**BH_0R**	3.8	0	/	/
	BH_45R	3.8	45	/	/
	BH_100R	3.8	100	/	/
SBS MODIFIED MASTICS	**MHL_0R**	3.8	0	1.00	28
	MHL_45R	3.8	45	1.00	28
	MHL_100R	3.8	100	1.00	28
2nd step: comparison among mastics, selecting 28L as reference mastic					
Influence of different filler dosages, choosing limestone as reference filler type					
SBS MODIFIED MASTICS	**14L_0R**	3.8	0	0.40	14
	14L_45R	3.8	45	0.40	14
	14L_100R	3.8	100	0.40	14
	42L_0R	3.8	0	1.90	42
	42L_45R	3.8	45	1.90	42
	42L_100R	3.8	100	1.90	42
	28L_0R	3.8	0	1.00	28
	28L_45R	3.8	45	1.00	28
	28L_100R	3.8	100	1.00	28
Influence of different filler types, fixing the value 28% as reference filler dosage					
SBS MODIFIED MASTICS	**28PC_0R**	3.8	0	1.16	28
	28PC_45R	3.8	45	1.16	28
	28PC_100R	3.8	100	1.16	28
	28B_0R	3.8	0	1.04	28
	28B_45R	3.8	45	1.04	28
	28B_100R	3.8	100	1.04	28
	28L_0R	3.8	0	1.00	28
	28L_45R	3.8	45	1.00	28
	28L_100R	3.8	100	1.00	28

Table 9.2. Basic properties of the fillers selected.

Filler type	Code	Particle density [g/cm^3]	Rigden voids (RV) [%]
Portland cement	**PC**	2.975	40.15
Basalt	**B**	2.684	33.50
Limestone	**L**	2.594	31.14

9.2 Test program

Two main phases constituted the laboratory experimental campaign: the first phase focused on the morphological analysis of the materials studied by means of a Scanning Electron Microscope (SEM), whereas the second one centred on the rheological characterisation of the blends by means of a Dynamic Shear Rheometer (DSR).
Besides the "classical" rheological investigation, more innovative test protocols and analyses were implemented in order to obtain an overall picture of the mechanical behaviour of the materials selected under different loading and temperature conditions and including self-healing capability and thixotropic contribution. Moreover, a further interpretation of the rheological results was provided by performing morphological analyses that allowed the assessment of bitumen-filler interaction within the corresponding mastics.
Details of each test are provided in the following section together with the corresponding experimental procedures. Table 9.3 shows a summary of the overall experimental plan in terms of number of replicates for each test carried out.

Table 9.3. Experimental program.

		Number of replicates for each test condition			
		SEM	**Frequency sweep**	**To find Isostiffness**	**Time sweep**
Bitumens	**BH_0R**	1	4	2	3
	BH_45R	1	4	2	3
	BH_100R	1	4	2	3
Mastics	**14L_0R**	-	-	2	3
	14L_45R	-	-	2	3
	14L_100R	-	-	2	3
	28L_0R	1	4	2	3
	28L_45R	1	4	2	3
	28L_100R	1	4	2	3
	42L_0R	-	4	2	3
	42L_45R	-	4	2	3
	42L_100R	-	4	2	3
	28PC_0R	-	4	2	3
	28PC_45R	-	4	2	3
	28PC_100R	-	4	2	3
	28B_0R	-	4	2	3
	28B_45R	-	4	2	3
	28B_100R	-	4	2	3
TOTAL		**6**	**60**	**36**	**54**

9.2.1 Morphological investigation

Rheological testing methods and analyses developed to investigate the mechanical performance of bituminous materials are not always sufficient to completely characterise their intrinsic behaviour. For this reason, a supplementary morphological analysis was carried out in order to evaluate the interaction between bitumen and filler particles inside mastics and thus provide a better interpretation of the rheological results. To this aim, a Scanning Electron Microscope (SEM) was used, allowing the identification of mastic morphology and filler distribution inside the bituminous matrix, thus helping to explain the differences detected in rheological response between mastics and the associated bitumens.

9.2.2 Classical and advanced rheological investigation

Each material selected was preliminarily characterised in terms of complex shear modulus (G*), by performing Frequency sweep tests through a Dynamic Shear Rheometer (DSR) in

plate-plate configuration in accordance with the procedure discussed in a previous paragraph § 5.4.3, thus providing a "classical" rheological analysis of all the blends studied.
The same device was used to characterise the blends in terms of fatigue, self-healing and thixotropy, by implementing To find isostiffness tests and then Time sweep tests with multiple rest periods, as described in the following paragraphs (§ 9.3.3 and 9.3.4), and thus allowing an "advanced" rheological investigation to be carried out.

9.3 Laboratory equipments, test methods and data analysis

The overall experimental study required the use of sophisticated equipments commonly employed in the most of the research activities, as prescribed by the European and the American standards. In order to provide a better understanding of the results obtained through the laboratory investigation, the main operation principles of the equipments employed and the test protocols, as well as the basic theory behind the analysis methods applied to elaborate the test data are discussed in the following paragraphs.

9.3.1 SEM analysis

Rheological analyses were integrated by a morphological characterisation of the surface of the mastic samples performed using a Scanning Electron Microscope (SEM). The evaluation aimed at estimating the distribution of filler particles inside the bituminous matrix in order to determine possible relationships between microstructure and rheological performance.
The analysis was carried out on the surface of cylindrical mastic samples (8 mm large and 2 mm thick). As bituminous mastics are nonconductive materials, the surface of the samples was metalised by applying a thin coating of gold before performing the SEM analysis. The images were scanned in backscattered electron mode with an acceleration tension of the electronic beam equal to 20 kV. Samples were photographed at a range of magnifications from x20 to x3000. At medium magnification, features of interest were picked out and further magnified.

9.3.2 Frequency sweep test

Before carrying out self-healing investigation, frequency sweep tests were performed on the materials selected to obtain a comprehensive picture of the overall rheological behaviour. In fact, considering that bitumens and mastics are time-temperature dependent materials, in order to properly characterise them, it is necessary to run tests under different loading and temperature conditions.
Frequency sweep tests were implemented by means of a Dynamic Shear Rheometer (DSR) in plate-plate configuration by applying a sinusoidal load (controlled strain mode) in selected ranges of frequency (0.159-15.9 Hz) and temperature (4-82 °C, with 6 °C intervals).

9.3.3 To find Isostiffness test

Prior to performing time sweep tests, a fundamental step was the determination of iso-stiffness conditions variable depending on the materials investigated and guarantying to run healing tests at intermediate and comparable temperatures, as accurately described in the following paragraph (§ 9.3.4). However, regardless of the presence or not of filler and eventually its type and dosage, the influence of different aged bitumen contents was considered using an equi-stiffness temperature, in order to delete the effect of stiffness in the materials properties.
Iso-stiffness temperatures to be adopted for each material were determined by subjecting a specimen to tests conducted in 3 steps at 3 multiple decreasing temperatures in the DSR, at the same strain level (constant during each test, but variable depending on the presence or not of filler and its type and dosage) and with the same frequency (constant and equal to 10 Hz for all the materials tested), for a short duration so as to avoid inducing damage. During each test, the loss modulus $|G^*|\bullet\sin\delta$, which is representative of changes in dissipated energy, was monitored. Each test is preceded by a conditioning time of 15 minutes (except for the first conditioning phase setting equal to 30 minutes) applied before every test temperature to reach the material thermal equilibrium, followed by a measuring time of 1 minute.
It is possible to plot steady-state $|G^*|\bullet\sin\delta$ data as a function of temperature with the results obtained ($\text{Log}|G^*|\bullet\sin\delta$ versus T): the iso-stiffness temperatures corresponding to the target stiffness were back calculated through an interpolation of the test data at different temperatures inserting the linear regression in the plot to find the equation that describes the trend of the curve. Two replicates were carried out for each material selected and the temperature requested was obtained by making the average of the results obtained.
Below an example of one of the materials studied is provided:

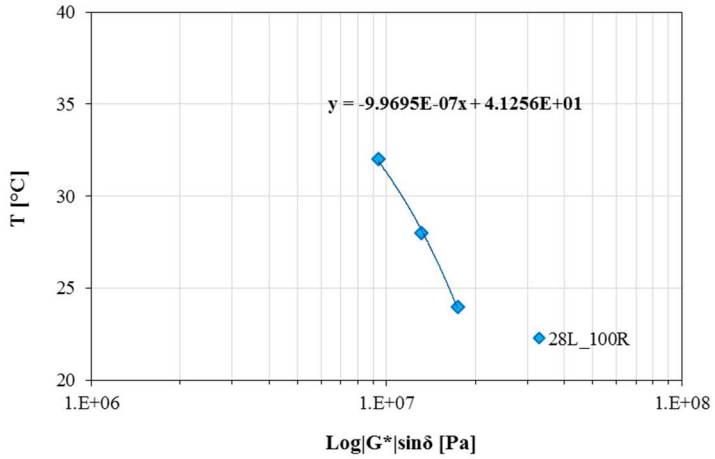

Figure 9.1. An example of To find iso-Stiffness test result (28L_100R investigation).

For example considering 28L_100R, the equation that describes its trend of temperature versus Log|G*|•sinδ curve is depicted in Figure 9.1 and the isostiffness temperature is calculated by substituting in "x" the isostiffness value selected and equal to 9 MPa, thus obtaining 32.3 °C, as showed below:

$$\boldsymbol{y = 9.9695 \cdot 10^{-7} x + 41.256}$$

Where $\boldsymbol{x = 9 \cdot 10^{6}\ Pa \rightarrow y = T = 32.3\ °C}$

The test temperatures used for each material based on this condition are provided in Table 9.4.

9.3.4 Time sweep test with multiple rest periods

Fatigue Endurance Limit concept is related to time-temperature dependent phenomena including damage accumulation, hardening, viscoelasticity, thixotropy and self-healing. Different methods exist to analyse this aspect in bituminous materials. The main one is based on initial modulus reduction, even though several researches suggest the evaluation of dissipated energy changes as a more appropriate approach (Santagata et al., 2009; Shen and Carpenter, 2005). In this study, self-healing potential was evaluated by means of a Dynamic Shear Rheometer (DSR) in a plate-plate configuration (diameter: 8 mm; gap: 2 mm). During each test, the loss modulus |G*|•sinδ, which is representative of changes in dissipated energy, was continuously monitored. Time sweep tests in strain-controlled mode were carried out with the insertion of multiple rest periods aimed at simulating field conditions. The loading stopped when the loss modulus |G*|•sinδ dropped down to 65% of its initial value (damage level corresponding to a 35% reduction of dissipated energy at each loading cycle) and started

again after 30 minutes of rest. A minimum of 12 load-rest phases were performed in all the test conditions and the stiffness recovery of the material was monitored also during rest period by applying a strain equal to 0.0001% and 0.001%, for mastics and the associated bitumens, respectively, that was low enough to avoid material stress and concurrently record data in accordance with minimum torque and torque resolution of the DSR used for testing. The frequency was set equal to 10 Hz, whereas test temperatures were selected so as to guarantee an iso-stiffness condition (i.e. loss modulus $|G^*|\bullet\sin\delta$ initial value) variable depending on the materials investigated, as summarised in Table 9.4. The higher the filler particle density and/or content, the higher the iso-stiffness level chosen to run tests at intermediate and comparable temperatures (Figure 9.2). The latter is an important aspect since self-healing is strongly influenced by temperature and heating is a way for enhancing this capability. The rate at which self-healing occurs increases with the increase in temperature, in agreement with the Arrhenius equation. This explains the importance of testing all the mastics composed of the same bituminous blend at comparable temperatures. Moreover, intermediate temperatures ensure enough molecular mobility that is essential for the occurrence of self-healing which is conversely inhibited at low temperatures. At the same time, too high temperatures, even if more beneficial in terms of self-healing, would not be significant for fatigue analyses since fatigue failure happens at low/intermediate temperatures.

The strain magnitude was selected to induce significant micro damage within the samples as well as acceptable testing times, concurrently allowing self-healing capability detection (Canestrari et al., 2015). The higher the filler percentage, the lower the strain value set, as shown in Table 9.4 which summarises the main testing conditions for all the mastics.

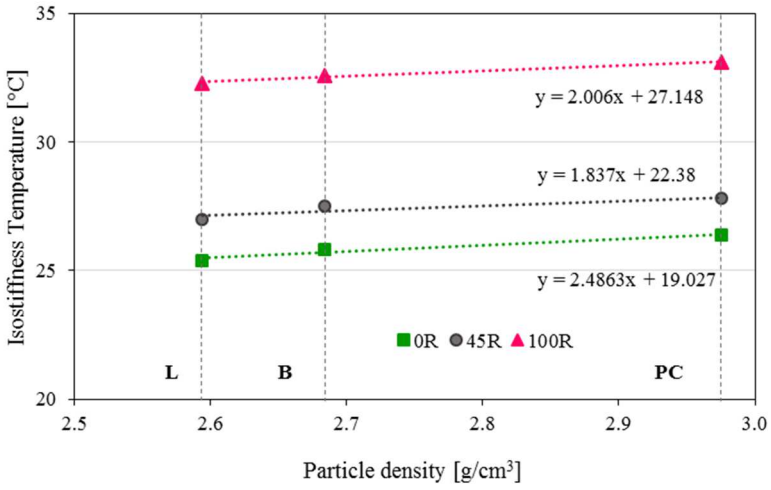

Figure 9.2. Mastic Isostiffness Temperatures versus filler particle densities.

Table 9.4. Test parameters for all the materials studied and compared.

Mastic	Strain [%]	Frequency [Hz]	Isostiffness |G*|•sinδ [MPa]	Temperature [°C]
1st step: comparison between mastics and the associated bitumens				
BB	5.0	10	3.0	19.5
BH_0R	5.0	10	3.0	21.5
BH_45R	5.0	10	3.0	22.5
BH_100R	5.0	10	3.0	29.0
MHL_0R	**1.0**	**10**	**9.0**	**25.4**
MHL_45R	**1.0**	**10**	**9.0**	**27.0**
MHL_100R	**1.0**	**10**	**9.0**	**32.3**
2nd step: comparison among mastics, selecting 28L as reference mastic				
Influence of different filler dosages, choosing limestone as reference filler type				
14L_0R	1.5	10	3.8	25.2
14L_45R	1.5	10	3.8	28.0
14L_100R	1.5	10	3.8	31.7
42L_0R	0.7	10	13.0	29.3
42L_45R	0.7	10	13.0	30.0
42L_100R	0.7	10	13.0	33.9
28L_0R	**1.0**	**10**	**9.0**	**25.4**
28L_45R	**1.0**	**10**	**9.0**	**27.0**
28L_100R	**1.0**	**10**	**9.0**	**32.3**
Influence of different filler types, fixing the value 28% as reference filler dosage				
28PC_0R	1.0	10	9.0	26.4
28PC_45R	1.0	10	9.0	27.8
28PC_100R	1.0	10	9.0	33.1
28B_0R	1.0	10	9.0	25.8
28B_45R	1.0	10	9.0	27.5
28B_100R	1.0	10	9.0	32.6
28L_0R	**1.0**	**10**	**9.0**	**25.4**
28L_45R	**1.0**	**10**	**9.0**	**27.0**
28L_100R	**1.0**	**10**	**9.0**	**32.3**

9.3.5 Interpretative model of multiple-rest test results

Self-healing capability was investigated by performing oscillatory tests which included multiple loading phases alternated with rest periods. The typical results and test parameters are shown in Figures 9.3 and 9.4, where the evolution of the loss modulus |G*|•senδ is depicted as a function of time and loading cycles, respectively. In each loading cycle, the first stage is characterised by a rapid decrease in stiffness, mainly due to thermal heating and thixotropy (artefact effects). In the second stage, where the loss modulus slightly decreases with an almost linear trend, the role of fatigue on the stiffness decrease is predominant. During this phase, the influence of artefact effects is less significant, yet it still needs to be taken into consideration (Di Benedetto et al., 2004).

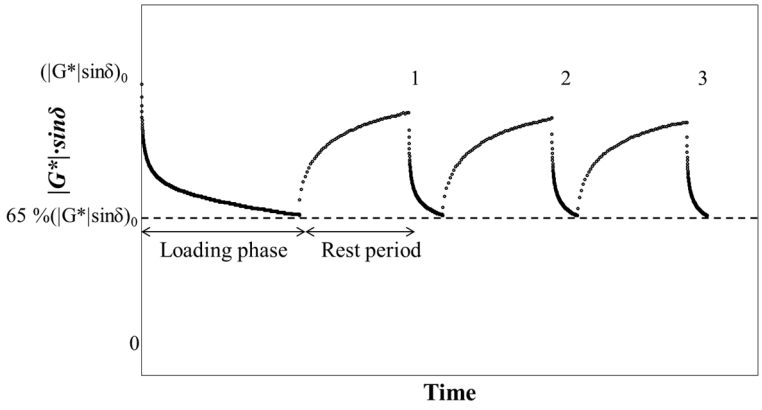

Figure 9.3. Evolution of |G*|•senδ versus time: general results (Mazzoni et al., 2016).

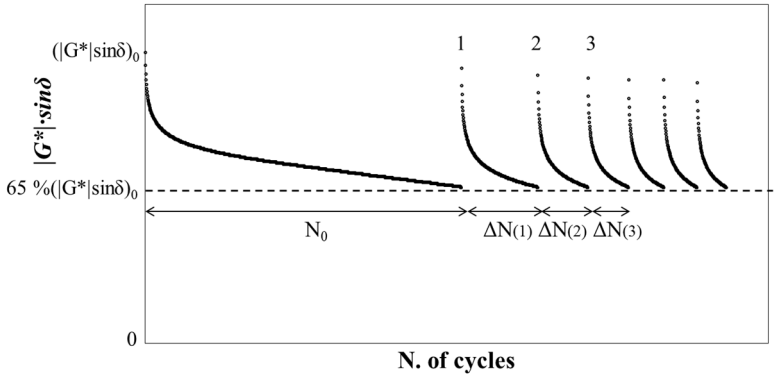

Figure 9.4. Evolution of |G*|•senδ versus number of loading cycles: general results (Mazzoni et al., 2016).

Results obtained were analysed using an innovative criterion developed for the characterisation of bitumens (Stimilli et al., 2014). The model proposed is based on the measurement of the number of initial loading cycles, N_0, and the number of loading cycles after each i-th rest period, ΔN_i, which are necessary to reach the damage level selected (65%|G*|•senδ). Test results show that ΔN_i decreases with a gradually lower rate as a function of the number of rest periods, until an asymptotical constant value is reached (Figure 9.5).
For bitumens, ΔN_i is assumed to be the result of two contributions, one provided by self-healing capability and the other related to time dependent phenomena, such as thixotropy. According to the definition of the latter (Mewis and Wagner, 2009; Mouillet et al., 2012), thixotropy exhibits its effect mainly when the material is unloading. Nevertheless, the thixotropic contribution developed during the rest phase has consequences also during the subsequent loading step: the higher the thixotropic recovery during the rest period, the higher the number of loading cycles that the material can resist when loaded. Also considering that thixotropy is an intrinsic property of a material, it is assumed to be a constant contribution, whereas self-healing capability tends to decrease as damage on the material increases. Thus, the asymptotical constant value of ΔN_i measured after infinite rest periods, when it can be assumed that the material has already reached complete failure, is attributed only to thixotropy and, based on the results obtained, this value (designated as ΔN_∞) is considered as a constant.

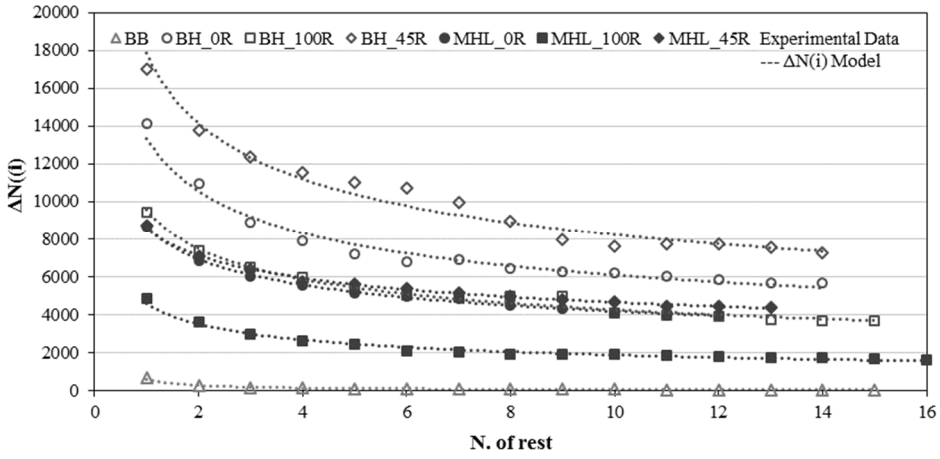

Figure 9.5. Recovered number of cycles versus number of rest periods: effects of modification, ageing and filler (Mazzoni et al., 2016).

Based on the previous concepts, the total number of cycles prior to material failure after "n" rest periods (N_{tot}) is considered to be the sum of more contributions, as summarised by the following equation:

$$N_{tot} = N_0 + \sum_{i=1}^{n} \Delta N_i \tag{9.1}$$

where N_0, which is related to the initial strength of the material, is the number of loading cycles that the material can sustain before reaching a 35% reduction in |G*|•senδ and ΔN_i is the number of recovered cycles after each rest period.
It is hypothesised that, for each loading cycle after a rest period, ΔN_i is the sum of a variable contribution due to self-healing ΔN^h_i and a constant contribution due to thixotropy ΔN_∞, as follows:

$$\Delta N_i = \Delta N_h^i + \Delta N_\infty \tag{9.2}$$

Thus, the self-healing contribution is calculated as the number of loading cycles recovered after "n" rest periods once the constant value of thixotropy is deducted, for each loading phase, per the following expression:

$$N_h^n = \sum_{i=1}^{n} \Delta N_h^i = \sum_{i=1}^{n} (\Delta N_i - \Delta N_\infty) = \sum_{i=1}^{n} \Delta N_i - n \cdot \Delta N_\infty \tag{9.3}$$

Based on the above-mentioned considerations, after an infinite number of rest periods, the total number of loading cycles converges to a finite value N_{fH} (material parameter) (Figure 9.6) modelled by Canestrari et al. (2015) as follows:

$$N_h^n = N_{fH} \cdot \left[1 - e^{\frac{-3n}{n_{95}}} \right] \tag{9.4}$$

where N_{fH} represents the maximum recoverable number of cycles due to self-healing and n_{95} is the number of rest periods necessary to reach the 95% of N_{fH}.

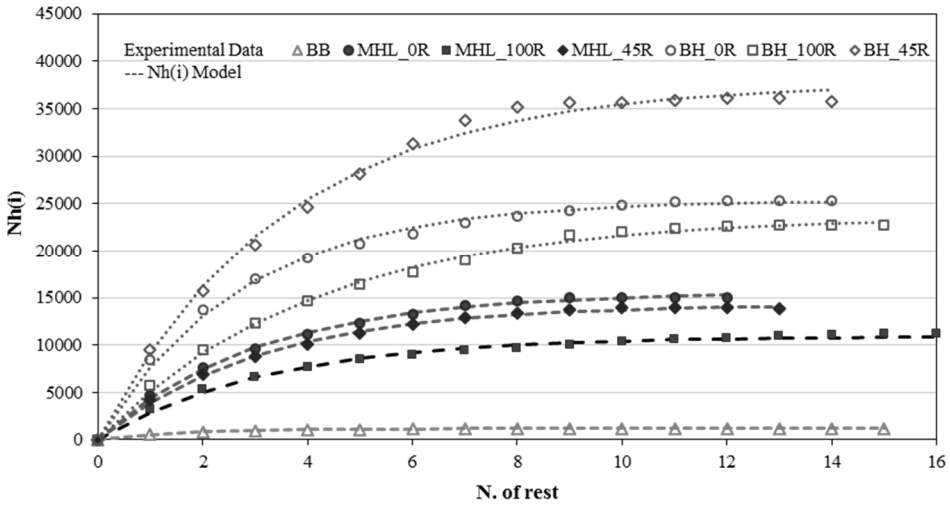

Figure 9.6. Self-healing contribution versus number of rest periods: effects of modification, ageing and filler.

Finally, by adding N_{fH} to N_0 it is possible to compute the global fatigue endurance limit prior to failure able to account for self-healing capability:

$$N_{fat} = N_0 + N_{fH} \quad (9.5)$$

Chapter 10.

Advanced experimental findings

10.1 Self-healing capability and thixotropy of bituminous materials: from bitumen to mastic

Fatigue resistance of bituminous materials is related to time-dependent phenomena, such as damage accumulation, hardening, viscoelasticity, thixotropy and healing.
In bituminous mixtures, damage due to fatigue processes mainly involves bitumen and its combination with filler (i.e. mastic).
Currently, there is the lack of a consolidated method that allows the quantification of bitumen fatigue endurance limit, considering also the phenomena above-mentioned, and limited work has been done on mastics.
To bridge this gap, the experimental investigation described in this study (Mazzoni et al., 2016) provides a comparison between bitumens and the corresponding mastics in terms of fatigue, self-healing and thixotropy. Effect of polymer modification on material response was accounted for the bitumens and the corresponding mastics investigated by adding a Styrene Butadiene Styrene (SBS) content equals to 3.8% by bitumen weight. In addition, long-term aged materials were also taken into consideration in order to identify potential detrimental effects on self-healing caused by oxidation phenomena, evaluating the possible inclusion of Reclaimed Asphalt Pavement (RAP) for the production of bituminous mixtures. Data analysis was based on an innovative test method previously implemented for bitumens and carried out by means of a Dynamic Shear Rheometer (DSR). Moreover, the influence of morphological properties of filler on filler-bitumen interactions was assessed by means of a Scanning Electron Microscope (SEM).
Results show that the above-mentioned analysis method is also suitable for analysing bituminous mastics and is able to identify the role of filler as well as the influence of ageing on self-healing process of bituminous materials. The investigation confirms that a certain amount of aged bitumen (up to 45%) added to a virgin bitumen/mastic is able to considerably enhance the overall fatigue performance, suggesting significant benefits when dealing with recycled mixtures including RAP contents.

10.1.1 SEM analysis

The interaction between bitumen and filler particles inside mastics was evaluated by means of SEM imaging analysis (according to ASTM E986) for a better interpretation of the rheological results (Mazzoni et al., 2016). This approach allowed the identification of mastic

morphology and filler distribution inside the bituminous matrix, thus helping to explain the differences detected in fatigue and self-healing behaviour between bitumens and mastics. Figures 10.1 and 10.2 show the SEM micrograph output obtained by SEM imaging for two mastics, captured at two resolution levels (i.e. 20 µm, 100 µm).

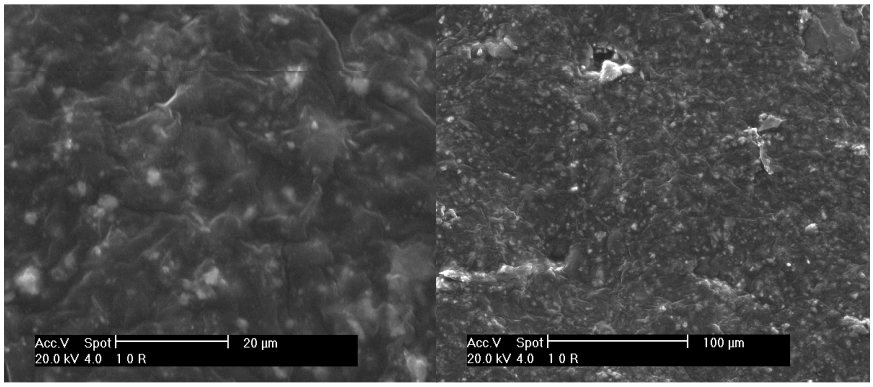

Figure 10.1. SEM imaging of MHL_0R (Mazzoni et al., 2016).

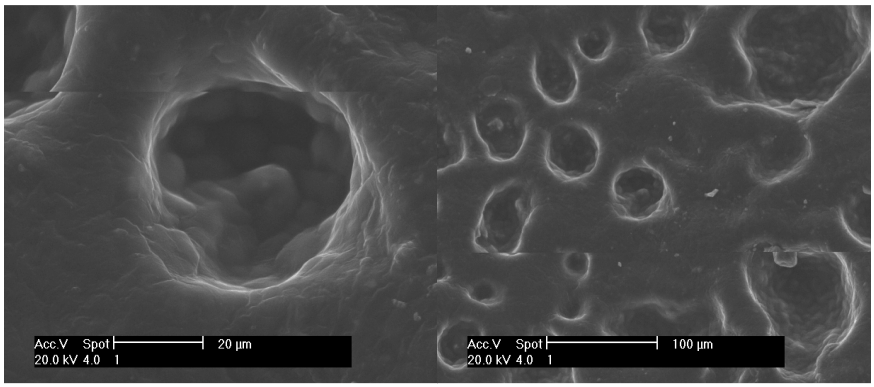

Figure 10.2. SEM imaging of MHL_100R (Mazzoni et al., 2016).

In agreement with the findings by Antunes et al. (2015), in SEM images limestone filler exhibits angular, smooth or slightly rough particles, with low propensity to agglomerate. By analysing the SEM images of the materials investigated in this study (Figures 10.1 and 10.2) on the basis of the description above-mentioned, the presence of filler in the mastic prepared with totally aged bitumen (MHL_100R) can be easily identified in the form of discontinuous globules. On the contrary, it is worth noting that in the case of the unaged mastic (MHL_0R) the SEM image shows a continuous network where no clear distinction between bitumen and filler is detected. Such a different behaviour can be related to the different internal molecular structures characterising unaged and aged bitumens. When an SBS modified bitumen

undergoes oxidation phenomena, it is subjected to a disruption in the butadiene functional group of SBS chains. In turn, this implies the formation of shorter polymer structures in the bituminous phase of MHL_100R mastic which determine an internal discontinuous network which is not able to adequately englobe the filler particles. Differently, the unaged bitumen of MHL_0R mastic is composed of longer polymer chains which are able to completely surround filler particles. Therefore, the MHL_0R SEM image shows a more uniform material, since filler particles are better enclosed in the bituminous phase, creating a more efficiently collaborative morphological structure between bitumen and filler, whereas, in the case of the aged mastic, filler particles are less linked to bitumen and stand out from the bituminous matrix. This finding further supports the results summarised in the following paragraph (§ 10.1.4) in terms of lower fatigue and self-healing performance of the aged mastic compared to those of the unaged one and is coherent with the hypotheses proposed to explain the rheological behaviour in terms of fatigue and self-healing, which are therefore definitely reasonable.

10.1.2 Frequency sweep test

For thermorheologically simple materials, Time-Temperature Superposition Principle (TTSP) can be applied to obtain complex modulus and phase angle master curves. In particular, the master curves of complex modulus were implemented for all the materials investigated at a reference temperature of 34 °C (Figure 10.3) (Mazzoni et al., 2016). The modified CAM (Christensen-Anderson-Marasteanu) Model was adopted to analyse test data and find the relationship between the complex modulus norm and the reduced frequency, following a shift factor variation based on the Williams-Landel-Ferry equation. In Table 10.1 the calibrated values for the modified CAM model parameters are summarised.

Table 10.1. Calibrated parameters of the modified Christensen-Anderson-Marasteanu model for the materials investigated (Mazzoni et al., 2016).

CAM modified model	$G^* = G^*_e+(G^*_g-G^*_e)[1+(f_c/f)^k]^{-me/k}$						
	G^*_e [Pa]	G^*_g [Pa]	f_c [Hz]	k	m_e	$S=Log2(m_e/k)$	R^2
BB	0	1.0E+09	400	0.155	1.07	2.077	0.997
BH_0R	0	1.0E+09	306	0.101	0.84	2.504	0.990
BH_45R	0	1.0E+09	306	0.105	0.71	2.040	0.987
BH_100R	0	1.0E+09	280	0.101	0.64	1.901	0.978
MHL_0R	0	1.2E+09	140	0.118	0.80	2.041	0.986
MHL_45R	0	1.2E+09	140	0.106	0.69	1.960	0.990
MHL_100R	0	1.2E+09	118	0.103	0.63	1.824	0.970

Elastomeric polymers (e.g. SBS) modify bitumen rheology by enhancing bitumen elastic response. This behaviour resulted in a higher stiffness at low frequencies and a lower stiffness at high frequencies, as shown in Figure 10.4 comparing the master curves related to the base bitumen (BB) and the SBS modified bitumen (BH_0R). Furthermore, the addition of polymers caused a higher shape index S, which is a positive behaviour suggesting a lower sensitivity to frequency changes and, simultaneously, a lower crossover frequency f_c, as an indication of a greater overall elastic component in the behaviour (Table 10.1).
Moreover, the master curve trend showed a stiffening effect in the whole range of the frequencies investigated due to the addition of filler. It is worth noting that the master curves of all the modified bitumens (BH_0R, BH_45R, BH_100R) and the corresponding mastics (MHL_0R, MHL_45R, MHL_100R) are almost reciprocally shifted along the vertical axis (Figure 10.3). This behaviour is highlighted in Figure 10.4 considering the master curve related to the SBS modified bitumen (BH_0R) compared to that of the corresponding SBS modified mastic (MHL_0R).
As expected, the presence of the aged bitumen R implied an increase in stiffness both for bitumens and mastics: the higher the percentage of R, the higher the stiffness, as shown by comparing the master curves related to the materials with different percentages of R (Figures 10.3 and 10.5).

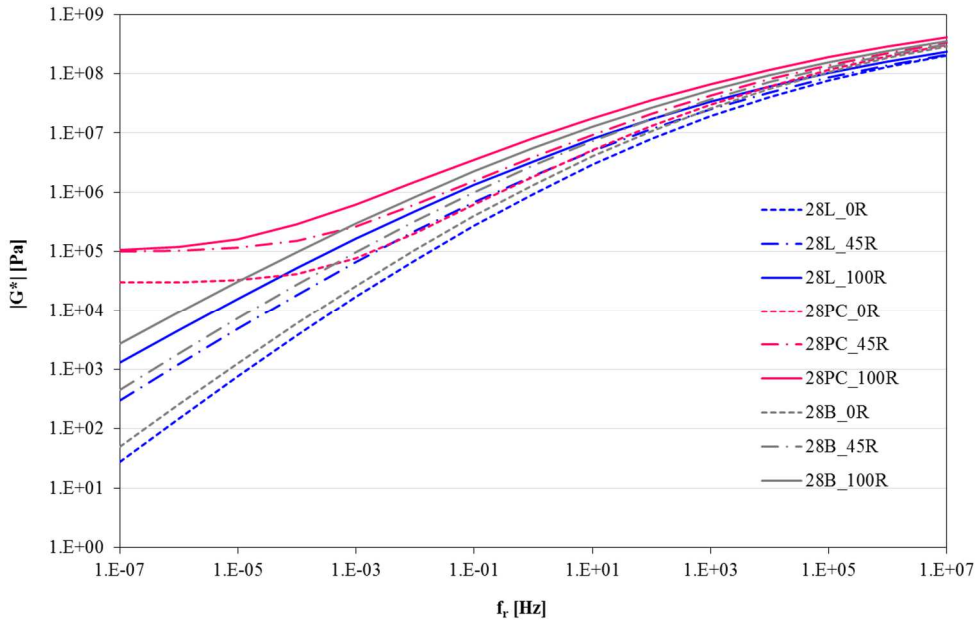

Figure 10.3. Master curves of |G*| at a reference T equal to 34 °C.

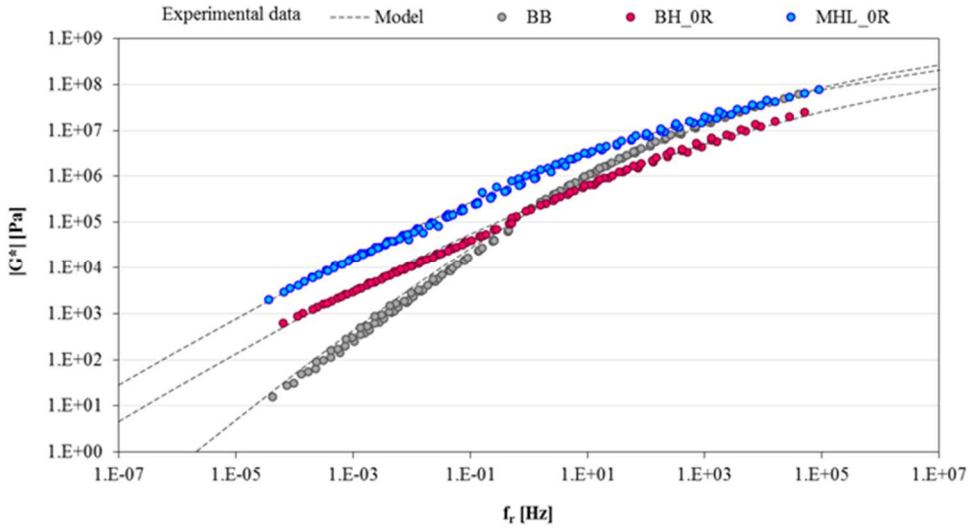

Figure 10.4. Effect of SBS modification and filler addition on the corresponding materials in terms of master curves of |G*| at a reference T equal to 34 °C (BH_0R Vs. BB and BH_0R Vs. MHL_0R).

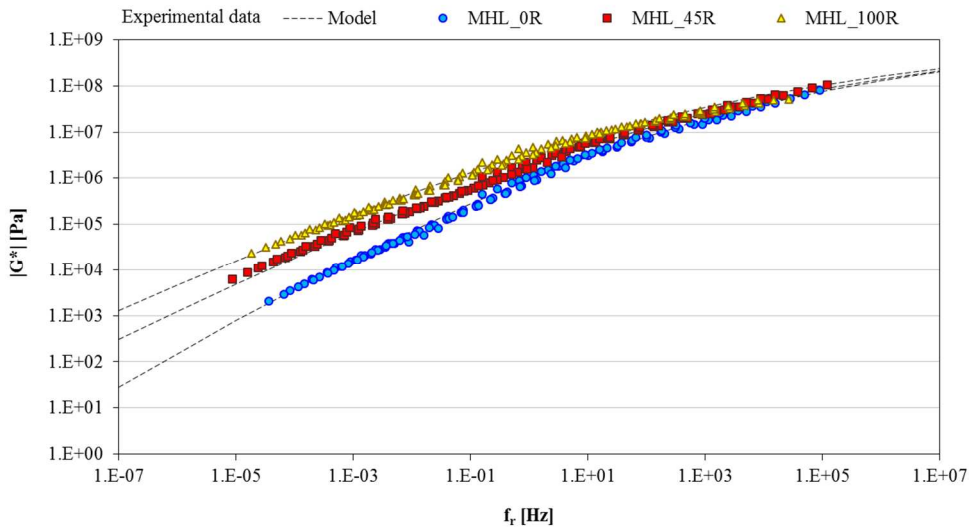

Figure 10.5. Effect of the inclusion of increasing aged bitumen R contents on the corresponding mastics in terms of master curves of |G*| at a reference T equal to 34 °C.

10.1.3 To find Isostiffness test

Results summarised in Table 9.4 were obtained following the procedure described in paragraph § 9.3.3 starting from the raw data represented in the table below.

Table 10.2. Isostiffness temperatures obtained for all the materials investigated.

Material	Strain [%]	Temperature [°C]	|G*|•sinδ [MPa]	Isostiffness |G*|•sinδ [MPa]	Isostiffness T [°C]
BB	5	28	0.37	3	19.5
		24	0.86		
		20	2.89		
BH_0R	5	28	0.77	3	21.5
		24	1.48		
		20	3.72		
BH_45R	5	28	0.83	3	22.5
		24	1.93		
		20	4.25		
BH_100R	5	28	3.55	3	29.0
		24	5.93		
		20	8.15		
MHL_0R	1	32	5.46	9	25.4
		28	7.57		
		24	9.80		
MHL_45R	1	32	6.04	9	27.0
		28	8.12		
		24	11.00		
MHL_100R	1	32	9.39	9	32.3
		28	13.10		
		24	17.40		

10.1.4 Time sweep test with multiple rest periods

Based on the test method described in paragraph § 9.3, the materials investigated were characterised in terms of self-healing capability and fatigue resistance (Mazzoni et al., 2016). The comparison between bitumens and mastics for each percentage of aged bitumen R (i.e. 0%, 45% and 100%) is depicted in Figure 10.6 where the parameter $|G^*| \bullet sen\delta$ is plotted as a function of the number of loading cycles. Regardless of the percentage of bitumen R considered, it can first be observed that the addition of filler to the bitumen caused a decrease in material resistance (i.e. a lower number of loading cycles). Subsequently, the effect of ageing on fatigue properties can be analysed. The aged bitumen R (BH_100R) exhibited a significant lower resistance compared to the virgin bitumen (BH_0R), as demonstrated by a faster damage accumulation during a single n-th loading cycle. However, the presence of a limited amount of aged bitumen blended with the virgin one seemed to provide benefits in terms of damage evolution (BH_0R Vs. BH_45R).
An identical trend was found for the corresponding mastics. In fact, even when a certain amount of filler was added to the aged bitumen R (MHL_100R), a significant decrease in material resistance was detected compared to the unaged mastic (MHL_0R). Also in this case, a blend of virgin and aged bitumen positively affected the corresponding mastic (MHL_45R) in terms of damage accumulation during each loading cycle, consistently with the bitumen trend.
All the test parameters determined for each material are summarised in Table 10.3 and each parameter is depicted in Figures 10.7 and 10.8, where the comparison between bitumens and the corresponding mastics is provided.

Table 10.3. Model parameters for all the materials investigated (Mazzoni et al., 2016).

Material	N_{fat}	N_0	N_{fH}	ΔN_∞	n_{95}
BB	4391	3180	1211	35	5.30
BH_0R	81095	55780	25315	5680	8.23
BH_100R	56036	32340	23696	3640	12.31
BH_45R	107248	69520	37728	7520	10.69
MHL_0R	34082	16580	15562	3980	9.17
MHL_100R	20866	9940	10926	1580	9.79
MHL_45R	37541	20940	14281	4440	9.32

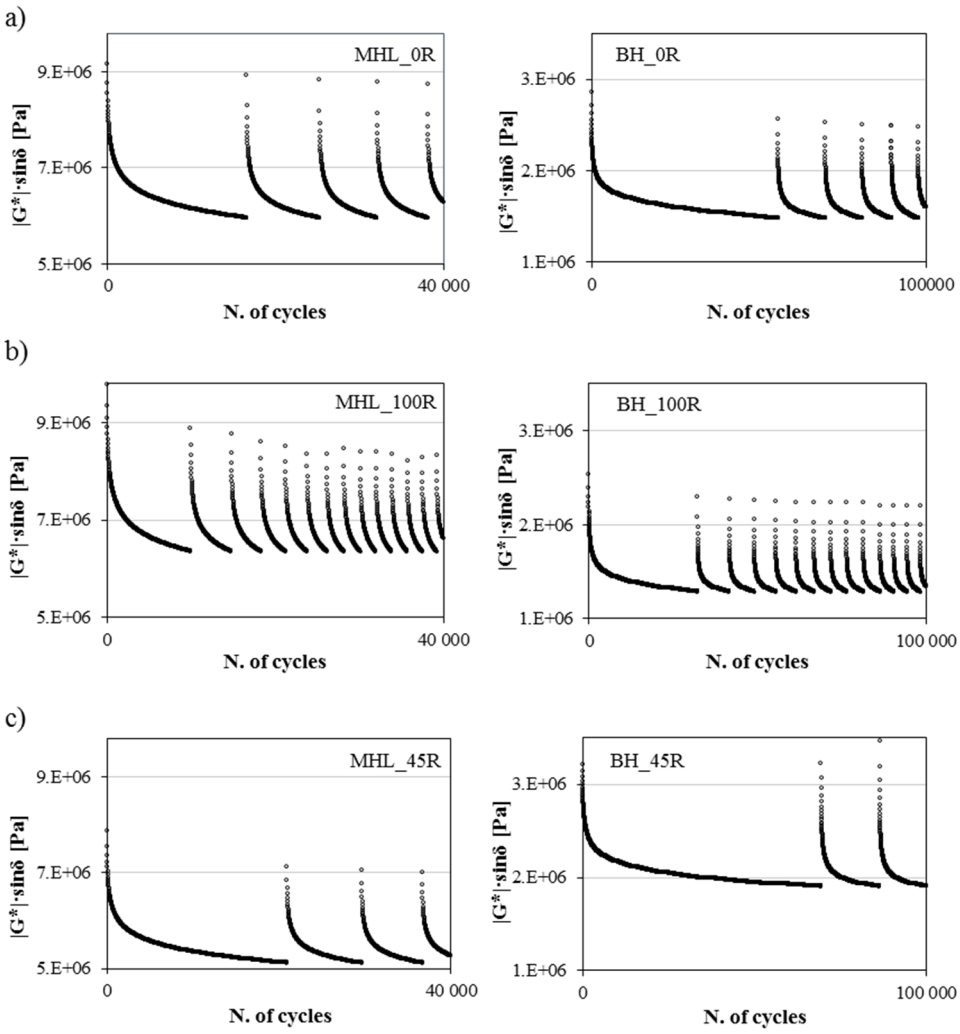

Figure 10.6. Evolution of |G*|•senδ versus number of loading cycles: a) mastic MHL_0R versus bitumen BH_0R; b) mastic MHL_100R versus bitumen BH_100R; c) mastic MHL_45R versus bitumen BH_45R (Mazzoni et al., 2016).

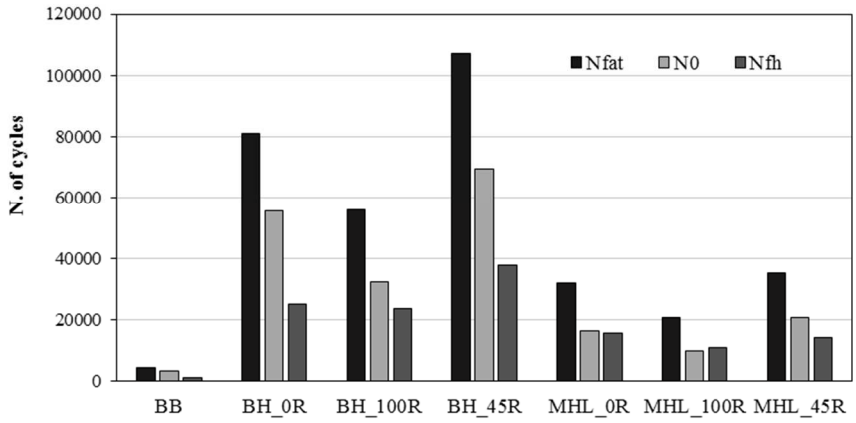

Figure 10.7. Initial strength N_0, self-healing potential N_{fH} and fatigue endurance limit N_{fat} of the materials studied (Mazzoni et al., 2016).

As far as the comparison between bitumens and mastics is concerned, the lower values of the parameter N_0 for mastics suggests that the presence of filler promoted a faster damage accumulation, whatever the amount of aged bitumen R. This behaviour could be attributed both to the unknown real strain effectively acting on the bituminous phase of mastic at a micro-scale level and to the involvement of chemical and mechanical mechanisms related to the interactions between the bituminous phase and the lytic component (i.e. filler) in fatigue process. In fact, the presence of filler, an interference element within the continuous bituminous phase, further complicates crack propagation by altering the overall cohesive potential of the effective binder component of a mixture (i.e. mastic).
The latter aspect, which is inherently linked to filler mineralogy (i.e. limestone), has consequences also on the cohesive self-healing capability. The presence of filler appeared detrimental in terms of self-healing (the lower N_{fH}, the lower the self-healing capability) due to the inhibition of bitumen interdiffusion, the main mechanism occurring at the crack surfaces (Wool et al., 1981).
Also the thixotropic component was slightly affected by the presence of filler, even if a less significant decrease in the related model parameter (ΔN_∞) was recorded, according to the consideration that thixotropy is an intrinsic bitumen property and acts independently of the presence of cracks.

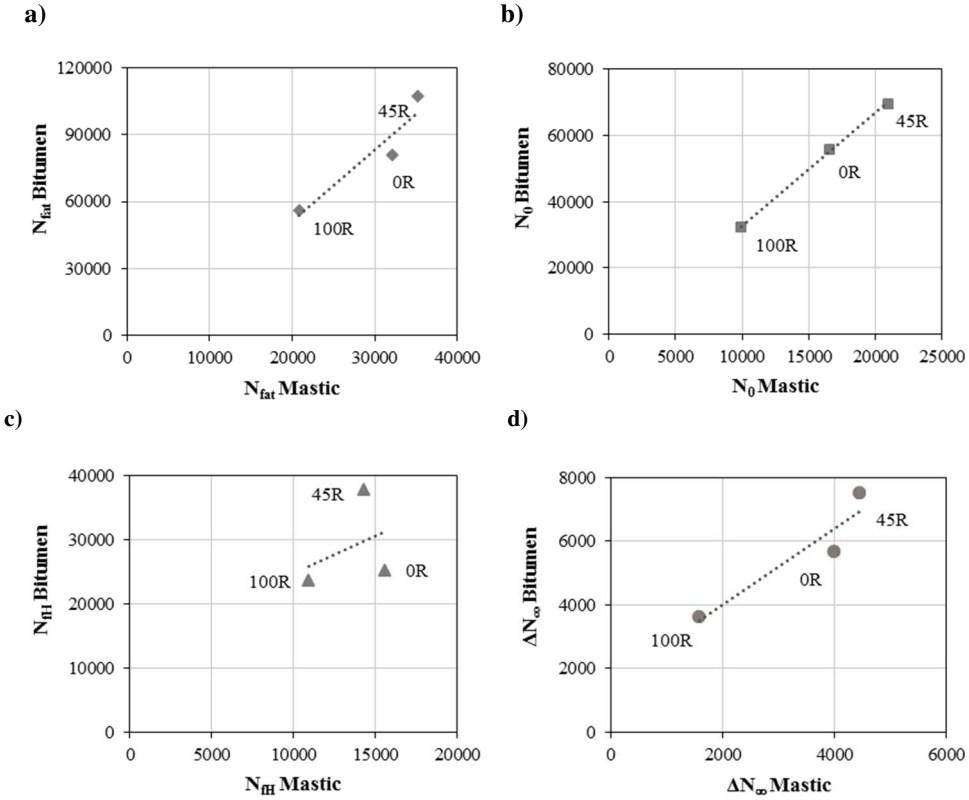

Figure 10.8. Comparison between bitumens and the corresponding mastics about: a) fatigue endurance limit N_{fat}; b) initial strength N_0; c) self-healing potential N_{fH}; d) thixotropic contribution ΔN_∞ (Mazzoni et al., 2016).

With respect to the influence of ageing, it can be noted that perfect agreement between bitumens and mastics was detected in terms of initial fatigue resistance (N_0) when different amounts of aged bitumen R were analysed, as supported by the linear trend in Figure 10.8-b. Oxidation seemed to cause a performance loss measurable with a decrease in the number of loading cycles N_0 and N_{fat} for the aged material compared to the corresponding virgin one, for both bitumen and mastic. However, the presence of a limited aged bitumen R content (i.e. 45%) in the blend provided slight benefits to the overall fatigue performance compared to the unaged material. Also in terms of thixotropy (ΔN_∞), which does not affect the fatigue performance, a similar correspondence can be found between bitumens and mastics (Figure 10.8-d). The aged materials were characterised by lower ΔN_∞ values, whereas a certain percentage of aged bitumen R blended with unaged material did not cause negative effects on thixotropy.

On the contrary, by analysing the influence of ageing on self-healing capability, different effects on bitumens and mastics were found (see ΔN_{fH} in Table 10.3 and Figure 10.8-c). In fact, the blend containing virgin bitumen and 45% of aged bitumen R exhibited an improved self-healing capability compared to the virgin bitumen. The interactions between shorter polymer chains (created by the disruption of the butadiene functional group due to oxidation phenomena undergone by the aged bitumen R) (Stimilli et al., 2014) and intact unaged polymer chains (provided by the virgin modified bitumen) improved self-healing capability by creating an internal network which was even more effective for fatigue performance. Moreover, virgin and aged bitumens were characterised by comparable self-healing performances, as shown by ΔN_{fH} values in Table 10.3, thus demonstrating that polymer is still able to provide its contribution after the ageing process, even after undergoing polymer chains disruption.

On the contrary, with regards to the corresponding mastics, MHL_45R containing 45% of aged bitumen R exhibited a self-healing performance comparable to that of the unaged mastic MHL_0R (Table 10.3). Such a difference in behaviour between bitumens and mastics is linked to the presence of filler which creates a skeleton that, acting as volume filling (Buttlar et al., 1999), obstructs the interactions between unaged and aged polymer chains, thus compromising the internal network above-mentioned.

In addition, mastic MHL_0R, which is characterised by a bituminous phase with longer molecular chains, is likely able to enhance the interaction with filler particles inside this network, positively affecting the overall material response. Such a statement is supported by the more remarkable difference in terms of self-healing potential recorded between unaged and aged mastic (MHL_0R Vs MHL_100R) compared to the corresponding bitumens (BH_0R Vs. BH_100R).

Moreover, as previously mentioned, also chemical interactions between bitumen and filler must be considered for the evaluation of mastic self-healing capability. Probably, the unaged mastic exhibits a higher chemical affinity with filler particles, thus developing an improved cooperation in terms of self-healing. On the contrary, the oxidation subjected by the aged bitumen reduces such affinity, thus compensating the enhanced internal network provided by the coexistence of long and short polymer chains (MHL_45R). Such a behaviour does not occur in bitumens, due to the absence of chemical filler-bitumen interactions which further complicate the analysis. Nonetheless, it is worth noting that, also for mastics, the overall self-healing potential was not hindered by the presence of aged bitumen R and the final fatigue performance (N_{fat}) was still improved compared to that of the unaged mastic, in accordance with the results obtained for bitumens (Table 10.3, Figures 10.7 and 10.8-a).

Since mastic is the effective binder component of bituminous mixtures, such an outcome leads to the expectation that recycled bituminous mixtures prepared with SBS modified bitumen and a certain amount of RAP (which releases a percentage of the same SBS modified aged bitumen) can exhibit an enhanced fatigue resistance compared to virgin mixtures. This observation agrees with the results obtained through specific studies on fatigue performance of recycled Hot Mix Asphalts (HMAs) prepared with the same SBS modified bitumens

(Stimilli et al., 2016), which showed improvements in terms of fatigue and cracking resistance when a given amount of RAP is added.

10.2 Fatigue, self-healing and thixotropy of bituminous mastics including aged SBS modified bitumens and different filler contents

Bituminous mastic is a self-healing viscoelastic material. Recoverable phenomena, such as thixotropy and self-healing capability, are recognised as an important resource for the development of sound road pavements.
The experimental investigation described in this study and implemented through a Dynamic Shear Rheometer (DSR) provides a comparison among mastics blended with different percentages of aged SBS modified bitumen, new virgin SBS modified bitumen and filler in terms of fatigue, self-healing and thixotropy (Mazzoni et al., 2017b).
Data analysis is based on a model adopted in previous studies for polymer modified bitumens in order to calculate the fatigue endurance limit.
Results show that the presence of increasing percentages of filler negatively affects mastic fatigue performance which can be, anyway, offset by the addition of a certain amount of aged SBS modified bitumen. In fact, whatever the filler content considered, a percentage of aged SBS modified bitumen (up to 45%) added to mastics improves the fatigue endurance limit suggesting significant benefits when dealing with sustainable recycled mixtures containing Reclaimed Asphalt (RA) aggregates.

10.2.1 Frequency sweep test

Time-Temperature Superposition Principle (TTSP) was applied to obtain complex modulus master curves at a reference temperature of 34 °C for all the materials investigated (Figure 10.9) (Mazzoni et al., 2017b). Test data were analysed by adopting the modified Christensen-Anderson-Marasteanu (CAM) Model to relate the complex modulus norm to the reduced frequency following a shift factor variation based on the Williams-Landel-Ferry (WLF) law. The calibrated values for the modified CAM model and the WLF law are summarised in Table 10.4.

Table 10.4. Calibrated parameters of the modified Christensen-Anderson-Marasteanu model and Williams-Landel-Ferry law for the materials investigated (Mazzoni et al., 2017b).

CAM modified model + WLF law	$G^* = G_e^* + \frac{G_g^* - G_e^*}{[1+(\frac{f_c}{f})^k]^{\frac{m_e}{k}}}$							$Log(a_t) = \frac{C_1(T-T_0)}{C_2+(T-T_0)}$		
	G^*_e [Pa]	G^*_g [Pa]	f_c	k	m_e	S	R^2	C_1	C_2	T_0 [°C]
42L_0R	100	5.0E+09	133	0.110	0.80	2.166	0.990	15	150	34
42L_45R	100	5.0E+09	134	0.105	0.71	2.036	0.998	22	200	34
42L_100R	100	5.0E+09	110	0.101	0.62	1.844	0.999	23	220	34
28L_0R	0	1.2E+09	140	0.118	0.80	2.041	0.986	15	150	34
28L_45R	0	1.2E+09	140	0.106	0.69	1.960	0.990	22	200	34
28L_100R	0	1.2E+09	118	0.103	0.63	1.824	0.970	22	220	34

$$\text{with } S = \text{Log}\frac{2^{\frac{m_e}{k}}}{1+(2^{\frac{m_e}{k}}-1)\cdot\frac{G_e^*}{G_g^*}}$$

The presence of the aged bitumen R led to an expected increase in mastic stiffness: the higher the percentage of R, the higher the stiffness, as shown by comparing the master curves corresponding to mastics with different percentages of R (Figure 10.9). Considering the model parameters summarised in Table 10.4, the presence of higher aged bitumen R contents implied the following effects: 1) lower shape index S and viscous asymptote m_e, indicating a higher sensitivity to frequency changes; 2) higher |G*| values and lower crossover frequency f_c, indicating a greater overall elastic component in the behaviour; 3) higher C_1 and C_2 values, according to the reduction in fractional free volume (i.e. reduction of molecular mobility).
Moreover, regardless of the aged bitumen content considered, the higher the filler percentage, the higher the fixed bitumen as well as the mastic stiffness (Figures 10.9 and 10.10), as confirmed by the model parameters summarised in Table 10.4. In details, the master curves of the mastics containing a higher filler percentage (42L_0R, 42L_45R, 42L_100R) are almost shifted along the vertical axis compared to the corresponding mastics blended with less filler (28L_0R, 28L_45R, 28L_100R) (Figures 10.9 and 10.10). In particular, the increase in filler content determined higher values of the glassy modulus G_g^* and the appearance of the equilibrium complex modulus G_e^* in the mastics blended with 42% of limestone by mastic volume, suggesting a stronger bitumen-filler interaction (Figure 10.11).

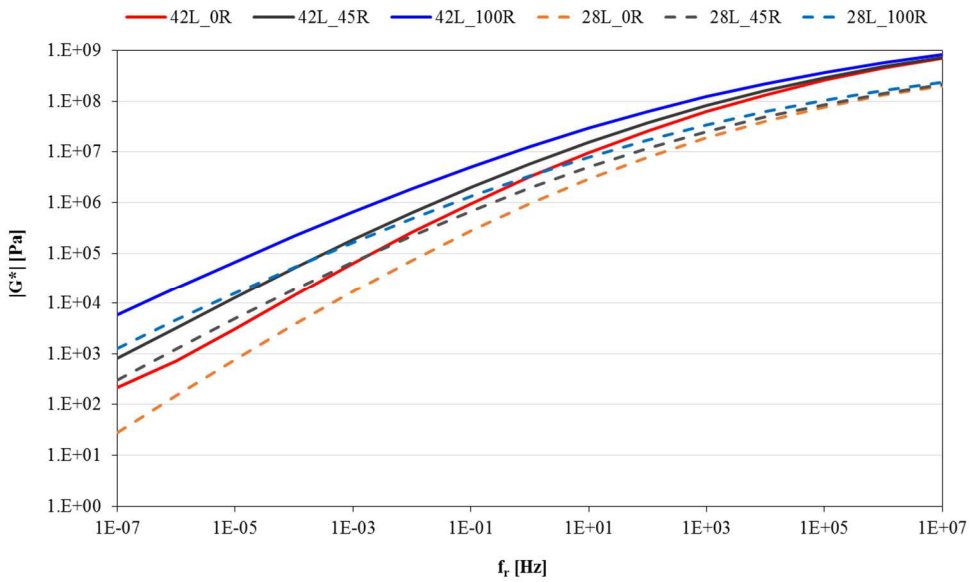

Figure 10.9. Master curves of |G*| at a reference T equal to 34 °C.

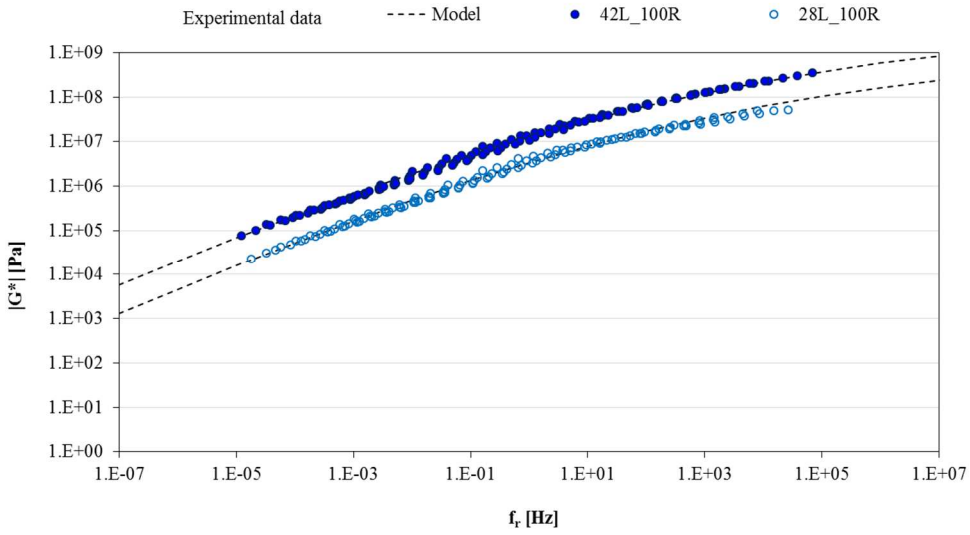

Figure 10.10. Comparison among master curves of |G*| at 34 °C related to the mastics composed of the same bituminous blend (100R) and different amounts of limestone filler (42% and 28% of limestone by mastic volume).

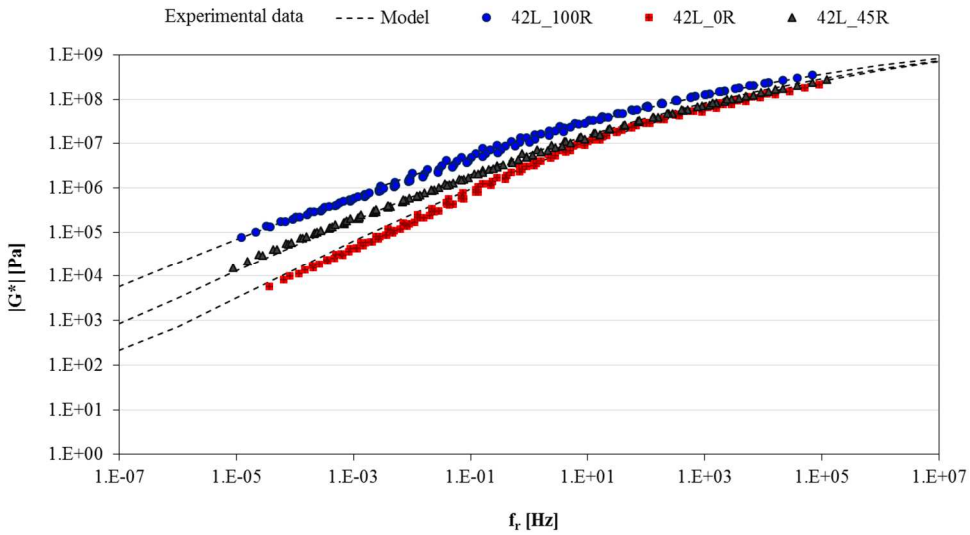

Figure 10.11. Comparison among master curves of |G*| at 34 °C related to the mastics blended with 42% of limestone by mastic volume.

10.2.2 To find Isostiffness test

Results summarised in Table 9.4 were obtained following the procedure described in paragraph § 9.3.3 starting from the raw data represented in the table below. In particular, the higher the filler percentage, the higher the iso-stiffness value (i.e. initial |G*|•sinδ value) chosen to run tests at intermediate and comparable temperatures.

Table 10.5. Isostiffness temperatures obtained for all the materials investigated.

Material	Strain [%]	Temperature [°C]	|G*|•sinδ [MPa]	Isostiffness |G*|•sinδ [MPa]	Isostiffness T [°C]
42L_0R	0.7	32	9.46	13.0	29.3
		28	14.90		
		24	19.80		
42L_45R	0.7	32	10.40	13.0	30.0
		28	15.50		
		24	20.60		
42L_100R	0.7	33	14.10	13.0	33.9
		31	16.20		
		29	18.50		
28L_0R	1.0	32	5.46	9.0	25.4
		28	7.57		
		24	9.80		
28L_45R	1.0	32	6.04	9.0	27.0
		28	8.12		
		24	11.00		
28L_100R	1.0	32	9.39	9.0	32.3
		28	13.10		
		24	17.40		
14L_0R	1.5	28	2.84	3.8	25.2
		24	4.15		
		20	5.82		
14L_45R	1.5	28	3.85	3.8	28.0
		24	5.20		
		20	6.94		
14L_100R	1.5	32	3.74	3.8	31.7
		29	4.69		
		26	5.89		

10.2.3 Time sweep test with multiple rest periods

Based on the test method described in paragraph § 9.3, all the materials were characterised in terms of self-healing capability and fatigue resistance (Mazzoni et al., 2017b).
For all the mastics investigated, the behaviour detected in terms of damage accumulation after each rest period is depicted in Figure 10.12 where the parameter $|G^*|\bullet\sin\delta$ is plotted as a function of the number of loading cycles.
Based on test data, it is possible to determine the main model parameters that provide a quantitative evaluation of fatigue, self-healing and thixotropy properties, as summarised in Table 10.6 and depicted in Figures 10.13 and 10.14 for a more direct comparison among the mastics investigated.
Analysis of all the parameters suggests important observations about the influence of filler and aged bitumen on the overall fatigue behaviour of materials.
Regardless of the percentage of bitumen R considered, it can be observed in Figure 10.12 that the addition of increasing filler contents to the bituminous phase caused a decrease in the mastic fatigue resistance (i.e. lower number of loading cycles to reach the same damage level corresponding to a 35% reduction of the loss modulus at each loading phase).
Besides, also the effect of aged bitumen on mastic fatigue properties was analysed. Whatever the percentage of filler considered, blending a certain amount of aged bitumen R with virgin bitumen H provided positive effects on the corresponding mastic in terms of damage accumulation over time, as demonstrated by the highest damage resistance of mastics prepared with 45% of bitumen R (45R) (Figure 10.12). However, when the bituminous phase was totally composed of aged bitumen (100R), a resistance decrease compared to the corresponding mastic prepared exclusively with virgin bitumen (0R) was detected, particularly for lower filler contents (14L and 28L).

Table 10.6. Model parameters for all the mastics investigated (Mazzoni et al., 2017b).

Mastic	N_{fat}	N_0	N_{fH}	ΔN_∞	n_{95}
14L_0R	37230	20380	16850	3700	9.09
14L_45R	43576	24780	18796	3520	8.72
14L_100R	27380	12320	15060	2540	9.98
28L_0R	32142	16580	15562	3980	9.17
28L_45R	35221	20940	14281	4440	9.32
28L_100R	20866	9940	10926	1580	9.79
42L_0R	12777	5260	7517	1480	11.95
42L_45R	18141	9300	8841	1520	12.29
42L_100R	16949	8680	8269	1480	11.19

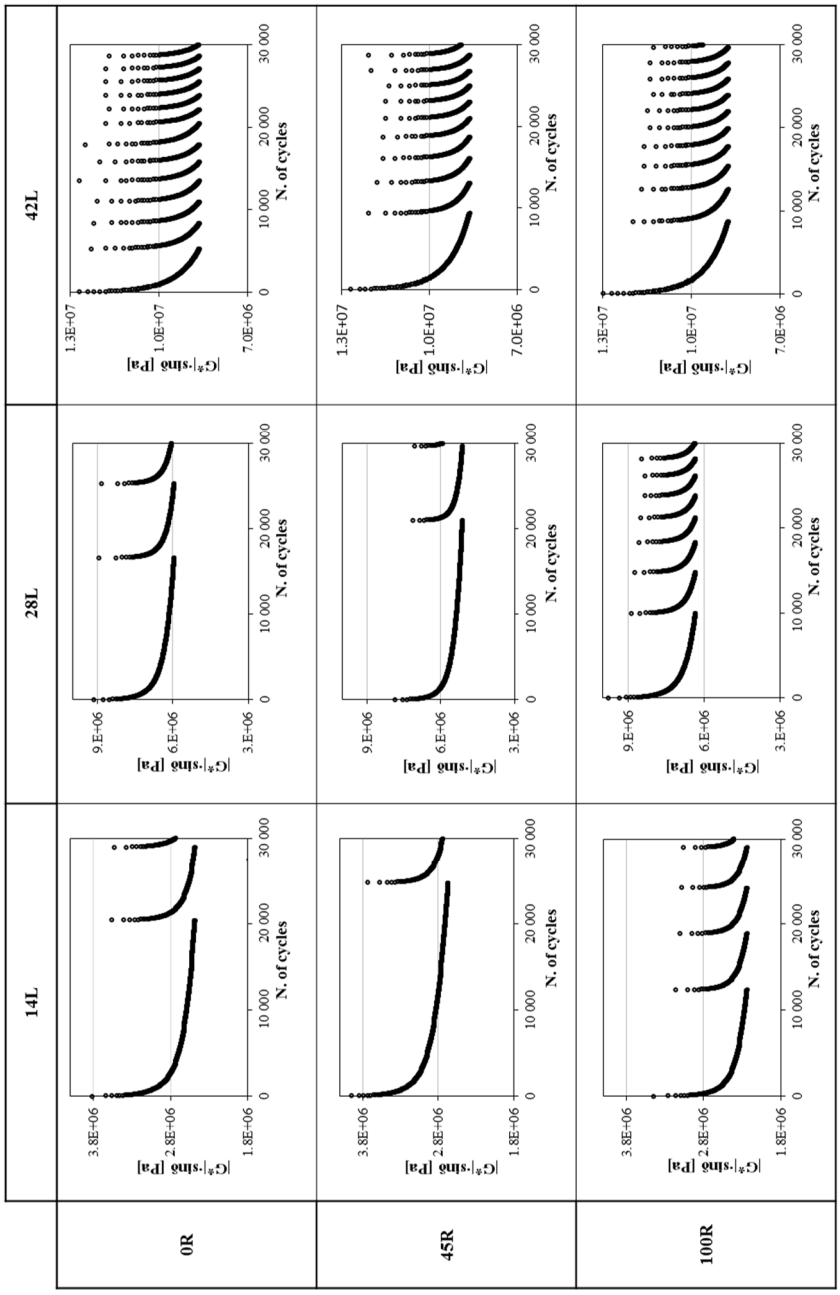

Figure 10.12. Comparison among all the mastics investigated about the evolution of |G*|•sinδ versus number of loading cycles (Mazzoni et al., 2017b).

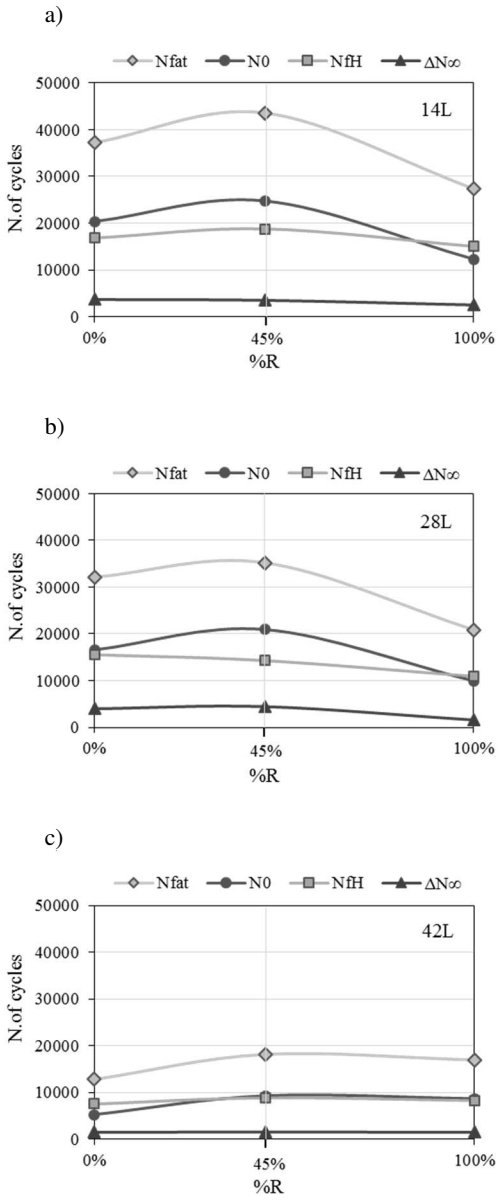

Figure 10.13. Model parameters (i.e. fatigue endurance limit N_{fat}, initial strength N_0, self-healing potential N_{fH} and thixotropy ΔN_∞) for: a) mastic with 14% of filler, by volume; b) mastic with 28% of filler, by volume; c) mastic with 42% of filler, by volume (Mazzoni et al., 2017b).

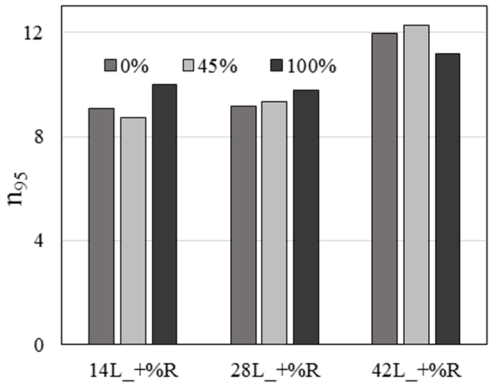

Figure 10.14. Comparison among all the mastics investigated in terms of the parameter n_{95} (Mazzoni et al., 2017b).

Moreover, results in terms of model parameters (Table 10.6 and Figure 10.13) confirmed what previously mentioned based on raw test data (Figure 10.12). The higher the percentage of filler, the faster the damage accumulation and the lower the values of the parameters N_0, N_{fH} and N_{fat}. This behaviour could be attributed to the involvement in fatigue process of chemical and mechanical phenomena, in turn related to the interactions between the bituminous phase and the lytic component (i.e. filler). In fact, filler constitutes an interference element within the bituminous matrix, since it interrupts the continuous bituminous phase by creating a discontinuous medium, further complicating crack propagation. Besides, oxidation seemed to cause a weakening of the material as detectable with a decrease in N_0, N_{fH} and N_{fat} for mastics including aged bitumen (100R) compared to the corresponding mastics prepared with virgin bitumen (0R), particularly for lower percentages of filler (14L and 28L) (Table 10.6 and Figures 10.13a and 10.13b). On the opposite, the presence of 42% of filler by mastic volume led to comparable performance, regardless of the amount of aged bitumen R (0R, 45R, 100R) contained in each mastic (Figure 10.13c). That is likely due to the predominance of the filler component over the bituminous phase within the mastic. The increase in filler content inhibits the dependence on bitumen chemistry. However, the addition of a limited amount of aged bitumen R (45%) provided benefits to the overall fatigue performance (N_{fat} and N_0) of the corresponding mastics without hindering their self-healing capability (N_{fH}), if compared to the mastics composed of only virgin bitumen (0R), confirming what previously observed for pure bitumens (Stimilli et al., 2014; Canestrari et al., 2015; Mazzoni et al., 2016). The simultaneous presence of shorter polymer chains (from bitumen R due to ageing) and intact chains (from virgin bitumen) optimises self-healing capability by creating an internal network which is even more effective for fatigue performance.

Furthermore, mastics exhibited a thixotropic behaviour as demonstrated by the constant contribution ΔN_∞, in agreement with previous experimental results obtained for pure

bitumens (Stimilli et al., 2014; Canestrari et al., 2015; Mazzoni et al., 2016). In particular, although it is an intrinsic bitumen property, also thixotropy (occurring due to molecular rearrangements within the bituminous phase) was negatively affected by increasing the amount of filler. In fact, regardless of the aged bitumen R content considered, the higher the percentage of filler, the lower the value of the thixotropic parameter ΔN_∞. In addition, oxidation led to lower ΔN_∞ values for mastics including only aged bitumen (100R) compared to the corresponding mastics prepared with virgin bitumen (0R), whereas the addition of 45% of aged bitumen R to the virgin bitumen (45R) did not cause detrimental effects on the corresponding mastic in terms of thixotropy (Table 10.6 and Figure 10.13). It is worth noting the case of mastics composed of 42% of filler by mastic volume (42L). Results showed substantially the same thixotropy value ΔN_∞ for all the percentages of bitumen R selected (0R, 45R, 100R) (Table 10.6 and Figure 10.13c). A comparable ΔN_∞ value was obtained also for mastic 28L_100R suggesting the existence of a minimum thixotropic threshold equal for all the bitumens (Table 10.6 and Figure 10.13b). When this threshold is reached, increasing the percentage of aged bitumen and/or filler does not cause further worsening in thixotropic performance.

As far as the parameter n_{95} is concerned, a previous study conducted on bitumens denoted a great influence due to modification and/or ageing (Stimilli et al., 2014). In particular, for SBS modified bitumens, the n_{95} value increased with the increase in aged bitumen R. In fact, oxidation phenomena induce a disruption in the butadiene functional group of polymer chains, thus creating shorter polymer structures that guarantee a better interdiffusion of bitumen components. On the contrary, no evident changes in n_{95} value were recorded in mastics characterised by different amounts of filler or bitumen R (Table 10.6 and Figure 10.14). The presence of filler creates a skeleton which, acting as volume filling (Buttlar et al., 1999) and interference element, prevails on bitumen chemistry and SBS polymer chains interactions. Finally, it should be highlighted that the SBS polymer percentage was the same for all the mastics investigated, hence only the effect due to the presence of aged bitumen on the final material acted on the n_{95} performance.

The results above-mentioned lead to the expectation that a recycled bituminous mixture prepared with an SBS modified bitumen and a certain amount of RAP (which releases a percentage of the same SBS modified aged bitumen) can exhibit improved fatigue and cracking resistance compared to a virgin mixture. This observation complies with the results obtained through specific studies on fatigue performance of recycled bituminous mixtures prepared with the same SBS modified bitumens which showed enhancements in terms of fatigue and cracking resistance when a given amount of RA was involved (Stimilli et al, 2015; Stimilli et al., 2016).

Moreover, results demonstrate how the filler/bitumen ratio highly influences the overall fatigue performance. In particular, it should be emphasised that a filler/bitumen ratio by weight equal to 1.0 (28L), in accordance with Superpave specifications, guarantees a fatigue performance not dissimilar from that one obtained with a filler/bitumen ratio by weight below the lower limit and equal to 0.4 (14L). Based on test data, the latter determines the best overall

fatigue and self-healing response. However, it should be taken into account that such a low filler content could cause other problems on the final blend (e.g. rutting). On the contrary, the choice of a filler/bitumen ratio by weight above the upper limit and equal to 1.9 (42L) leads to detrimental effects on the overall material response.

10.3 Influence of different fillers and SBS modified bituminous blends on fatigue, self-healing and thixotropic performance of mastics

The prediction of asphalt pavement performance is closely linked to the behaviour of mastic, consisting of filler and bitumen, which can be modelled as viscoelastic material.
The purpose of this study is to investigate the effect of different fillers and bituminous blends on mastic fatigue response, considering recoverable phenomena in viscoelastic materials (thixotropy and self-healing) that concurrently occur (Mazzoni et al., 2017c).
Three fillers (limestone, basalt and Portland cement) and three aged SBS modified bitumen contents (0%, 45% and 100%) were blended with a virgin SBS modified bitumen obtaining nine mastics characterised in terms of fatigue, self-healing and thixotropy using a Dynamic Shear Rheometer (DSR).
Data recorded are analysed through a model previously adopted for polymer modified bitumens and mastics, allowing the determination of the fatigue endurance limit.
Results show that the presence of filler with increasing particle density and/or Rigden voids (RV) causes a higher mastic stiffness without a clear trend on fatigue performance. In fact, great attention should be put on filler-bitumen interactions based on the physicochemical nature of filler. Moreover, whatever the filler considered, an enhancement in fatigue endurance limit occurs in the mastics blended with a limited percentage of aged SBS modified bitumen (up to 45%), promoting the addition of Reclaimed Asphalt Pavement (RAP) to obtain more performing and sustainable recycled mixtures.

10.3.1 Frequency sweep test

Time-Temperature Superposition Principle (TTSP) was applied to obtain complex modulus master curves at a reference temperature of 34 °C for all the materials investigated (Mazzoni et al., 2017c) (Figure 10.15). Test data were analysed by adopting the modified Christensen-Anderson-Marasteanu (CAM) Model to relate the complex modulus norm to the reduced frequency following a shift factor variation based on the Williams-Landel-Ferry (WLF) law. The calibrated values for the modified CAM model and the WLF law are summarised in Table 10.7.

Table 10.7. Calibrated parameters of the modified Christensen-Anderson-Marasteanu model and Williams-Landel-Ferry law for the materials investigated (Mazzoni et al., 2017c).

CAM modified model + WLF law	$G^*=G_e^*+\frac{G_g^*-G_e^*}{[1+(\frac{f_c}{f})^k]^{\frac{m_e}{k}}}$							$Log(a_t)=\frac{C_1(T-T_0)}{C_2+(T-T_0)}$		
	G^*_e [Pa]	G^*_g [Pa]	f_c	k	m_e	S	R^2	C_1	C_2	T_0 [°C]
28PC_0R	3E+04	2.2E+09	140	0.104	0.75	2.170	0.996	18.0	185	34
28PC_45R	1E+05	2.2E+09	140	0.099	0.65	1.975	0.998	22.0	225	34
28PC_100R	1E+05	2.2E+09	118	0.098	0.58	1.765	0.998	26.0	255	34
28B_0R	0	1.8E+09	140	0.111	0.79	2.161	0.991	17.6	185	34
28B_45R	0	1.8E+09	140	0.106	0.69	1.963	0.997	22.0	220	34
28B_100R	0	1.8E+09	118	0.104	0.62	1.800	0.998	24.0	240	34
28L_0R	0	1.2E+09	140	0.118	0.80	2.041	0.986	15.0	150	34
28L_45R	0	1.2E+09	140	0.106	0.69	1.960	0.990	22.0	200	34
28L_100R	0	1.2E+09	118	0.103	0.63	1.824	0.970	22.0	220	34

with $S = \mathrm{Log}\frac{2^{\frac{m_e}{k}}}{1+(2^{\frac{m_e}{k}}-1)\cdot\frac{G_e^*}{G_g^*}}$

The presence of the aged bitumen R led to an expected increase in mastic stiffness: the higher the percentage of R, the higher the stiffness, as shown by comparing the master curves corresponding to mastics with different percentages of R (Figure 10.15). Considering the model parameters summarised in Table 10.7, the presence of higher aged bitumen R contents implied the following effects: 1) lower shape index S and viscous asymptote m_e, indicating a higher sensitivity to frequency changes; 2) higher |G*| values and lower crossover frequency f_c, denoting a greater overall elastic component in the behaviour; 3) higher C_1 and C_2 values, according to the reduction in fractional free volume (i.e. reduction of molecular mobility).
Moreover, although the filler content by mastic volume was the same for all the mastics investigated (28%), the different physicochemical properties of the fillers and the related differences in filler-bitumen interactions determined evident changes in the rheological response of the corresponding mastics. In particular, regardless of the aged bitumen content considered, the higher the filler particle density and Rigden voids (RV), the higher the fixed bitumen as well as the mastic stiffness (Figure 10.16). This result is confirmed by the model parameters summarised in Table 10.7. In particular, the increase in filler particle density determined higher values of the glassy modulus G_g^* and the appearance of the equilibrium complex modulus G_e^* in the mastics blended with Portland cement (characterised by the highest particle density), suggesting a stronger bitumen-filler interaction (Figure 10.17).

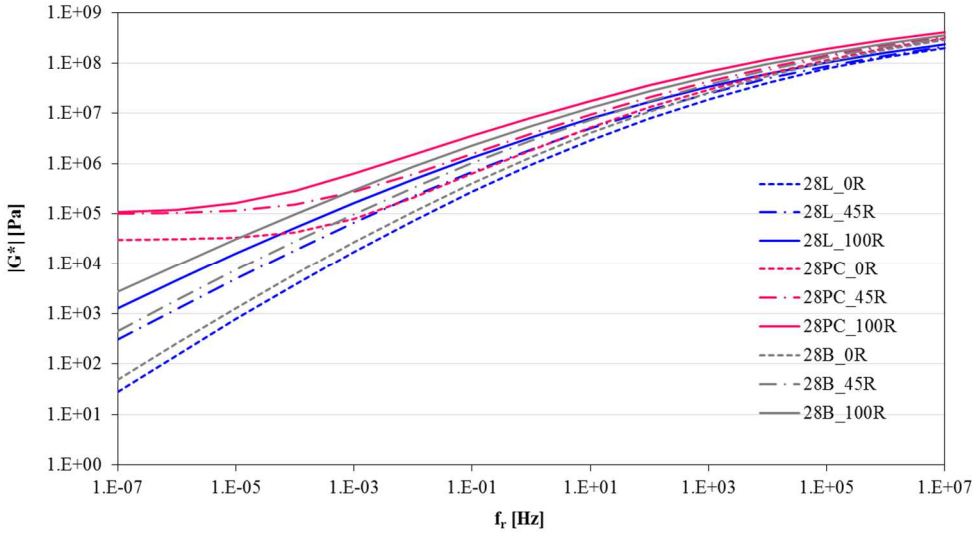

Figure 10.15. Master curves of |G*| at 34 °C.

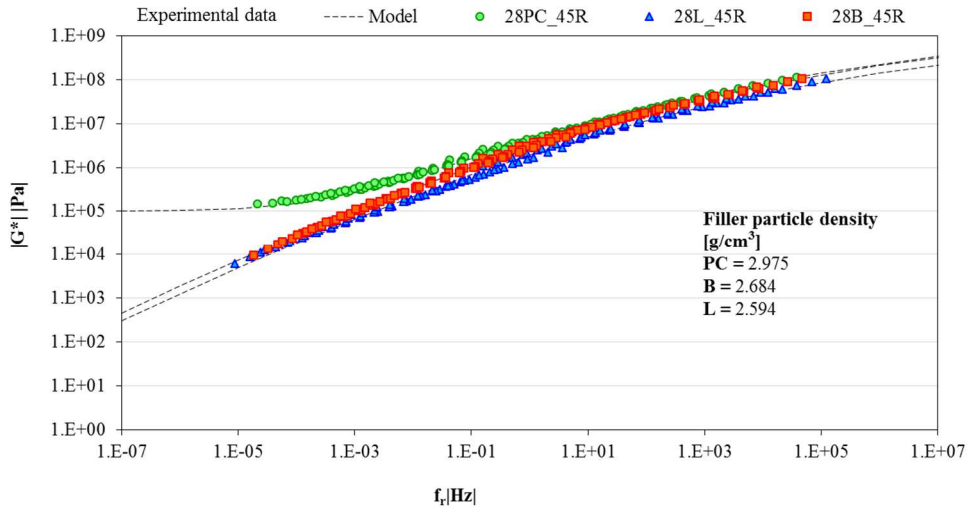

Figure 10.16. Comparison among master curves of |G*| at 34 °C related to the mastics composed of the same bituminous blend (45R) and different types of fillers (B, L and PC).

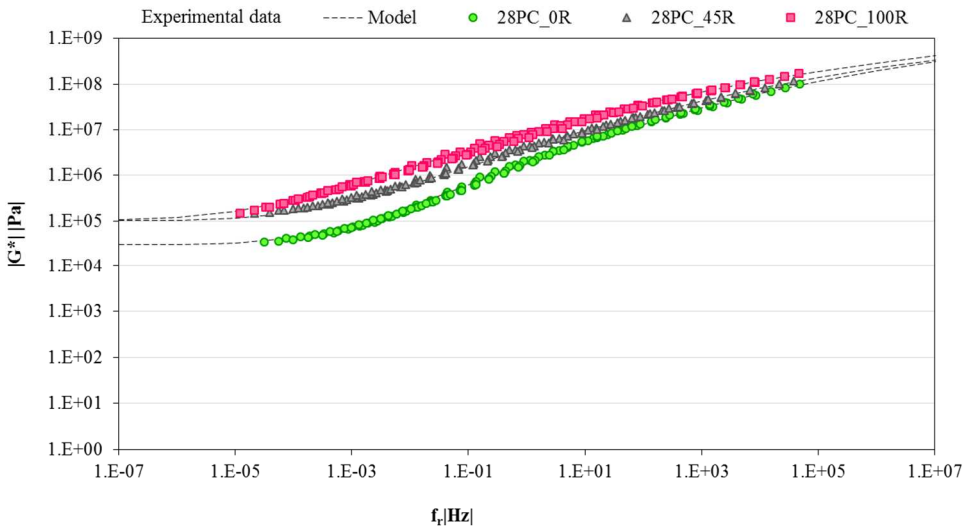

Figure 10.17. Comparison among master curves of |G*| at 34 °C related to the mastics blended with Portland cement.

10.3.2 To find Isostiffness test

Results summarised in Table 9.4 were obtained following the procedure described in paragraph § 9.3.3 starting from the raw data represented in the table below.
In particular, asphalt pavement fatigue damage, or cracking, caused by traffic loads is influenced by the stiffness properties of the mix and the distribution of stress and strains through the layer. For this reason, an equi-stiffness temperature was used, in order to delete the effect of stiffness in the materials properties, and obtained by fixing constant strain and frequency equal to 1% and 10 Hz, respectively.

Table 10.8. Isostiffness temperatures obtained for all the materials investigated.

Material	Strain [%]	Temperature [°C]	|G*|•sinδ [MPa]	Isostiffness |G*|•sinδ [MPa]	Isostiffness T [°C]
28PC_0R	1	32	5.36	9	26.4
		28	7.64		
		24	10.80		
28PC_45R	1	32	6.35	9	27.8
		28	8.74		
		24	11.60		
28PC_100R	1	33	9.13	9	33.1
		31	10.40		
		29	12.00		
28B_0R	1	26.5	8.28	9	25.8
		25.5	9.42		
		24.5	10.30		
28B_45R	1	28	8.46	9	27.5
		27	9.59		
		26	10.70		
28B_100R	1	33	8.67	9	32.6
		32	9.58		
		31	10.70		
28L_0R	1	32	5.46	9	25.4
		28	7.57		
		24	9.80		
28L_45R	1	32	6.04	9	27.0
		28	8.12		
		24	11.00		
28L_100R	1	32	9.39	9	32.3
		28	13.12		
		24	17.41		

10.3.3 Time sweep test with multiple rest periods

Based on the test method described in paragraph § 9.3, all the mastics were characterised in terms of self-healing capability, thixotropy and fatigue resistance, providing useful insights into the influence of filler and bitumen properties as well as their interactions (Mazzoni et al., 2017c).

Raw data analysis

All the mastics were compared in terms of damage resistance after each rest period, as depicted in Figure 10.18, where the parameter $|G^*| \bullet \sin\delta$ is plotted as a function of the number of loading cycles.
In particular, as far as the limestone filler is concerned, the behaviour associated with the corresponding mastics was analysed in previous researches (Mazzoni et al., 2016, Mazzoni et al., 2017b) showing positive effects in terms of damage accumulation over time, as confirmed by the highest fatigue resistance of the mastic prepared with 45% of bitumen R (28L_45R). On the opposite, the presence of Portland cement and, especially, basalt in mastic causes a worsening of fatigue performance (i.e. lower number of loading cycles to reach the same damage level corresponding to a 35% reduction of the loss modulus at each loading phase), whatever the aged bitumen content considered (Figure 10.18).
Also the effect of aged bitumen on mastic fatigue properties was analysed. It should be noted that the presence of a totally aged bituminous phase (100R) determines comparable fatigue behaviour, regardless of the type of filler contained in each mastic. However, when the bituminous phase is composed of higher amounts of aged bitumen (45R and 100R), a resistance increase compared to the corresponding mastic prepared exclusively with virgin bitumen (0R) occurs, particularly for higher filler particle densities or RV (28B and 28PC) (Figure 10.18).

Model parameters analysis

The results in terms of model parameters confirmed what previously mentioned based on raw test data (Figure 10.18). In particular, the main model parameters providing a quantitative evaluation of fatigue, self-healing and thixotropic properties are calculated, as summarised in Table 10.9 and depicted in Figure 10.19 for a more direct comparison among the mastics investigated.

Fatigue response including self-healing capability

Regardless of the aged bitumen content considered, mastics composed of fillers with a higher particle density (i.e. B and PC) suffer a faster damage accumulation and consequently present lower values of the parameters N_0, N_{fH} and N_{fat} (Table 10.9 and Figure 10.19a). This is likely due to the predominance of filler properties in terms of physicochemical interactions between bitumen and filler, as the fines are embedded in the bitumen and, thus, generate the majority of the surface area (Anderson et al., 1992) and create a discontinuous medium that interrupts the continuous bituminous phase, further complicating crack propagation (Mazzoni et al.,

2016, Mazzoni et al., 2017b). With respect to limestone filler, the corresponding mastics exhibit the best overall fatigue response, as confirmed by the higher values of the parameters N_0, N_{fH} and N_{fat}, except 28L_100R. In fact, the latter presents a slightly lower fatigue endurance limit, N_{fat}, than 28PC_100R, but it should be noted that their fatigue behaviour has the same order of magnitude and can be considered comparable. The result above-mentioned could be explained with the high affinity between limestone and bitumen, which determines the development of strong chemical bonds. On the opposite, whatever the aged bitumen content considered, the presence of basaltic filler in mastic causes the worst performance in terms of fatigue and self-healing, as suggested by the lower values of the parameters N_0, N_{fH} and N_{fat}. In fact, both bitumen and basalt are characterised by the presence of a majority of acid groups causing a poor bitumen-basalt affinity and consequently weak chemical bonds.
Also the effect of aged bitumen on mastic fatigue properties was analysed (Table 10.9 and Figure 10.19a). Regardless of the type of filler contained in each mastic, the presence of a totally aged bituminous phase (100R) leads to comparable fatigue performances, especially in terms of self-healing, as suggested by the similar values of the parameters N_{fat} and N_{fH}. That is likely linked to the predominance of the bituminous phase over the filler component or their interaction within the mastic. Moreover, oxidation seems to cause an enhancement in the material response, as detectable with an increase in N_0, N_{fH} and N_{fat} values for mastics including aged bitumen (100R) compared to the corresponding mastics prepared with virgin bitumen (0R), particularly for higher filler particle densities (B and PC). In fact, a better interdiffusion of bitumen components could be allowed by the shorter polymer structures created by the disruption in the butadiene functional group of polymer chains, as a consequence for oxidation phenomena (Negulescu, 2006).
However, whatever the filler considered, the addition of a limited amount of R (45%) to the corresponding mastics provides benefits to their overall fatigue performance (N_{fat} and N_0) without hindering their self-healing capability (N_{fH}) compared to the mastics composed of only virgin bitumen (0R). The simultaneous presence of shorter polymer chains (from aged bitumen R) and intact ones (from virgin bitumen) creates a more effective internal network for self-healing occurrence and fatigue performance (Canestrari et al., 2015).

Thixotropic contribution

As far as the parameter ΔN_∞ is concerned and regardless of the filler considered, mastics exhibit a thixotropic behaviour, as demonstrated by the constant contribution ΔN_∞ (Table 10.9 and Figure 10.19b), in agreement with what observed for pure bitumens in previous experimental tests (Stimilli et al., 2014, Canestrari et al., 2015). The nature of filler and the consequent bitumen-filler interaction clearly affect thixotropy, although it is an intrinsic bitumen property. In particular, whatever the aged bitumen R content considered, the presence of limestone determines a positive thixotropic contribution on the corresponding mastic, thanks to its high affinity with bitumen. On the opposite, the weak bonds between basaltic filler and bitumen cause a considerable decrease in the thixotropic value.

In addition, oxidation leads to higher ΔN_∞ values for the mastics containing only aged bitumen (100R) compared to the corresponding mastics prepared with virgin bitumen (0R), particularly for higher particle densities or RV of filler (28B and 28PC). That is likely due to a strengthening of the chemical bonds between short polymer chains in aged bitumen and lytic particles in filler characterised by higher RV that positively affects molecular rearrangements within the aged bituminous phase. Whereas the addition of 45% of aged bitumen R to the virgin bitumen (45R) determined an increase in the thixotropic contribution of the respective mastic, if compared to the corresponding mastic composed of a totally virgin bitumen (0R), whatever the filler considered (Table 10.9 and Figure 10.19b).
Based on the results above-mentioned, an improvement in terms of fatigue and cracking resistance is reasonably expected for a recycled bituminous mixture containing an SBS modified bitumen and a certain amount of RA (which releases a percentage of the same SBS modified aged bitumen). This observation complies with the results obtained through specific studies on recycled Hot Mix Asphalts (HMAs) prepared with the same SBS modified bitumen, which showed an enhancement in fatigue response when dealing with a given amount of RAP (Stimilli et al., 2015, Stimilli et al., 2016).
Moreover, the results obtained demonstrate the great influence of the physicochemical nature of filler on the overall fatigue performance, suggesting significant benefits when limestone was involved.

Table 10.9. Model parameters for all the mastics investigated (Mazzoni et al., 2017c).

Mastic	N_{fat}	N_0	N_{fH}	ΔN_∞	n_{95}
28PC_0R	7562	4100	3462	1500	8.19
28PC_45R	19382	9720	9662	1720	8.78
28PC_100R	21560	10520	11040	1640	11.89
28B_0R	2227	1080	1147	340	9.89
28B_45R	8343	3520	4823	1000	14.29
28B_100R	18289	7280	11009	1300	12.65
28L_0R	32142	16580	15562	3980	9.17
28L_45R	35221	20940	14281	4440	9.32
28L_100R	20866	9940	10926	1580	9.79

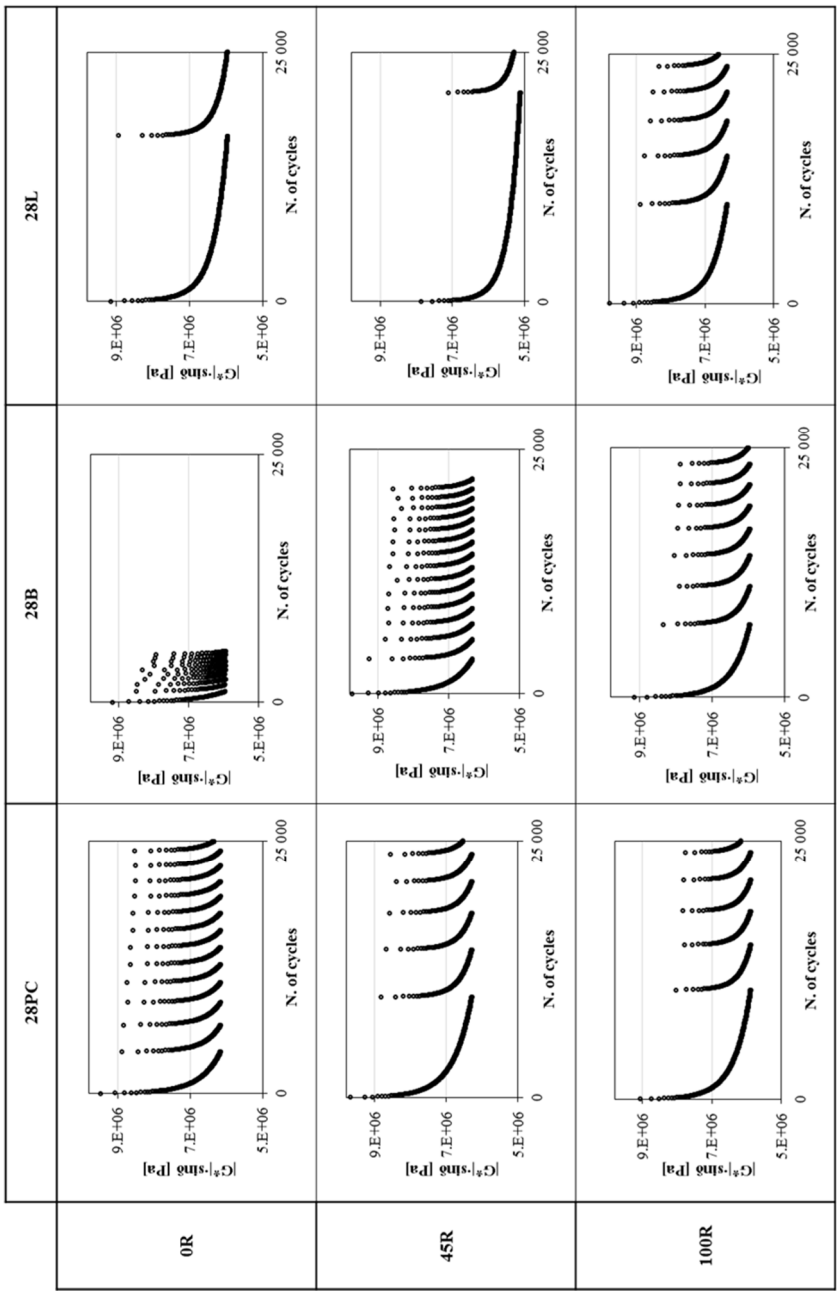

Figure 10.18. Comparison of the evolution of |G*|•sinδ versus number of loading cycles in all the mastics investigated (Mazzoni et al., 2017c).

a)

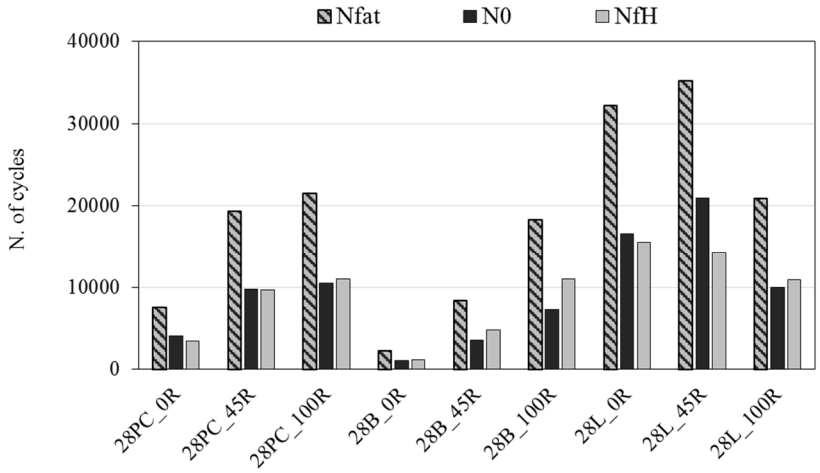

b)

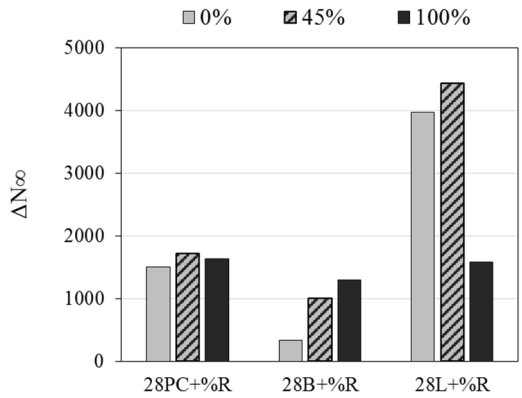

Figure 10.19. Comparison of: a) fatigue endurance limit N_{fat}, initial strength N_0, self-healing potential N_{fH}; b) thixotropy ΔN_∞ in all the mastics investigated (Mazzoni et al, 2017c).

10.4 Summary

The experimental research described in the second phase of Ph.D investigation proposes an evaluation of the overall response of bitumens and the corresponding mastics composed of different dosages and types of filler, when different aged SBS modified contents are involved, in terms of fatigue, self-healing and thixotropy. Based on the rheological and morphological results obtained, the following conclusions can be drawn:

1. The analytical method used to elaborate test data, which had been previously implemented for bitumens, was found suitable also to interpret mastic behaviour. The proposed model allowed a useful comparison between bitumens and the corresponding mastics investigated in terms of fatigue, self-healing and thixotropy, representing in this sense a reliable tool for the ranking of materials with different characteristics;
2. Perfect agreement was detected between the behaviours of bitumens and the corresponding mastics in terms of initial fatigue resistance, when different amounts of aged bitumen R were involved. Fatigue performance was lower for long-term aged materials due to oxidation effects which determine the formation of shorter SBS polymer chains within the bitumen, hence creating a bituminous phase which is less prone to interact and efficiently collaborate with the lytic component of mastic (i.e. filler particles). This interpretation is consistent with the morphological analysis performed by SEM imaging. Moreover, oxidation could determine a deterioration of the chemical interactions of bitumen with filler particles, thus negatively affecting the overall material response;
3. Whatever the filler dosage and type, the presence of lytic phase caused detrimental effects on the corresponding mastic in terms of fatigue and self-healing performance, if compared to the associated bitumen;
   Stand-alone filler particles are unable to self-heal. Hence, filler acts as an interference component within the mastic creating an inhomogeneous structure that further complicates crack propagation (the formation of the crack at the interface between bitumen and filler) and inhibits the occurrence of interdiffusion at the filler-bitumen crack interface, which is the main mechanism responsible for self-healing development;
4. Regardless of the amount of aged bitumen R considered, an increasing in filler content determined a worse behaviour of mastic in terms of fatigue, self-healing and thixotropy;
5. High filler content (42L) led to comparable performance of mastics blended with different amounts of aged bitumen R (0R, 45R, 100R). In fact, the higher the filler content, the lower the bituminous phase, the lower the effects due to different amounts of bitumen R on mastic properties, such as damage resistance, self-healing and thixotropy;

6. Mastics composed of fillers with higher particle densities (i.e. B and PC) suffered a faster damage accumulation because of the predominance of filler properties in terms of physicochemical interactions between bitumen and filler. The fines are embedded in the bitumen and, thus, generate the majority of the surface area and create a discontinuous medium that interrupts the continuous bituminous phase, further complicating crack propagation and altering interdiffusion and cohesive potential of the real binder component of a mixture (i.e. mastic);
7. Regardless of the amount of aged bitumen R considered, the presence of the limestone filler L guaranteed the corresponding mastics positive effects in terms of damage accumulation over time, thanks to the high affinity between limestone and bitumen, which determines the development of strong chemical bonds;
8. The presence of a limited amount of aged bitumen R (up to 45%) blended with virgin bitumen appeared to be beneficial in terms of self-healing, with positive repercussions on the overall fatigue response, independently of the presence or not of filler and eventually its dosage and type. This finding is explained by the positive interactions between short polymer chains (provided by the aged bitumen) and long polymer chains (provided by the unaged bitumen), which create an internal network able to promote higher interdiffusion and elasticity;
9. When lower percentages of filler were added (14L and 28L), mastics prepared with only aged bitumen (100R) exhibited the lowest fatigue performance due to oxidation effects that determine the formation of shorter SBS polymer chains within the bitumen, hence creating a bituminous phase less prone to interact and efficiently collaborate with the lytic component of mastics (i.e. filler particles);
10. When fillers with higher particle densities were added (B and PC), mastics prepared with only virgin bitumen (0R) exhibited lower fatigue performances. This is likely due to a more difficult interaction and inefficient collaboration between unaged bitumen characterised by long SBS polymer chains and the lytic component characterised by a higher particle density (i.e. filler particles). Whereas, a totally aged bituminous phase (100R) led to comparable performance of the mastics blended with different types of filler (L, B and PC), indicating the predominance of the bituminous phase over the filler component or their interaction within the aged mastics;
11. Thixotropy, an intrinsic ability of the bituminous phase, is still detectable in mastics, independently of the presence of cracks. However, thixotropy was affected not only by the different aged bitumen contents, but also by the amount and physicochemical nature of filler and the consequent bitumen-filler interactions. In particular, the presence of a certain amount of aged bitumen (45%R) and limestone filler (28%L) involved the highest thixotropic contribution for the corresponding mastic (28L_45R);
12. Regardless of the amount of aged bitumen R considered, the higher the filler content, the particle density and/or the RV, the higher the fixed bitumen as well as

the mastic stiffness. Similarly and as expected, an increase in mastic stiffness was obtained by increasing the amount of aged bitumen R, whatever the filler type or dosage considered.

In conclusion, this experimental study provides an important contribution to understand and quantify time-temperature dependent phenomena (i.e. self-healing and thixotropy) of bituminous materials, accounting for the effect of different dosages and types of filler, when different aged SBS modified bitumen contents are involved.

Based on the findings above-described, it is reasonable to expect that recycled bituminous mixtures prepared with SBS modified bitumens and a certain amount of RAP (which releases a percentage of the same SBS modified aged bitumen) can exhibit improved fatigue and cracking resistance compared to virgin mixtures, whatever the filler type and the filler/bitumen ratio considered. However, it should be underlined that the choice of the most suitable filler type and filler/bitumen ratio (i.e. the bitumen thickness within the mastic) represents a fundamental step to optimise the final mixture behaviour. In details, low filler/bitumen ratio improves fatigue and self-healing response, but could worsen rutting resistance, whereas high ratio leads to an opposite behaviour. Moreover, as expected, bitumen-filler affinity should be guaranteed by adopting a basic (e.g. limestone) filler and not an acid (e.g. basalt) one, thus determining the development of strong chemical bonds with the acid groups characterising bitumens. In addition, although Portland cement is often considered an alternative for limestone in common pavement applications, its use as filler in bituminous materials is discouraged, since it causes a worsening of the final fatigue performance.

Summary of the overall experimental study

Chapter 18.

Concluding remarks

The objective of this doctoral dissertation was to scientifically validate the possibility to incorporate in flexible pavements high RAP contents without negatively affecting the final recycled Hot Mix Asphalts (HMAs) in terms of performance. It is expected that fatigue cracking represents the main distress for flexible pavements whose field performance is mainly led by mastic phase and its components (i.e. filler and bitumen). In such a pavement high RAP contents cause a further worsen due to the high oxidation, and consequently viscosity (stiffness), of the aged RAP bitumen included. For this reason, the experimental study focused on analysing the interactions among different types and dosages of RAP bitumens, rejuvenators and fillers. Besides the "classical" rheological characterisation, more innovative tests and analyses were implemented in order to get an overall picture of the mechanical behaviour of the materials investigated under different loading and temperature conditions. In details, an innovative experimental approach was applied in order to quantify the overall fatigue endurance limit, considering self-healing contribution after the deduction of other simultaneous contributions due to viscoelastic phenomena, such as thixotropy, since the latter does not affect the fatigue life.

The first phase of the experimental investigation focused on the assessment of the rheological properties of different paving grade bitumens during their overall service life including the reuse in hot recycling by adopting different rejuvenators. To this purpose, bitumen properties were evaluated simulating different conditions of the service life: before and after HMA production, at the end of pavement service life, during hot recycling process, after laying of recycled HMA and, finally, at the end of the recycled HMA service life. Whereas in the second phase mastics and the related associated bituminous components of HMAs, including different RAP contents, were investigated with advanced morphological and rheological tests. The main objective of this phase was to quantify fatigue response, self-healing potential and thixotropy of bituminous materials and concurrently identify useful insights for fillers and bituminous blends.

The results acquired through the first experimental phase demonstrated that recycled bituminous mixtures prepared with virgin bitumens, rejuvenators and high amounts of RAP (which releases a percentage of the same aged bitumen) suffer less ageing phenomena and could also be less stiff than virgin mixtures. However, great importance must be given to the type and dosage of rejuvenators and bitumens and their related interactions since they mainly influence the final performance due to compatibility. Also the second phase results confirmed the findings above-described. In particular, thanks to the implementation of RAP obtained from highways, and consequently including Styrene Butadiene Styrene (SBS) copolymer modified bitumen that limits oxidation and enhances elastic response, improved fatigue

cracking resistance for final recycled HMA compared to virgin was detected, whatever the filler type and dosage considered and without adding rejuvenators. However, also in this experimental phase the choice of the most suitable components proved to be a fundamental step in optimising the final mixture behaviour.
More detailed results of these investigations can be found in the Summary section of each chapter. Based on the overall findings, the inclusion of higher RAP contents appears possible, without negatively affecting the final mixture performance, when an appropriate design is considered. In particular, source, properties and dosage of RAP, bitumen, filler and, eventually, rejuvenator need to be properly selected so as to improve low and intermediate temperature properties of the mixture without penalising its high temperature performance.

Lists of 3-years Ph.D publications

Mazzoni G., Stimilli A. and Canestrari F., "Self-healing capability and thixotropy of bituminous mastics." International Journal of Fatigue 2016; 92 (1): 8-17
doi: 10.1016/j.ijfatigue.2016.06.028;

Mazzoni G., Stimilli A., Cardone F. and Canestrari F., "Fatigue, self-healing and thixotropy of bituminous mastics including aged modified bitumens and different filler contents", Construction and Building Materials 2017, 131, 496-502
doi: 10.1016/j.conbuildmat.2016.11.093;

Mazzoni G., Virgili A. and Canestrari F., "Influence of different fillers and bituminous blends on fatigue, self-healing and thixotropic performance of mastics", submitted on Road Materials and Pavement Design 2017;

Mazzoni G., Bocci E. and Canestrari F., "Influence of rejuvenators on bitumen ageing in hot recycled asphalt mixtures", under revision on Journal of Traffic and Transportation Engineering (English edition) 2017.

Lists of 3-years Ph.D awards

SIIV Award 2017_Best presentation of the research activities during the 2nd edition of SIIV Arena within SIIV Summer School 2017;

SIIV Award 2015_Best presentation of the research activities during SIIV Summer School 2015.

References

Abo-Qudais S. and Suleiman A., Monitoring fatigue damage and crack healing by ultrasound wave velocity. Nondestructive Testing and Evaluation 20 (2005) 125-145, doi:10.1080/10589750500206774.

Airey G.D., Liao M.C. and Thom N.H., Fatigue behaviour of bitumen-filler mastics. In: 10th International Conference on Asphalt Pavements, Quebec City, 2006.

Airey G.D., Use of black diagrams to identify inconsistencies in rheological data. Road Materials and Pavement Design 3 (4) (2002) 403–424, doi: 10.1080/14680629.2002.9689933.

Al-Qadi I.L., Elseifi M.A. and Carpenter S.H., Reclaimed asphalt pavement: a literature review. Report Number FHWA-ICT-07-001, Springfield: Illinois Center for Transportation, 2007.

Anderson D.A. and Goetz W.H., Mechanical behavior and reinforcement of mineral filler-asphalt mixtures. Journal of the Association of Asphalt Paving Technologists 42 (1973) 37-66.

Anderson D.A., Bahia H.U. and Dongre R., Rheological properties of mineral filler-asphalt mastics and its importance to pavement performance. ASTM Special Technical Publication 1147 (1992) 131-153.

Antunes V., Freire A.C., Quaresma L. and Micaelo R., Effect of the chemical composition of fillers in the filler-bitumen interaction. Construction and Building Materials 104 (2016) 85-91, doi: 10.1016/j.conbuildmat.2015.12.042.

Antunes V., Freire A.C., Quaresma L. and Micaelo R., Influence of the geometrical and physical properties of filler in the filler-bitumen interaction. Construction and Building Materials 76 (2015) 322-329, doi: 10.1016/j.conbuildmat.2014.12.008.

Ashouri, M., Modeling Microdamage Healing in Asphalt Pavements Using Continuum Damage Theory (PhD dissertation). North Carolina State University, Raleigh, North Carolina, USA, 2014.

Asli H., Ahmadinia E., Zargar M. and Karim M.R., Investigation on physical properties of waste cooking oil – rejuvenated bitumen binder. Construction and Building Materials 37 (2012) 398–405.

Asphalt Research Correspondent. University of Wisconsin Madison leads testing of the Linear Amplitude Sweep (LAS) procedure to specify fatigue resistance, 2013.

Ayar P., Moreno-Navarro F. and Rubio-Gámez M.C., The healing capability of asphalt pavements: a state of the art review. Journal of Cleaner Production 113 (2016) 28-40, doi: 10.1016/j.jclepro.2015.12.034.

Bahia H.U. and Anderson D., The pressure aging vessel (PAV). A test to Simulate Rheological Changes due to field aging. Physical Properties of Asphalt Cement Bitumens: ASTM STP 1241, pp. 67-89, 1995.

Bahia H.U., Hanson D.I., Zeng M., Zhai H. Khatri M.A. and Anderson R.M., Characterization of modified asphalt binders in Superpave mix design, NCHRP Report 459, National Cooperative Highway Research Program, Transportation Research Board, National Research Council, Washington, D.C., 2001.

Bahia H.U., Zhai H., Bonnetti K. and Kose S., Non-linear viscoelastic and fatigue properties of asphalt binders. Journal of the Association of Asphalt Paving Technologists 69 (1999) 1-34.

Barnes H.A., Thixotropy - a review. Journal of Non-Newtonian Fluid Mechanics 70 (1997) 1-33.

Bazin P., Saunier J., Deformability, fatigue, and healing properties of asphalt mixes. In: Proceedings of the 2nd International Conference on the Structural Design of Asphalt Pavements. Ann Arbor, Michigan, USA, 1967.

Bell C., Summary Report on Aging of Asphalt-Aggregate Systems, SHRP Report A-305. Washington D. C.: National Research Council; 1989.

Bhasin A., Branco V.T.C., Masad E. and Little D.N., Quantitative comparison of energy methods to characterize fatigue in asphalt materials. Journal of Materials in Civil Engineering 21(2) (2009) 83-92.

Bocci E., Cardone C. and Grilli A., Mix design and volumetric analysis of hot recycled bituminous mixtures using a bio-additive. In: AIIT International Congress on Transport Infrastructure and Systems (TIS 2017), Rome, Italy, 10-12 April 2017, pp. 267-274, doi: 10.1201/9781315281896-37.

Bodin D., Soenen H. and de La Roche C. Temperature effects in binder fatigue and healing tests. In: Proceeding of the 3rd Eurasphalt and Eurobitume Congress held Vienna 2004: 1996-2004.

Bommavaram R., Bhasin A. and Little D., Determining intrinsic healing properties of asphalt binders: role of dynamic shear Rheometer. Transportation Research Record 2126 (2009) 47-54.

Bonnaure F.P., Huibers A.H.J.J. and Boonders A., A laboratory investigation of the influence of rest periods on the fatigue characteristics of bituminous mixes. Journal of the Association of Asphalt Paving Technologists 51 (1982) 104-128.

Boomquist D., Diamond G., Oden M., Ruth B., Tia M., Engineering and environmental aspects of recycled materials for highway construction, Report No. FHWA-RD-088, FHWA, Washington, DC, 1993.

Booshehrian A., Mogawer W.S., Bonaquist R., How to construct an asphalt binder master curve and assess the degree of blending between RAP and virgin binders. Journal of Materials in Civil Engineering (2013) 1813–1821.

Bowers B.F., Huang B., Shu X. and Miller B.C., Investigation of Reclaimed Asphalt Pavement blending efficiency through GPC and FTIR. Construction and Building Materials 50(15) (2014) 517–523.

Branthaver J.F., Petersen J.C., Robertson R.E., Duvall J.J., Kim S.S., Harnsberger P.M., et al., Binder Characterization and Evaluation – vol. 2 Chemistry, SHRP Report A-368. Washington D. C.: National Research Council; 1994.

Bressi S., Carter A., Bueche N. and Dumont A.G., Impact of different ageing levels on binder rheology. International Journal of Pavement Engineering (2015) 1–11, doi: 10.1080/10298436.2014.993197.

Brundtland G. H., Our common future: Brundtland-report, Oxford University Press, Oxford, 1987.

Butt A.A., Birgisson B. and Kringos N., Optimizing the highway lifetime by improving the self healing capacity of asphalt. Proc. Soc. Behav. Sci. 48 (2012) 2190-2200, doi: 10.1016/j.sbspro.2012.06.1192.

Buttlar W.G., Bozkurt D., Al-Khateeb G.G. and Waldhoff A.S., Understanding asphalt mastic behavior through micromechanics. Transportation Research Record 1681 (1999) 157-169.

Canestrari F., Virgili A., Graziani A. and Stimilli A. Modeling and assessment of self-healing and thixotropy properties for modified binders. International Journal of Fatigue 70 (2015) 351-360, doi: 10.1016/j.ijfatigue.2014.08.004.

Cardone F., Frigio F., Ferrotti G. and Canestrari F., Influence of mineral fillers on the rheological response of polymer-modified bitumens and mastics. Journal of Traffic and Transportation Engineering (English Edition) 2 (6) (2015) 373-381, doi: 10.1016/j.jtte.2015.06.003.

Carpenter S.H. and Wolosick J.R., Modifier influence in the characterization of hot mix recycled material Transportation research record 777, Transportation Research Board, National Research Council, Washington DC, 1980. pp. 15–22.

Castro M. and Sanchez J.A., Fatigue and healing of asphalt mixtures: discriminate analysis of fatigue curves. Journal of Transportation Engineering 132 (2006) 168-174, doi:10.1061/(ASCE)0733-947X(2006)132:2(168).

Celauro C., Bernardo C. and Gabriele B., Production of innovative, recycled and high performance asphalt for road pavements. Resources, Conservation and Recycling 54 (6) (2010) 337–347, doi: 10.1016/j.resconrec.2009.08.009.

Chen J.S., Huang C.C., Chu P.Y. and Liu K.Y., Engineering characterization of recycled asphalt concrete and aged bitumen mixed recycling agent. Journal of Materials Science 42 (2007) 9867–9876, doi: 10.1007/s10853-007-1713-8.

Chen M., Xiao F., Putman B., Leng B. and Wu S., High temperature properties of rejuvenating recovered binder with rejuvenator, waste cooking and cotton seed oils. Construction and Building Materials 59 (2014) 10–16.

Chung K., Lee S., Park M., Yoo P. and Hong Y., Preparation and characterization of microcapsule-containing self-healing asphalt. Journal of Industrial and Engineering Chemistry 29 (2015) 330-337, doi: 10.1016/j.jiec.2015.04.011.

Copeland A., Reclaimed asphalt pavement in asphalt mixtures: state of the practice. FHWA US Department of Transportation, 2011.

Corbett L.W. and Swarbrick R.E., Composition analysis used to explore asphalt hardening. Journal of the Association of Asphalt Paving Technologists 29 (1960) 104-112.

Corbett L.W., Composition of asphalt based on generic fractionation, using solvent deasphaltening, elution-adsorption chromatography and densimetric characterization. Anal Chem 41 (1969) 576–579.

Cussler E.L., Diffusion—Mass Transfer in Fluid Systems, 2nd ed., Cambridge University Press, London, 1997.

Daniel J.S. and Kim Y.R., Laboratory evaluation of fatigue damage and healing of asphalt mixtures. Journal of Materials in Civil Engineering 13 (2001) 434-440.

Das Kumar P., Jelagin D., Birgisson B. and Kringos N., Atomic force microscopy to characterize the healing potential of asphaltic materials. In: Bellitto, V. (Ed.), Atomic Force Microscopy e Imaging, Measuring and Manipulating Surfaces at the Atomic Scale. InTech, Rijeka, Croatia, ISBN 978-953-51-0414-8, 2012, doi: 10.5772/37008.

de La Roche C. et Marsac P., Caractérisation expérimentale de la dissipation thermique dans un enrobé bitumineux sollicité en fatigue. First International Eurobitume and Eurasphalt Congress (1996b).

de La Roche C., Module de rigidité et comportement en fatigue des enrobes bitumineux. Expérimentation et nouvelles perspective d'analyse, Thése de Doctorat, EC Paris (1996).

de La Roche C., Piau J.M. and Dangla P., Modelisation of thermal effects in fatigue tests on asphalt mixes', Workshop on accelerated load testing and advanced modelling of asphalt pavements, Delft, The Netherlands, March, 1996a.

de La Roche C., Van de Ven M., Planche J.P., Van den Bergh W., Grenfell J., Gabet T., Mouillet V., Porot L., Farcas F. and Ruot C., RILEM STATE-OF-THE-ART REPORT: Advances in Interlaboratory Testing and Evaluation of Bituminous Materials, Chapter 6 "Hot Recycling of Bituminous Mixtures", State-of-the-Art Report of the RILEM Technical Committee 206-ATB, 2012.

Delaporte B., Di Benedetto H., Chaverot P. and Gauthier G., Linear viscoelastic properties of bituminous materials: from binders to mastics. Journal of association of asphalt paving technologists 76 (2007) 455-94.

Di Benedetto H., Ashayer Soltani M.A. and Chaverot P., Fatigue damage for bituminous mixtures: a pertinent approach. Journal of the Association of Asphalt Paving Technologists 65 (1996).

Di Benedetto H., Ashayer Soltani M.A. and Chaverot P., Fatigue damage for bituminous mixtures. Proceedings of the 5th int. RILEM Symposium MTBM, Lyon (1997a) 263-270.

Di Benedetto H., de La Roche C., Baaj H., Pronk A. and Lundström R., Fatigue of bituminous mixtures. Materials and Structures 37(3) (2004) 202-216, doi: 10.1007/BF02481620.

Di Benedetto H., Francken L. and de la Roche C., Fatigue of bituminous mixtures: Different approaches and RILEM interlaboratory tests. Proceedings of the Fifth International RILEM Symposium MTBM LYON 97, France, 1997b, 15-26.

Di Benedetto H., Nguyen Q. and Sauzeat C., Non linearity, heating, fatigue and thixotropy during cyclic loading of asphalt mixtures. Road Materials and Pavement Design 11 (1) (2011) 129-58.

Dondi G., Mazzotta F., Simone A., Vignali V., Sangiorgi C. and Lantieri C., Evaluation of different short-term aging procedures with neat, warm and modified binders. Construction and Building Materials 106 (2016) 282–289, doi: 10.1016/j.conbuildmat.2015.12.122.

Dony A., Colin J., Bruneau D., Drouadaine I. and Navaro J., Reclaimed asphalt concretes with high recycling rates: changes in reclaimed binder properties according to rejuvenating agent. Construction and Building Materials 41 (2013) 175–181.

Faheem A.H. and Bahia, H.U., Modelling of asphalt mastic in terms of filler-bitumen interaction. Road Materials and Pavement Design 11 (S1) (2010) 281-303, doi: 10.1080/14680629.2010.9690335.

Farcas F., Étude d'une méthode de simulation du vieillissement des bitumes surroute, LCPC Research report CR21, Paris (France): LCPC Ed., 1998.

Frigio F., Ferrotti G. and Cardone F., Fatigue rheological characterization of polymer-modified bitumens and mastics. RILEM Bookseries 11 (2016) 655 – 666, doi: 10.1007/978-94-017-7342-3_53.

Frigio F., Pasquini E., Canestrari F., Laboratory Study to Evaluate the Influence of Reclaimed Asphalt Content on Performance of Recycled Porous Asphalt. Journal of Testing and Evaluation 43 (6) (2015) 1308-1322, doi: 10.1520/JTE20140024.

Fwa T.F., Evaluation of Engineering Benefits of RJ Seal: , Research Report, National University of Singapore, 2006.

Garcia Á., Norambuena-Contreras J., Bueno M. and Partl M.N., Single and multiple healing of porous and dense asphalt concrete. Journal of Intelligent Material Systems and Structures (2014), doi: 10.1177/1045389X14529029.

García Á., Schlangen E. and van de Ven M., Properties of capsules containing rejuvenators for their use in asphalt concrete, Fuel 90 (2011) 583–591.

García Á., Schlangen E., van de Ven M., Sierra-Beltrán G., Preparation of capsules containing rejuvenators for their use in asphalt concrete, J. Hazard. Mater. 184 (2010) 603–611.

García Á., Self Healing of open cracks in asphalt mastic. Fuel 93 (2012) 264-272, doi: 10.1016/j.fuel.2011.09.009.

Gaskin J., On Bitumen Microstructure and the Effects of Crack Healing (PhD dissertation). University of Nottingham, Nottingham, UK, 2013.

Grabowski W. and Wilanowicz J., The structure of mineral fillers and their stiffening properties in filler-bitumen mastics. Materials and Structures 41 (2008) 793-804, doi: 10.1617/s11527-007-9283-4.

Grant T.P., Determination of Asphalt Mixture Healing Rate Using the Superpave Indirect Tensile Test (MSc dissertation). University of Florida, Gainesville, Florida, USA,2001.

Grilli A., Bocci E., Bocci M., Hot recycling of reclaimed asphalt using a tall oil-based additive. In: 8th International RILEM-SIB Symposium, Ancona, October 2015, doi:10.1007/978-94-017-7342-3_76.

Grilli A., Graziani A. and Bocci M., Compactability and thermal sensitivity of cement-bitumen-treated materials. Road Materials and Pavement Design 13 (2012) 599-617, doi: 10.1080/14680629.2012.742624.

Grilli A., Iorio Gnisci M. and Bocci M., Effect of ageing process on bitumen and rejuvenated bitumen. Construction and Building Materials 136 (2017) 474–481, doi: 10.1016/j.conbuildmat.2017.01.027.

Groenendijk J., Accelerated Testing and Surface Cracking of Asphalt Concrete Pavements. Delft University of Technology, Delft, The Netherlands, 1998.

Groupe National Bitume, Susceptibilité au vieillissement des bitumes –Expérimentation A08, LCPC Research report CR19, Paris (France): LCPC Ed., 1997.

Hansen K. and Newcomb D., Asphalt Pavement Mix Producion Survey on Reclaimed Asphalt Pavement, Reclaimed Asphalt Shingles, and Warm-Mix Asphalt Usage. National Asphalt Pavement Association, 2011.

Harris B.M. and Stuart K.D., Analysis of mineral fillers and mastics used in stone matrix asphalt. Journal of the Association of Asphalt Paving Technologist 64 (1) (1995) 54-95.

Hefer A. and Little D.N., Adhesion in Bitumen-aggregate Systems and Quantification of the Effects of Water on the Adhesive Bond (Research report ICAR-505-1). Texas Transportation Institute, Texas A&M University, College Station, Texas, USA, 2005.

Huang B., Li G., Vokosavljevic D., Shu X. and Egan B., Laboratory investigation of mixing hot-mix asphalt and Reclaimed Asphalt Pavement. Trans Res Rec: J Trans Res Board 1929 (2005) 37–45.

Huang J., In: Usmani AM, editor. Oxidation of asphalt fractions in Asphalt Science and Technology. New York: Marcel Dekker; 1997. p. 119–34.

Huang S-C., Qin Q., Grimes R.W., Pauli A.T. and Glaser R., Influence of rejuvenators on the physical properties of RAP binders. Journal of Testing and Evaluation 43 (2015) 594–603.

Huang W., Lv Q. and Xiao F., Investigation of using binder bond strength test to evaluate adhesion and self-healing properties of modified asphalt binders. Construction and Building Materials 113 (2016) 49–56, doi: 10.1016/j.conbuildmat.2016.03.047.

Hugener M., Partl M.N., Morant M., Cold asphalt recycling with 100% reclaimed asphalt pavement and vegetable oil-based rejuvenators. Road Materials and Pavement Design 15 (2014) 239–258.

Im S., Zhou F., Lee R. and Scullion T., Impacts of rejuvenators on performance and engineering properties of asphalt mixtures containing recycled materials. Construction and Building Materials 53 (2014) 596–603.

Ipavec A., Marsac P. and Mollenhauer., Synthesis of the European national requirements and practices. In 5th Euroasphalt & Eurobitume Congress, Istanbul, 2012.

Isaccson, Zeng H., Cracking of asphalt at low temperature as related to bitumen rheology. J Mater Sci 33 (2003) 2165–2170.

Jakarni F.M., Adhesion of asphalt mixtures [PhD thesis], University of Nottingham (2012).

Jiménez-Mateos J.M., Quintero L.C. and Rial C., Characterization of petroleum bitumens and their fractions by thermogravimetric analysis and differential scanning calorimetry. Fuel 1996;75:1691–700.

Jones A.S., Dutta H., Fatigue life modeling of self-healing polymer systems. Mechanics of Materials 42 (2010) 481-490, doi: 10.1016/j.mechmat.2010.02.002.

Joseph C., Lark R., Jefferson T. and Gardner D., Potential Application of Self-healing Materials in the Construction Industry. Cardiff University, Cardiff, UK, 2009.

Kandhal P.S., Lynn C.Y. and Parker J., Characterization tests for mineral fillers related to performance of asphalt paving mixtures. NCAT Report 98-2(1998), USA: National Center of Asphalt Technologies.

Kandhal P.S., Mallick R., Pavement Recycling Guidelines for State and Local Governments, 1997.

Karki P., Li R. and Bhasin A., Quantifying overall damage and healing behaviour of asphalt materials using continuum damage approach. International Journal of Pavement Engineering 16 (2014) 350-362, doi: 10.1080/10298436.2014.942993.

Karlsson R. and Isacsson U., Application of FTIR-ATR to characterization of bitumen rejuvenator diffusion. Journal of Materials in Civil Engineering 15 (2003) 157–165.

Karlsson R. and Isacsson U., Material-related aspects of asphalt recycling: state-of-the-art. Journal of Materials in Civil Engineering 18 (1) (2006) 81-92, doi: 10.1061/(ASCE)0899-1561(2006)18:1(81).

Kats B.I., Glotova N.A. and Kudryashova A.I., Study of aging of asphalts from Romashkino and Ust'-Balyk under natural conditions. Chemistry and Technology of Fuels and Oils 12 (1976) 121–124.

Kazmee H., Tutumluer E. and Beshears S., Using accelerated pavement testing to evaluate reclaimed asphalt pavement materials for pavement unbound granular layers. Journal of Materials in Civil Engineering 29 (2) (2017), doi: 10.1061/(ASCE)MT.1943-5533.0001729.

Kennedy T.W., Huber G.A., Harrigan E.T., Cominsky R.J., Hughes C.S., Von Quintus H. and Moulthrop J.S. (1994). Superior performing asphalt pavement (Superpave): the product of the SHRP asphalt research program.

Khandal P., Foo K.Y., Designing Recycled Hot Mix Asphalt Mixtures Using Superpave Technology. National Center for Asphalt Paving Technology (NCAT) Report 96 (5) (1997) 7–22.

Kim B. and Roque R., Evaluation of healing property of asphalt mixtures. Transportation Research Record 1970 (2006) 84-91, doi: 10.3141/1970-10.

Kim Y.H. and Wool R.P., A theory of healing at a polymer-polymer interface. Macromolecules 16 (1983) 1115-1120.

Kim Y.R., Little D.N. and Benson F.C., Chemical and mechanical evaluation of healing mechanisms in asphalt concrete. Journal of Association of Asphalt Paving Technologist 59 (1990) 240-275.

Kim Y.R., Little D.N. and Lytton R.L., Use of dynamic mechanical analysis (DMA) to evaluate the fatigue and healing potential of asphalt binders in sand asphalt mixtures. Journal of Association of Asphalt Paving Technologist 71 (2002) 176-199.

Kim Y.R., Little D.N. and Lytton, R.L., Fatigue and healing characterization of asphalt mixtures. Journal of Materials in Civil Engineering 15 (2003) 75-83, doi: 10.1061/(ASCE)0899-1561(2003)15:1(75).

Kim Y.R., Modeling of asphalt concrete. McGraw-Hill Professional (2008).

King G.N., King H.W., Spray Applied Surface Seal, Federal Highway Administration to the Foundation for Pavement Preservation, 2007. Final Report.

Koots J.A. and Speight J.G., Relation of petroleum resins to asphaltenes. Fuel 54 (1975) 179–184.

Kuang D., Yu J., Chen H., Feng Z., Li R., Yang H., Effect of rejuvenators on performance and microstructure of aged asphalt. Journal of Wuhan University of Technology-Materials Science Edition 29 (2014) 341–345.

Lamontagne J., Dumas P., Mouillet V. and Kister J., Comparison by Fourier transform infrared (FTIR) spectroscopy of different ageing techniques: application to road bitumens. Fuel 80 (2001) 483–488.

Lee H.-J., Daniel J.S. and Kim, Y.R., Laboratory performance evaluation of modified asphalt mixtures for inchon airport pavements. International Journal of Pavement Engineering 1 (2000) 151-169, doi: 10.1080/10298430008901703.

Lee N.K., Morrison G.R. and Hesp S.A.M., Low temperature fracture of polyethylene-modified asphalt binders and asphalt concrete mixes. Journal of Association of Asphalt Paving Technologists 64 (1995) 534-574.

Lemaitre J. and Desmarat R., Engineering Damage Mechanics. New York: Springer, 2005.

Lesueur D., Gerard J.F., Claudy P., Letoffe J.M., Planche J.P. and Martin D., A structure-related model to describe bitumen linear viscoelasticity. Proceedings of the Eurasphalt and Eurobitume Congress, Session 5, Binders-Functional properties and performance testing, E&E.5.114, Strasbourg, 1996.

Lesueur D., The colloidal structure of bitumen: Consequences on the rheology and on the mechanisms of bitumen modification. Advances in Colloid and Interface Science 145 (2009) 42-82, doi: 10.1016/j.cis.2008.08.011.

Levesque M., Derrie K., Baptiste D. and Gilchrist M.D., On the development and parameter identification of Schapery-type constitute theories. Mechanics of Time-Dependent Materials 12(2) (2008) 95–127, doi: 10.1007/s11043-008-9052-y.

Lin J., Guo P., Wan L., Wu S., Laboratory investigation of rejuvenator seal materials on performances of asphalt mixtures. Construction and Building Materials 37 (2012) 41–45.

Lin J., Hong J., Huang C., Liu J. and Wu S., Effectiveness of rejuvenator seal materials on performance of asphalt pavement. Construction and Building Materials 55 (2014) 63–68.

Lin P-S., Wu T-L., Chang C-W. and Chou B-Y, Effects of recycling agents on aged asphalt binders and reclaimed asphalt concrete. Materials and Structures 44 (2011) 911–921.

Little D.N. and Bhasin A., Exploring mechanism of healing in asphalt mixtures and quantifying its impact. In: Self Healing Materials, P. S. van der Zwaag, Ed. Springer, The Netherlands (2007) 205-218.

Little D.N., Bhasin A. and Darabi M.K., Damage healing in asphalt pavements: theory, mechanism, measurement, and modelling. Advances in Asphalt Materials 56 (2015) 205-242, doi: 10.1016/B978-0-08-100269-8.00007-6.

Little D.N., Lytton R.L., Williams A.D. and Chen C.W., Microdamage healing in asphalt and asphalt concrete, 1: Microdamage and Microdamage Healing (2001).

Little D.N., Lytton R.L., Williams D.A. and Kim Y.R., An analysis of the mechanism of microdamage healing based on the application of micromechanics first principles of fracture and healing. Journal of Association of Asphalt Paving Technologists 68 (1999) 501e542.

Liu Q., Schlangen E., van de Ven M.F.C., van Bochove G. and van Montfort J., Evaluation of the induction healing effect of porous asphalt concrete through four point bending fatigue test. Construction and Building Materials 29 (2012) 403-409, doi:10.1016/j.conbuildmat.2011.10.058.

Liu, Q., Induction Healing of Porous Asphalt Concrete (PhD dissertation). Delft University of Technology, Delft, The Netherlands, 2012.

Lu X., Investigation of the Fracture Healing and Mechanism of Asphalt Binders (PhD dissertation). Washington State University, Pullman, Washington, USA, 2013.

Lu X., Soenen H. and Laukkanen O.V., Aging of bituminous binders in asphalt pavements and laboratory tests. In: 10th International Conference on the Bearing Capacity of Roads, Railways and Airfields (BCRRA), Athens, Greece, 28-30 June 2017, doi: 10.1201/9781315100333-40.

Lu X., Soenen H., Redelius P., Fatigue and Healing Characteristics of Bitumens studied using Dynamic Shear Rheometer. In: 6th International Rilem Symposium on Performance Testing and Evaluation of Bituminous Materials (2003) 408-15.

Lv Q., Huang W., X. Zhu and Xiao F., On the investigation of self-healing behavior of bitumen and its influencing factors. Materials and Design 117 (2017) 7–17, doi: 10.1016/j.matdes.2016.12.072.

Lv Q., Huang W., Zhu X. and Xiao F., On the investigation of self-healing behavior of bitumen and its influencing factors. Materials and Design 117 (2017) 7–17, doi: 10.1016/j.matdes.2016.12.072.

Lytton, R., Characterizing asphalt pavements for performance. Transportation Research Record 1723 (1) (2000) 5-16.

Malkin A.Y., Nonlinearity in rheology: an essay of classification. Rheological Acta 34, no. 1 (1995) 27-39.

Masad E., Huang C.W., D'Angelo J. and Little D.N., Characterization of asphalt binder resistance to permanent deformation based on nonlinear viscoelastic analysis of multiple stress creep recovery (MSCR) test. Journal of the Association of Asphalt Paving Technologists 78 (2009) 535–566.

Mazzoni G., Bocci E. and Canestrari F., Influence of rejuvenators on bitumen ageing in hot recycled asphalt mixtures. Journal of Traffic and Transportation Engineering (English edition) (2017a).

Mazzoni G., Stimilli A. and Canestrari F., Self-healing capability and thixotropy of bituminous mastics. International Journal of Fatigue 92(1) (2016) 8-17, doi: 10.1016/j.ijfatigue.2016.06.028.

Mazzoni G., Stimilli A., Cardone F. and Canestrari F., Fatigue, self-healing and thixotropy of bituminous mastics including aged modified bitumens and different filler contents. Construction and Building Materials 131 (2017b) 496-502, doi: 10.1016/j.conbuildmat.2016.11.093.

Mazzoni G., Virgili A. and Canestrari F., Influence of different fillers and bituminous blends on fatigue, self-healing and thixotropic performance of mastics. Road Materials and Pavement Design (2017c), doi: 10.1080/14680629.2017.1417150.

McDaniel R.S., Shah A., Huber G.A. and Copeland A., Effects of Reclaimed Asphalt Pavement content and virgin binder grade on properties of plant produced mixes. Association of Asphalt Paving Technologists 81 (2012) 369–401.

Meadows D.H., Meadows D.L., Rander J. and Behrens W.W., The limits to growth: A report for the Club of Rome's project on the predicament of mankind. Universe Books, New York, 1972.

Menozzi A., Garcia A., Partl M.N., Tebaldi G. and Schuetz P., Induction healing of fatigue damage in asphalt test samples. Construction and Building Materials 74 (2015) 162-168, doi: 10.1016/j.conbuildmat.2014.10.034.

Mewis J. and Wagner N.J., Thixotropy. Advances in Colloid and Interface Science 147-148 (2009) 214-227, doi: 10.1016/j.cis.2008.09.005.

Mogawer W.S., Austerman A., Roque R., Underwood S., Mohammad L. and Zou J., Ageing and rejuvenators: evaluating their impact on high RAP mixtures fatigue cracking characteristics using advanced mechanistic models and testing methods. Road Materials and Pavement Design 16 (2015) 1–28.

Mogawer W.S., Bennert T., Daniel J.S., Bonaquist R., Austerman A. and Boosherian A., Performance characteristics of plant-produced high RAP mixtures. Road Materials and Pavement Design 13(S1) (2012) 183–208, doi: 10.1080/14680629.2012.657070.

Mogawer W.S., Booshehrian A., Vahidi S. and Austerman A.J., Evaluating the effect of rejuvenators on the degree of blending and performance of high RAP, RAS, and RAP/RAS mixtures. Road Materials and Pavement Design 14 (2013) 193–213.

Molenaar A.A.A., Design of Flexible Pavement. Delft University of Technology, Delft, The Netherlands, 2007.

Moreno-Navarro F., Sol-Sanchez M., Rubio-Gamez M.C., Exploring the recovery of fatigue damage in bituminous mixtures: the role of healing. Road Materials and Pavement Design (2015) 1-15, doi: 10.1080/14680629.2015.1029706.

Mortazavi M. and Moulthrop J.S., SHRP Materials Reference Library, SHRP report A-646. Washington D. C.: National Research Council; 1993.

Moschopedis S.E. and Speight J.G., Influence of metal salts on bitumen oxidation. Fuel 57 (1978) 235–240.

Motamed A., Bhasin A. and Liechti K.M., Constitutive modeling of the nonlinearly viscoelastic response of asphalt binders; incorporating three-dimensional effects. Mechanics of Time-Dependent Materials 17(1) (2013) 83–109, doi: 10.1007/s11043-012-9178-9.

Motamed A., Bhasin A. and Liechti K.M., Interaction nonlinearity in asphalt binders. Mechanics of Time-Dependent Materials 16(2) (2012) 145–167, doi: 10.1007/s11043-011-9141-1.

Mouillet V., De La Roche C., Chailleux E. and Coussot, P., Thixotropic behavior of paving-grade bitumens under dynamic shear. Journal of Materials in Civil Engineering 24 (2012) 23-31, doi: 10.1061/(ASCE)MT.1943-5533.0000354.

Nahar S., Qiu J., Schlangen E., Shirazi M., van de Ven M., Schitter G. and Scarpas A., Turning back time: rheological and microstructural assessment of rejuvenated bitumen. In: 93rd Annual Meeting of the Transportation Research Board, Washington, D.C., 2014.

Narayan SPA, Little DN, Rajagopal KR. A nonlinear viscoelastic model for describing the response of asphalt binders within the context of a Gibbspotential based thermodynamic framework. Journal of Engineering Mechanics 124(1) (2013) 32–40, doi: 10.1061/(ASCE)EM.1943-7889.0000682.

National Cooperative Highway Research Program (NCHRP) Report 459, Characterization of Modified Asphalt Binders in Superpave Mix Design. Transportation Research Board - National Research Council, 2001.

Navaro J., Bruneau D., Drouadaine I., Colin J., Dony A. and Cournet J., Observation and evaluation of the degree of blending of reclaimed asphalt concretes using microscopy image analysis. Construction and Building Materials 37 (2012) 135–143, doi: 10.1016/j.conbuildmat.2012.07.048.

Nayak P. and Sahoo U.C., A rheological study on aged binder rejuvenated with Pongamia oil and Composite castor oil. International Journal of Pavement Engineering 13 (2015), doi: 10.1080/10298436.2015.1103851.

Nazzal M., Kaya S. and Abu-Qtaish L., Evaluation of WMA healing properties using atomic force microscopy. In: Scarpas, A., Kringos, N., Al-Qadi, I., Loizos, A. (Eds.), 7th RILEM International Conference on Cracking in Pavements 4 (2012) 1125-1134, doi: 10.1007/978-94-007-4566-7_107.

Negulescu I., Mohammad L., Daly W., Abadie C., Cueto R., Daranga C., Glover I., Kluttz R., Huber G.M., Stephens J. and Davis R., Chemical and rheological characterization of wet and dry aging of SBS copolymer modified asphalt cements: laboratory and field evaluation. Asphalt Paving Technology: Association of Asphalt Paving Technologists-Proceedings of the Technical Sessions 75 (2006) 267–96.

Nellensteyn F.J., The constitution of asphalt. J Inst Pet Technol 10 (1924) 311–325.

Nguyen V.H., Effects of Laboratory Mixing Methods and RAP Materials on Performances of Hot Recycled Asphalt Mixtures (Thesis), University of Nottingham, 2009.

Noferini L., Simone A., Sangiorgi C. and Mazzotta F., Investigation on performances of asphalt mixtures made with Reclaimed Asphalt Pavement: Effects of interaction between virgin and RAP bitumen. International Journal of Pavement Research and Technology 10 (4) (2017) 322-332, doi: 10.1016/j.ijprt.2017.03.011.

Ongel A. and Hugener M., Impact of rejuvenators on aging properties of bitumen. Construction and Building Materials 94 (2015) 467-474, doi: 10.1016/j.conbuildmat.2015.07.030.

Otto S., Bedeutung und Verwendung der Begriffe nachhaltige Entwicklung und Nachhaltigkeit: Eine empirische Studie, Dissertation, Jacobs Univ. Bremen, Jacobs Center on Lifelong Learning and Institutional Development, Germany, 2007.

Pan X., York D., Preece J.A., Zhang Z., Size and strength distributions of melamine-formaldehyde microcapsules prepared by membrane emulsification, Powder Technology 227 (2012) 43–50.

Park S. Development of a nonlinear thermo-viscoelastic constitutive equation for particulate composites with growing damage. PhD dissertation. University of Texas, Austin, Austin, TX, 1994.

Pepper D., Modern environmentalism: An introduction, Routledge, London, 2005.

Pereira P., Oliveira J. and Picado-Santos L., Mechanical characterization of hot mix recycled materials. International Journal of Pavement Engineering 5 (4) (2004) 211–220, doi: 10.1080/10298430412331333668.

Pérez-Jiménez F.E., Botella R. and Mirò R., Differentiating between damage and thixotropy in asphalt binder's fatigue tests. Construction and Building Materials 31 (2012) 212-9, doi: 10.1016/j.conbuildmat.2011.12.098.

Petersen J.C., Asphalt oxidation — an overview including a new model for oxidation proposing that physicochemical factors dominate the oxidation kinetics. Fuel Science and Technology International 11 (1993) 57–87.

Pfeiffer J.P. and Saal R.N.J., Asphaltic bitumen as colloid systems. The Journal of Physical Chemistry 44 (1940) 139–149.

Phillips M.C., Multi-step models for fatigue and healing, and binder properties involved in healing. In: Proceedings of Eurobitume Workshop on Performance Related Properties for Bituminous Binders, Luxembourg 1998 (Paper 115).

Piéri N., Etude du Vieillissement Simulé et In-Situ des Bitumes Routiers par IRTF et Fluorescence UV en Excitation-Emission Synchrones, Ph. D. Thesis: Univ. Aix-Marseille St-Joseph (France), 1995.

Pradyumna T.A., Mittal A. and Jain P.K., Characterization of reclaimed asphalt pavement (RAP) for use in bituminous road construction. Procedia - Social and Behavioral Sciences 104 (2013) 1149–1157.

Prapaitrakul N., Freeman T., Glover C.J., Analyze existing fog seal asphalts and additives: literature, review, 2005. FHWA/TX-06/0-5091-1.

Pronk A.C. and Cocurullo A., Investigation of the PH model as a prediction tool in fatigue bending tests with rest periods. Advanced Testing and Characterization of Bituminous Materials (2009).

Pronk A.C. and Hopman P.C., Energy dissipation: the leading factor of fatigue. In: Highway Research: Sharing the Benefits, Thomas Telford Publishing (1991) 255-267.

Pronk A.C., Partial healing model - curve fitting. Report WDWW- 2000-047. Delft: DWW; 2000.

Pronk A.C., PH model in 4PB test with rest periods. Road Materials and Pavement Design 10 (2009) 417-426.

Puzinauskas V.P., Filler in asphalt mixtures. Research Report 69-2 (1969) Asphalt Institute, Maryland.

Qiu J., Self-healing of asphalt mixtures towards a better understanding of the mechanism (PhD dissertation 2012. Delft University of Technology, Delft, The Netherlands).

Qureshi N.A., Tran N.H., Watson D., Jamil S.M., Effects of rejuvenator seal and fog seal on performance of open-graded friction course pavement. Maejo International Journal of Science and Technology7 (2013) 189–202.

Raithby K.D., Sterling A.B., The effect of rest periods on the fatigue performance of a hot-rolled asphalt under repeated loading. Association of Asphalt Paving Technologists 39 (1970) 134-152.

Rajagopal K.R. and Srinivasa A.R., Mechanics of the inelastic behavior of materials. Part I, theoretical underpinnings. International Journal of Plasticity 14(10–11) (1998) 945–967, doi: 10.1016/S0749-6419(98)00037-0.

Read J. and Whiteoak D. The Shell Bitumen Handbook. 5th Ed. London: Thomas Telford Publishing; 2003.

Redelius P., Bitumen solubility model using Hansen solubility parameter. Energy and Fuels 18(4) (2004).

Ridgen P.J., The Use of Fillers in Bituminous Road Surfacing. A Study of Filler-Binder System in Relation to Filler Characteristics. Journal of Society of Chemical Industry 66 (1947) 299–309.

Roberts F., Kendhal P., Brown E.R., Lee D.Y. and Kennedy T., Hot mix asphalt materials, mixture design and construction. Third Edition ed., Lanham, MD: National Asphalt Pavement Association Research and Education Foundation, 2009.

Roque R., Simms R., Chen Y., Koh C. and Lopp G., Development of a Test Method that Will Allow Evaluation and Quantification of the Effects of Healing on Asphalt Mixture. Department of Civil and Coastal Engineering, University of Florida, Gainesville, Florida, USA (Project No.: 00084223), 2012.

Rosinger A., Beiträge zur Kolloidchemie des Asphalts. Kolloid-Z 15 (1914) 177–179.

Rostler F.S. and White R.M., Rejuvenation of Asphalt Pavements, Materials Research and Development Inc, Oakland, California, 1970. Under Air Force Systems Command Contract F29601-69-C-0129.

Rubio M.C., Martínez G., Baena L. and Moreno F., Warm mix asphalt: an overview. Journal of Cleaner Production 24 (2012) 76–84, doi: 10.1016/j.jclepro.2011.11.053.

Saal R.N.J. and Labout J.W.A., Rheological properties of asphaltic bitumens. The Journal of Physical Chemistry 44 (1940) 149–165.

Santagata E., Baglieri O. and Dalmazzo D., Experimental investigation on the fatigue damage behaviour of modified bituminous binders and mastics. Journal of the Association of Asphalt Paving Technologists 77 (2008) 851-883.

Santagata E., Baglieri O., Dalmazzo D. and Tsantilis L., Investigating cohesive healing of asphalt binders by means of a dissipated energy approach. International Journal of Pavement Research and Technology (2017), doi: 10.1016/j.ijprt.2017.06.004

Santagata E., Baglieri O., Dalmazzo D. and Tsantilis L., Rheological and chemical investigation on the damage and healing properties of bituminous binders. Journal of the Association of Asphalt Paving Technologists 78 (2009) 567-595.

Santagata E., Baglieri O., Tsantillis L. and Chiappinelli G., Fatigue and healing properties of nano-reinforced bituminous binders. International Journal of Fatigue 80 (2015) 30-39, doi: 10.1016/j.ijfatigue.2015.05.008.

Schapery R.A., A theory of mechanical behavior of elastic media with growing damage and other changes in structure. Journal of the Mechanics and Physics of Solids 38 (2) (1990) 215–253, doi: 10.1016/0022-5096(90)90035-3.

Schapery R.A., A theory of non-linear thermoviscoelasticity based on irreversible thermodynamics. In: Proc 5th U.S. natl cong appl mech. Minneapolis, MN, 1966. p. 511–30.

Schapery R.A., Correspondence principles and a generalized J-integral for large deformation and fracture analysis of viscoelastic media. Int J Fract 25(3) (1984) 195–223, doi: 10.1007/BF01140837.

Schapery R.A., On the characterization of nonlinear viscoelastic materials. Polymer Engineering & Science 9(4) (1969) 295–310, doi: 10.1002/pen.760090410.

Schmets A., Kringos N., Pauli T., Redelius P. and Scarpas T., On the existence of wax-induced phase separation in bitumen. International Journal of Pavement Engineering 11 (2010) 555-563, doi: 10.1080/10298436.2010.488730.

Self healing materials, concept and applications. NL Agency. Publication 3ISHM1001, 2010.

Shan L., Tan Y., Underwood B.S. and Kim Y.R., Application of thixotropy to analyze fatigue and healing characteristics of asphalt binder. Transportation Research Record 2179 (2010) 85-92, doi: 10.3141/2179-10.

Shashidhar N. and Romero, P., Factors affecting the stiffening potential of mineral fillers. Transportation Research Record 1638 (1998) 94-100.

Shen J., Amirkhanian S. and Miller J.A., Effects of rejuvenating agents on superpave mixtures containing reclaimed asphalt pavement. Journal of Materials in Civil Engineering 19 (5) (2007a) 376–384, doi: 10.1061/(ASCE)0899-1561(2007)19:5(376).

Shen J., Amirkhanian S. and Tang B., Effects of rejuvenator on performance-based properties of rejuvenated asphalt binder and mixtures. Construction and Building Materials 21(5) (2007b) 958–964, doi: 10.1016/j.conbuildmat.2006.03.006.

Shen S. and Carpenter S.H., Application of the dissipated energy concept in fatigue endurance limit testing. Transportation Research Record: Journal of the Transportation Research Board 1929 (2005) 165-173.

Shen S. and Carpenter S.H., Dissipated energy concepts for HMA performance: fatigue and healing (COE report no. 29). Centre of Excellence for Airport Technology, Department of Civil and Environmental Engeenering, University of Illinois at Urbana-Champaign, Champaign-Urbana Metropolitan Area, Illinois, USA, 2007.

Shen, S., Sutharsan, T., Quantification of cohesive healing of asphalt binder and its impact factors based on dissipated energy analysis. Road Materials and Pavement Design 12 (2011) 525-546, doi: 10.1080/14680629.2011.9695259.

Shirodkar P., Mehta Y.A., Nolan A., Sonpal K., Norton A., Tomlinson C., DuBois E. et al., A study to determine the degree of partial blending of reclaimed asphalt pavement (RAP) binder for high RAP hot mix asphalt, Construction and Building Materials 25 (2011) 150–155.

Shu X., Huang B., Shrum E.D. and Jia X., Laboratory evaluation of moisture susceptibility of foamed warm mix asphalt containing high percentages of RAP. Construction and Building Materials 35 (2012) 125–130.

Simonen M., Blomberg T., Pellinen T. and Valtonen J., Physicochemical properties of bitumens modified with bioflux. Road Materials and Pavement Design 14 (2012) 36–48.

Soleymani H.R., Anderson M., McDaniel R. and Abdelrahman M., Investigation of the black rock issue for recycled asphalt mixtures. Journal of the Association of Asphalt Paving Technologists 69 (2000) 366–390.

Soltani A. and Anderson D.A., New test protocol to measure fatigue damage in asphalt mixtures. Road Materials and Pavement Design 6 (2005) 485-514, doi: 10.1080/14680629.2005.9690017.

Song I., Little D.N., Masad E. and Lytton, R.L., Comprehensive evaluation of damage in asphalt mastics using X-ray CT, continuum mechanics, and micromechanics. Journal of the Association of Asphalt Paving Technologists 74 (2005) 885-920.

Speight J. G., The Chemistry and Technology of Petroleum, 3rd. Ed. New-York: Marcel Dekker; 1999.

Speight J.G., Petroleum asphaltenes. Part 1. Asphaltenes, resins and the structure of petroleum. Oil Gas Science Technology 59 (2004) 467–477.

Stimilli A., Ferrotti G., Conti C., Tosi G. and Canestrari F., Chemical and rheological analysis of modified bitumens blended with “artificial reclaimed bitumen”. Construction and Building Materials 63 (2014) 1-10, doi: 10.1016/j.conbuildmat.2014.03.047.

Stimilli A., Ferrotti G., Radicioni D. and Canestrari F., Performance evaluation of hot recycled mixtures containing sbs modified binder. Bituminous Mixtures and Pavements VI - Proceedings of the 6th International Conference on Bituminous Mixtures and Pavements, ICONFBMP (2015) 607-616.

Stimilli A., Hintz C., Li Z., Velasquez R. and Bahia H.U., Effect of healing on fatigue law parameters of asphalt binders. Transportation Research Record 2293 (2012) 96-105, doi: 10.3141/2293-12.

Stimilli A., Virgili A. and Canestrari F., New Method to Estimate the "Re-Activated" Binder Amount in Recycled HMA. Road Materials and Pavement Design 16 (2015) 442-459, doi: 10.1080/14680629.2015.1029678.

Stimilli A., Virgili A., Giuliani F. and Canestrari F., In plant production of hot recycled mixtures with high reclaimed asphalt pavement content: A performance evaluation. RILEM Bookseries 11 (2016) 927-939, doi: 10.1007/978-94-017-7342-3_74.

Stimilli A., Virgili A., Giuliani F. and Canestrari F., Mix design validation through performance-related analysis of in plant asphalt mixtures containing high RAP content. International Journal of Pavement Research and Technology 10 (2017) 23-37, doi: 10.1016/j.ijprt.2016.07.002.

Su J.F., Qiu J. and Schlangen E., Self-healing bitumen by microcapsules containing rejuvenator. In: Proceedings of the 4th International Conference on Self-healing Materials (ICSHM 2013), Ghent, Belgium, 2013a.

Su J-F, Qiu J. and Schlangen E., Stability investigation of self-healing microcapsules containing rejuvenator for bitumen, Polymer Degradation and Stability 98 (2013) 1205–1215.

Su Z., A sustainable maintenance solution for porous asphalt pavements via rejuvenation technology, in: Sustainable Construction Materials (2012) – Proceedings of the 2nd International Conference on Sustainable Construction Materials – Design, Performance, and Application, Wuhan, China, 2012, pp. 387–403.

Tabakovi A., Braak D., van Gerwen M., Copuroglu O., Post W., Garcia S.J. and Schlangen E., The compartmented alginate fibres optimisation for bitumen rejuvenator encapsulation. Journal of Traffic and Transportation Engineering (English edition) 4 (4) (2017) 347-359, doi: 10.1016/j.jtte.2017.01.004.

Tan Y., Shan L., Kim Y. R. and Underwood B.S., Healing characteristics of asphalt binder. Construction and Building Materials 27 (2012) 570–577, doi:10.1016/j.conbuildmat.2011.07.006.

Tan Y., Shan L., Underwood B.S. and Kim Y.R., Thixotropic characteristics of asphalt binder Journal of Materials in Civil Engineering 2011.

Tebaldi G., Dave E., Marsac P., Muraya P., Hugener M., Graziani A., Grilli A. et al., Synthesis of specimen preparation and curing processes for cold recycled asphalt mixes. In: 2nd International Symposium on Asphalt Pavement & Environment, ISAP TC APE, Fortaleza, Brasil 2012a.

Tebaldi G., Dave E., Marsac P., Muraya P., Hugener M., Pasetto M., Graziani A., Grilli A. et al., Classification of recycled asphalt pavement (RAP) material. 2nd International Symposium on Asphalt Pavement & Environment, ISAP TC APE, Fortaleza, Brasil 2012b.

Traxler R.N. and Coombs C.E., The colloidal nature of asphalt as shown by its flow properties. The Journal of Physical Chemistry 40 (1935) 1133-1147.

Traxler R.N., Relation between asphalt composition and hardening by volatilization and oxidation. Proceedings of Association of Asphalt Paving Technologists 30 (1961) 359–372.

Tsai B.W., Monismith C.L., Dunning M., Gibson N., D'Angelo J., Leahy R., King G., Christensen D., Anderson D., Davis R. and Jones D., Influence of asphalt binder properties on the fatigue performance of asphalt concrete pavements. In: Asphalt Paving Technology: Association of Asphalt Paving Technologists-Proceedings of the Technical Sessions 74 (2005) 733-89.

Underwood B.S. and Kim Y.R., A nonlinear viscoelastic constitutive model for asphalt cement and asphalt mastic. International Journal of Pavement Engineering 16(6) (2015) 510–529, doi: 10.1080/10298436.2014.943133.

Underwood B.S., A continuum damage model for asphalt cement and asphalt mastic fatigue. International Journal of Fatigue 82 (2016) 387-401, doi: 10.1016/j.ijfatigue.2015.08.020.

Underwood B.S., Kim Y.R. and Guddati M.N., Improved calculation method of damage parameter in viscoelastic continuum damage model. International Journal of Pavement Engineering 11(6) (2010) 459–476, doi: 10.1080/10298430903398088.

Valdés G., Pérez-Jiménez F., Miró R., Martínez A. and Botella R., Experimental study of recycled asphalt mixtures with high percentages of reclaimed asphalt pavement (RAP). Construction and Building Materials 25 (3) (2011) 1289–1297.

Van den Bergh W., The Effect of Ageing on the Fatigue and Healing Properties of Bituminous Mortars (PhD dissertation). Delft University of Technology, Delft, The Netherlands, 2011.

Van der Poel C., A general system describing the visco-elastic properties of bitumen and its relation to routine test data. Journal of Applied Chemistry 4 (1954) 221-236.

Van Dijk W., Moreaud H., Quedeville A. and Uge, P., The fatigue of bitumen and bituminous mixes. In: Proceedings of the 3th International Conference on the Structural Design of Asphalt Pavements, London, England, 1972.

Van Gooswiligen G., de Hilster E. and Robertus C., Changing needs and requirements for bitumen and asphalts. In: Proceedings of the 6th Conference on Asphalt Pavements for Southern Africa, Cape Town, South Africa, 1994.

Verstraeten J., Fatigue of bituminous mixes and bitumen thixotropy. XIXth World Road Congress, AIPCR. Marrakech (1991) 766-769.

Wang H., Al-Qadi I.L., Faheem A.F., Yang S.-H. and Reinke G.H., Effect of mineral filler characteristics on asphalt mastic and mixture rutting potential. Transportation Research Record 2208 (2011) 33-39, doi: 10.3141/2208-05.

Wang W., Chen J., Sun y., Xu B., Li J. and Liu J., Laboratory performance analysis of high percentage artificial RAP binder with WMA additives. Construction and Building Materials 147 (2017) 58-65, doi: 10.1016/j.conbuildmat.2017.04.142.

Wen H. and Bahia H.U., Characterizing fatigue of asphalt binders with viscoelastic continuum damage mechanics. Transportation Research Record: Journal of the Transportation Research Board 2126 (2009) 55–62, doi: 10.3141/2126-07.

Williams D., Little D.N., Lytton R.L., Kim Y.R. and Kim Y., Microdamage Healing in Asphalt and Asphalt Concrete: Laboratory and Field Testing to Assess and Evaluate Microdamage and Microdamage Healing (Research report no. FHWA0RD-98-142). Texas Transportation Institute, The Texas A&M University System, College Station, Texas, USA, 2001.

Wool R.P. and O'Connor K.M., A theory of crack healing in polymers. Journal of Applied Physics 52(10) (1981) 5953-5963, doi: 10.1063/1.328526.

Wool R.P. and O′Connor K.M., Time dependence of crack healing. Journal of Polymer Science: Polymer Letters Edition 20 (1982) 7-16.

Wool R.P., Self-healing materials: a review. Soft Matter 4 (2008) 400-418, doi: 10.1039/b711716g.

Wright J.R., Weathering: theoretical and practical aspects of asphalt durability. In: Hoiberg AJ, editor. Bituminous Materials: Asphalts, Tars and Pitches. New York: Interscience Publishers; 2(1) (1965) 249–306.

Wu D.Y., Meure S. and Solomon D., Self-healing polymeric materials: a review of recent developments. Progress in Polymer Science 33 (2008) 479-522.

Wu S-P., Huang X-M., Zhao Y-L., The development of recycling agent for asphalt pavement. Journal of Wuhan University of Technology-Materials Science Edition 17 (3) (2002) 63–65.

Yousefi Rad F., Estimating Blending Level of Fresh and Rap Binders in Recycled Hot Mix Asphalt. Master of Science, University of Wisconsin Madison, 2013.

Yu X., Zaumanis M., dos Santos S. and Poulikakos L., Rheological, microscopic, and chemical characterization of the rejuvenating effect on asphalt binders. Fuel 135 (2014) 162–71, doi: 10.1016/j.fuel.2014.06.038.

Zargar M., Ahmadinia E., Asli H. and Karim M.R., Investigation of the possibility of using waste cooking oil as a rejuvenating agent for aged bitumen. Journal of Hazardous Materials 233–234 (2012) 254–258.

Zaumanis M., Mallick R., Review of very high-content reclaimed asphalt use in plant-produced pavements: state of the art. International Journal of Pavement Engineering (2015) 39–55, doi: 10.1080/10298436.2014.893331.

Zaumanis M., Mallick R.B. and Frank R. 100% Recycled hot mix asphalt: a review and analysis. Resources, Conservation and Recycling (2014), doi: 10.1016/j.resconrec.2014.07.007.

Zaumanis M., Mallick R.B. and Frank R., Evaluation of different recycling agents for restoring aged asphalt binder and performance of 100% recycled asphalt. Materials and Structures 48 (2015) 2475–2488, doi: 10.1617/s11527-014-0332-5.

Zaumanis M., Mallick R.B. and Frank R., Evaluation of rejuvenator's effectiveness with conventional mix testing for 100% reclaimed asphalt pavement mixtures. Transportation Research Record 2370 (2013) 17–25, doi: 10.3141/2370-03.

Zaumanis M., Mallick R.B., Poulikakos L. and Frank R., Influence of six rejuvenators on the performance properties of reclaimed asphalt pavement (RAP) binder and 100% recycled asphalt mixtures, Construction and Building Materials 71 (2014) 538–550.

Zhang Z., Identification of Suitable Crack Growth Law for Asphalt Mixtures Using the Superpave Indirect Tensile Test (IDT) (PhD dissertation). University of Florida, Gainesville, Florida, USA, 2000.

Zhang Z., Rogue R., Birgisson B. and Sangpetngam B., Identification and verification of a suitable crack growth law. In: Proceedings of the Association of Asphalt Paving Technologists Volume 70 (2001) 206-241.

Zhao S., Bowers B.F., Huang B. and Shu X., Characterizing rheological properties of binder and blending efficiency of asphalt paving mixtures containing RAS through GPC. Journal of Materials in Civil Engineering 26(5) (2014) 941–946.

Zhao S., Huang B., Shu X. and Woods M., Comparative evaluation of Warm Mix Asphalt containing high percentages of Reclaimed Asphalt Pavement. Construction and Building Materials 44 (2013) 82–100.

Zhao S., Huang B., Shu X., Jia X. and Woods M., Laboratory performance evaluation of warm-mix asphalt containing high percentages of reclaimed asphalt pavement. Transportation Research Record: Journal of the Transportation Research Board 2294 (2012) 98–105.